

# The WEST research plan

v1.0  
February 2015

P. Ghendrih, E. Tsitrone, C. Bourdelle, S. Brémond, J. Bucalossi, Y. Corre, A. Ekedahl, G. Giruzzi, R. Guirlet, P. Maget, Y. Marandet, M. Missirlian, P. Moreau, E. Nardon, B. Pégourié

With contributions from:

**CEA/DSM/IRFM, F-13108 Saint-Paul-lez-Durance, France:**

T. Alarcon, J.F. Artaud, M.H. Aumenier, V. Basiuk, M. Bécoulet, C. Bottereau, H. Bufferand, M. Chantant, M. Chatelier, G. Ciraolo, F. Clairet, L. Colas, G. Colledani, X. Courtois, E. Delchambre, L. Delpech, P. Devynck, G. Dif-Pradalier, D. Douai, R. Dumont, D. Elbèze, N. Fedorczak, C. Fenzi, M. Firdaouss, X. Garbet, J. Garcia, L. Gargiulo, E. Gauthier, C. Gil, M. Goniche, C. Grisolia, A. Grosman, D. Guilhem, J. Gunn, J. Hillairet, T. Hoang, M. Houry, F. Imbeaux, E. Joffrin, T. Loarer, P. Lotte, L. Manenc, D. Mazon, O. Meyer, D. Molina, P. Mollard, P. Monier-Garbet, J.Y. Pascal, Y. Peysson, C. Reux, R. Sabot, Y. Sarazin, F. Saint Laurent, S. Salasca, M. Schneider, J.M. Travère, P. Tamain, S. Vartanian

**Aix-Marseille Université, CNRS, PIIM, UMR 7345, 13013 Marseille, France:** Y. Marandet

**CCFE, Abingdon, Oxon, OX14 3DB, UK / EUROfusion Programme Management Unit, D-85748 Garching, Germany:** M.L. Mayoral

**Centre de Recherches en Physique des Plasmas, Ecole Polytechnique Fédérale de Lausanne, Switzerland :** J. Decker

**Ecole Polytechnique, LPP, CNRS UMR 7648,91128 Palaiseau, France :** P. Hennequin, L. Vermare

**Associazione ENEA-Euratom sulla Fusione, Frascati, Italy:** A. Tuccillo

**EUROfusion Programme Management Unit; Culham Science Centre; Abingdon, UK:** X. Litaudon

**Max Planck Institut für Plasmaphysik, D-85748 Garching, Germany:** C. Angioni, V. Bobkov, T. Eich, A. Kallenbach

**Forschungszentrum Jülich, D-52425 Jülich, Germany:**

S. Brezinsek, J. Coenen, J. Linke, C. Linsmeier, T. Loewenhoff, M. Wirtz

**Fusion for Energy F4E, Barcelona, Spain:**

P. Lorenzetto

**Institute of Plasma Physics and Laser Microfusion, EURATOM/IPPLM Association, Warsaw, Poland:**

I. Ivanova-Stanik, R. Zagorski

**ITER Organization, F-13115 Saint Paul lez Durance, France:** R. A. Pitts, F. Escourbiac, M. Merola,

G. De Temmerman, J. Snipes

**Japan Atom Energy Agency, Naka, Ibaraki, Japan:**

M. Yoshida

**Japanese Domestic Agency (JADA), Japan Atom Energy Agency, Naka, Ibaraki, Japan:** K. Ezato, S. Suzuki, Y. Seki, K. Yokoyama, K. Mohri, T. Hirayama, S. Kakudate

**EcoTopia Science Institute, Nagoya University, Nagoya 464-8603, Japan:** S. Kajita, N. Ohno

**Center for Energy Research, University of California at San Diego, 9500 Gilman Drive, La Jolla, CA 92093-0417, USA:** R. Doerner



# Foreword

---

The present document corresponds to the first update of the WEST Research Plan (version 1.0, February 2015), taking into account the input of WEST international partners. This was performed through a dedicated workshop devoted to WEST scientific programme, organized in summer 2014. Recommendations from an international panel assessing WEST as a EUROfusion facility were also considered.

This is a living document, which will evolve with the project and will be discussed with the WEST partners on a regular basis. The next update is proposed at the end of the first phase of WEST exploitation.

The authors wish to warmly thank all the participants to the 1<sup>st</sup> international WEST workshop for their contribution, and in particular Dr M. L. Mayoral (CCFE, UK), J. Linke (FZJ, Germany), A. Kallenbach (IPP, Germany), R. Doerner (UCSD, USA) and M. Yoshida (JAEA, Japan) for having taken the duty to review the WEST topical research areas as external experts.

# Executive Summary

---

Finding a reliable scheme for power exhaust in magnetic fusion devices has been identified as one of the main challenge towards a future fusion reactor. In next step fusion devices, such as ITER and DEMO, the plasma facing components will experience extreme heat and particle loads. In addition, these devices, aiming at steady state operation, will run much longer plasma discharges than present day facilities. The cumulated particle fluence<sup>1</sup> and energy on the plasma facing components will reach unprecedented levels, with hours of plasma exposure for the components and gigajoules of energy to extract in a single discharge. In order to address these challenges, an integrated approach, relying on progress in technology, plasma operation and exhaust physics, is required.

Tore Supra has been leading the way towards mastering power exhaust over long pulse operation over the past 25 years, developing a unique expertise to solve the associated technological, operational and physics issues. With the WEST project (Tungsten (W) Environment in Steady State Tokamak), this expertise is turned in support of the ITER divertor. The divertor is a crucial component, handling the highest heat and particle loads in the vessel, and allowing access to high plasma confinement regimes (H mode). ITER plans to operate with an actively cooled tungsten divertor, bringing specific challenges.

- From the technology point of view, although prototypes have been successfully built and tested for ITER, large scale industrial manufacturing of actively cooled tungsten components has never been performed and remains a challenging step.
- From the operation point of view, these components have been tested in dedicated high heat flux facilities or plasma wall interaction linear devices, but have never been run in a tokamak environment under combined heat and particle loads.
- From the physics point of view, using tungsten plasma facing components restrains the operational window, as the tolerable tungsten concentration in the plasma ( $\ll 10^{-4}$ ) is much lower than for carbon (few %). Acceptable tungsten control has been obtained in JET and AUG. However, the control of tungsten contamination over long discharges has not yet been addressed so far.

The WEST project is targeted at solving these issues, minimizing risks for the ITER divertor procurement (in terms of cost, delays, performance) and gaining time for its operation. It consists of implementing a divertor configuration and installing an ITER like actively cooled tungsten divertor in the Tore Supra tokamak, taking full benefit of its unique long pulse capability.

Tore Supra is already fully equipped for long pulse operation with actively cooled components (superconducting magnets, pressurized water loop, steady state heating and fuelling systems ...) and is therefore the most cost effective facility to tackle the issues mentioned above.

---

<sup>1</sup> Defined as the integrated particle flux. For instance, the deuterium fluence will reach  $1.5 \cdot 10^{27}$  D/m<sup>2</sup> at the ITER strike point within one nominal discharge. This is equivalent to several years of operation for JET.

## Executive Summary

WEST complements the ongoing effort on tungsten R&D worldwide, as it provides an integrated test environment, bringing together the high heat flux technology of the ITER divertor and long pulse tokamak operation.

WEST will also open new possibilities to demonstrate the sustainability of plasma scenarios over relevant plasma wall equilibrium timescale (~minutes), as required for steady state operation. Indeed, extending plasma operation to long pulse brings additional constraints (high current drive efficiency, control of MHD at vanishing loop voltage ...) and can evidence new issues which do not appear on short pulses, in particular in the field of particle control. WEST provides an opportunity to anticipate current unknowns on the way to long pulse operation in a metallic environment before they are encountered in ITER, and identify solutions.

The main mission of WEST is therefore twofold:

- Paving the way towards the ITER actively cooled tungsten divertor procurement and operation,
- Mastering integrated plasma scenario over relevant plasma wall equilibrium time scale in a metallic environment.

The high level deliverables expected from WEST include:

- The optimization of industrial scale production processes ahead of ITER divertor procurement
- The assessment of power handling capabilities / lifetime of ITER high heat flux tungsten divertor components in tokamak environment
- A validated scheme for actively cooled metallic plasma facing component protection
- The demonstration of integrated long pulse H mode scenario, including the optimization of RF heating, the control of tungsten contamination and plasma density over plasma wall equilibrium time scale
- The investigation of advanced scenario regimes (fully non inductive H mode operation, highly radiating scenario in preparation for DEMO, high bootstrap discharges in preparation for JT-60SA)

The main driver of the WEST planning is to provide timely answers for ITER. It is therefore aligned with the ITER divertor procurement and operation planning. The WEST platform is scheduled to be operational in 2016. WEST operation is planned to be phased, to make the best use of the WEST ITER like divertor elements as they become available. In phase 1 (2016-2017), it is planned to operate with a mix of actively cooled ITER like tungsten divertor elements and inertial tungsten coated divertor start up elements. In this phase, full power will be available, but plasma operation will be limited in time by the inertial divertor elements (typically ~10 s at high power). In phase 2 (2018-early 2020's), the full actively cooled ITER like tungsten divertor will be available, allowing long pulse operation, up to 1000s. The contributions of WEST are foreseen in 3 steps:

- WEST divertor production : optimization of the industrial large scale production
- WEST operation phase 1 : power handling capabilities of the ITER like divertor

## Executive Summary

- WEST operation phase 2 : high fluence plasma divertor exposure / demonstration of integrated long pulse H mode / investigation of advanced regimes

The WEST project and its research plan are open to the international fusion community. The programme foreseen for WEST, using the unique long pulse capability of Tore Supra in support of the ITER divertor, is in line with the European Fusion Roadmap, where the success of ITER is seen as the highest priority for Horizon 2020. The WEST platform will be run as a user facility, open to the EUROfusion Consortium and all ITER partners. Major fusion partners have already demonstrated their interest for WEST and participate to the construction phase. In particular, partnership agreements have been signed with China, India, Japan, Korea, USA and European laboratories, as well as with the European Domestic Agency F4E. Further contacts with other potentially interested laboratories or institutions in and outside Europe are ongoing.

The project has been initiated based on a joint analysis of tungsten divertor R&D needs with the ITER Organization. In addition, a strong connection is being developed with the Domestic Agencies in charge of procuring the ITER divertor targets (F4E for Europe and JADA for Japan), as well as with the ITER partners. In particular, the programme of WEST is developing strong links with superconducting long pulse fusion devices (such as EAST, JT-60SA, KSTAR, SST-1, or the W7X stellarator), as well as with tokamaks running with metallic walls (AUG and JET) and plasma wall interaction devices (Judith, Gladis, Magnum PSI, PISCES). At the national level, WEST is supported by the French Federation of Research on Magnetic Confinement Fusion (FR-FCM), gathering the efforts of French research institutions in the field of fusion.

The present document aims at defining the research plan associated with the WEST project to fulfill the mission previously described. This document is also meant to ensure an efficient operation and a timely implementation of the experimental programme over the period foreseen for WEST exploitation. The West Research Plan is structured around 2 topical headlines:

- Headline 1 : Operating and testing ITER grade Plasma Facing Components in tokamaks
- Headline 2 : Towards long pulse H mode and steady state operation

They are detailed in the document where associated deliverables and milestones are described, as well as a proposal for priorities and phasing.

The present version of the document corresponds to the first update of the WEST Research Plan (version 1.0, February 2015), taking into account the input of the international WEST partners. This a living document, which will evolve with the project and will be discussed with the WEST partners on a regular basis, through scientific workshops as well as through presentation at the WEST Governing Board. The next update is proposed at the end of the first phase of WEST exploitation.

# Outline

---

<b>Foreword</b>	<b>2</b>
<b>Executive Summary</b>	<b>3</b>
<b>Outline</b>	<b>6</b>
<b>Chapter 1: Strategy of the WEST project</b>	<b>11</b>
I. Background: the challenge of power exhaust in fusion devices	11
II. R&D needs for the ITER divertor	13
III. The mission of WEST	14
IV. WEST high level deliverables	15
V. The WEST schedule: providing answers in time for ITER	18
VI. WEST: a user facility open to the international fusion community	20
VII. Main objectives of the document	22
VIII. Guidelines for the reader	23
<b>Chapter 2: the WEST project in a nutshell</b>	<b>25</b>
I. Turning Tore Supra into the WEST configuration	25
II. WEST main parameters	27
III. WEST ITER like divertor and plasma facing components	29
IV. The diagnostics and control system	31
Plasma control system	31
Heat and particle fluxes, SOL physics	31
W sources, radiation, and transport	32
Core and pedestal profiles (Figure 11)	32
Turbulence and MHD	33
V. WEST plasma scenarios outlook	34
<b>Chapter 3: WEST Research Plan</b>	<b>38</b>
<b>W1. Headline 1 – Testing and operating ITER-grade PFC in tokamak</b>	<b>38</b>
<b>W1.1 Pre- and post-characterization of ITER-grade PFCs (phase-1 and phase-2)</b>	<b>41</b>
W1.1.1 PFC pre characterization	41
W1.1.2 Monitoring of PFC exposure conditions	41

## Outline

W1.1.3	PFC post characterization _____	41
<b>W.1.2</b>	<b>Power exhaust balance &amp; controlling the heat flux deposition (phase-1) _____</b>	<b>42</b>
W1.2.1	Steady state heat load pattern including strike point & SOL widths _____	42
W1.2.2	ELM heat load pattern _____	42
W1.2.3	Disruption heat load pattern and impact on PFC _____	42
W1.2.4	Validated power balance _____	43
<b>W.1.3</b>	<b>Towards a reliable wall protection system (phase-1 and phase-2) _____</b>	<b>43</b>
W1.3.1	Validated IR temperatures _____	43
W1.3.2	Reliable PFC surface temperature control _____	44
W1.3.3	Wall Monitoring System for transients _____	44
<b>W.1.4</b>	<b>Metallic Wall conditioning (phase-1 and phase-2) _____</b>	<b>45</b>
W1.4.1	Reliable conditioning of tungsten walls, with control of light impurities _____	45
W1.4.2	Efficient wall conditioning procedures with magnetic fields _____	45
<b>W.1.5</b>	<b>Divertor operation with different configurations in deuterium and helium (mostly phase-1) _____</b>	<b>46</b>
W1.5.1	Lower and upper divertor operation _____	46
W1.5.2	Plasma density control and optimized pumping for steady state operation _____	47
W1.5.3	Helium divertor operation _____	47
W1.5.4	Baffle and divertors plasma response to ELMs _____	48
W1.5.5	Controlled divertor conditions for long pulse H-mode operation _____	48
<b>W.1.6</b>	<b>Power handling of ITER PFCs @10 MW/m<sup>2</sup> (mostly phase-1) _____</b>	<b>49</b>
W1.6.1	Test with ITER nominal steady state heat flux _____	49
W1.6.2	Validation of the ITER gap and shaping requirements _____	51
W1.6.3	Evolution of the power handling capability of ITER PFCs under thermal cycling _____	52
<b>W.1.7</b>	<b>Tungsten melting and damage (end of phase 1) _____</b>	<b>53</b>
W1.7.1	Operation with pre-damaged PFC _____	53
W1.7.2	Melting & operation with misaligned PFC _____	53
<b>W.1.8</b>	<b>Power handling under extreme heat loads (phase-1 and phase-2) _____</b>	<b>54</b>
W1.8.1	Upper energy flux limit of ITER grade PFC _____	54
W1.8.2	Component ageing with 10 <sup>6</sup> ELM cycles _____	55
<b>W.1.9</b>	<b>Tungsten surface modification with helium plasmas (end of phase-1 and phase-2) _____</b>	<b>56</b>
W1.9.1	Structural changes of tungsten PFCs under He operation and impact on subsequent plasma operation _____	57
<b>W.1.10</b>	<b>PFC ageing with long pulse operation (mostly phase-2) _____</b>	<b>57</b>
W1.10.1	Development of long pulse scenarios for PFC ageing campaigns _____	58
W1.10.2	PFC ageing with long pulse deuterium operation _____	58
W1.10.3	PFC ageing with long pulse helium operation _____	58
W1.10.4	PFC ageing with long pulse impurity seeded discharges _____	59
<b>W.1.11</b>	<b>PFC ageing: arcing and dust monitoring (phase-1 and phase-2) _____</b>	<b>59</b>
W1.11.1	Arcing data base _____	60
W1.11.2	Dust data base _____	60
W1.11.3	UFO data base _____	60
<b>W.1.12</b>	<b>Fuel inventory build up in actively cooled tungsten PFCs (phase -2) _____</b>	<b>61</b>
W1.12.1	Fuel retention in actively cooled tungsten PFCs _____	61
W1.12.2	Control of fuel inventory in actively cooled tungsten PFCs _____	61
<b>W.1.13</b>	<b>Testing innovative concepts (end of phase-2) _____</b>	<b>62</b>
W1.13.1	Testing new materials for DEMO _____	62

## Outline

W1.13.2	Testing liquid metal PFCs in WEST	62
<b>W2.</b>	<b>Headline 2 – Towards long pulse H-mode &amp; steady-state operation</b>	<b>64</b>
<b>W.2.1</b>	<b>Controlling plasma start-up and soft landing (phase-1 and phase-2)</b>	<b>65</b>
W2.1.1	Optimizing plasma breakdown and ramp-up	65
W2.1.2	Developing plasma soft landing scenarios	66
<b>W.2.2</b>	<b>Optimizing robust heating scenarios (phase-1)</b>	<b>66</b>
W2.2.1	Edge density for optimum LHCD performance	66
W2.2.2	Edge density for optimum ICRH performance	67
W2.2.3	Interplay of divertor density and radio-frequency heating systems	67
W2.2.4	ICRH absorption and ripple losses	67
W2.2.5	ICRH electron to ion heating ratio dependence on H minority concentration	68
W2.2.6	Lower Hybrid coupling and fast electron ripple losses	68
W2.2.7	Lower Hybrid Current Drive efficiency at high density	69
W2.2.8	Interplay between LHCD and ICRH operation	69
<b>W.2.3</b>	<b>Density and tungsten control in long pulses (phase-1 and 2)</b>	<b>70</b>
W2.3.1	Tungsten erosion and tungsten source pattern	71
W2.3.2	Divertor impurity screening	71
W2.3.3	Tungsten transport in the confined plasma	72
W2.3.4	Tungsten transport during MHD relaxation	72
W2.3.5	Control of tungsten accumulation	72
W2.3.6	Tungsten control for low collisionality pedestal performance	73
<b>W.2.4</b>	<b>Access to long pulse H-mode (phase-1 and phase-2)</b>	<b>74</b>
W2.4.1	H-mode power threshold	74
W2.4.2	Impact of aspect ratio and magnetic ripple	74
W2.4.3	Impact of X-point height, main ion species and effective charge	75
W2.4.4	Long pulse H mode operation	75
<b>W.2.5</b>	<b>Optimizing confinement for long pulse H-mode operation (phase 1 and phase 2)</b>	<b>76</b>
W2.5.1	Particle confinement and pedestal degradation with fuelling	76
W2.5.2	Pedestal height, width and location	77
W2.5.3	Obtaining low collisionality pedestal conditions	77
W2.5.4	ELM properties and their control	77
W2.5.5	ELM resilient matching and improved arc detection	78
W2.5.6	Confinement dependence on the aspect ratio and edge safety factor	78
W2.5.7	Optimizing intrinsic rotation	79
<b>W.2.6</b>	<b>Towards disruption-free campaigns (phase 1 and phase 2)</b>	<b>80</b>
W2.6.1	Disruption and VDE characterization	80
W2.6.2	Disruption and runaway electrons mitigation	80
W2.6.3	Disruption-free long pulse campaigns	80
<b>W.2.7</b>	<b>Current profile control and MHD stability (mostly phase 2)</b>	<b>81</b>
W2.7.1	Assisted plasma breakdown and current ramp-up	81
W2.7.2	Stability of low safety factor operation	81
W2.7.3	Fast ions and electrons interplay with MHD	81
W2.7.4	Operational space without double tearing mode	82
W2.7.5	Statistics for Neoclassical Tearing Modes in long pulse operation	82
<b>W.2.8</b>	<b>Advanced tokamak scenarios (phase 2 mostly)</b>	<b>82</b>



## Outline

W2.8.1	Fully non inductive H-mode discharges	82
W2.8.2	Pellet fuelling in LH heated discharges	83
W2.8.3	High bootstrap discharges	83
W2.8.4	Internal Transport Barrier regimes	84
W2.8.5	Long pulse hybrid scenario	84
<b>W.2.9</b>	<b>Controlled high density and high radiation regimes (phase 2 mostly)</b>	<b>85</b>
W2.9.1	Controlled high radiation regimes	85
W2.9.2	Operation at high Greenwald fraction (>1)	85
<b>W.2.10</b>	<b>Control of slowly evolving burning plasmas (phase 2)</b>	<b>86</b>
W2.10.1	Cyclic scenario	86
W2.10.2	Simulation of alpha heating & Real Time control	86
	<b>Tentative timeline for WEST exploitation</b>	<b>88</b>
	<b>Chapter 4: Conclusions and prospects</b>	<b>93</b>
	<b>Annexes of the WEST research plan</b>	<b>95</b>
	<b>Annex 1: contributions of WEST to the EU fusion roadmap for Horizon 2020</b>	<b>96</b>
	<b>Annex 2: WEST partnerships</b>	<b>101</b>
	<b>Annex 3: The WEST magnetic configurations</b>	<b>102</b>
	<b>Annex 4: The plasma facing components of WEST</b>	<b>105</b>
I.	Testing ITER technology: the lower divertor	105
II.	The coated plasma facing components	107
1.	Start up divertor : W coatings on graphite	108
2.	Upper divertor, baffle, ripple/VDE protections : W coatings on copper	108
3.	Inner bumpers, outer limiter : W coatings on CFC	108
4.	Antenna protections : tungsten or boron coatings on CFC	108
	<b>Annex 5: The heating systems of WEST</b>	<b>110</b>
I.	Ion Cyclotron Resonance Heating (ICRH)	110
II.	Lower Hybrid Current Drive (LHCD)	111
III.	Electron Cyclotron Resonance Heating (ECRH)	113
	<b>Annex 6: The fuelling/pumping systems</b>	<b>115</b>
I.	Fuelling	115
II.	Pumping	117
	<b>Annex 7: overview of WEST diagnostics</b>	<b>119</b>
I.	Overview of the diagnostic set for WEST	119
II.	Detailed description of WEST diagnostics	125
1.	Plasma operation and control	125

## Outline

2.	Core plasma and pedestal profiles	128
3.	Plasma facing components	132
4.	Plasma wall interaction	136
5.	Radiation and impurities	140
6.	Coupling of Heating systems	144
7.	Turbulence and MHD	148
<b>Annex 8: WEST scenario modelling</b>		<b>152</b>
1.	Introduction	152
2.	Expected heat flux on the divertor target	153
3.	High frequency plasma heating	156
4.	Fuelling and pumping capabilities	160
5.	L-H power threshold, pedestal and ELMs	161
6.	Expected density profiles	164
7.	W sources and contamination	166
8.	Integrated standard scenarios	169
9.	Conclusions	172
<b>Annex 9 : theory and modelling</b>		<b>175</b>
I.	The Tungsten cycle	175
1.	Global simplified approaches	175
2.	SOL / Edge physics at prescribed transport coefficients	176
3.	Synthetic diagnostics for interpreting W related data	177
4.	Nonlinear edge transport models	177
II.	Transport and L-H transition	180
III.	Scenario development	181
IV.	Magneto-Hydro-Dynamics issues	182
V.	Disruptions and Runaway electrons	183
<b>Annex 10 : risk assessment for the WEST programme</b>		<b>187</b>
W3.	I – Methodology	187
W4.	II - Main risks identified for the WEST programme	188
<b>Annex 11 : Commissioning and power ramp up</b>		<b>195</b>
I.	Step 1 : Commissioning the WEST platform	195
II.	Step 2 : Power ramp up in L mode	197
III.	Step 3 : Achievement of H mode operation	199
<b>Annex 12 : Summary of the 1<sup>st</sup> WEST international workshop</b>		<b>201</b>
<b>Annex 13 : List of figures</b>		<b>208</b>
<b>Annex 14 : List of tables</b>		<b>214</b>

# Chapter 1: Strategy of the WEST project

---

This chapter gives an overview of the strategy of the WEST project (Tungsten (W) Environment in Steady State Tokamak), implementing an ITER like tungsten actively cooled divertor in the long pulse Tore Supra tokamak.

As background to the project, the challenge of power exhaust in fusion devices is shortly summarized in section I, underlining the importance of the divertor, which has to handle the highest heat and particle loads in the vessel. The R&D needs for the ITER divertor are reviewed in section II. The mission of WEST, targeted at minimizing risks for the ITER divertor and mastering integrated plasma scenario over long pulses, is then presented in section III, as well as the associated high level deliverables in section IV. The schedule and the operation phases foreseen for WEST in order to provide timely answers for ITER are described in section V. WEST will be run as a user facility, open to the international fusion community, as explained in section VI. Finally, the main objectives of this document as well as guidelines for the reader are given in section VII and VIII respectively.

The present version of the document corresponds to the version 1 of the WEST research plan, taking into account the input of the international WEST partners<sup>2</sup>. This a living document, which will evolve with the project and will be discussed with the WEST partners on a regular basis.

## I. Background: the challenge of power exhaust in fusion devices

As has been identified in the European Fusion Roadmap [EUroadmap2012], a reliable solution to the problem of heat exhaust is probably the main challenge towards the realisation of magnetic confinement fusion. This is presently considered as a challenge for ITER, and a potential showstopper for DEMO.

Mastering plasma wall interactions is essential for successfully operating next step fusion devices, as well as for reaching full performance in terms of fusion gain. The wall of fusion devices is composed of plasma facing components, which must provide adequate protection of in-vessel structures, sufficient heat exhaust capability and be compatible with the requirements of plasma purity [Pitts2011]. In next step fusion devices, the plasma facing components will experience extreme heat and particle loads. In particular, thermal transients (ELMs, disruptions) will be generated on a scale unattainable in current devices and require adequate mitigation. In

---

<sup>2</sup> This has been achieved through a dedicated international workshop, organized in summer 2014 (June 30 – July 2<sup>nd</sup> 2014, Aix en Provence, France, see <http://west.cea.fr/Workshop2014/> and annex 12 on the workshop summary for more details). Recommendations from an international panel assessing WEST as a EUROfusion facility were also considered (see “Recommendations from the panel in charge of the evaluation of WEST as a EUROfusion facility”, B. Sharkov et al., EUROfusion General Assembly July 08-09 2014)

## Chapter 1: Strategy of the WEST project

addition, these devices will aim at steady state operation, as is required for a future fusion reactor: they will run much longer plasma discharges than present day facilities<sup>3</sup>. The cumulated particle fluence<sup>4</sup> and energy on the plasma facing components will reach unprecedented levels, with hours of plasma exposure for the components and gigajoules of energy to extract in a single discharge (see [Pitts2011b] for ITER, [Unterberg2012] for DEMO).

In order to address these challenges, an integrated approach, relying on progress in technology, plasma operation and exhaust physics, is required.

Thanks to its superconducting magnets and actively cooled plasma facing components, Tore Supra has been leading the way towards mastering power exhaust over long pulse operation over the past 25 years, developing a unique expertise within the French Institute of Research on Magnetic Fusion (IRFM)<sup>5</sup> to solve the associated technological, operational and physics issues. With the WEST project, this expertise is turned in support of the ITER divertor.

The constraints for the ITER divertor<sup>6</sup>, which handles the highest heat and particle loads in the vessel, are many. They include:

- Extracting high power fluxes in steady state, in the range 10-20 MW/m<sup>2</sup>
- Handling thermal transients, such as ELMs and disruptions
- Ensuring acceptable lifetime of the plasma facing components, by minimizing material erosion by the plasma
- Ensuring particle control, in particular exhaust of the helium ashes from the fusion reaction
- Ensuring acceptable plasma contamination by material eroded from the plasma facing components, in order not to degrade plasma performance

On the technology side, this requires the development of high heat flux components, using active cooling in order to extract the power in steady state. This is a major step forward from inertial components used in most present day short pulse devices. Tore Supra has pioneered the design, manufacturing and operation of several generations of actively cooled components over the past decades [Garin2001], while new superconducting devices are presently taking this step (in particular EAST in China on the tokamak side, and W7X in Germany on the stellarator side). Most present day tokamaks in Europe and US are still equipped with inertial components.

---

<sup>3</sup> Discharges in the range 100-1000 s for ITER, hours/days for DEMO, to be compared with 1-20 s in most present day fusion devices.

<sup>4</sup> Defined as the integrated particle flux. For instance, the deuterium fluence will reach  $1.5 \cdot 10^{27}$  D/m<sup>2</sup> at the ITER strike point within one nominal discharge. This is equivalent to several years of operation for JET [Pitts2011b].

<sup>5</sup> IRFM is part of the Physical Science Division of the French Alternative Energies and Atomic Energy Commission (CEA), a large scale research organization, focused on innovation from research to industry.

<sup>6</sup> For DEMO and fusion reactors, an additional constrain comes from the impact of the 14 MeV fusion neutrons on the materials. While this issue remains moderate for ITER (~1 dpa end of life), this is a major challenge for DEMO (> 10 dpa) and future fusion reactors (~100 dpa).

On the physics side, this requires the development of an integrated exhaust scheme, combining a high radiation fraction to reduce the heat loads carried by charged particles as well as plasma facing component erosion, adequate mitigation of the thermal transients and good plasma core performance. This is being investigated in present day metallic walls tokamaks (see [Neu2013] for AUG, [Matthews2013] for JET). However, the robustness of these scenarios has to be demonstrated on relevant plasma discharge duration, taking into account typical time constants from the different processes involved, from plasma turbulence ( $\sim\mu\text{s}$ ) up to current diffusion ( $\sim\text{s}$ ) and plasma wall equilibrium ( $\sim$  minutes) [Saoutic2002]. The latter plays an important role for particle control issues, which can be a serious limitation preventing long pulse operation, as has been evidenced in several experiments [Tsitrone2007] [Guirlet2003] [Grisolia1999]. This aspect can only be investigated in devices with long pulse capability. Unlike most present day short pulse fusion devices, Tore Supra is able to reach typical ITER pulse length [VanHoutte2004].

Finally, on the operation side, adequate control tools and machine protection systems are needed. In particular, actively cooled components bring specific issues in terms of monitoring [Bucalossi2013]. The limit on the component surface temperature for safe operation does not translate in a limit on the pulse duration, as for inertial components implemented in most present day devices, but rather on whether a given plasma scenario can be achieved or not. The impact in case of component failure is also more severe, with potential water leaks in the vessel resulting in long shutdowns. The wall protection system has therefore to be optimized in order to ensure safe operation of the plasma facing components while not overconstraining the plasma operational window. The Tore Supra team has gained significant operational know how and developed specific control tools in this area [Travere2012].

## II. R&D needs for the ITER divertor

The divertor is a crucial plasma facing component, fulfilling all of the requirements for power exhaust described in the previous section, and allowing access to high plasma confinement regimes (H mode). ITER plans to operate with an actively cooled tungsten divertor<sup>7</sup>, bringing specific challenges [Pitts2013], in particular compared to carbon components widely used in tokamaks over the last decades.

The main challenges associated with using a tungsten actively cooled divertor for ITER are shortly summarized below, from the technology, operation and physics points of view:

- From the technology point of view, although prototypes have been successfully built and tested for ITER, large scale industrial manufacturing of actively cooled tungsten components has never been performed. From past experience of procurement of actively cooled components (Tore Supra and W7X), the step from prototyping to industrial production can result in significant delay.

---

<sup>7</sup> The ITER Council has approved in 2013 the ITER Organisation proposal to start ITER operation with a full tungsten divertor from day 1 [IC 13, 21 November 2013], instead of starting with a mixed carbon tungsten divertor in the non nuclear phase and changing to a full tungsten divertor in the nuclear phase. This makes the R&D related to a full tungsten divertor all the more urgent to complete.

## Chapter 1: Strategy of the WEST project

In addition, the detailed design of the components (in particular regarding the shaping of the tungsten monoblocks to avoid exposing leading edges to the plasma) still needs to be further refined.

- From the operation point of view, these components have been tested in dedicated high heat flux facilities (electron or ion beams) or plasma wall interaction linear devices, but have never been run in a tokamak environment. The evolution of tungsten actively cooled components under combined heat and particle loads in tokamak conditions, as well as the potential impact on plasma performance, needs further investigation, in particular after hours of plasma exposure. Indeed, it has been shown that exposure to a large number of thermal transients or high deuterium and/or helium particle fluence can lower the damage threshold of the component, induce cracks development within the material, degrade its thermal conductivity, eventually leading to enhanced erosion [Loewenhoff2012] [Wirtz2013] [De Temmerman2013]. The interactions of tungsten with helium are of particular interest, as helium will be used in the non nuclear phase of ITER to gain margin for H mode access (helium will also be present in the nuclear phase as ashes from the D-T fusion reaction).

In addition, assessing the impact of major component damage (tungsten component melting and subsequent melt layer motion) on plasma operation is also a high priority issue for ITER.

Finally, efficient monitoring of actively cooled components in a metallic environment has to be demonstrated.

- From the physics point of view, using tungsten plasma facing components restrains the operational window, as the tolerable tungsten concentration in the plasma ( $\ll 10^{-4}$ ) is much lower than for carbon (few %) in order not to degrade plasma performance. This has been documented in AUG and JET, running with metallic walls. In particular, AUG and JET have demonstrated that adequate tungsten control can be achieved, provided central electron heating, high ELM frequency and adjusted fuelling are used. However, the control of tungsten contamination over long discharges (~minutes) has not yet been addressed so far.

Addressing these issues is part of the WEST mission, described in the next section.

### III. The mission of WEST

The WEST project (Tungsten (W) Environment in Steady State Tokamak) is targeted at supporting the ITER divertor strategy, minimizing risks for its procurement and gaining time for its operation. It consists of implementing a divertor configuration and installing an ITER like actively cooled tungsten divertor in the Tore Supra tokamak, taking full benefit of its unique long pulse capability.

It should be noted that Tore Supra is already fully equipped for long pulse operation (superconducting magnets, pressurized water loop for plasma facing component cooling, steady

## Chapter 1: Strategy of the WEST project

state heating and fuelling systems ...). It is therefore the most cost effective facility to tackle the issues mentioned in the previous section.

WEST complements the worldwide ongoing effort on tungsten R&D. Tokamaks such as JET and AUG investigate plasma performance in a metallic environment, but use inertial components and are not equipped to explore long pulse operation<sup>8</sup>. On the other hand, ITER relevant actively cooled tungsten components are being tested in high heat flux facilities and plasma wall interaction linear devices but these cannot address the impact of component aging on tokamak plasma performance. WEST provides an integrated test environment, bringing together the high heat flux technology of the ITER divertor and long pulse tokamak operation<sup>9</sup>.

WEST will also open new possibilities to demonstrate the sustainability of plasma scenarios foreseen for next step fusion devices over relevant plasma wall equilibrium timescale (~minutes). Indeed, extending operation to long pulse brings additional constraints (high current drive efficiency, control of MHD at vanishing loop voltage ...) and can evidence new issues which do not appear on short pulses, in particular in the field of particle control where the interplay with the wall plays a major role. WEST provides an opportunity to anticipate current unknowns on the way to long pulse operation in a metallic environment before they are encountered in ITER, and identify solutions.

The main mission of WEST is summarized as follows :

- Paving the way towards the ITER actively cooled tungsten divertor procurement and operation
- Mastering integrated plasma scenario over relevant plasma wall equilibrium time scale in a metallic environment

The next section describes the high level deliverables expected from WEST.

## IV. WEST high level deliverables

The programme foreseen for WEST, using the unique long pulse capability of Tore Supra in support of the ITER divertor, is in line with the European Fusion Roadmap, where the success of ITER is seen as the highest priority for Horizon 2020<sup>10</sup> [EUroadmap2012]. In particular, WEST addresses Mission 1 on plasma regimes of operation and Mission 2 on heat exhaust systems of the European Fusion Roadmap.

---

<sup>8</sup> plasma duration of a few seconds for AUG, typically < 30 s for JET.

<sup>9</sup> WEST and the superconducting EAST tokamak in China have a complementary programme : both will test an actively cooled tungsten divertor in the coming years, but EAST relies on in house divertor technology and presently has a mixed PFC configuration (carbon on the lower divertor, molybdenum on the first wall, tungsten on the upper divertor).

<sup>10</sup> “constructing ITER within scope, schedule and cost; securing the success of future ITER operation and preparing the ITER generation of scientists, engineers and operators” has been identified as the overarching objective for Horizon 2020 in the European Fusion Roadmap [EUroadmap2012].

## Chapter 1: Strategy of the WEST project

Table 1 summarizes the high levels deliverables expected from WEST, sorted by research areas as defined in the WEST mission.

As far as minimizing risks for the ITER divertor procurement is concerned, WEST will reproduce as closely as possible the manufacturing route foreseen for ITER (same manufacturers, assembling technologies, material grades etc), in close connection with the domestic agencies in charge (F4E for Europe, JADA for Japan). WEST will therefore allow optimizing the manufacturing processes for a large scale industrial production ahead of the ITER divertor procurement. The WEST project involves the procurement of more than 15 000 tungsten monoblocks (roughly 15 % of the ITER divertor needs), which provides significant statistics to assess the component rejection rate. In case it is needed, a repair process could be developed and qualified. WEST will also validate the component qualification procedure and the acceptance criteria foreseen for the ITER divertor. Finally, WEST will allow assessing the manufacturing and assembly tolerances, on which stringent requirements are put for ITER.

Concerning the ITER divertor operation, WEST will provide relevant steady state heat fluxes (in the range 10-20 MW/m<sup>2</sup>) to test the power handling capabilities of the tungsten components under tokamak conditions. Concerning thermal transients, the ELMs foreseen for WEST are of course benign compared to larger machines, but the long pulse capability of Tore Supra will allow cumulating a large number of sub damage threshold ELMs and assessing the impact on component damage development. WEST will also provide high particle fluence (both helium and deuterium operation are foreseen) on the plasma facing components, and will allow an accelerated lifetime test of the ITER like divertor elements under combined heat and particle loads in tokamak conditions. It is also planned to run dedicated experiments to expose pre damaged components or perform in situ tungsten melting experiments, in close connection with the ITER R&D needs. Finally, WEST will develop operational know how for actively cooled plasma facing component monitoring in a metallic environment, and the associated control tools (wall protection system).

Concerning long pulse operation for next step devices, WEST will contribute to developing integrated long pulse H mode scenario in a metallic environment, which requires optimization of the power coupling from the Radio Frequency (RF) heating systems, control of the tungsten plasma contamination as well as of the plasma density, while maintaining good plasma performance. In addition, WEST will allow progressing in the understanding of the underlying physics, as it exhibits specific features besides its long pulse capability (large aspect ratio, dominant electron heating, compact divertor geometry). Finally, WEST will allow investigating advanced scenario issues for next step fusion devices, in particular in support of the JT-60SA programme (high performance/high bootstrap discharges) or on a wider perspective for DEMO (high radiation/high Greenwald fraction discharges). Fully non inductive H mode operation will also be explored in preparation of future steady state operation, relying on the IRFM expertise in this area.

The corresponding high levels deliverables are listed in the table below, and further detailed in this document (see chapter 3 to chapter 6 describing the content of the WEST research plan).



Research area	High level WEST deliverables
Paving the way towards ITER divertor procurement and operation	Optimization of industrial scale production processes ahead of ITER divertor procurement
	Evaluation of manufacturing / assembly divertor tolerances
	Assessment of power handling capabilities of ITER high heat flux tungsten divertor components in tokamak environment
	Impact of high particle fluence plasma wall interactions on ITER tungsten divertor component lifetime, including helium and deuterium operation
	Assessment of plasma operation on damaged/melted tungsten components
	Validated scheme for actively cooled metallic PFC protection and monitoring
Mastering integrated plasma scenario over relevant plasma wall equilibrium time scale in a metallic environment	Optimization of RF heating in long pulse H mode / metallic environment
	Demonstration of control of tungsten contamination over long pulse H mode
	Demonstration of density control over long pulse H mode
	Demonstration of fully non inductive H mode operation
	Investigation of advanced scenario regimes (highly radiating scenario for DEMO, high bootstrap discharges for JT-60SA)

Table 1 : overview of the high level deliverables expected from WEST

WEST will also generate a strong accompanying theory and modelling programme (see annex 9 for more details), contributing to the deliverables listed above. For instance, the development of specific plasma edge modelling tools, such as SOLEDGE2D (using plasma grids to the walls, and realistic PFC geometry [Bufferand2013]), contributes to improving the predictive capability in this area, in particular for power exhaust issues. WEST plasma scenarios will be prepared using integrated modelling tools, which will be continuously improved (impact of tungsten or core-edge coupling in the CRONOS code [Artaud2010]). Efforts are also planned on first principle theory, from plasma edge turbulence (development of the Tokam3X code [Tamain2013]) to transport gyrokinetic codes (introducing impurities in the gyrokinetic code GYSELA [Grandgirad2006] to address W transport issues) or non linear MHD codes (ELMs and disruption physics with the JOREK code [Huysmans2007], core instabilities with the XTOR code [Lütjens2010]).

Finally, WEST will contribute to training the ITER generation. WEST will be open to the international fusion community (see section VI for details) and will train teams of engineers, physicists and operators in manufacturing and operating an actively cooled tungsten divertor, as well as other long pulse specific systems (superconducting coils, steady state heating and fuelling systems etc) in advance of ITER.

The next section describes the time schedule foreseen for WEST.

## V. The WEST schedule: providing answers in time for ITER

The main driver of the WEST planning is to provide timely answers for ITER : the schedule of WEST is therefore aligned with the planning of the ITER divertor procurement and operation (see Figure 1 for illustration). The most constraining part is given by the ITER divertor procurement, initially planned to start in 2016<sup>11</sup>, while ITER divertor operation is foreseen in 2023, leaving ample time to investigate long pulse related issues.

The WEST platform is scheduled to be operational in 2016. WEST operation is planned to be phased, to make the best use of the WEST ITER like divertor elements (and in a later stage of advanced PFC concepts) as they become available.

In phase 1 (2016-mid 2017), it is planned to operate the WEST divertor with a mix of actively cooled ITER like tungsten elements and inertial tungsten coated start up elements. In this phase, full power will be available, but plasma operation will be limited in time by the inertial divertor elements (typically ~10 s at high power).

In phase 2 (2018-early 2020's), the full actively cooled ITER like tungsten divertor will be available. This will therefore allow long pulse operation, up to 1000s.

The Table 2 summarizes the main features of the 2 operation phases foreseen for WEST.

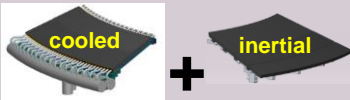
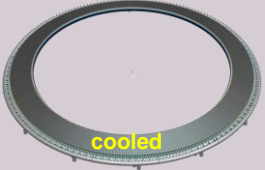
	Phase 1 (2016-2017)	Phase 2 (2018-early 2020's)
WEST ITER like divertor	Mix of actively cooled ITER like and inertial start up elements 	Full actively cooled ITER like divertor 
Heating power	Full power	Full power
Plasma duration	~10 s	Up to 1000 s

Table 2 : comparison of the main features of the 2 operation phases foreseen for WEST.

As schematically illustrated in Figure 1, the contributions of WEST for minimizing the risks for the ITER divertor and mastering integrated scenario over relevant plasma wall equilibrium time constant are foreseen in 3 steps :

- WEST divertor production : optimization of the industrial large scale production
- WEST operation phase 1 : power handling capabilities of the ITER like divertor
- WEST operation phase 2 : high fluence plasma divertor exposure / demonstration of integrated long pulse H mode / investigation of advanced regimes

<sup>11</sup> The dates given in this section are subject to revision, as the planning of the ITER divertor is being reviewed and might shift to a later time (a 2 years shift could be contemplated). In any case, the schedule of the WEST ITER like elements procurement will be adapted to match the planning of ITER divertor procurement and operation and provide timely answers.

## Chapter 1: Strategy of the WEST project

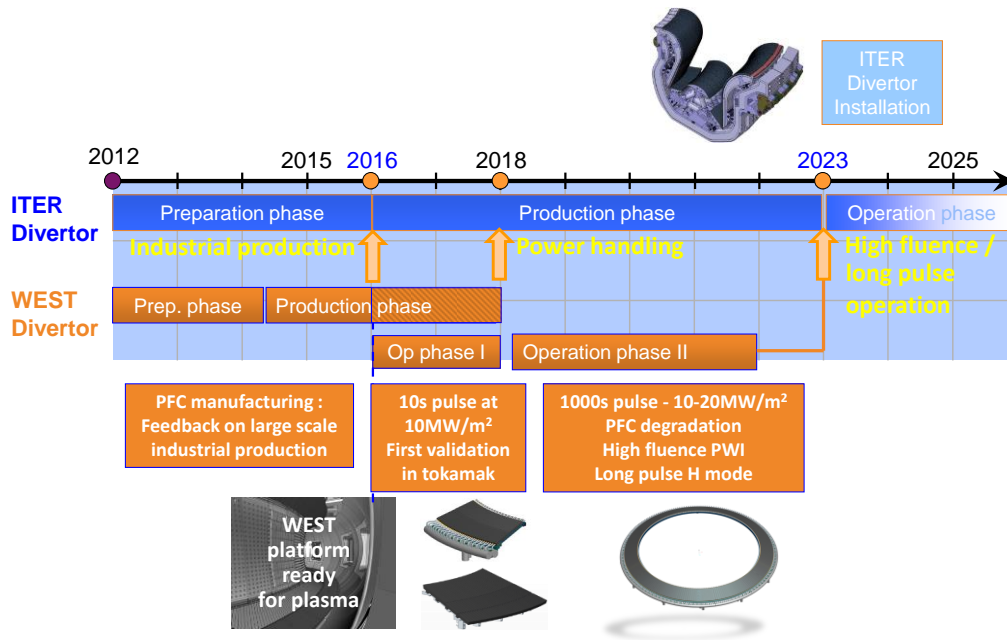


Figure 1 : comparison of the ITER and WEST divertor procurement and operation phases. The timing foreseen for the main inputs of WEST to ITER is also indicated. (NB : the dates shown here are subject to revision, see <sup>11</sup>)

As shown in Figure 1, the ITER divertor procurement is presently in the preparation phase, and should enter the production phase in 2016<sup>11</sup>. The start of plasma operation with the ITER divertor is presently planned in 2023.

The WEST divertor has entered its production phase in 2014. This allows providing a first feedback on the optimization of the manufacturing processes at the industrial scale in time for the ITER divertor production phase.

Phase 1 will be mainly focused on testing the power handling capabilities of the ITER like divertor. For this purpose, the plasma duration foreseen (~10 s) is well adapted, as it is larger than the thermal equilibrium constant of the monoblock (~5 s). This phase will also give a first feedback from divertor plasma operation, which could still provide input for the detailed ITER design (monoblock shaping for instance) at this stage. Preparation work for long pulse H mode operation will also take place.

At the beginning of phase 2 (2018-2020), the main focus will be on exploring high fluence plasma wall interactions, providing an accelerated lifetime test of the ITER like divertor significantly in advance of ITER operation. Power handling studies under extreme conditions (after long term plasma exposure, large number of ELM cycles, high steady state heat fluxes ...) will complete the results obtained during phase 1. Integrated long pulse H mode operation will be a prerequisite for this purpose, and will be thoroughly investigated (RF heating, control of tungsten contamination ...). Work on advanced scenarios will be started, in support of the JT-60SA programme.

## Chapter 1: Strategy of the WEST project

The end of phase 2 (early 2020's typically) could be devoted to exploring innovative divertor concepts, that could be used for ITER second divertor and/or DEMO. The programme of this phase is however very preliminary at this stage.

The next section describes the collaborative framework in which the WEST platform is expected to be exploited with the ITER partners.

### VI. WEST: a user facility open to the international fusion community

The WEST project and its research plan are open to the international fusion community. The WEST platform will be available for plasma operation from 2016 and will be run as a user facility. It will be open to the EUROfusion Consortium and all ITER partners. The French Institute of Research on Magnetic Fusion (IRFM), running Tore Supra, is committed to provide easy and efficient access to WEST to interested fusion laboratories.

A collaboration network is being built around WEST, as illustrated in Figure 2.

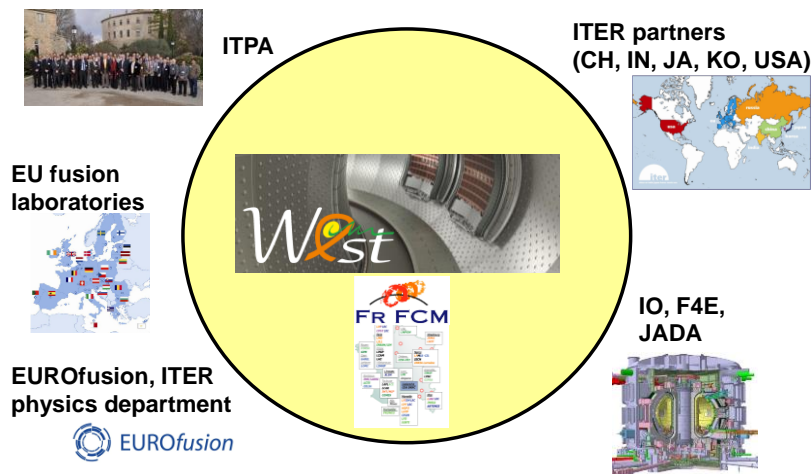


Figure 2 : building the WEST network

Major fusion partners have already demonstrated their interest for WEST and participate to the construction phase. Partnership agreements have been signed with China, India, Japan, Korea, USA and European laboratories, as well as with the European Domestic Agency F4E. Further contacts with other potentially interested laboratories or institutions in and outside Europe are planned

The project has been initiated based on a joint analysis of tungsten divertor R&D needs with the ITER Organization, and follows a dedicated recommendation of the ITER council towards ITER partners to support the ITER divertor procurement and commissioning. In addition to the ITER Organization, a strong connection is being developed with the Domestic Agencies in charge of procuring the ITER divertor targets (F4E for Europe and JADA for Japan), as well as with the ITER partners.

The ITPA topical groups (International Tokamak Physics Activities), targeted at high priority R&D issues for ITER, have examined in 2013 the impact of running ITER with a full tungsten divertor from day 1 and underlined inter alia the importance of gaining operational experience with EAST and WEST.

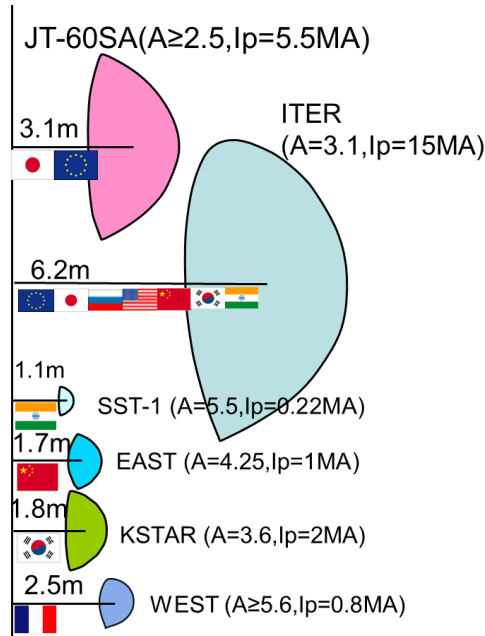


Figure 3 : the worldwide family of superconducting long pulse tokamaks (in operation or under construction). WEST is presently the only superconducting tokamak located in Europe [courtesy Y. Kamada]

The programme of WEST is developing strong links with the long pulse tokamaks operating or under construction in Asia (EAST, KSTAR, SST-1, JT-60SA). It should be noted that Tore Supra is presently the only long pulse tokamak located in Europe (see Figure 3). In particular, both EAST and WEST will explore operation with actively cooled tungsten components in the coming years. The capabilities of WEST to develop advanced scenario in support of the JT-60SA programme will be fully exploited, in the framework of the Broader Approach between Europe and Japan. Within Europe, collaboration on common issues related to long pulse operation is also being established with the stellarator W7X.

At the European level, WEST is part of the EUROfusion facilities<sup>12</sup> and complements the substantial effort on tungsten related issues ongoing both in tokamaks (AUG, JET) and Plasma Wall Interaction devices (Magnum PSI, Judith, Gladis, PISCES ...), by providing an integrated test environment for the ITER divertor operation. Collaborations are in particular foreseen with the EU fusion laboratories interested in Mission 2 on heat exhaust systems (cf. EU fusion roadmap).

Finally, at the national level, WEST is supported by the French Federation of Research on Magnetic Confinement Fusion (FR-FCM), gathering the efforts of French research institutions in the field of fusion. Experts from the FR-FCM have been involved, in particular in the field of diagnostics, from the early phase of the project.

More information on WEST partnerships can be found in annex 2.

<sup>12</sup> Following the decision of the EUROfusion General Assembly (23-24 September 2014), based on recommendations made by an international panel in charge of evaluating WEST as a EUROfusion facility.

## VII. Main objectives of the document

The main objective of this document is to define the research plan associated with the WEST project to fulfill the mission described in section 3. In particular, the WEST research plan should allow to:

- provide answers in due time for ITER to issues related to manufacturing and operating an actively cooled tungsten divertor
- fully exploit the capabilities of WEST to prepare long pulse operation over relevant plasma wall equilibrium time constant

This document is also meant to ensure an efficient operation and a timely implementation of the experimental programme over the period foreseen for WEST exploitation (2016-early 2020's).

The West Research Plan is structured around 2 topical headlines, detailed in the document:

- Headline 1 : Operating and testing ITER grade Plasma Facing Components in tokamaks
- Headline 2 : Towards long pulse H mode and steady state operation

Headline 1 addresses the issues related to preparing actively cooled tungsten divertor operation for ITER, assessing PFC power handling and ageing in tokamak conditions, in particular under high fluence plasma wall interactions. Headline 2 addresses the issues related to mastering long pulse operation, for H mode regimes as well as for advanced tokamak modes, in particular in support of JT-60SA.

These headlines should be not be seen as isolated, but rather as complementary parts of a consistent programme. For instance, progress in H mode operation under Headline 2, dealing with control of W contamination or coupling of the RF systems, is essential to prepare plasma scenarios for Headline 1, aiming at high power fluxes on the divertor, or optimizing the particle fluence on the divertor within a reasonable operational time.

An important output of this document is the logical order of the programme blocks and the necessary prerequisites for them, both in terms of auxiliary hardware or diagnostics availability and output from previous steps in the plan. Durations for the programme to address each of the headlines have been assigned, but are necessarily uncertain at this stage, particularly as the plan progresses. They are not detailed yet in this document.

The WEST research plan is built assuming that the project delivers the WEST platform according to schedule and scope. All the WEST sub-systems are therefore assumed to run at nominal performance. A risk analysis on the WEST programme is carried out in annex 10.

The present version of the document corresponds to the first update of the WEST Research Plan, taking into account the input of the international WEST partners to revise the initial draft. This was performed through a dedicated workshop devoted to WEST scientific programme, organized in summer 2014 (see annex 12 for the summary of the workshop). It is planned to continue discussing the scientific programme with WEST partners on a regular basis through a series of such workshops. This will be done in close connection with the general process

## Chapter 1: Strategy of the WEST project

foreseen for operating the European tokamaks through the EUROfusion consortium. The Research Plan is also discussed at the annual WEST Governing Board meeting, where all members participating to the project are represented. The next update of the Research Plan is proposed at the end of the first phase of WEST exploitation.

The research plan will also be enriched as results from current R&D and, later, from the experimental exploitation of WEST, become available. It is thus to be viewed as a living document that evolves with the project. In addition, it serves as a baseline from which the consequences of design, planning changes or unforeseen events can be determined.

## VIII. Guidelines for the reader

After an overview of the WEST strategy in Chapter 1, Chapter 2 shortly describes the main features of WEST. For more details on the WEST configuration and sub-systems capabilities, the reader is referred to the technical annexes of the document (magnetic configuration in annex 3, plasma facing components in annex 4, heating systems in annex 5, fuelling/pumping systems in annex 6, diagnostics and plasma control systems in annex 7). These annexes are in particular useful for the reader not familiar with the Tore Supra environment.

Chapter 2 also gives a short overview of the plasma scenario designed to reach the objectives of the WEST programme. More details on integrated scenario modelling for WEST can be found in annex 8, while annex 9 presents the theory and modelling effort associated with the WEST programme.

The reader interested by the WEST Research Plan should proceed directly to Chapter 3, which describes the 2 headlines foreseen for WEST (the description of the phase planned for the restart of Tore Supra in the WEST configuration can be found in Annex 11). The content of the Research Plan has been updated from the initial version 0 draft to take into account the input from the international WEST partners (see list of main changes below). For each headline, deliverables and major milestones are identified. A synthetic table is given at the end of Chapter 3 to provide a tentative timeline for the WEST exploitation phase.

Chapter 4 summarizes the document and describes longer term prospects, while Annex 10 presents the risk assessment performed for the WEST programme.

Finally, Annex 12 gives the summary of the first WEST international workshop.

References are listed at the end of each chapter of the document. A list of figures and a list of tables of the document can be found in Annex 13 and 14 respectively.

### **WEST Research Plan : main changes from version 0 to version 1**

The main changes from version 0 to version 1 of the Research Plan are listed below :

- The Research Plan has been structured into a reduced number of research areas : 2 headlines instead of 4, corresponding to the 2 missions of WEST, with Headline 1

## Chapter 1: Strategy of the WEST project

“Operating and testing ITER grade Plasma Facing Components in tokamaks”<sup>13</sup> and Headline 2 “Towards long pulse H mode and steady state operation”<sup>14</sup>. The description of the Research Plan is now gathered in a single chapter (with Chapter 3 replacing Chapters 3 to 6 of the previous version).

- A list of deliverables has been added for each sub topic within the headlines. Major milestones have been identified, in particular for the first phase of WEST exploitation.
- Recommendations from the 1<sup>st</sup> WEST international workshop have been taken into account. This includes for instance :
  - as far as the experimental timeline is concerned : the proposal for a short pulse helium campaign at the end of the first phase of WEST exploitation in addition to the long pulse helium campaign initially foreseen in phase-2. This was motivated by the high priority of this topic for ITER, and by the fact that the tungsten surface modification by helium appears at a modest helium fluence.
  - as far as the scientific content is concerned : more emphasis on selected topics, such as the ELM pattern characterization, since the WEST divertor is well adapted for these studies, or investigation of operation at low edge safety factors.
  - as far as diagnostics are concerned : an additional high resolution infrared camera is now planned to better handle detailed heat load patterns, as required for assessing leading edges power handling or monitoring tungsten melting experiments.
- An annex (annex 12) has been added to present the main outcome of the workshop.

Additional changes include technical updates in Chapter 2 and annexes, or the revision of the section dealing with partnerships, as WEST is now a EUROfusion facility.

---

<sup>13</sup> This corresponds to the previous Headline 1 “Testing ITER tungsten Plasma Facing Components” and Headline 3 “Exploring high fluence Plasma Wall Interactions” of the Research Plan – version 0

<sup>14</sup> This corresponds to the previous Headline 2 “Towards long pulse H mode operation” and Headline 4 “Preparing advanced tokamak modes” of the Research Plan – version 0



# Chapter 2: the WEST project in a nutshell

The WEST project builds on the assets of Tore Supra (superconducting toroidal field coils, active cooling loop for the plasma facing components, steady state heating/fuelling systems etc) to address the strategic lines described in Chapter 1.

This chapter gives an overview of the WEST project. Section 1 describes how Tore Supra is turned into the WEST configuration. The main parameters of WEST are presented in section 2. The WEST ITER like divertor as well as the plasma facing components are described in section 3, while the diagnostics and control systems are shortly summarized in section 4. The plasma scenarios foreseen are presented in section 5.

More detailed technical information can be found in [Bucalossi2011] and [Grosman2013], as well as in the technical annexes of this document. See annex 3 for the magnetic configuration, annex 4 for plasma facing components, annex 5 for the heating systems, annex 6 for the fuelling/pumping systems, and annex 7 for the diagnostics and plasma control systems. In addition, annex 8 describes the status of WEST scenarios integrated modelling.

## I. Turning Tore Supra into the WEST configuration

In order to go from the previous CIEL configuration of Tore Supra to WEST, the main change is two-fold, as schematically illustrated in Figure 4:

- For the magnetic configuration: going from a circular limiter plasma to an elongated D shaped divertor plasma
- For the Plasma Facing Components (PFCs): going from a carbon actively cooled environment to a tungsten actively cooled environment

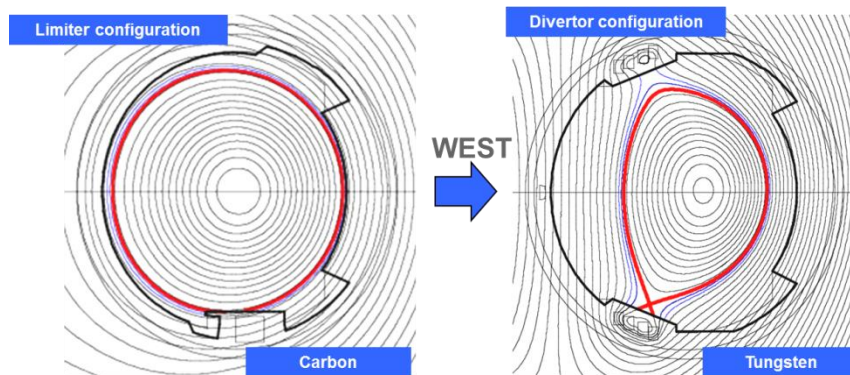


Figure 4: going from the CIEL (left) to the WEST (right) configuration of Tore Supra

## Chapter 2: the WEST project in a nutshell

To obtain the new magnetic configuration, divertor coils (copper coils) are inserted inside the vacuum vessel at the top and the bottom. Stabilizing plates are added to improve vertical instability control.

For the PFCs, a new actively cooled metallic environment is being developed. The ITER like tungsten divertor will be installed in the lower part of the vessel, while most of the other PFCs will be tungsten coated elements. A pumping baffle is added to optimize particle exhaust.

Concerning the heating systems, major changes are foreseen for the Ion Cyclotron Resonant Heating (ICRH) system, where three new antennas are provided to ensure ELM resilience and long pulse operation. The Lower Hybrid (LH) system already has long pulse operation capability but the launchers have been slightly adapted to fit the curvature of the WEST plasmas. The Electron Cyclotron Resonant Heating (ECRH) system remains unchanged.

Concerning the diagnostic systems, new or strongly modified diagnostics are being implemented to fulfill the WEST programme requirements. In particular, the extensive infrared (IR) system already used for CIEL is being significantly renewed to be adapted to the WEST configuration. WEST also includes new PFC and plasma edge diagnostics (tungsten spectroscopy, Langmuir probes, thermocouples, Helium jet, etc.) as well as new plasma core diagnostics (such as the 2D X spectrometer). The Plasma Control System (PCS), as well as the Wall Monitoring System (WMS) or the Data Handling system, are also updated.

Finally, auxiliary subsystems (power supplies, cooling loops, fuelling, conditioning and pumping) are also modified to adapt to the new configuration.

A view of the Tore Supra chamber in the CIEL and WEST configuration is shown in Figure 5.

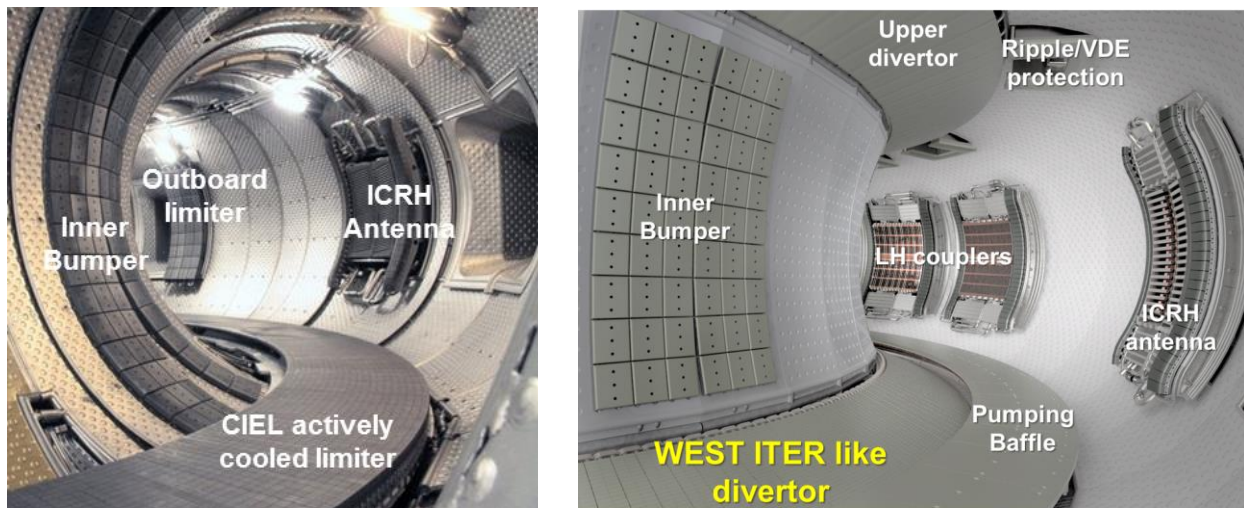


Figure 5: Internal view of Tore Supra in the previous CIEL configuration (left) and the foreseen WEST configuration (right)

## II. WEST main parameters

Table 3 summarizes the main parameters of the new WEST configuration of Tore Supra, which are discussed below.

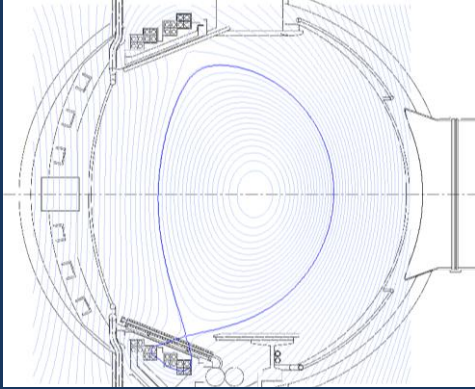
	Main WEST parameters	
	Plasma current	1 MA ( $q_{95} \sim 2.5$ )
	Toroidal field	3.65 T @ R=2.5m
	Major radius	2.5 m
	Minor radius	0.5 m
	Aspect ratio	~ 5-6
	Elongation	1.3 - 1.8
	Triangularity	0.5 - 0.6
	Plasma volume	15 m <sup>3</sup>
	Greenwald density (at 1 MA)	$1.5 \cdot 10^{20} \text{ m}^{-3}$
	Maximum heating power :	
	ICRH	9 MW
	LHCD	7 MW
	ECRH	0.7 MW
Flat-top duration	up to 1000 s	

Table 3: Main parameters of WEST

The plasma current can reach up to 1 MA. Routine operation is foreseen in the range 0.5-0.8 MA. At higher plasma currents, the flat-top duration will be limited due to divertor coils limits (~20s at 1 MA), while discharges up to 1000 s are foreseen in the range 0.5-0.8 MA (see annex 3 for details).

The toroidal field is unchanged compared to the previous Tore Supra configuration and reaches 3.65 T @ R = 2.5m (corresponding to 490 MJ of magnetic energy). It should be noted that, due to the finite number of toroidal field coils (18 coils), the ripple reaches 2.3 % @ R= 2.93 m (typical outboard midplane boundary).

WEST allows flexible magnetic configurations to be performed, from lower/upper single null to double null. Two typical configurations will be used to test the ITER tungsten divertor: the far (from the divertor target) X-point and the close X-point configurations, as illustrated in Figure 6. The X point height allows fine tuning of the heat fluxes on the divertor, by changing the magnetic flux expansion (see Figure 14 in chapter 3 for an illustration of the heat load pattern variation with the X point height). Figure 6 also shows the position of the inner wall on the high field side, and typical position of the heating antennas on the low field side, as well as the upper and lower stabilizing plates and the pumping baffle. The WEST plasmas are highly shaped (typical elongation 1.5, triangularity 0.5). The highest elongation achievable ( $\delta=1.75$ ) can reach values typical for the ITER plasmas (see annex 3 for more details on the magnetic configurations achievable).

## Chapter 2: the WEST project in a nutshell

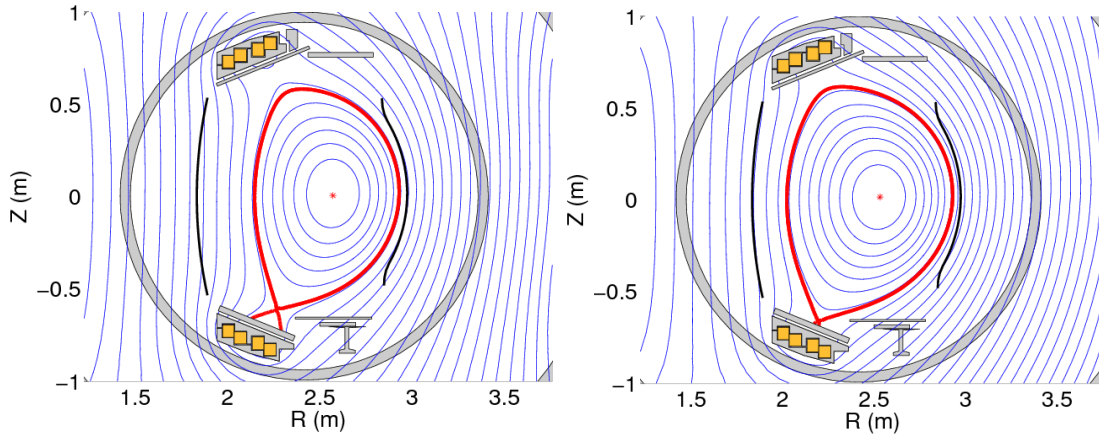


Figure 6: Typical magnetic configurations foreseen for WEST: the far X-point (left) and close X-point (right) configurations

WEST has a large aspect ratio ( $A \sim 5$  for  $R=2.5$  m and  $a = 0.5$  m), allowing a good complementarity with the other EU tokamaks (see Figure 7).

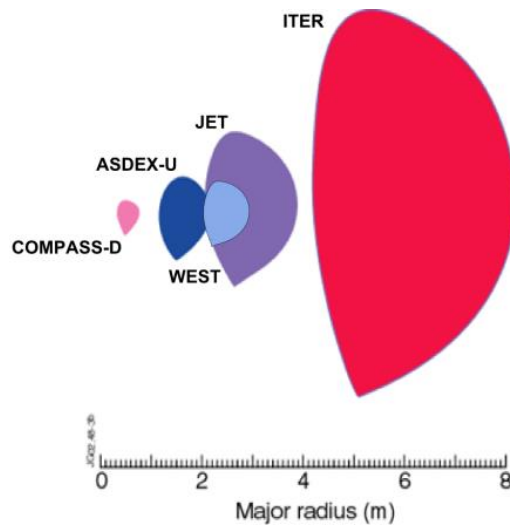


Figure 7: WEST plasma size compared to ITER and the other EU tokamaks

Plasma volume is in the range  $10\text{-}15$  m<sup>3</sup>. Maximal thermal energy content of the order of 1MJ is expected (see annex 8 on integrated modelling of WEST plasma scenarios).

The Greenwald limit at 1 MA is around  $1.5 \cdot 10^{20}$  m<sup>-3</sup> (central line averaged density), which should allow operating through a large range of density. Typical volume line averaged densities are expected to range between  $5$  to  $9 \cdot 10^{19}$  m<sup>-3</sup> depending on the plasma scenario (see scenario description in annex 8).

Tore Supra is equipped with 3 high-frequency (HF) heating systems, delivering a maximum total additional power of 15 MW: a Lower Hybrid (LH) current drive system, an Ion Cyclotron Resonant Heating (ICRH) system and an Electron Cyclotron Resonant Heating (ECRH) system. It should be noted that while the LH system is fully steady state (7 MW – 1000s), the ICRH system is steady-state up to 3 MW and has limitation in time above (typically 9MW 30s / 6MW

## Chapter 2: the WEST project in a nutshell

60s). The ECRH system can provide 0.7 MW-5s. More technical details on the heating systems are given in annex 5.

WEST counts on Tore Supra versatile fuelling system (gas injection, supersonic molecular beam injection, pellet injection) able to provide steady state particle injection. New gas introduction modules will be implemented to fuel the divertor. Gas injection is also foreseen in the vicinity of heating systems. The pumping system is almost unchanged compared to the previous CIEL configuration (turbo molecular pumping) but could be upgraded (cryopumps) if deemed necessary from the first phase of WEST operation. More technical details on the fuelling/pumping systems are given in annex 6.

The water cooling loop will be set at 70°C during operation, to match ITER conditions. For conditioning purposes, the baking temperature of the vessel can go up to 200°C. The glow discharge system, as well as a boronisation system (based on diborane injection) will rely on 6 fixed electrodes. Ion Cyclotron Wall Conditioning (ICWC) can also be performed.

The duty cycle of WEST is expected to be the following: a high power / 30s long discharge or a medium power / 60s long discharge every 30 minutes, a 1000s long discharge every hour.

### III. WEST ITER like divertor and plasma facing components

WEST will provide a fully metallic actively cooled environment, as is illustrated in Figure 8.

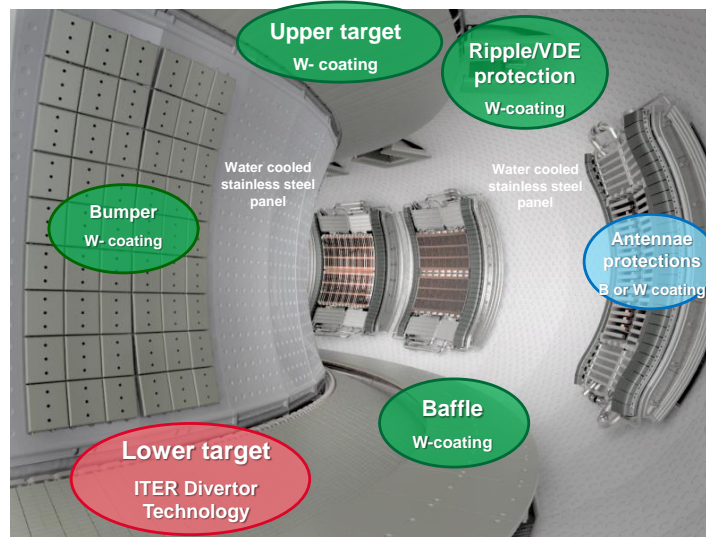


Figure 8 : overview of the WEST plasma facing components

The lower divertor of WEST will reproduce the high heat flux flat part of the ITER divertor targets. It corresponds to a scale 1 reproduction of the strike point area of the ITER divertor targets, as is illustrated in Figure 9. It is based on the ITER technology: massive tungsten monoblocks joined to a copper heat sink with water cooling, and assembled in a Plasma Facing Unit (PFU).

## Chapter 2: the WEST project in a nutshell

Table 4 gives a comparison of the main characteristics of the ITER and WEST divertors. WEST will provide significant statistics to optimize the ITER divertor manufacturing processes at a large industrial scale: more than 15 000 tungsten monoblocks are required for the WEST divertor, which corresponds to 14% of the ITER divertor inner vertical target. The operational conditions will be similar in terms of thermal hydraulics (inlet water at 70°C and  $v = 10$  m/s).

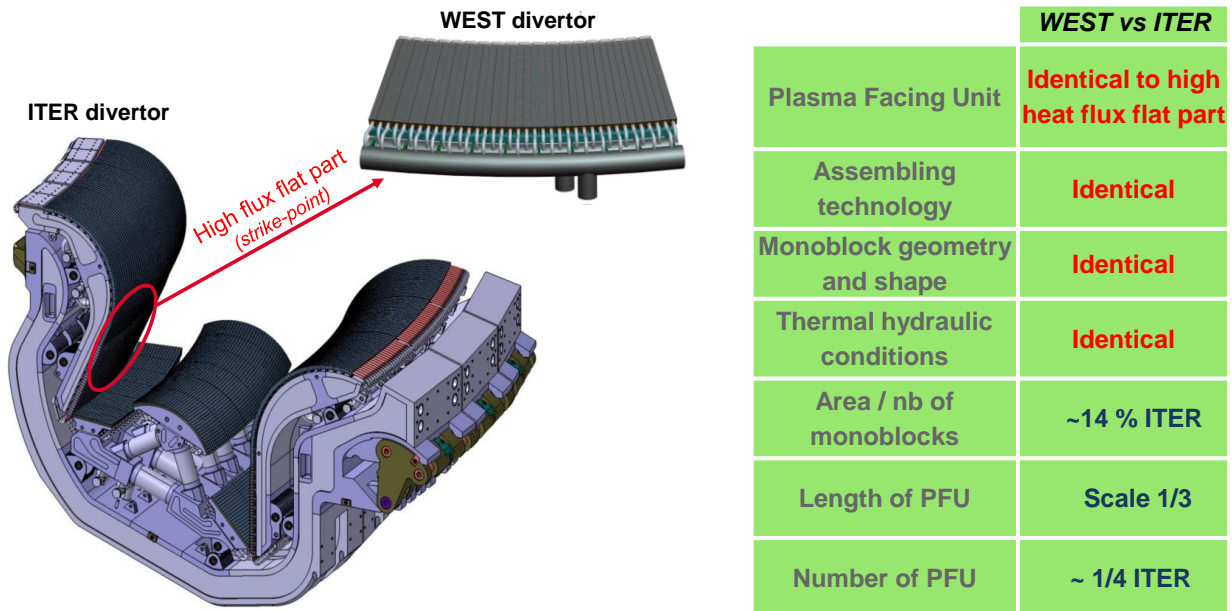


Figure 9 : comparison of the ITER and WEST divertor. WEST reproduces at scale 1 the flat high heat flux part of the ITER divertor.

Table 4 : comparison of the main characteristics of the ITER and WEST divertor

The WEST lower divertor consists of 12 independent toroidal sectors of 30°. This modular design allows for testing variants (e.g. detailed design shaping, tungsten grades...) or running dedicated experiments (e.g. deliberately damaged or misaligned components ...), as well as for post mortem analysis of the components or for refurbishment if needed. These sectors can be dismantled in a relatively short time: typically 1 month shutdown from plasma to plasma for the replacement of one sector by a new one, 2 months if the sector needs to be refurbished before going back inside the vacuum vessel.

As is shown in Figure 8, the remaining plasma facing components will use tungsten coatings. Note that the heating systems antennas protections could use tungsten or boron coatings to avoid excessive tungsten plasma contamination.

The upper divertor consists of actively cooled tungsten coated copper elements, allowing for steady state operation, although at lower performance compared to the ITER like elements (typically up to 8 MW/m<sup>2</sup>). In phase 1 of WEST exploitation, the lower divertor includes inertial start up elements (tungsten coating on graphite) to complement the available actively cooled ITER like divertor elements. They are the only non actively cooled components of the WEST configuration, which will be temporarily installed during phase 1 as start up components while waiting for the complete ITER like divertor assembly. They are designed to allow testing the neighboring ITER like elements under relevant heat fluxes, but over limited duration, as they are

inertially cooled. It should be noted that lower and upper divertor elements are designed to be compatible, so that they can be swapped, providing flexibility for the experimental program.

The remaining vessel will be protected by water cooled stainless steel panels. More details on the WEST plasma facing components can be found in annex 4.

## **IV. The diagnostics and control system**

WEST is equipped with more than 40 diagnostics, as well as with a sophisticated real time control system. A brief overview of key diagnostics connected with the WEST research areas is given here (in the field of plasma control, SOL physics, W sources and transport characterization, core and pedestal physics and turbulence). A more comprehensive description of all diagnostics can be found in annex 7.

It should be noted that the WEST diagnostic set is expected to evolve (with diagnostics adapted to phase 1 and phase 2 of WEST operation for instance, see the diagnostic overview Table 10 in annex 7).

### **Plasma control system**

The real time control system of Tore Supra is being thoroughly updated to address advanced tokamak control needs. It will contribute to preparing the ITER plasma control system. It features a time segmented approach to define the plasma discharge, as well as a real time event detection to deal with unexpected phenomena which may occur during the discharge. A wall monitoring system (WMS), using a multi diagnostics approach (infrared, spectroscopy, etc.), is being developed for ensuring real time PFC protection, addressing the challenge of surface temperature measurement in a metallic environment.

### **Heat and particle fluxes, SOL physics**

Measuring surface temperature and corresponding heat fluxes is at the core of the WEST programme for testing the ITER like divertor tungsten components. Seven upper ports are equipped with an IR endoscope, allowing a full coverage of the lower ITER like divertor and the plasma heating antennas. The measurements are connected to the Wall Monitoring System for real time PFC protection. Two high resolution IR cameras viewing the lower divertor are also implemented for dedicated physics studies. A set of thermocouples embedded in various PFCs allows measuring their bulk temperature (100-1300°C) and thus calibrating the IR measurements independently of the W PFC emissivity evolution. A sophisticated calorimetry system yields a detailed power and energy balance reconstruction on PFCs. More than sixty flush mounted Langmuir probes complement the IR measurements on the upper and lower divertors, the inboard limiter and the baffle. Two reciprocating probes are equipped with exchangeable probe heads for measurements of e.g. electron density, electron and ion temperature, Mach number etc, allowing for detailed SOL physics studies in complement with other diagnostics (edge reflectometer, He jet beam ...). The movable outboard limiter is also housing two “pecker” probes. In addition, a remote handling system (Articulated Inspection Arm)

## Chapter 2: the WEST project in a nutshell

is available to monitor the plasma facing components without breaking vacuum or impacting conditioning.

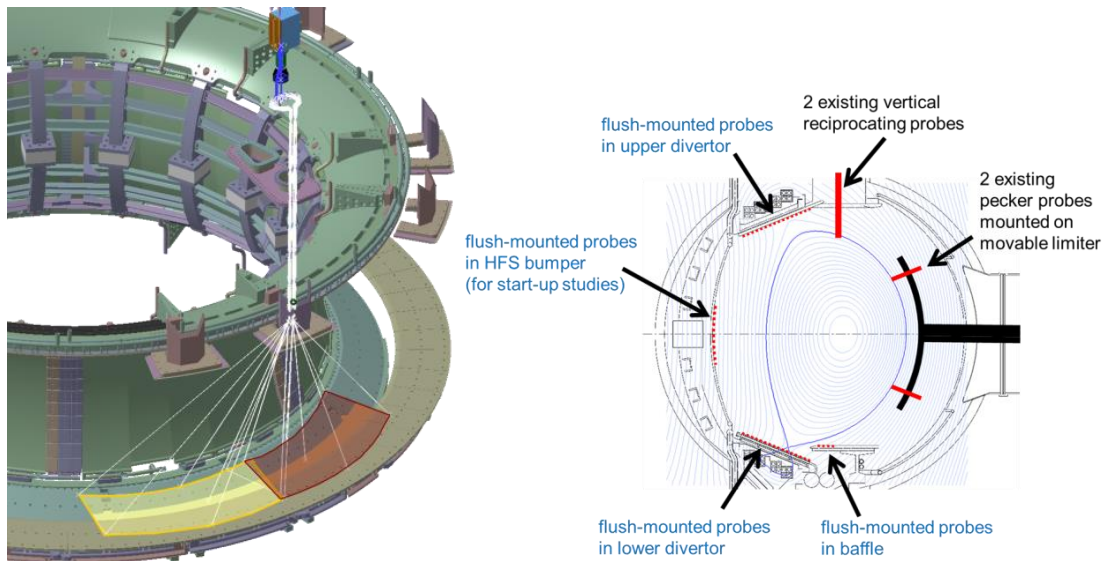


Figure 10 : field of view of an IR endoscope (left) and Langmuir probe set-up (right)

### W sources, radiation, and transport

The control of W contamination will be an important research area for the WEST programme. Tungsten and other impurity sources, as well as recycling fluxes, are monitored by an extensive visible spectroscopy system (200 lines of sight), covering most PFCs in the vessel (lower and upper divertors, HFS limiters, antenna and launcher protection limiters). In addition to the standard time resolution, a high speed mode is also possible for ELM studies. Two VUV spectrometers are also available. The first system has a high spectral resolution and a mobile line of sight, allowing for scans of the lower divertor region. The second system is particularly suited for impurity transport studies in conjunction with the laser blow-off system.

WEST will be equipped with three bolometric cameras in a horizontal port and one or two cameras located in an upper vertical port. The system will allow estimate of the total radiated power.

The soft X-ray diagnostic is going through major refurbishment based on the GEM (Gas Electron Multiplier) detector technique. An array of GEM is planned in an upper vertical port, giving a full coverage of the plasma. In addition, a second GEM based camera is planned in a horizontal port, allowing for tomographic reconstruction. Slow (ms) and fast ( $\mu$ s) acquisition modes are foreseen.

### Core and pedestal profiles (Figure 11)

The electron density profile is measured by a 10-chord interferometry diagnostic and two X-mode reflectometers which give access to the entire LFS profile and part of the HFS profile. These diagnostics allow an accurate determination of the density profile in the confined plasma with a time resolution allowing density fluctuation measurements over the entire profile. The 32-



## Chapter 2: the WEST project in a nutshell

point ECE radiometer provides the  $T_e$  measurements over the same radial range with 5% accuracy and a millisecond time resolution. A new 2D X-ray crystal spectrometer is planned to provide  $T_i$ ,  $T_e$ ,  $V_\phi$  and  $V_\theta$  measurements. In a first stage, the system will be limited to central measurements (5 points around the magnetic axis). It will be further improved at a later stage, with additional measurement points including the pedestal (15 measurements in total). The  $q$  profile is deduced from the interferopolarimetry diagnostic.

The existing Thomson scattering diagnostic could be modified to focus on the electron and temperature profiles in the pedestal region, with about 10 points over a radial range of about 10 cm and a spatial resolution around 6 mm. The edge reflectometer will also provide part of the necessary density measurements. The outer views of the imaging 2D X-ray spectrometer will provide few  $T_i$  measurement points. The radial electric field will be provided by a direct measurement by the Doppler reflectometer and can also be inferred from the velocity measurements of the 2D X-ray spectrometer.

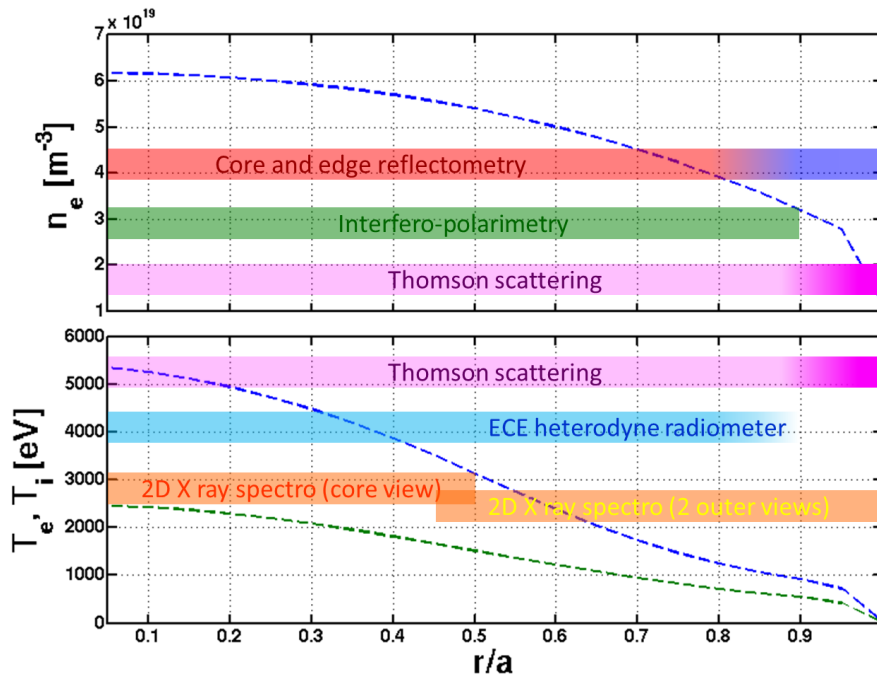


Figure 11: Typical electron density (top) and temperature (bottom) profiles with radial intervals measured by the various profile diagnostics. The Thomson scattering diagnostic will have 6 measurement points in the pedestal region (around  $r/a = 0.9-1$ ). The overlap region between core and edge reflectometers and the outermost radius measured by ECE depend on the plasma conditions. The outer views of the 2D X ray spectrometer will not be available at the beginning of operation.

### Turbulence and MHD

With the WEST project comes a unique set of diagnostics dedicated to fluctuation measurements. With their microsecond time resolution capability, the two reflectometers presented in the paragraph above provide fluctuation profiles over the entire LFS half of the plasma and part of the HFS half. An Upper Hybrid Resonance Scattering (UHRS) reflectometer is proposed for small scale density fluctuation measurements. The Doppler reflectometer already

present on Tore Supra provides frequency spectra with a radial and wavenumber scan capability. A fast camera tangential view will allow observation of disruptions, gas or pellet injections and edge plasma turbulence. A 2D ECE imaging diagnostic will record  $52 \times 18 \text{ cm}^2$  images of the electron temperature at 250 kHz for ELM dynamics and core MHD studies.

## V. WEST plasma scenarios outlook

An essential asset of WEST is its capability of integrating scientific, technological and operational issues on long pulses, combining plasma edge and core confinement issues. In order to prepare these highly integrated operating modes, a preliminary investigation of the simultaneous requirements on the plasma scenario has been carried out, investigating the heat flux on the divertor target, the heating schemes, the expected behaviour of the L-H threshold and of the pedestal and the potential W sources. These aspects are discussed in details in annex 8.

In order to fulfil the missions of WEST, three categories of plasma scenario are foreseen. A standard scenario at medium power (12 MW) will be the workhorse for testing the ITER plasma facing components and demonstrating integrated H mode long pulse operation, ensuring relevant heat fluxes on the divertor (in the range  $10\text{-}20 \text{ MW/m}^2$ ) and relevant time scale ( $\sim 60 \text{ s}$ ). For the study of plasma wall interactions at high particle fluence, scenario for longer discharges will be studied, aiming at 1000 s operation. This scenario will be performed at lower density for efficient current drive, and will use the full power available from LHCD (7 MW). Finally, a high power scenario at 15 MW will be developed for high performance discharges, using the full ICRH power available (9 MW) on shorter discharges (30 s).

The scenarios have been investigated for 2 reference configurations: close X point at 0.8 MA and far X point at 0.6 MA (see Figure 6 for an illustration of the magnetic configurations, as well as annex 3). The high power scenario has been studied at 0.8 MA, while the standard and the high fluence scenario have been studied at 0.6 MA.

At the stage of the present report, integrated modeling of the three classes of scenarios has been done with the 0D version of CRONOS [Artaud2010], called METIS. The main assumptions used for METIS settings are described below. Eleven JET-ILW and one AUG plasmas have been modeled using METIS, meaning that the temperature and density profiles, the radiated power and the total energy have been simultaneously reproduced. This METIS setting has then been used for WEST scenarios (see annex 8).

Based on a fair agreement obtained on these 12 cases, WEST pulses have been modelled. For ICRH a power absorption within  $\rho=0.4$  is modelled, based on EVE/AQL results, with a ratio of 50% of the power coupled to the bulk ions and 50% to the electrons. LH waves are absorbed at mid radius with CD efficiency from 0.07 to  $0.1 \times 10^{20} \text{ A.W}^{-1}.\text{m}^{-2}$  consistent with C3PO/LUKE simulations. The density peaking from [Weisen2005] is used, based on the relative success in reproducing JET profiles. A density at the separatrix from [Mahadavi2003] coherent with SOLEDGE2D-Eirene expectations is assumed. A pedestal width of 5% is taken, which was found coherent with JET observations. A tungsten concentration at the separatrix such that

## Chapter 2: the WEST project in a nutshell

$n_w/n_e = 5 \times 10^{-4}$  is taken, in the range used to reproduce the radiated power of the 12 studied cases. Such a  $W$  concentration is in the right order of magnitude, in case of target temperatures around 50 eV and some light impurity content [Dux2009]. A flat  $n_w$  profile is assumed. In the future simultaneous turbulent and neoclassical transport should be accounted for. The radiative power,  $P_{rad}$ , is determined using the revised  $W$  cooling rate from [Putterich2010]. The  $H$  factor from [ITER1999] is taken to be 1 and sensitivity tests in the range 0.7 to 1.2 have been carried out. The pedestal energy based on the ITPA scaling [McDonald2007] adjusted to the  $H$  factor is used. It was shown to be below the ideal MHD limit for  $\Delta_{ped}=2.3$  cm and to reproduce well the 12 cases.

All scenarios are for 3.7 T at 2.5 m. The duration of the standard and high power scenarios are limited by the ICRH system capabilities while the high fluence scenario has no known limitation. The three scenarios are summarized in Table 5.

Scenario	High power	standard	High fluence
$I_p$ (MA)	0.8	0.6	0.6
$n_e$ ( $10^{19}m^{-3}$ )	8.0	7.0	7.0
$f_{GW}$ (%)	70	70	70
$P_{heat}$ (MW)	15	12	10
LHCD (MW)	6	6	7
ICRH (MW)	9	6	3
$P_{rad}$ (MW)	5.0	3.0	3.0
$\beta_N$	2.7	2.2	1.7
$T_{ped}$ (keV)	0.7	0.4	0.4
$n_{ped}$ ( $10^{19}m^{-3}$ )	5.0	5.0	4.5
$W_{th}$ (MJ)	0.9	0.6	0.5
Bootstrap fraction (%)	30	35	35
LHCD fraction (%)	30	50	60
<b>Pulse length (s)</b> min(14 Wb or IC time limit)	<b>30</b>	<b>60</b>	<b>1000</b>
<b>Expected heat load (MW/m<sup>2</sup>), 2/3 vs 1/3 asym.</b>	<b>10 to 20</b> depending on X point height and $\lambda_q$		
<b>Operation time to reach one ITER pulse fluence</b>	~6 months	~2 months	<b>few days</b>

Table 5: overview of the plasma scenarios foreseen for WEST

In particular, one can note that the Greenwald fraction is between 60 to 70%, which is comparable with the fraction at which metallic wall machines such as JET-ILW [Beurskens2013] and ASDEX Upgrade [Kallenbach2011] routinely operate. The pedestal density is at most  $5 \times 10^{19} m^{-3}$  which should be compatible with LH wave accessibility discussed in section 3. The bootstrap fraction is around 30 to 35% and the fraction of LH driven current up to 60%. On Figure 12, the profiles for the 3 scenarios are illustrated. The density profiles are peaked due to the scaling used [Weisen2005], this should be revisited using CRONOS and realistic transport codes. The electron temperature reaches up to 6 keV in the core of the high power case. The  $q$  profiles do not go below 1 for the two scenarios at 0.6 MA. The  $q$  profile is even expected to be strongly reversed in the high fluence scenario due to the off-axis LHCD absorption. No ITB model has been included here.

15 MW, 0.8 MA, 30 s 12 MW, 0.6 MA, 60 s 10 MW, 0.6 MA, 1000 s

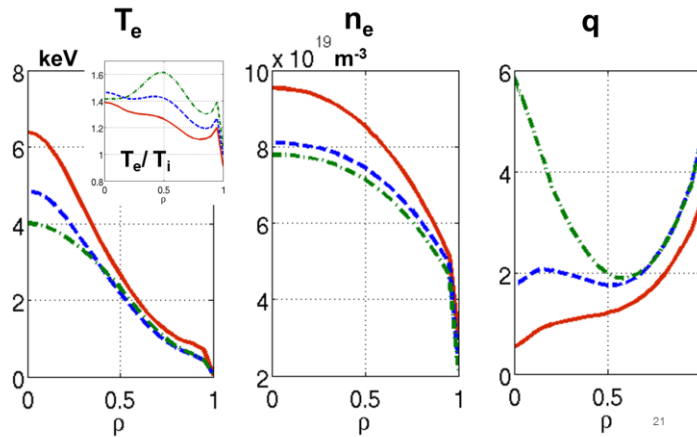


Figure 12: Temperature, density and q profiles of the 3 scenarios summarized in Table 5.

Moreover advanced tokamak modes are expected to be accessible thanks to the LHCD long-pulse capability at high power and their investigation will be an important research axis of WEST. Note that a 30 s pulse is as long as 20 resistive times. These scenarios will allow developing real-time control expertise for long pulse scenarios, exploring some advanced regimes and their control. This programme will participate to JT60-SA operation preparation.

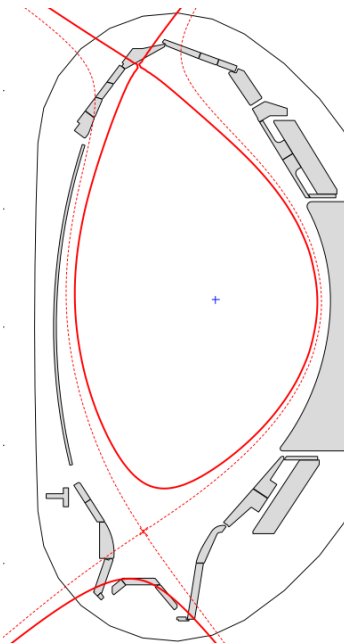


Figure 13 : illustration of a WEST like close X point configuration run on the upper divertor of AUG [Meyer2013]

In addition to this integrated modelling effort, additional simulations have been carried out on specific issues: RF heating (LH and ICRH absorptions using the CP30-LUKE and EVE codes respectively), radiated power (using the COREDIV code to estimate W contamination levels) or plasma edge modelling (using coupled SOLEDGE2D-Eirene calculations). The overall consistency of the plasma scenarios foreseen with the peak heat loads on the divertor has also been checked. This is described in annex 8.

Finally, the above simulations effort is being consolidated with experimental results: a WEST like configuration has been performed in AUG, showing that high power operation is possible [Meyer2013]. Further work is proposed to investigate additional issues in AUG (ICRH only heated plasmas, impact of low pumping on H mode performance etc).

The next chapter presents the WEST research plan, structured around the two topical headlines described in Chapter 1.

### References of chapter 2:

[Artaud2010] J.F. Artaud et al, Nuclear Fusion (2010) 50 043001

## Chapter 2: the WEST project in a nutshell

[Beurskens2014] M. Beurskens et al Nucl. Fusion 54 (2014) 043001

[Bucalossi2011] J. Bucalossi, A. Argouarch, V. Basiuk et al., Feasibility study of an actively cooled tungsten divertor in Tore Supra for ITER technology testing, Fusion Engineering and Design 86 (2011) 684–688

[Dux2009] R. Dux et al Journal of Nuclear Materials 390–391 (2009) 858–863

[Grosman2013] A. Grosman, J. Bucalossi, L. Doceul et al., The WEST programme: Minimizing technology and operational risks of a full actively cooled tungsten divertor on ITER, Fusion Eng. Des. (2013), <http://dx.doi.org/10.1016/j.fusengdes.2013.02.039>

[ITER1999] ITER Physics Nucl. Fusion 39 2175 (1999)

[Kallenbach2011] A. Kallenbach et al Nucl. Fusion 51 (2011) 094012 (11pp)  
doi:10.1088/0029-5515/51/9/094012

[Loarte2003] A. Loarte et al, Plasma Physics and Controlled Fusion (2003)

[Mahdavi2003] Mahdavi et al. Phys. Plasmas, Vol. 10, No. 10, October 2003 Physics of pedestal density profile formation and its impact on H-mode density limit in burning plasmas

[Martin2008] Y.R. Martin et al. Journal of Physics: Conference Series 123 (2008) 012033

[McDonald2007] McDonald D C et al, Nuclear Fusion 2007

[Meyer2013] O. Meyer, E. Belonohy, J. Bucalossi et al., “WEST Like Divertor geometry experiments in ASDEX Upgrade”, 40th European Physical Society Conference on Plasma Physics, Espoo, Finland, 2013

[Mikhailovskii1997] Mikhailovskii A.B.et al., Plasma Phys. Rep. 23 844–57 (1997)

[Peysson2012] Y. Peysson, J. Decker & L. Morini. Plasma Phys. Control. Fusion 54 (2012) 045003

[Pütterich2010] Pütterich T et al Nucl. Fusion 50 (2010) 025012

[Weisen2005] Weisen et al. Nucl. Fusion 45 (2005) L1–L4 Collisionality and shear dependences of density peaking in JET and extrapolation to ITER

[Zarzoso2011] Zarzoso D et al, Nuclear Fusion 2011

# Chapter 3: WEST Research Plan

---

This chapter is dedicated to the WEST Research Plan. The latter is developed along two headlines: Headline-1 “Testing and operating ITER-grade PFC in tokamaks” and Headline 2 “Towards long pulse H-mode & steady-state operation”, described in the next sections.

The staged implementation of the actively cooled components, with an initial set-up, phase-1, which includes non-actively cooled lower divertor Plasma Facing Units, and phase-2 with the complete actively cooled lower divertor, leads to a staged research plan for both headlines. As readily expected, the research plan for phase-1 is more detailed than for phase-2. The headlines are organized in areas of research, with deliverables attached either to phase-1 or to phase-2 or both. Milestones are identified and correspond to high priority deliverables of the program.

A tentative timeline is proposed at the end of the chapter, to give an overview of the program phasing during WEST exploitation.

NB : in what follows, W1 and W2 refer to WEST Headline 1 and WEST Headline 2 respectively.

## **W1. Headline 1 – Testing and operating ITER-grade PFC in tokamak**

This section describes Headline-1 of the WEST research plan, “Testing and operating ITER-grade PFC in tokamaks”, dedicated to testing tungsten actively cooled plasma facing components under a tokamak environment. The first priority of Headline-1 is risk minimization of PFC procurement and operation in ITER. Headline-1 is focused on assessing the power handling capabilities of tungsten components both in terms of peak head load and ageing. Operation and physics issues that govern the power handling capability of WEST, as well as its control, are part of Headline-1.

The deliverables of Headline-1 listed in this section are related to tokamak operation of PFCs with ITER grade technology. Although this is not described in detail here, WEST also provides output on the optimization of industrial scale production processes ahead of the ITER divertor procurement. In particular, WEST allows assessing the component rejection rate during industrial production and developing repair processes if needed. It also allows validating the qualification procedure and acceptance criteria: the performance of the tungsten monoblocks under high heat flux exposure in WEST will be cross correlated with the results from the qualification procedure. Finally WEST allows one checking the manufacturing/assembly tolerances, and investigating the impact of component misalignment on plasma operation as well as on the component operational limit.

## Motivation and objectives

Assessing the performance of the ITER like tungsten divertor under combined plasma loads in a tokamak environment (steady state and transient heat loads, combined particle/heat loads etc.) is a high priority issue to ensure efficient ITER operation.

As far as power handling is concerned, Headline-1 is focused on testing the ITER like tungsten divertor under relevant steady state heat fluxes (10-20 MW/m<sup>2</sup>) as well as under a large number of sub threshold transients ( $> 10^5$  ELMs). The modular design of the WEST divertor sectors provides a means to accommodate “à la carte” experiments such as testing different material grades, investigating monoblock geometry and shaping, ageing of pre-damaged or misaligned components, melting experiments, etc. It will also allow one comparing components supplied by different manufacturers.

Although focused on ITER divertor tungsten components, Headline-1 encompasses the power handling capability of all in-vessel PFC, including in particular the baffle and upper divertor as well as the ICRH antenna and LHCD launcher protections.

As far as PFC ageing is concerned, experiments with high integrated particle flux to the vessel walls, comparable to that of a nominal ITER discharge, typically  $\sim 10^{27}$  D/m<sup>2</sup> at the strike point for the nominal 400 s, Q = 10 discharge, are planned under Headline-1. Reaching these values of the integrated particle flux requires years of operation in short pulse fusion devices, but is achievable within days/weeks with WEST. The synergistic effects of combined exposure of the components to steady state heat loads / transient heat loads / high integrated particle flux, to be addressed within Headline-1 during WEST phase-2, is a high priority issue for ITER, as it might impact PFC lifetime and plasma performance (see [Loewenhoff2012], [Wirtz 2013] and [DeTemmerman2013]). This part of the program relies on dedicated wall loading campaigns with repetitive long pulses, and includes the impact of helium operation on tungsten components. These WEST campaigns will be supplemented by thorough post-mortem analysis, allowing one to quantify wall erosion, changes in tungsten morphology of exposed surfaces, dust production and fuel retention.

Furthermore, the physics and operation issues that determine and constrain the heat loads are also included in Headline-1 so that edge plasma conditions and their control are investigated together with PFC testing. Consequently, the physics of power exhaust are also addressed within Headline-1, for instance the Scrape-Off Layer width, taking advantage of WEST edge diagnostics: extensive IR coverage, backed up by thermocouples and calorimetry, versatile Langmuir probe systems, helium jet and edge reflectometers.

Regarding operation, conditioning of the all metal WEST facility is also part of Headline-1 together with specific control issues regarding safe PFC operation, such as developing the wall protection system including both the control tools and associated diagnostics. These aspects are highly relevant for ITER.

### General remarks for Headline 1 (W1):

- Headline-1 requires H-mode operation for several facets of its program, of course that related to ELM transients but also to increase the energy flux to the target plate by narrowing the inter-ELM Scrape-Off Layer width. The H-mode scenario developed within Headline-2 must open the way to routine confinement improvement over durations larger than the time constant for thermal equilibrium of the W monoblocks ( $\sim 5$  s) during the initial research phase, phase-1, and repetitive long-pulse H-mode operation during phase-2.
- Various operation scenarios are considered in phase-2 for repetitive long pulse operation in helium, deuterium and deuterium with impurity seeding. The plasma parameters (energy and particle fluxes, plasma edge temperature, PFC surface temperature etc) of these scenarios must be carefully optimized for a meaningful comparison of the various experiments. The development of such scenarios is a high priority for phase-2.
- The Headline-1 program will be adapted as a function of the ITER grade divertor elements available, as well as the components to be tested. Openings in the course of WEST operation to add or change actively cooled components is part of the facility program. These shutdowns are important aspects of the program and have to be adapted to the needs of PFC testing and optimized regarding the other issues of the program.
- In view of the need of comparing various technologies and manufacturers, heterogeneous divertor sectors will be operated, not only in phase-1 but also in phase-2. This has strong implication on the tests, which have to be optimized to deliver results with significant statistics, given the number of monoblocks of a given grade available to be operated under similar conditions.
- Operational limits on the tungsten surface temperatures will be set to perform staged component testing, with typically three steps:
  - Tungsten temperature below recrystallization,  $T_{\text{rec}} \approx 1200^\circ\text{C}$ , for both steady state and ELM excursion.
  - ELM induced temperature transients exceeding  $T_{\text{rec}} = 1200^\circ\text{C}$  and leading to recrystallization, possibly requiring to redefine the temperature threshold  $T_{\text{rec}}$ .
  - Steady state temperature operation above  $T_{\text{rec}}$ .
- Visual inspection of PFCs is essential to monitor component damage and surface morphology changes. Regular visual inspections of the PFC are planned (in particular after significant exposure to high heat flux and/or off normal events), taking advantage of the Tore Supra articulated arm to perform this monitoring without breaking vacuum.
- Wall loading campaigns have been staged according to the planned operation of ITER: deuterium campaign followed by a helium campaign, corresponding to ITER non-nuclear phase, followed by high power deuterium discharges with impurity seeding, corresponding to nominal ITER discharges in the nuclear phase. The order of these



ageing experiments can be modified depending on the most urgent R&D needs of ITER Organization and ITER partners.

The following sections are a presentation of Headline-1 blocks of experiments. Key deliverables identified in Phase-1 or Phase-2 experiments and corresponding modeling effort are emphasized.

### **W.1.1 Pre- and post-characterization of ITER-grade PFCs (phase-1 and phase-2)**

#### **W1.1.1 PFC pre characterization**

In order to assess the manufacturing technologies to be used for ITER Plasma Facing Units, the characterization of all Plasma Facing Units to be tested on WEST must be as complete as possible prior to assembly in the WEST divertor, and should be systematically performed before introducing new ITER-grade PFC in WEST. The technology qualification tests of the Domestic Agencies, the manufacturing qualification test of the component and the WEST qualification test as well as available tests in linear devices should provide a rather complete pre-characterization survey. Precise coordination of the WEST agenda of component mounting and removal and PFC pre-characterization and post-characterization will have to be organized in order to optimize the WEST operation timeline.

#### **W1.1.2 Monitoring of PFC exposure conditions**

Traceability of tile behavior and test conditions during plasma operation (as well as conditioning phases, machine shutdowns etc) must be prepared, with a comprehensive database archiving the PFC exposure conditions (such as plasma exposure duration, plasma edge parameters, surface temperature, number of thermal cycling, off normal events etc).

#### **W1.1.3 PFC post characterization**

A number of selected ITER grade tungsten elements will be dismantled after plasma exposure and send for post mortem analysis (metallurgy, chemical composition, structural morphology change, erosion and deposition, fuel uptake). This will be performed in particular after high heat flux exposure and/or long pulse wall loading campaigns.

Relevant criteria to assess the PFU technologies should be determined with the partners. The statistical error bars of the results of the test based on the number of available components and on the history of the test must be determined. The operation risk associated to accepting PFUs that stand below acceptance criteria, damaged components and repaired components must be assessed to determine the time line for their introduction and removal from WEST.

#### **Deliverables, priority and timeline**

Deliverable W1.1.1: PFC pre-characterization (phase 1 and 2)

Deliverable W1.1.2: Monitoring of PFC exposure conditions (phase 1 and 2)

Deliverable W1.1.3: PFC post-characterization (phase 1 and 2)

## **W.1.2 Power exhaust balance & controlling the heat flux deposition (phase-1)**

### **W1.2.1 Steady state heat load pattern including strike point & SOL widths**

The preliminary step towards testing the tungsten components is to determine the heat flux deposition pattern and identify the fast particle contribution. This requires in particular determining the structure of the Scrape-Off Layer width regarding the energy channel and particle channel. The heat load pattern will be characterized as a function of the plasma parameters, heating power, plasma current and density, and of the divertor configuration far / near X-point, and single-down, double and single-up divertor. This will be performed in L-mode, then in H-mode. A control scheme will be assessed to ensure a given heat flux on the divertor, using the real time features of the Wall Monitoring System.

A comparison between the measured and the predicted heat flux pattern will be performed, using the “engineering” code PFCFLUX, as well as the more physics oriented code package SOLEDGE-Eirene (see annex 9 for the description of the modelling tools mentioned here).

### **W1.2.2 ELM heat load pattern**

The WEST geometry is quite appropriate to analyze the key features of the ELM energy deposition pattern, including the wetted area, peaking factor and in/out asymmetries. Using several diagnostics, one should be able to determine the characteristic time scales. The phase-2 long pulse H-modes will offer a unique capability to develop ELM statistical analysis on a single shot as well as during repetitive shots with quasi-constant conditions.

For PFC testing purposes, careful monitoring of the surface temperature during the ELM cycle is required with precise back-up simulation of both the component thermal response and the Infra-Red measurement system. This experiment is particularly delicate since the PFCs thermal response and ELMs energy deposition pattern are heterogeneous. Statistics over the whole divertor are mandatory to investigate the evolution of the PFCs and estimate their damage threshold. A critical issue is determining the ELM energy deposition pattern with appropriate space and time resolution, for each ELM, given an expected but yet unknown statistical dispersion. A prerequisite for such an experiment is therefore a high level of expertise regarding ELM properties during long pulse H-mode plasmas, an issue to be addressed within Headline-2. Infra-Red cameras with high space –determined by the structure of the deposition pattern on a monoblock– and time –determined by the ELM dynamics– resolution are required but might not be sufficient for a complete characterization. It is proposed to tackle this issue through a multi-diagnostic analysis implemented within the Wall Monitoring System. The use of laser induced heat loads would certainly be valuable to calibrate an advanced Infra-Red camera highly resolved in space and time and develop the appropriate know-how required by such an experiment.

### **W1.2.3 Disruption heat load pattern and impact on PFC**

Disruptions can lead to large energy fluxes onto reduced areas, eventually damaging PFC. The heat load pattern during disruptions will be studied in the metallic environment of WEST (heat load pattern broadening, distribution between the in vessel components, characteristics of

current quench / thermal quench etc) to complete the existing database of disruptions heat loads in metallic devices, of high interest for ITER.

In addition, disruptions at large plasma current can drive strong forces on PFCs depending on the circulation of the induced currents. Of particular interest in that respect is the case of a PFC that has been subject to melting (with for instance melted material filling the gaps between tiles, so that castellation is no longer efficient). This can be studied in WEST if requested.

Finally, it should be noted that disruptions should be avoided during PFC ageing experiments (see also W.2.6), in order not to impact on the PFC surface evolution. The constraint introduced by avoiding disruptions during hundreds of long pulses dedicated to PFC ageing being very severe, it would be very valuable to assess as early as possible what is the actual impact of disruptions on PFCs with tungsten armor under WEST conditions.

### W1.2.4 Validated power balance

The power balance will be validated by a thorough crosscheck of all relevant diagnostics and quantify the heat load pattern on the PFCs, electron and ion energy flux through the separatrix. This can be achieved in L mode, early in phase 1. However, a significant cumulated energy, e.g. high power and/or long pulse, will improve the accuracy of the calorimetry system. The thermocouples inserted into the inertial divertor sectors during phase 1 will also provide valuable information when completed with appropriate modeling. The output of this phase is a complete and validated power balance, giving in particular a consistent coupled power ( $P_{\text{add}}$ ), radiated power (core and edge) and conducted power onto the PFCs. A precise power balance can in particular provide an estimate of the ion energy which is a key input in shallow angle energy deposition and the issue of gaps and tile shaping.

### Deliverables, priority and timeline

Deliverable W1.2.1: Steady state heat load pattern (phase 1)

Deliverable W1.2.2: ELM heat load deposition pattern (phase 1)

Deliverable W1.2.3: Disruption heat load deposition pattern (phase 1)

Deliverable W1.2.4: Validated power balance (phase 1, high priority)

W1-2 is a high priority item. Initial results are required at the beginning of phase-1, and must be consolidated throughout WEST operation.

## W.1.3 Towards a reliable wall protection system (phase-1 and phase-2)

### W1.3.1 Validated IR temperatures

Validating the temperature data from the IR system is identified as a challenging issue at the start of phase-1 (issue of W emissivity, reflections etc.). Indeed, a correct estimate of the component temperature is required to characterize the thermal cycles and tungsten evolution such as recrystallization. A thorough comparison between the divertor IR data, the divertor Langmuir probes data, the calorimetry and the divertor thermocouples data will be performed.

The output of this effort is validated surface temperature measurements of the Plasma Facing Units. The chain going from raw IR data up to surface temperatures and finally heat fluxes will be tested.

### **W1.3.2 Reliable PFC surface temperature control**

Developing operational know-how and specific tools for PFC protection relevant to ITER is one of the objectives pursued with the WEST platform. Actively cooled plasma facing components bring specific issues in terms of wall protection, as the limit when running at high power is not the discharge duration as for inertial components but whether the plasma scenario can be performed or not [Bucalossi2013].

The Wall Monitoring System of WEST is targeted at protecting the PFCs while allowing high plasma performance. It is required for high heat flux operation of WEST and will have direct implications for developing protection systems for the safe operation of ITER divertor. It is based on a multi-diagnostic approach: Infra-Red imaging, calorimetry, thermocouples, spectroscopy, etc. and is developed in a staged way, building on the experience gained during the previous operation of Tore Supra. It will cover the divertor as well as the heating systems, and include real time sophisticated control schemes and event recognition, such as arcing [Travere2012], as well as exception handling. Proving reliable PFC surface temperature control is a milestone for phase-1 of the WEST research plan.

For phase-1 of WEST operation, the PFC surface temperature will be used to determine the controlled energy flux to specific areas of the divertor where the PFCs under test are located. Alternatively it can be used directly for feed-backed operation at controlled surface temperatures of the PFCs under test. Furthermore, it will be required to monitor the protection of other PFCs, in particular the antennas.

### **W1.3.3 Wall Monitoring System for transients**

Improvement and further development of the Wall Monitoring System is to be pursued throughout phase-1 and phase-2. In particular, a multi-diagnostic version will be required to monitor the ageing tests with ELM transients during phase-2, in order to access the ELM deposition pattern resolving energy deposition and time. The use of laser induced heat loads and other in situ inspection technics is important to determine the component ageing and very valuable when developing the Wall Monitoring System to include ageing as part of the survey.

A version 1 of the Wall Monitoring System must be operational from the start of phase-1. Improvement and further development is to be pursued throughout phase-1 and phase-2, in particular towards a multi-diagnostic scheme allowing one to address fast transients, developing a database of arcing and dust and evolving towards DEMO grade wall monitoring. It is planned to allocate specific days for the Wall Monitoring System validation early in phase-1. From then on the system will benefit from regular use during plasma operation that will provide time for testing and validating the ongoing development.

### **Deliverables, priority and timeline**

Deliverable W1.3.1: Validated IR temperature (phase 1)

Milestone W1.3.2: Reliable PFC surface temperature control (high priority, phase 1)

Deliverable W1.3.3: Wall monitoring system for transients (phase 1 and 2)

#### **W.1.4 Metallic Wall conditioning (phase-1 and phase-2)**

##### **W1.4.1 Reliable conditioning of tungsten walls, with control of light impurities**

An efficient conditioning strategy is a key issue to operate WEST as a PFC test facility. Indeed, new components are to be introduced in the vessel on a regular basis. Conditioning will then play a major role to resume operation with well controlled plasmas, otherwise components subject to different conditions are difficult to compare, in particular regarding the change of the surface morphology. A key uncertainty is the duration of the conditioning period; hence how fast reliable plasma breakdown conditions are obtained. A second open issue is how to proceed to obtain reproducible intrinsic impurity content.

One of the main questions to be investigated is the control of light impurities. These play a deleterious role both with respect to tungsten erosion and to enter H-mode confinement. Indeed, when light impurities are reduced enough, the electron temperature can reach the 10-20 eV range before tungsten erosion becomes significant. With light impurities present at a higher level, the electron temperature of the plasma has to be reduced and the operational space is consequently narrowed towards the challenging detached divertor conditions.

Two species of light impurities are expected to require specific attention during conditioning, namely carbon and oxygen. The former should be related to the manufacturing and mounting processes, provided the tungsten coated carbon elements are not deteriorated, leading to a carbon source during operation as a consequence of carbon erosion by the plasma. Regarding oxygen, the main sources include tungsten oxides formation on the component surfaces and residual air leakage.

A possibility to control the intrinsic carbon and oxygen level is to boronize the vessel. However, this procedure introduces another light impurity, boron that will contribute to tungsten erosion. Furthermore, the effect of boronization is limited in duration, typically a couple of minutes of plasma operation. Such a technic is therefore neither appropriate to long pulse operation nor to repetitive plasma tests with comparable conditions. Although the boronization system will still be operational on WEST, this conditioning process cannot be regarded as part of routine operation

##### **W1.4.2 Efficient wall conditioning procedures with magnetic fields**

Next step devices such as ITER will require conditioning procedures that can be performed with the magnetic field on, as is the case for WEST. The baseline strategy for WEST relies on vessel baking at 200°C, and on deuterium glow discharges prior to operation, thus with the toroidal magnetic field down. In addition to this, other conditioning procedures compatible with the magnetic field are available, such as Ion Cyclotron Wall Conditioning and Taylor Cleaning Discharges. Once conditions for plasma breakdown are reached, plasma operation is an efficient way to improve the conditioning.

Other issues that could require conditioning actions are related to the main species behavior with two issues. First, the limited pumping capability can trigger disruptions early in the plasma

current ramp down. Furthermore, the transient particle uptake by the wall could respond differently with actively cooled components due to the very short duration of the thermal equilibration of the PFC at the pulse end. The rapid decay of the particle transport within the tungsten could then lead to much larger particle trapping in the cooled tungsten. This could require specific conditioning action to provide reliable plasma breakdown and density ramp-up in following shots. Furthermore, the control of the concentration of the hydrogen isotope, which is needed for ICRH hydrogen minority heating scheme, is another point that could require specific action. All of the above should be performed with magnetic fields on.

### **Deliverables, priority and timeline**

Deliverable W1.4.1: Reliable conditioning of tungsten walls, with control of light impurities (phase 1 and 2)

Deliverable W1.4.2: Efficient wall conditioning procedures with magnetic fields (phase 1 and 2)

Conditioning will be addressed immediately after successful pump-down at the beginning of phase-1. It will remain a high priority issue during all the life time of the PFC test facility.

### **W.1.5 Divertor operation with different configurations in deuterium and helium (mostly phase-1)**

The WEST PFCs and control system will allow one operating in single lower null, single upper null and double null configurations as well as intermediate cases characterized by the distance between the two separatrices. This will offer considerable flexibility in investigating divertor physics. The WEST divertors are tight divertors without high-field side baffles and with the X-point rather close to the target plate. The lower divertor, with its baffle on the low-field side providing a plenum for pumping, is reminiscent of the lower divertor of DIII-D albeit for the choice of armor material. Another difference is the aspect ratio that could play a role in decoupling the divertor operation point from that of the pedestal, hence facilitating detached divertor operation combined to low collisionality pedestal.

#### **W1.5.1 Lower and upper divertor operation**

L-mode characterization of the lower and upper divertors must be achieved early in phase-1 in particular to identify the divertor density regimes, the effect of the large aspect ratio and that of the ion vertical drift direction.

As soon as possible, this characterization should be completed by that in H-mode. The interplay between divertor and H-mode conditions must also be investigated experimentally using as figure of merit vanishing tungsten erosion conditions.

At least two reference scenarios with different X-point heights must be documented for the PFC test experiments, as this can be used to tune the heat flux pattern on the divertor. High recycling regime, detached divertor regime with divertor plugging and detachment without neutral control in the divertor volume must be investigated. The transition point between these divertor states must be determined both during density ramp-up and ramp-down experiments as well as with near steady-state conditions. The dynamics of the transition are also relevant since transition characteristic times close to a transition point can be quite long. As a rule, one should aim at achieving these transitions without extrinsic impurity

seeding, hence only based on the increased deuterium flux. In such a case, one should be able to combine a high energy flux onto the PFC as required for testing while achieving appropriate electron temperature conditions to suppress tungsten erosion. It is possible that such a regime is more readily achieved at high power as observed on DIII-D. Impurity seeding should only be contemplated when the divertor temperature is sufficiently low, and remains low, to avoid enhanced tungsten erosion by these impurities.

### **W1.5.2 Plasma density control and optimized pumping for steady state operation**

Since WEST operation is dedicated to high energy flux operation onto the divertor target plates, the major role of the WEST divertor is to ensure the control of particle recirculation. In particular, a maximum particle-flux onto the target plate with standard core density values must be achieved. This decoupling is the figure of merit of the divertor. It requires that most of the neutral flux leaving the divertor target plates is ionized in the divertor volume. This plugging effect must be ensured by the plasma itself since the existing baffle is mainly implemented for pumping purposes. Neutral particle leakage out of the divertor volume into the large volumes on the high field side or on the low field side will gradually change the divertor operating point. Signs of this evolution should be visible with the onset of recycling at the strike point of the secondary separatrix onto the other divertor target plate. Some tuning of the relationship between divertor particle flux and core density can be achieved by changing the X-point height.

Another important issue of divertor plasma conditions is that of pumping. One can readily expect that plasma plugging of the neutral particle outflux from the pumping plenum is critical for the pumping efficiency. The latter is mandatory for reaching steady-state conditions while allowing for gas injection to improve ICRH and Lower Hybrid coupling, or pellet injection to modify core density profiles. Operation wise, pumping during the plasma current ramp-down is regarded as crucial in avoiding density limit disruptions while the plasma current is still large. Finally, compensating any slow evolution of edge plasma conditions towards increasing densities can only be achieved by increasing the pumping efficiency, hence the plasma plugging of the pumping plenum, most likely by modifying the strike point, either by a radial displacement or an increased X-point height. Monitoring the pumping efficiency is a requirement for feed-back controlled steady-state operation.

Pumping in all metallic wall devices is a critical issue. With moderate pumping capability WEST scenarios must ensure the consistency between the total gas injected during plasma build-up and plateau and the pumping phase during the plasma plateau and ramp-down. A transient wall uptake would alleviate this constraint.

### **W1.5.3 Helium divertor operation**

Operating helium plasma will be most interesting regarding divertor physics. Indeed the atomic physics change considerably from deuterium to helium (in particular, a large fraction of the complex atomic and molecular processes ongoing in detached deuterium plasmas do not take place in helium plasmas).

The changes in divertor plasma behavior between deuterium and helium plasmas will thus provide considerable insight into the divertor physics. Such experimental evidence is also most important to test the modeling effort and assess the role of atomic processes in divertor plasma detachment. It could also have some relevance for the ITER program during the non-nuclear phase where operation with helium plasmas is foreseen.

Should the decision be taken to operate WEST plasmas in helium at the end of phase-1 for PFC testing purposes, dedicated scenario development including helium divertor operation should be implemented in phase 1.

### **W1.5.4 Baffle and divertors plasma response to ELMs**

The edge plasma cannot be considered as steady state during H-mode operation due to the ongoing ELM relaxation events followed by a recovery time. The particle recirculation scheme also responds to this cyclic drive of energy and particle flux. Maintaining divertor plugging conditions as well as low enough electron divertor temperature during the ELM cycles is then essential. The ELM energy flux deposition will also affect the plasma that develops in the vicinity of the secondary separatrix. Furthermore, ELMs will most probably interact with the baffle and generate transient plasmas and recycling patterns on this component. JOREK, SOLEDGE modeling in support of this physics will be important because of the time scale gap between the ELM relaxation event and the gradual pump-out of these secondary plasmas. Determining potential correlations between slow drifts of edge plasma conditions and ELM cycling will be a challenge that will require multi-diagnostic analysis and global modeling. ELM cycling requires a specific effort to maintain average steady state conditions.

### **W1.5.5 Controlled divertor conditions for long pulse H-mode operation**

The working point of divertor plasmas with controlled tungsten erosion of divertor PFCs requires a low electron temperature plasma in the divertor that is usually achieved in a partially detached divertor regime. As a consequence, long pulse H-mode operation must integrate core plasma properties suitable for current drive and edge plasma properties suitable for divertor operation. Achieving the regime, which combines controlled divertor and core operation, is thus a milestone of the WEST program. An issue raised in the Headline-1 plasma scenarios for phase-2 and PFC ageing program is that of the flexibility of such a scenario in order to accommodate various divertor plasma conditions, and therefore ageing conditions, while maintaining low tungsten erosion conditions. The possibility of achieving a rather large operating space for this scenario, while minimizing tungsten erosion in the divertor is a challenge, which should be addressed during phase-1 in preparation of phase-2.

## **Deliverables, priority and timeline**

Deliverable W1.5.1: Mastering lower and upper divertor operation (phase-1)

Deliverable W1.5.2: Plasma density control and optimized pumping for steady state operation (phase-1 and 2)



Deliverable W1.5.3 : Helium divertor operation (end of phase-1 and phase-2)

Deliverable W1.5.4 : Baffle and divertors plasma response to ELMs (phase-1)

Milestone W1.5.5 : Controlled divertor conditions for long pulse H-mode operation (high priority, phase-1 and phase-2)

Experimental days at the beginning of phase-1 must be dedicated to mastering the divertor operation. As plasma performance is increased, further dedicated days will be required for appropriate investigation of the operation point, especially when switching to H-mode in both phases 1 and 2.

Steady-state control of particle recirculation and plasma density as a fixed point or via feed-back control is an important issue for phase-1 and even more for long pulse operation in phase-2. This aspect will have to be integrated in WEST scenario developments although the physics and modeling back-up will be more divertor specific.

Long pulse H mode operation is the reference scenario for phase-2, and must be developed during phase-1.

## W.1.6 Power handling of ITER PFCs @10 MW/m<sup>2</sup> (mostly phase-1)

### W1.6.1 Test with ITER nominal steady state heat flux

The objective of this block of experiments is to test the thermal behavior of ITER like tungsten Plasma Facing Units (PFUs) under nominal steady state conditions. The first step will be to develop the best plasma scenario to reach the 10 MW/m<sup>2</sup> milestone at the divertor target, over duration larger than the thermal equilibrium time of the Plasma Facing Units ~ 5 s. This is a milestone of the WEST Research Plan that will be performed in close connection with Headline-2.

The WEST configuration has been optimized for maximizing the heat flux on the divertor. Present estimates [Missirlian2013] indicate that the ITER nominal steady state heat flux target, 10 MW/m<sup>2</sup>, should be within reach at medium power, in the range 5-12 MW of coupled power. The two main control parameters are the heating power and flux surface expansion controlled with the X point height. It is to be noted that all WEST actively cooled PFCs must be tested at their nominal steady state heat flux. This extends this topic beyond the case of the ITER components to a comprehensive analysis that will include, in particular, loads on the baffle nose, which will depend on the clearance between the separatrix and this component.

This is illustrated on Figure 14 where the heat load pattern on the WEST lower divertor is plotted for 2 magnetic configurations (close and far X-point). This PFCFLUX calculation is performed for 10 MW of power into the Scrape-Off Layer and a characteristic Scrape-Off Layer width  $\lambda_q = 5$  mm. The calculation takes into account the 3D magnetic field, hence including the toroidal field ripple, but only accounts for parallel projection and does not take into account tile shadowing stemming from the toroidal chamfer of the tungsten monoblocks foreseen for ITER, see annex 4 for a description of the tungsten monoblocks. This could lead to increased peak heat loads driven by up to 70% tile shadowing in the high heat flux area. Furthermore, the latest ITPA Scrape-Off Layer width scaling in H-mode [Eich2013] predicts  $\lambda_q \sim 2-4$  mm for WEST conditions. This would also govern higher peak heat loads than obtained here with  $\lambda_q \sim 5$  mm.

Operation in the medium-high density range is foreseen to maintain W contamination at acceptable levels. See Chapter 2 for an overview of the foreseen plasma scenarios.

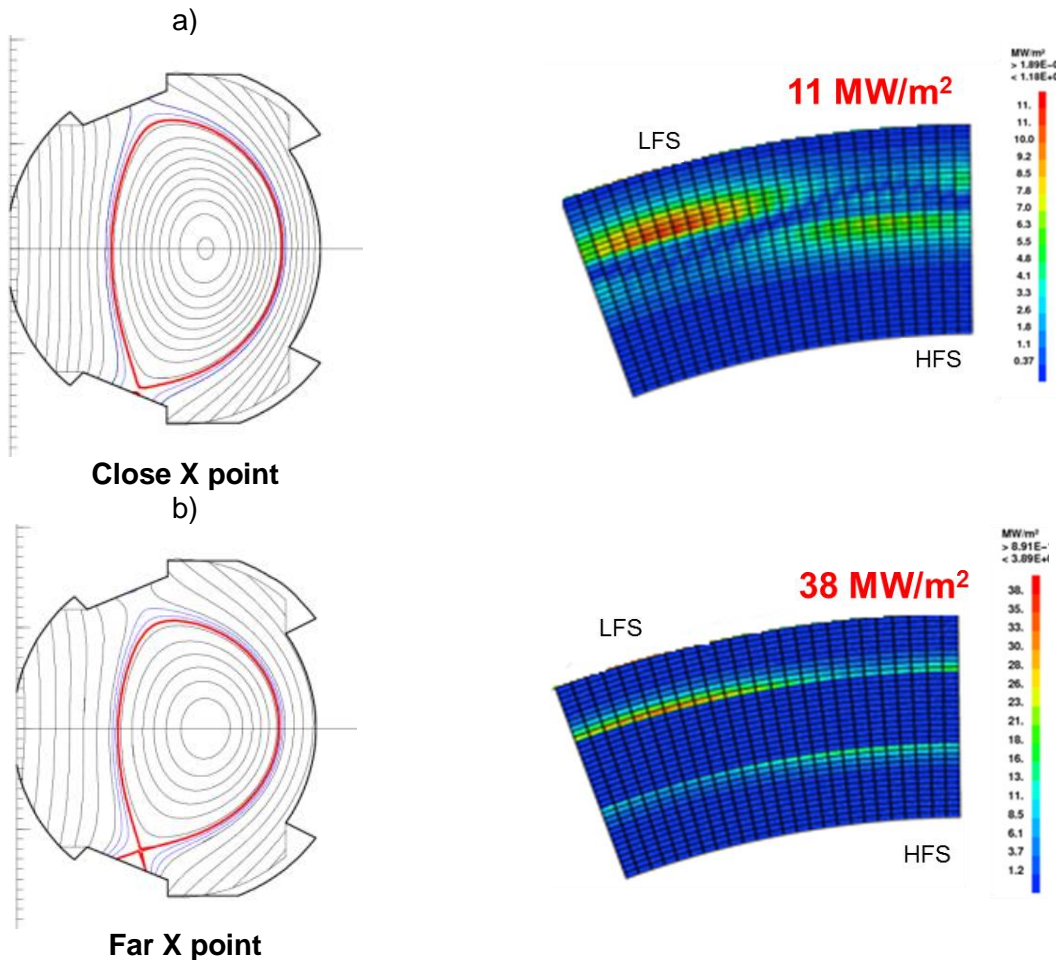


Figure 14 : PFCFLUX calculations of the heat load pattern on the WEST divertor for PSOL = 10 MW and  $\lambda_q = 5$  mm for the 2 standard magnetic configuration, the close X point (a) and the far X point (b)

Preliminary experiments in ASDEX Upgrade have already shown that high power operation is possible in a WEST like configuration [Meyer2013]. Simulations with edge plasma codes (such as SOLPS and SOLEDGE-Eirene) are also ongoing.

The milestone of steady state nominal operation of ITER Plasma Facing Units will open the way to comparison with other tests achieved during the Plasma Facing Units qualification phase, High Heat Flux and/or SATIR testing [Durocher2009]. Similarly thermo-mechanical simulations will be compared to the experimental data.

Follow-up steps in this block of experiments address the following possible deliverables:

- Cycling at steady state nominal operation of ITER,
- Reaching this operating point over a maximum number of monoblocks to improve the statistics,

After inserting new components, similar series of experiments can be performed to test:

## Chapter 3: WEST Research Plan

- Plasma Facing Units supplied by different manufacturers,
- Tungsten monoblocks with lower heat extraction capability, as evaluated during the qualification phase or rejected after the manufacturers qualification test
- Components with prescribed defects,
- Repaired Plasma Facing Units
- Aged Plasma Facing Units (for instance with high energy ion beams induced defects to simulate neutron impact).

These data will then be available for updating the acceptance criteria set by ITER for the Plasma Facing Units.

During this block of experiments, in-situ visual inspection of the Plasma Facing Units is planned after high heat flux exposure and/or disruptions. Post-mortem analysis of the components removed from WEST will also be undertaken.

### W1.6.2 Validation of the ITER gap and shaping requirements

In addition to the power handling capabilities of the Plasma Facing Units, a particular attention will be paid to the behavior of the leading edges of the monoblocks. This milestone of the WEST research plan requires a high resolution Infra-Red camera to obtain a detailed image of the tungsten monoblocks, on a narrower field of view. If available, the performance of different shaping geometries will be compared. The present reference for the ITER like divertor sectors in WEST is a single toroidal chamfer of height 0.5 mm. However, other geometries can readily be tested (in particular, the no shaping option can be assessed). The gap between Plasma Facing Units can also be varied if requested, in particular to study the behavior of larger gaps depending of the effective misalignment tolerance, the present ITER reference being 0.3 mm.

The WEST divertor will be a unique opportunity to validate the gap and shaping management in ITER given the uncertainty on manufacturing and in-vessel mounting tolerances. Experimental data will be compared with thermo-mechanical calculations. PIC code calculations are required to extrapolate the WEST results to the ITER operation point [Dejarnac2007]. Shallow angle energy flux deposition must be analyzed in 6D phase space for collisionless plasma target interaction. The thermal loading of the flat surface of the monoblocks versus the side of the monoblocks exposed because of the gaps, partly governed by the ion gyration movement, hence the 3D properties of the particle trajectories, is most sensitive to the ion energy, both in the perpendicular and parallel direction. It will also depend on the electric field, which can be quite large, since charge separation builds-up in the gaps due to the difference in transverse geometries of the ion and electron trajectories. Sensitivity to ELM transients and to changes in magnetic equilibrium must also be assessed. A significant modelling activity is thus needed to contribute to tile shaping optimization of the Plasma Facing Units in the ITER divertor. It is to be noted that the issue of gaps must be addressed for all WEST components and include fast particle deposition, such as ion ripple losses, as well as the robustness of the shaping strategy defined for the non-cooled components of the divertor during phase-1.

### W1.6.3 Evolution of the power handling capability of ITER PFCs under thermal cycling

This block of experiments is dedicated to assessing the evolution of ITER grade PFC performance under thermal cycling in a tokamak environment.

Given the fact that heterogeneous Plasma Facing Units are likely to be used, at least during phase-1 and probably during part of phase-2, the ageing process will be sensitive to the fuse effect, such that the weakest component will set the upper operation limit. Furthermore, carefully monitored experiments should enable to determine the upper cycle limit prior to degradation of the component performance. These experiments can be achieved during phase-1, but the repetitive character foreseen will be characteristic of phase-2 experimental campaigns.

Two types of experiments could be addressed : thermal cycling repeating dedicated pulses at a given steady state heat flux, or monitoring the PFC behavior during the campaigns using a reference shot performed periodically. Both approaches could also be used in a complementary way. This should be done first at nominal heat flux ( $10 \text{ MW/m}^2$ ) then repeated in the heat flux range foreseen for slow transients (up to  $20 \text{ MW/m}^2$ ). The detailed PFC cycling procedure will be discussed with the ITER organization and the Domestic Agencies providing the ITER grade PFC. Below are given a few details for both options.

#### **PFC repetitive thermal cycling**

Operation at nominal steady state conditions : the issue is the component fatigue, including leading edges, with thermal cycling and the consequent ageing of the components.

Operation for slow transient conditions, a priori up to  $20 \text{ MW/m}^2$ : the issue is the monoblock fatigue in the tungsten bulk or at the interface between tungsten and the copper heat sink.

Careful visual inspection, correlation with tungsten spectroscopy and modelling in the course of the test should enable detecting the early signs of ageing and assessing the limit in the cycling process without reaching component degradation.

It is to be noted here that a complex shaping strategy with several different shapes will render a comprehensive test of the shapes under thermal cycling very demanding in run time. This experiment can be accommodated within phase-1 for nominal steady state conditions. It would then be the phase-1 heavy experiment in terms of run time. Experiments at higher heat flux could also be performed during phase-1, but the upper limit will be determined by the performance of the divertor tungsten coated start up elements.

#### **PFC fatigue monitoring using a reference shot :**

The power handling capability of the ITER like Plasma Facing Units will be surveyed during the WEST experimental campaigns, using reference shots at ITER nominal operation points with steady state conditions, hence  $10 \text{ MW/m}^2$ . A robust scenario for these reference shots, heating power waveform, energy flux pattern... must be determined. It will be based on the know-how gained during the WEST phase-1 operation and progress in Headline-1.

These shots will be repeated throughout campaigns. The frequency at which the reference shot will be performed will be evaluated as a feedback from the first experimental results, but will probably be a function of cumulated energy/operation time at high power. The evolution of defects on the tungsten monoblocks will be monitored. The change in thermal response will be analyzed in view of the data base of reference shots.

Results will be compared with the output from the qualification phase, High Heat Flux and SATIR testing, and used as a feedback on the acceptance criteria for ITER Plasma Facing Units. The impact of recrystallization will also be addressed with the reference shot database. In addition, post-mortem analysis of default monoblocks will be performed at need to investigate the ageing process leading to a degradation of the energy extraction capability.

It should be noted that although starting in phase-1, these experiments will also benefit from long pulse operation planned in phase-2, with alternative ageing process of the component governed by the evolution of the tungsten surface morphology under high integrated particle flux.

### **Deliverables, priority and timeline**

**Milestone W1.6.1: Test with ITER nominal steady-state heat flux (phase 1, high priority)**

Deliverable W1.6.2: Validation of the ITER gap and shaping requirements (phase 1, high priority)

Deliverable W1.6.3: Evolution of power handling of ITER PFCs under thermal cycling (phase 1 and 2, high priority)

W.1.6 is a high priority item of the WEST program, with a significant part of the experimental time, in particular during phase-1. The output of W.1.6 is expected to be used to optimize the detailed ITER divertor design, tile shaping for instance, and gain confidence in the ITER divertor power handling capability in tokamak conditions. This part of the program should therefore be executed in close connection with the planning of the ITER divertor procurement, see the general WEST timeline shown in Chapter 1. Milestone W1.6.1 and Milestone W1.6.2 are to be achieved early in phase-1 of WEST. The reference shots to monitor the ageing of the components should become important towards the end of phase-1 and when addressing the long pulse ageing of phase-2.

### **W.1.7 Tungsten melting and damage (end of phase 1)**

The consequences of tungsten PFCs damage/melting on subsequent plasma operation are a high priority issue for ITER. This block of experiments is therefore to be performed in close connection with requests of ITER Organization, completing tungsten melting experiments already performed in other fusion devices. Two different blocks of experiments are presently contemplated.

#### **W1.7.1 Operation with pre-damaged PFC**

The aim is simulating ITER operation after tungsten PFC damage by transients. While the damage cannot be achieved in situ with WEST transients, the impact of droplet expulsion, damage propagation, etc. on plasma operation as a function of damage location can be investigated with carefully designed pre-damaged components. For this purpose, the High Heat Flux testing phase could be used to produce cracking, local melting, droplets, etc on the components.

#### **W1.7.2 Melting & operation with misaligned PFC**

The aim is simulating damage due to PFC misalignment in ITER. This would be performed with dedicated misaligned elements implemented in WEST. A precise mapping of the position of

misaligned elements once assembled in the machine should be planned. Melting of leading edges, damage propagation and impact on plasma operation as a function of damage location can be addressed.

It should be noted that this experiment requires a careful planning and designing of pre-damaged/misaligned PFCs, to be defined in connection with ITER Organization. It also requires optimization of shutdowns during phase-1 to implement “pre-damaged” and “misaligned” elements at the end of phase-1. As underlined in Chapter 2, the time line for component changes includes the one month shutdown needed to replace a divertor sector or a single Plasma Facing Unit by a new one, as well as the time to resume operation with comparable plasma properties.

### **Deliverables, priority and timeline**

Deliverable W1.7.1: Operation with pre-damaged PFC (end of phase 1, high priority)

Milestone W1.7.2: Melting & operation with misaligned PFC (end of phase 1, high priority)

W.1.7 is presently seen as a high priority item, but the priority and the content of the experiment will have to be reassessed depending on the output of melting experiments presently ongoing in other tokamaks/Plasma-Wall Interaction devices. It is proposed to run W.1.7 at the end of phase-1, using dedicated divertor elements.

### **W.1.8 Power handling under extreme heat loads (phase-1 and phase-2)**

This block of experiments is dedicated to testing the performance of ITER like PFUs under extreme conditions, in terms of steady state heat loads (with heat fluxes up to  $20 \text{ MW/m}^2$  as foreseen during ITER slow transients) or large number of ELM cycles (typically  $>10^5$ , given the fact that ITER is expected to experience  $\sim 10^5$  ELMs during the nominal 400 s shot). Similarly to PFC cycling described in W1.6.3, these tests do not aim at component degradation but at testing the actual operational limit. Furthermore, when testing heterogeneous Plasma Facing Units, the “fuse” effect will take place, providing information on the weakest component and a lower limit for the others. For these tests, in-situ component inspections are mandatory.

#### **W1.8.1 Upper energy flux limit of ITER grade PFC**

ITER divertor plasma facing components are designed to handle slow transients, with an energy flux up to  $20 \text{ MW/m}^2$ . The WEST experiments can be used to investigate such events and thus assess the slow transient operation capability. Achieving this milestone of the WEST program will require a very careful and progressive heat load increase from  $10 \text{ MW/m}^2$  up to  $20 \text{ MW/m}^2$ , as local damage of the monoblocks (increased material roughness, cracks swelling, local melting) has been observed in previous High Heat Flux testing [Missirlian2011] in this range of thermal loads. It should also be noted that for these heat fluxes, the corresponding monoblock steady state surface temperature will exceed the tungsten recrystallization temperature. Frequent visual inspection of the PFCs will be required, as the power will be progressively ramped up.

The plasma scenario will benefit from the experience gained when achieving PFC testing at nominal heat fluxes in W.1.6. The experiments will consist of a progressive additional power increase with intermediate steps of energy flux deposition, from 10 to 20 MW/m<sup>2</sup>. This ramp-up scenario must also be used to investigate the impact on operation of exceeding the recrystallization temperature.

Careful modelling, compared to precise surface temperature measurements, as well as empirical scaling, should provide the trend, and allow one extrapolating to the limit without having to perform the limit test with the risk of component degradation.

The thermal behavior of the ITER like Plasma Facing Units under these extreme heat loads will be closely monitored, in particular to assess damage threshold and propagation, and to identify potential failure modes. The performance of Plasma Facing Units supplied by different manufacturers will be evaluated. Results will be compared with the output from the Plasma Facing Units qualification phase. These data will contribute to the validation of the acceptance criteria for ITER Plasma Facing Units. Experimental data will also be compared with thermo-mechanical simulations of the Plasma Facing Units. This performance test of ITER PFCs is a major milestone for WEST.

### W1.8.2 Component ageing with 10<sup>6</sup> ELM cycles

This milestone of the WEST program requires appropriate ELM characterization and high level expertise on ELM physics and deposition pattern to estimate the maximum temperature reached during the ELM transient energy deposition on the PFCs. Another demanding prerequisite is an efficient disruption control system, since the impact of a disruption on PFC may dominate the cumulative impact of numerous ELM cycles (the impact of disruptions on PFC will therefore be studied in advance of this block of experiments, see W1.2.3).

This block of experiments is targeted at investigating the behavior of the tungsten monoblocks under a large number of ELM cycles. In electron-beam testing facilities, the damage threshold has been observed to decrease with the number of ELM like cycles, down to a heat flux factor  $F_{HF} = 6 \text{ (MW/m}^2\text{) s}^{0.5}$  for crack appearance after 10<sup>5</sup> cycles, compared to the tungsten melting threshold  $F_{HF} \sim 50 \text{ (MW/m}^2\text{) s}^{0.5}$  without cycling [Loewenhoff2012]. WEST will allow one addressing this issue under plasma bombardment in a tokamak environment.

During long pulse operation of WEST in phase-2, a large number of ELMs cycles can be cumulated in one day of repetitive 1000 s long pulses, typically up to 10<sup>5</sup> ELMs per day. Such experiments will be coupled to the evolution of the tungsten surface morphology under high integrated particle flux. The output of such a block of experiments is the evolution of the surface temperature and its pattern, both for the steady state temperature and the peak temperature under transients. Preliminary estimates indicate that for steady state heat loads of 10 MW/m<sup>2</sup>, the ELMs should induce temperature cycles around the recrystallization temperature, as illustrated in Figure 14.

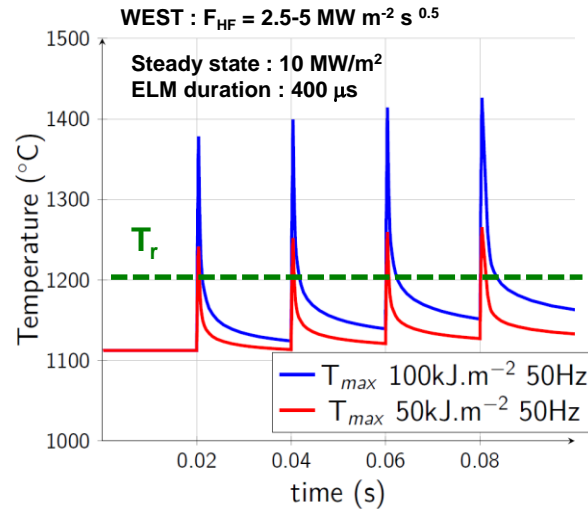


Figure 15 : preliminary estimate of the temperature increase of the W monoblocks linked to ELMs, showing that the temperature excursion can allow cycling around the recrystallisation temperature  $T_r$  (for a steady state heat load of  $10 \text{ MW/m}^2$ , and ELMs of  $50$  and  $100 \text{ kJ/m}^2$ , red and blue curve respectively,  $400 \text{ }\mu\text{s}$  duration,  $50 \text{ Hz}$  frequency).

### Deliverables, priority and timeline

Milestone W1.8.1: Upper energy flux limit of ITER grade PFC (end of phase 1 and/or phase 2, high priority)

Deliverable W1.8.2: Component ageing with  $10^6$  ELM cycles (phase 2, high priority)

W.1.8 is seen as a high priority item of the program, as it might have serious consequences for ITER divertor operation. W1.8.1 experiments can be initiated during phase-1 but might be limited by the operational limit of non actively cooled divertor elements for the highest power range foreseen. They will thus be complemented effectively during phase-2. W1.8.2 requires a campaign with long pulse and repetitive shots. As such it must be regarded as a demanding phase-2 experiment, presumably addressed not earlier than mid phase-2.

### W.1.9 Tungsten surface modification with helium plasmas (end of phase-1 and phase-2)

Helium operation is foreseen in the non-nuclear phase of ITER. Helium coming from the D-T fusion reaction will also be present during the nuclear phase. Interaction with helium is known to cause specific issues with tungsten PFCs, with potentially harmful structural changes. At high surface temperature,  $T_s > 700 \text{ }^\circ\text{C}$ , formation of nano-tendrils, called fuzz, is expected [Ueda2013]. Such fuzz has been grown in Plasma Wall Interaction devices and also evidenced in tokamaks, as in dedicated C-Mod experiments. Fuzz formation could be detrimental especially in presence of transient heat loads. In particular, fuzz has been shown to be prone to arcing, which in turn is likely to increase dust production. At lower surface temperature, nanobubbles formation has been evidenced [Ueda2013], degrading the thermal properties of the PFCs. Given the heat fluxes expected in WEST, both phenomenon could take place, with fuzz formation



localized around the strike point region where the peak steady state surface temperature should be 1100°C for 10MW/m<sup>2</sup> heat flux.

#### **W1.9.1 Structural changes of tungsten PFCs under He operation and impact on subsequent plasma operation**

A first series of shots in helium is to address the change in the tungsten PFC surface morphology as well as determine changes in plasma operation due to this surface evolution. This should be done towards the end of phase-1, and requires that the plasma scenario used for PFC testing is adapted to helium operation. In particular, the helium scenarios should be defined taking into account the conditions for helium related tungsten morphology change (forming tungsten fuzz requires a scenario with heat fluxes not far from 10MW/m<sup>2</sup> in order to reach the requested high surface temperatures. The plasma temperatures on the targets should be kept low while maintaining high heat fluxes, since some of the morphology change effects are sensitive to particle energy).

Depending on the needs of ITER Organization, a second helium campaign with repetitive long pulses will be scheduled in phase-2 to investigate the impact of a higher helium fluence (see W1.10.3).

Such experiments require precise monitoring of plasma conditions, most importantly of light impurities and residual deuterium, of the evolution of the component surface between shots with in-situ inspection, and finally precise component pre-characterization and post characterization. The formation of fuzz, which has optical properties markedly different from undamaged tungsten surfaces, will be followed in situ by visual inspection of the PFCs.

#### **Deliverables, priority and timeline**

**Milestone W1.9.1 : structural changes of tungsten PFC under He operation and impact on subsequent plasma operation (end of phase 1, high priority)**

#### **W.1.10 PFC ageing with long pulse operation (mostly phase-2)**

The experiments described below aim at investigating the ageing behaviour of actively cooled W PFCs in long pulse tokamak operation under high particle fluence. In particular, the impact of tungsten morphology change under plasma exposure (such as blisters under D bombardment or tungsten nanostructures under He bombardment) on the component lifetime and power handling capability, as well as on subsequent plasma operation will be investigated.

The order proposed below for the 3 different wall loading campaigns has been chosen so as to mimic the situation foreseen for ITER operation : first a pure D campaign, then a pure He campaign, corresponding to ITER non nuclear H/He phase. It would be followed by high power deuterium discharges with impurity seeding, corresponding to the situation of nominal ITER discharges in the nuclear phase. This set of experiments, planned in phase 2 of WEST, should provide operational guidelines in time for the ITER divertor exploitation. However, the order of the experiments can be modified as required by the ITER Organization, depending on the most urgent R&D needs.

Such experiments require precise monitoring of plasma conditions, most importantly of light impurities including seed, of the evolution of the component surface between shots with in-situ inspection, and finally precise component pre-characterization and post characterization.

#### **W1.10.1 Development of long pulse scenarios for PFC ageing campaigns**

The plasma scenarios developed for PFC ageing campaigns should allow reaching large particle fluences while optimizing the experimental time. This will be performed in close collaboration with Headline-2. These scenarios should be both reliable, that is for instance not too demanding on the heating systems (power, discharge duration), and well suited for long discharge operation (optimized flux consumption, current drive). The conditions close to the divertor plates should be as relevant as possible because of the importance of synergistic effects (heat loads, particles fluxes, transients, ...).

Determining the optimum plasma scenario to operate such campaigns is challenging : one must identify what are the key parameters responsible for PFC ageing, and which should be kept constant for comparing the various experiments (incident particle flux or fluence, heat flux, plasma temperature, surface temperature etc ...) and extrapolate to ITER conditions. For instance, the introduction of seed impurities is likely to modify the plasma scenario in particular regarding the divertor plasma conditions, compared to the pure deuterium case. Scaling laws and their extrapolation to ITER conditions might then be required for this scientific achievement.

#### **W1.10.2 PFC ageing with long pulse deuterium operation**

The behavior of tungsten actively cooled components under high integrated particle flux relevant for ITER discharges (several  $10^{27}$  D<sup>+</sup>/m<sup>2</sup>) will be investigated by performing repetitive identical shots, typically several tens of long discharges, i.e. one to two weeks of operation, followed by a shutdown and post-mortem analysis of selected tungsten monoblocks. This selection will be made so as to cover a broad range of power fluxes over a divertor sector, and account for the possible presence of test monoblocks (advanced shaping, repaired elements...). The fluence reached should be larger than that accumulated during the previous experiments, in order to be discriminated in the post mortem analysis. This first set of experiments will be carried out in deuterium, without impurity seeding, to serve as a reference.

Tungsten gross erosion will be monitored by visible spectroscopy during the campaigns, and compared to confocal microscopy measurements giving access to net erosion/redeposition. The latter must be performed both prior to and after the campaign, and will be calibrated using marker tiles [see for instance Maier2013]. A wide range of post-mortem analysis techniques will be applied on the selected monoblocks, in collaboration with other laboratories, in order to evidence possible structural changes, monitor fuel retention (see also W.1.12), look for cracks development, possible blistering or helium nanobubbles on the surface. The quantity of dust formed during the campaign will be assessed by careful collection.

#### **W1.10.3 PFC ageing with long pulse helium operation**

Depending on the output from the short pulse helium exposure performed during phase 1 (see W.1.9), experiments at higher helium fluence could be performed during phase 2. The experiment will consist in replicating the loading campaign of W1.10.2 in Helium, and perform

post-mortem analysis of the PFCs with similar tools. Operation on virgin PFCs (replacement of Plasma Facing Units after the campaign of W1.10.2) will allow one to assess the effects incurred by prior deuterium exposition. The quantity of dust collected after shutdown will be compared to that formed during the W1.10.2 campaign.

#### **W1.10.4 PFC ageing with long pulse impurity seeded discharges**

In ITER impurity seeding will be mandatory so as to reduce the power load on the divertor PFCs to an acceptable level. Currently, Argon, Neon and Nitrogen are considered as good candidates for seeding (even though Nitrogen might be an issue for the tritium plant). It is therefore important to investigate the effects of these impurities on ITER relevant divertor PFCs (e.g. formation of tungsten nitrides  $WN/WN_2$  [Rubel2011]), as well as operational problems that may occur during long discharges). For instance, it is known that  $N_2$  seeding has a strong wall loading memory effect, and that Neon can accumulate via co-deposition [Rubel2011]. The dust formation rate in seeded discharges might also be larger than expected [Grisolia]. Depending on the outcome of the helium loading campaign or of R&D on the effects of helium on W PFCs, these discharges might be run with helium injection too, in order to come closer to the actual ITER operation conditions.

The experiment will again consist in replicating the loading experiment W1.10.2 using impurity seeding (with impurities considered as relevant at the time of the experiments), and performing post-mortem analysis on selected components, as well as dust collection. As for W1.10.3, possible options include exposing virgin PFC (replacement of Plasma Facing Units) combined with PFC already exposed to the previous high fluence campaigns.

#### **Deliverables, priority and timeline**

Deliverable W1.10.1 : development of long pulse scenarios for ageing campaigns (phase 1 and phase 2)

Milestone W1.10.2: PFC ageing with long pulse deuterium operation (phase 2, high priority)

Milestone W1.10.3 : PFC ageing with long pulse helium operation (phase 2, high priority)

Milestone W1.10.4 : PFC ageing with long pulse impurity seeded discharges (phase 2, high priority)

Experiments mentioned in this section have a high priority as they address the question of PFCs ageing under tokamak conditions, which is a key contribution for ITER. They must be carried out during phase 2 since they require long discharges to reach high fluences. Developing optimized “loading” scenarios for these campaigns is thus also a high priority, and preparatory experiments are planned during the first phase of operation in order to be ready as quickly as possible after the start of phase 2. The implementation of these campaigns requires careful scheduling because of the need for shutdowns (1 to 2 months depending whether some mono-blocks are exchanged). For these reasons, one loading campaign per year of operation is typically foreseen.

#### **W.1.11 PFC ageing: arcing and dust monitoring (phase-1 and phase-2)**

Arcs and dust production are indicative of the evolution of PFCs. They can also have serious consequences on operation as well as regarding safety issues. Aside from dedicated

experimental time and diagnostics, a data base of the events must be developed in conjunction with the Wall Monitoring System.

#### **W1.11.1 Arcing data base**

A proper discussion on arcs during RF operation will be most efficient if the history of these events is carefully recorded from day one allowing one to establish for instance correlations with ELMs, UFOs as well as ageing of the antenna and launchers. With full metal walls, arcing can also be expected on standard PFCs and contribute to changes in the surface morphology. During Helium plasma operation, fuzz formation in conjunction with arcing is likely to increase the dust production.

#### **W1.11.2 Dust data base**

Dust, that can appear as a fraction of a PFC surface with poor thermal binding to the heat sink, can first be indicative of the conditioning of the element. After the introduction of a new component, the dust survey can be indicative of the surface properties of the manufactured component as well as the evolution of its conditioning with plasma operation. At later stages, in particular during high integrated particle flux to the PFCs, changes of the surface morphology can build-up to new layers with poor thermal bounds. This evolution would then be indicative of component ageing. Dust production during the early phase of the component operation, conditioning phase, and during the ageing phase will be monitored to provide a production history as detailed as possible.

Dust production is also a safety issue in future magnetized fusion devices. WEST should help characterizing dust production rates in tungsten environment, and thus provide valuable input mostly for DEMO studies. Indeed, regarding ITER, beryllium is expected to be dominant in dust production. Dust produced during WEST campaigns must be collected for post-mortem analysis. In order to characterize the behavior of dust grains in the plasma, fast cameras providing data for trajectory tracking, and possibly aerogel collection allowing determining the energy and impact direction should complete the data. This is important in identifying the production mechanism and how it is related to the evolution and ageing of the PFCs. The possibility of installing an ITER relevant dust collector will depend on requirement from ITER Organization.

#### **W1.11.3 UFO data base**

The occurrence of arcs and dust release during plasma operation can govern a transient influx of metallic impurities. These events labelled UFOs can be traced with spectroscopy and soft X-rays diagnostics. The impact on tokamak operation of the smaller and most frequent transients of the sort is still lacking. A UFO data base is required to complete the arc and dust data base. It can provide valuable information on the penetration of the event, its magnitude and its composition.

### **Deliverables, priority and timeline**

Deliverable W1.11.1 : Arcing data base (phase 1 and 2)

Deliverable W1.11.2 : Dust data base (phase 1 and 2)

Deliverable W1.11.3 : UFO data base (phase 1 and 2)

### **W.1.12 Fuel inventory build up in actively cooled tungsten PFCs (phase -2)**

Although retention in the bulk of tungsten PFCs is not expected to be a problem in ITER, where co-deposition with beryllium will dominate, it remains to be quantified in actively cooled tungsten components operated in realistic conditions. This is especially true in view of DEMO, where both the total amount of retention and the penetration depth of the fuel atoms will matter (tritium permeation to the cooling channels after hours/days of operation should be assessed for instance). As the material temperature plays a crucial role in fuel retention processes, it should be noted that the thermal cycle of actively cooled components will be very different from those experienced by inertial ones. The surface temperature will rise and decrease rapidly (~5 s for thermal equilibrium of a tungsten monoblock) at the beginning and at the end of the discharge, with a long flat top at constant temperature in between (assuming a steady state scenario). Furthermore, the temperature gradient between the surface and the cooling pipes should affect fuel diffusion inside the material. In this respect, WEST provides data on fuel retention in relevant actively cooled tungsten PFC.

#### **W1.12.1 Fuel retention in actively cooled tungsten PFCs**

Retention studies in WEST will be carried out in connection with the wall loading campaigns (see W.1.10). Gas balance studies will be conducted in a systematic way during these campaigns and will be complemented by post-mortem analysis. The impact of component ageing and the associated tungsten morphology changes (with processes such as crack development, He nanostructures etc) on the long term fuel uptake can also be studied.

The use of test monoblocks exposed to ion beam bombardment to simulate neutron damages is foreseen during this phase, and would provide valuable input for DEMO retention studies.

#### **W1.12.2 Control of fuel inventory in actively cooled tungsten PFCs**

Should significant long term fuel retention be observed, it is then crucial to determine and operate a plasma scenario avoiding such trapping mechanism.

In this case, fuel recovery processes can also be investigated. In terms of fuel trapping, WEST provides actively cooled W PFCs exposed to relevant plasma conditions. Fuel recovery studies can be performed either in situ or in the laboratory. The experiments performed in-situ are closely tied to conditioning experiments (see W.1.4). In particular, the divertor components can be baked during shutdowns (up to 200°C) at the start of the campaigns as part of conditioning, and gas balance can be used to measure the removal rate and the total quantity of gas removed. The efficiency of ICWC (Ion Cyclotron Wall Conditioning ) discharges may also be investigated. The originality of laboratory experiments involving PFCs exposed in WEST is that the latter will provide a realistic test-bed to assess fuel removal techniques, for the reasons exposed above (actively cooled components, ...). These laboratory experiments would for instance consist of flash heating techniques (laser for instance), and would focus on monitoring the evolution of the fuel concentration profile (and total content) resulting from the cleaning attempt. Temperature controlled thermodesorption techniques (such as TDS, ...) will also be

used to assess the trapping energy distribution, and compare to numerical modelling of these experiments.

**Deliverables, priority and timeline**

Deliverable W1.12.1: Fuel retention in actively cooled tungsten PFCs (phase 2)

Deliverable W1.12.2: Control of fuel inventory in actively cooled tungsten PFCs (phase 2)

**W.1.13 Testing innovative concepts (end of phase-2)**

After testing the first ITER divertor, WEST could be used at a later stage to test innovative concepts (by the end of phase 2, in early 2020's). It should be noted that the integrated approach used to test the ITER divertor in a tokamak environment in WEST follows the same spirit as a Divertor Test Tokamak for the preparation of DEMO.

This could go from testing advanced tungsten material conventional PFCs, up to testing breaking technologies, such as liquid metals. The latter would however result in significant technological development of the WEST test bed and would require a thorough feasibility study, not yet performed at this stage. The content described below is therefore highly tentative at this stage, and will depend on the output of the R&D in the field of materials development and PFC technology carried out in the coming years.

**W1.13.1 Testing new materials for DEMO**

WEST allows exposing innovative tungsten PFCs to a tokamak environment in preparation for ITER second divertor and/or DEMO. New tungsten grades such as fiber reinforced tungsten, tungsten alloys, etc. could be tested once the technology for actively cooled components is developed with these materials. New assembly techniques like Cu-W functional gradients materials could also be tested. This would be performed in close collaboration with the material R&D and technological developments carried out in the French FR-FCM and the EU fusion laboratories involved in this topic.

**W1.13.2 Testing liquid metal PFCs in WEST**

Liquid metals such as lithium, gallium or tin are currently possible candidates for DEMO PFCs, because they would provide a solution to the PFC lifetime (and to some extent to the neutron damage) problem. At the end of phase 2 of WEST operation (early 2020's), depending on the results of R&D carried out in the years to come, the installation of a liquid metal divertor sector would allow for an integrated testing of such a technology in long pulse tokamak operation. This would provide invaluable experience in a view of the final choice of technology for DEMO.

**Deliverables, priority and timeline**

Deliverable W1.13.1 : Testing advanced tungsten PFCs (end of phase 2)

Deliverable W1.13.2 : Testing liquid metal PFCs in WEST (end of phase 2)

### **Chapter 3: WEST Research Plan**

This part of the research activity is foreseen by the end of phase-2 of the WEST program. It is possible that testing advanced tungsten armor material be shifted earlier, should the technology be mature enough for the components to be available for tokamak operation.

## W2. Headline 2 – Towards long pulse H-mode & steady-state operation

This chapter describes Headline-2 of the WEST Research Plan. This main task under Headline-2 is plasma operation towards long pulses with staged achievements.

First and starting with highest priority during phase-1 of WEST-operation, long pulse H-mode operation with different scenarios is both a highlight in extending ITER reference H-mode scenario towards long pulse operation and a high priority for Headline-1. Second, taking advantage of both the new divertor configuration and the long pulse capability of the machine and of its sub-systems, the aim is then exploring as well as validating advanced operation modes with enhanced confinement and steady-state conditions. The latter part of the program will constitute a valuable preparation and support not only to ITER, but also to JT-60SA and, in a wider perspective, to DEMO.

Besides its long pulse capability, the specific features of WEST offer unique opportunities to untangle some important parameters such as large aspect ratio, dominant electron heating, compact divertor geometry, no momentum source, etc. An important deliverable is therefore a productive interaction between experimental investigation and theory and modelling for improved understanding, scenario preparation and evaluating theory and modelling predictive capability regarding:

- the dynamics of the L-H and H-L transition
- ELMs and ELM transport
- tungsten sources and transport
- MHD stability including interplay with fast electrons and ions
- intrinsic rotation
- particle transport
- energy confinement

In addition, scenario required for testing ITER tungsten PFC under Headline-1 will be developed under Headline-2. During phase-1, a routine H-mode scenario with high heat flux onto the divertor, in 10-20 MW/m<sup>2</sup> range, and flat-top approaching 10 s is needed and will be used as reference scenario for PFC characterization throughout phase-1 and phase-2. Should an early helium phase take place towards the end of phase-1, this scenario should be adapted to helium operation. Furthermore, a scenario with large ELMs for thermal transient testing of the ITER-grade tungsten components will be also required. It should be characterized by long pulse capability and therefore lower hybrid current drive, to be used during testing campaigns of phase-2. Finally, three other scenarios are presently considered for phase-2 PFC testing. They should be characterized by comparable heat fluxes and particle fluxes to investigate changes of tungsten surface morphology during repetitive long pulse campaigns. The target pulse duration



that is contemplated is up to 1000 s in order to achieve high integrated particle flux first in deuterium plasmas, then in helium plasmas and finally in deuterium with extrinsic impurity injection.

IRFM has also developed a large expertise in the physics of steady-state non-inductive discharges [Bucalossi2009, Giruzzi2009]. Steady-state operation and related physics issues will become more and more important in view of the second phase of the ITER program and are also at the core of the research program of JT-60SA [Kamada2013]. This research effort is organized in view of the development of DEMO scenarios.

Since CEA is strongly committed in the construction of JT-60SA, and will be very likely also involved in its operation and scientific exploitation, R&D on advanced regimes will be mainly oriented to the preparation and support of the JT-60SA experimental program. The long pulse steady-state capability of WEST with full tungsten walls is thus an opportunity to assess the existing scenarios and investigate novel trends in support of both JT-60SA and ITER programs.

Below are listed the main experimental achievements requested to tackle the issues mentioned above. Several challenges of the fusion program are addressed: high performance RF heating, long pulse control of density profiles and tungsten impurity source and transport, low collisionality pedestal compatible with high density divertor operation, Lower Hybrid Current Drive efficiency in high performance H-mode, and steady-state operation with controlled enhanced confinement.

### **W.2.1 Controlling plasma start-up and soft landing (phase-1 and phase-2)**

Plasma breakdown followed by plasma current ramp-up and plasma landing at the end of the current ramp down phase are strongly coupled to the wall particle content. The operation of an all-metallic device, hence with different particle uptake by the wall, will modify considerably these regimes.

#### **W2.1.1 Optimizing plasma breakdown and ramp-up**

Controlled plasma breakdown, minimizing the loop voltage at breakdown, and therefore possible arcing, and preventing the generation of fast electron beams are important to reduce the impact of this early plasma phase on the wall properties. Switching to the divertor configuration and coupling HF heating early in the current ramp-up phase will contribute to extending the plasma current flat-top. Such a scenario also requires an appropriate control of the plasma density to minimize tungsten erosion governed by high electron temperature in the divertor as successfully achieved in JET-ILW for example [Mailloux2012].

For the ramp-up phase, the stability map at high aspect ratio with respect to MHD instabilities generated at rational edge safety factor values and favored by low plasma inductance will be studied. Developing safe scenarios, including that needed for addressing low safety operation during flat-top, will be needed. This is especially important to prevent disruption occurrences.

Furthermore, in the course of testing PFCs, with regular vessel opening for installing new components, possibly with different behavior during plasma operation, the wall conditions can vary. The use of the upper divertor for the early plasma phase could be a way to ensure stable wall conditions, with little impact of the plasma landing conditions at the lower divertor.

### W2.1.2 Developing plasma soft landing scenarios

During plasma ramp down, controlling the density is also mandatory to avoid reshuffling the wall conditions by hitting disruption conditions at the density limit too early in ramp-down and therefore at large plasma current. The operation with actively cooled PFCs, with thermal characteristic time comparable to the plasma current ramp-down phase can further modify the ramp down conditions. An important issue for this phase of plasma operation is the effectiveness of the WEST pumping system combined to the transient wall uptake in maintaining appropriate density conditions during all the current ramp-down phase. Advanced scenarios, such as ramp down with plasma heating, might be necessary to maintain divertor plugging and effective pumping capability.

These phases are tightly connected to the status of wall conditioning. Standard conditions with low wall outgassing at breakdown in will favor soft plasma breakdown strategy and controlled ramp-up scenarios. Similarly, low intrinsic light impurity content, carbon and oxygen, will reduce the disruption occurrence by plasma radiative collapse during ramp-down.

### Deliverables, priority and timeline

Deliverable W2.1.1: Optimizing plasma breakdown and ramp-up (mostly phase 2)

Deliverable W2.1.2: Developing plasma soft landing scenarios (mostly phase 1)

Part of the topics will be addressed during phase-1 in close connection with the conditioning program under Headline-1, W.1.4. However, full optimization in support of advanced operation modes will require dedicated experimental time during phase-2.

### W.2.2 Optimizing robust heating scenarios (phase-1)

Once the LHCD and ICRH systems are commissioned, operation at high enough power to enter the H-mode will be needed as early as possible during the restart phases. Optimizing the heating scenarios can then be addressed with the appropriate plasma conditions.

#### W2.2.1 Edge density for optimum LHCD performance

Lower Hybrid coupling is sensitive to the plasma density in the vicinity of the launcher. Controlled coupling conditions have been achieved with dedicated gas injection close to the launcher. This beneficial operation condition must be investigated together with the radial distance to the separatrix in different scenarios, in particular L-mode versus H-mode scenarios and balanced by the core density increase that will tend to reduce the current drive efficiency.

The edge conditions (gas, radial distance) need to be optimized taking into account the fact that two different LHCD launchers with different coupling characteristics are used. In this context, WEST will be a unique opportunity to validate the ITER-relevant LHCD launcher design in long duration H-mode plasmas.

The energy transferred to the fast electron beam in the Scrape-Off Layer plasma located radially in the vicinity just ahead of the launcher is proportional to the density there. Hence depending on conditions one can obtain very high energy fluxes to the PFCs connected along the field line. Optimizing the gas injection for LHCD coupling and appropriate edge density is therefore mandatory for plasma heating and current generation.

### W2.2.2 Edge density for optimum ICRH performance

The edge density is also crucial for efficient ICRH coupling. Here again, local gas injection appears to alleviate this coupling issue. The edge conditions (gas, radial distance) need to be optimized, with a trade off between the thermal load on the antenna and the density needed for efficient coupling (note that the WEST antennas are movable radially, which adds flexibility).

Part of the problem for ICRH is due to the development of large sheath potentials induced by the ICRH waves at the end of field lines that are close to the antenna front face. These potentials built by a rectified sheath effect accelerate the ions to high energy producing important impurity sources, a critical issue with tungsten wall. Furthermore, they tend to generate a large scale convection pattern in the Scrape-Off Layer depleting the density in some regions and increasing it at others. This large scale distortion of the Scrape-Off Layer density profile has a strong impact on all systems depending on edge conditions, such as density measurements and LHCD coupling.

In addition, ICRH coupling has been shown to be sensitive to ELMs : ELM resilient matching will have to be achieved (see also W2.5.5).

### W2.2.3 Interplay of divertor density and radio-frequency heating systems

The edge density plays an important role for LHCD and ICRH coupling as well as the divertor density regimes. Each element is equipped with a specific gas injection system. However, the edge density directly couples the density at all three locations and the synergy between the divertor density regimes and high performance LHCD and ICRH is to be achieved with dedicated experiments for different scenarios. Last and not least, the edge density and gas injection determine the core density. In particular, in steady state, particle balance between the injected gas and the pumping capability must be achieved to prevent a density limit disruption.

### W2.2.4 ICRH absorption and ripple losses

The amplitude of the toroidal magnetic field ripple at the outer separatrix will be of the order of 2%. The good confinement region depends on the value of the plasma current and on the shape of the current profile. For example, with plasma current smaller than 0.57 MA, and a parabolic current profile, no good confinement zone is expected. Hence a significant fraction

of ICRH power, up to 25 %, can be promptly deposited in ripple loss regions on the baffle. A proper accounting of these ripple losses is mandatory: first one must check that the deposition on the baffle does not exceed its heat extraction capability, second one must verify that ripple losses do not affect the baffle nose and the lower divertor, finally a precise value of the ICRH power coupled to the plasma is needed to obtain an accurate power balance.

It is also necessary to determine the ion current loss that will have an impact on the radial electric field profile, and consequently on the H-mode and ELM behavior,

Another point to be addressed is the use of ICRH as a limitation tool to prevent tungsten accumulation in the core plasma. It will then be necessary to search for the ideal trade-off between ripple losses and central ICRH absorption needed for tungsten accumulation control. Regarding the latter point, the impact of fast ion ripple losses on neoclassical transport can be an issue.

ICRH operation also generates ion acceleration by rectified sheath effects at the plasma edge. This is an issue for PFC operation and tungsten generation by ICRH as well as for a precise analysis of the ICRH power effectively coupled to the core plasma.

#### **W2.2.5 ICRH electron to ion heating ratio dependence on H minority concentration**

The hydrogen minority heating scheme will be the main scheme used in WEST. The isotopic ratio will be given by the  $H_{\alpha}$  and  $D_{\alpha}$  lines at the edge and in the pumping system. Request on a flexible ratio between electron and ion heating will depend on the development required for tungsten control and H-mode performance. The experience gained on Tore Supra will help minimizing the effort in developing these ICRH heating scenarios.

Modelling by a full wave solver with a Fokker–Planck module such as EVE/AQL will provide the balance between the ion and electron energy flux coupled to the core plasma and information on the expected impact of the hydrogen concentration. Precise modelling with the CRONOS code must then provide the balance between the ion and electron energy flux channels at the separatrix. The impact of the hydrogen concentration on ICRH losses must also be assessed as input to the power balance.

Furthermore, particle transport modelling must yield the hydrogen concentration in the core for given boundary values to be compared to ICRH heating models.

Finally, the trace hydrogen concentration provides a means to investigate the wall particle uptake and eventually an estimate for retention times exceeding the time between shots.

#### **W2.2.6 Lower Hybrid coupling and fast electron ripple losses**

At low collisionality, enhanced electron ripple losses due Lower Hybrid electron acceleration have been reported. A specific PFC has been installed to protect top components from these strongly localized heat deposition patterns. These losses must be determined for the WEST large aspect ratio. Dependences on key plasma parameters as well as the analysis of the power deposition on the ripple protection PFC must be achieved early in phase-1.

Possible, fast electron ripple deposition on the upper divertor must be investigated for safe operation of this component.

Power and current transport due to electron ripple losses must be determined for a precise power balance. Furthermore, LH generated edge electron beams, depending on edge density conditions must also be analyzed in the framework of Lower Hybrid heating.

#### W2.2.7 Lower Hybrid Current Drive efficiency at high density

Achieving adequate lower hybrid current drive efficiency is a milestone of the WEST program. Given the large aspect ratio in WEST and the pedestal density gradient foreseen during H-mode operation, experimental investigation can be required for achieving appropriate current drive efficiency and address H-mode long pulse operation. Indeed, the H-mode edge can hinder the Lower Hybrid wave propagation beyond the pedestal region and affect the current drive efficiency of the Lower Hybrid waves.

Studies of the Lower Hybrid power deposition profile and current drive efficiency will be carried out, using the Hard X-ray diagnostics, which will be compared with predictions from the ray-tracing and Fokker-Planck, codes C3PO/LUKE. Different  $N_{\parallel}$  spectra will be tested in the foreseen scenarios, in order to achieve simultaneously efficient current drive and good Lower hybrid wave penetration into the plasma core. In addition, a trade-off between optimum current drive efficiency, favoring lower collisionality operation and therefore low plasma density, and the control of tungsten source favoring high density operation will have to be addressed. Operation at high pedestal density will most likely be particularly demanding.

#### W2.2.8 Interplay between LHCD and ICRH operation

Combined operation of LHCD and ICRH is a high priority to achieve high performance scenarios. It will be pursued in phases 1 and 2. This will require a trade-off between various aspects: ripple losses, LHCD and ICRH coupling, LHCD current drive efficiency, tungsten source monitoring. Compatibility of the local gas injection systems, with possible cross talk between LHCD and ICRH via the edge density, with the pumping capability and divertor operation are addressed under Headline-1 as part of the edge particle balance. Mastering the combined operation of LHCD and ICRH is a key point to develop high performance scenarios both to test ITER-grade PFCs and to develop long pulse H-modes as well as advanced confinement and steady-state operation.

#### Deliverables, priority and timeline

Deliverable W2.2.1: Edge density for optimum LHCD performance (phase 1)

Deliverable W2.2.2: Edge density for optimum ICRH performance (phase 1)

Deliverable W2.2.3: Interplay of divertor density and radio-frequency heating systems (phase 1)

Deliverable W2.2.4: ICRH absorption and ripple losses (phase 1)

Deliverable W2.2.5: ICRH electron to ion heating ratio dependence on H minority concentration (phase 1)

Deliverable W2.2.6: Lower Hybrid coupling and fast electron ripple losses (phase 1)

Milestone W2.2.7: Lower Hybrid Current Drive efficiency at high density (phase 1 and 2, high priority)

Deliverable W2.2.8: Interplay between LHCD and ICRH operation (phase 1 and 2, high priority)

Determining appropriate conditions for LHCD and ICRH operation will be addressed early during phase-1 and yield precise information on the various loss channels. This will be part of the experiments in view of establishing robust H-mode scenarios.

Regarding ICRH, request on a flexible ratio between electron and ion heating will depend on the development required for tungsten control and H-mode performance mainly during phase 1. The experience gained on Tore Supra will help minimizing the effort in developing these ICRH heating scenarios.

Establishing Lower Hybrid Current Drive scenarios in WEST H-modes is a high priority task. Several experimental days during phase-1 will have to be dedicated to this key issue of the program in preparation for phase 2.

Combined operation of LHCD and ICRH is a high priority to achieve high performance scenarios. It will be pursued in phases 1 and 2.

### W.2.3 Density and tungsten control in long pulses (phase-1 and 2)

This task will require both dedicated experimental effort as well as appropriate adjustment with pulse duration and PFC ageing leading to changes of the tungsten source pattern. Compared to high performance short pulse experiments, where the duration can be limited by overwhelming core tungsten radiation, the aim is here to operate long H-mode pulses with constant tungsten source and without accumulation in the plasma core, hence core concentration remaining below the  $10^{-4}$  limit. As the pulse length gets longer this requires either a strict operation point with known tungsten source or appropriate feedback methods to maintain the tungsten source constant on average. In a full tungsten-PFC environment, tungsten impurity can be produced:

- by deuterium sputtering,
- by light intrinsic or extrinsic impurities sputtering,
- by self-sputtering that can lead to a runaway in the tungsten source.

Transient sources can occur, either governed by arcing and/or dust. ELMs also play a role in generating additional tungsten source. Slow evolution of the tungsten source can then stem from:

- an increase of the light impurity content,
- a slow increase of the electron temperature at the plasma-wall interaction region,
- ill-operation due to uncontrolled ion acceleration by rectified ICRH sheaths,
- operation with a damaged PFC.

The source pattern, from the divertor, main chamber wall, antennas and launchers governs different edge plasma penetration probability. This will modify both the effective impact on operation and the characteristic time scale.

Given the tungsten penetration into the edge plasma, core transport properties further transform the response of the system in terms of core tungsten concentration and dynamics. These

transport properties can also be characterized by a slow drift that can only be observed and therefore addressed in the framework of long pulse operation. Two unfavorable mechanisms are reported to favor tungsten impurity accumulation in the plasma core: an inward edge pinch that drags the impurities into the plasma despite the H-mode barrier, and neoclassical impurity peaking. The latter generates a tungsten peaking factor, which is that of the main ion species at the power  $Z_w$  where  $Z_w$  is the tungsten charge. The peaking exponent  $Z_w$  can exceed 40. As a consequence, any peaking of the main species will govern strong tungsten peaking, close to a factor 10 for a main species peaking factor of 1.05.

Tungsten accumulation in the core governs an increase of line radiation that can generate a radiative collapse and lead to a disruption or to the termination of the high performance phase of the pulse. It is therefore essential to determine means limiting both tungsten sources and core accumulation.

WEST with its long pulse operation capability then appears as a key facility to demonstrate that steady-state conditions are effectively achieved and that there is no slow drift of plasma conditions that will ultimately drive tungsten accumulation. It will thus provide experimental evidence of safe long pulse operation with metallic walls, as will be required in ITER.

### W2.3.1 Tungsten erosion and tungsten source pattern

The location of the source of tungsten impurity is a question that deserves run time. The impact of light impurities on the tungsten impurity source also deserves attention. Because of its large mass, tungsten erosion by deuterium and tritium is expected to be negligible for most divertor conditions. In present experiments one finds that light impurities are the main responsible for tungsten erosion, which require that operation conditions reach sufficiently low electron temperature, typically smaller than 10 eV in the divertor.

WEST divertor combining extensive visible spectroscopic diagnostic and simplified divertor geometry will offer an opportunity to clarify the tungsten impurity source from the divertor. The ELM impact on the wall will also be studied, taking benefit of visible spectroscopy lines of sight. ICRH power required for WEST operation might also lead to additional tungsten sources by the rectified sheaths, see W2.2.2. This specific tungsten source and the contemplated effect of central ICRH heating to prevent tungsten accumulation will be the two terms of the trade-off that will determine the usefulness of ICRH for tungsten control. Finally, tungsten enhanced penetration with dust, generating UFOs, as well as arcing could play a role.

### W2.3.2 Divertor impurity screening

Divertors have demonstrated very strong screening capability, especially for heavy impurities. It has been argued that most of the eroded tungsten would experience prompt redeposition due to the very small ion Larmor orbit of the singly charged tungsten ion. Simulations with COREDIV have been carried out to address this topic in the WEST configuration [Marandet2013] (see annex 8). Finally, ELM conditions at the divertor in present experiments are such that tungsten erosion by deuterium can dominate the tungsten source during the ELM. The divertor impurity screening and divertor tungsten migration must be assessed experimentally.

### W2.3.3 Tungsten transport in the confined plasma

Tungsten accumulation in the plasma center will lead to an early termination of the high performance plasma required to sustain long pulses. Control of the tungsten source and core transport is therefore mandatory for the WEST program. At least two different scenarios, both for long pulse discharges and with controlled tungsten accumulation, are required: a high density scenario, with moderate pedestal performance and conversely a low collisionality scenario with a high pedestal performance.

Given the large charge of the tungsten impurity, tungsten collision effects are enhanced by a factor  $Z_W^2$ , where  $Z_W$  is the tungsten charge. This transport mechanism can then compete with turbulence to determine the tungsten transport and in particular its density profile. This is the standard case in the plasma center, where weak turbulence and large neoclassical transport can lead to tungsten peaking. Neoclassical transport also depends on the magnetic field ripple as well as on the radial electric field profile, and consequently for WEST on the heating scheme and on turbulence

One can thus readily expect that the WEST data base will provide cases where neoclassical transport appears to be dominant, possibly with transitions in space and time between turbulent and neoclassical regimes.

Central heating has been used to control tungsten peaking. It is then understood that turbulent transport is enhanced, up to the stage where it can balance neoclassical transport. However, the intricate transport mechanisms taking place require precise experimental analysis backed by comprehensive modeling. As an example, tungsten transport is coupled to plasma rotation and to the electric field, both being related to neoclassical transport, turbulent transport, as well as to heating schemes. Again tungsten can be used to improve our understanding of the interplay between these transport mechanisms. Last and not least, the dependence of turbulent transport on the aspect ratio will reduce the impact of trapped particles in the transport mechanism and provide a means to differentiate the role of different instabilities.

### W2.3.4 Tungsten transport during MHD relaxation

MHD relaxation events, such as sawteeth and ELMs, are known to contribute to maintaining the tungsten impurity at a low value. During the transient relaxation event, impurity flush out is then considered to take place. However, a precise understanding of such a process and its efficiency in terms of impurity control mechanism remains to be assessed. This can also apply to helium ash control required in next step devices. Experimental evidence with trace tungsten could then be used in conjunction with non-linear MHD modeling to provide an accurate representation of the impact of MHD relaxation transients on impurity transport.

### W2.3.5 Control of tungsten accumulation

Control of tungsten during long pulse operation is a major issue for the WEST program. A robust means to prevent tungsten accumulation is to prevent density peaking. Empirically this appears to be the most reliable control procedure. Core heating, inducing confinement



degradation, and consequently flat density profiles is considered to be a good actuator to control the issue of tungsten peaking. Given the complexity of the transport processes, and the important benefit in terms of fusion power of achieving density peaking, a comprehensive investigation of this physics must be addressed. Regarding the aim of the WEST project, the development of a robust scenario allowing one to prevent tungsten accumulation, and thus opening the way to long pulse H-modes is however sufficient. WEST will be heated by LH and ICRH, hence mostly electron heating, which should contribute to preventing W accumulation. Feed-back control of tungsten accumulation with core heating is a milestone regarding the development of phase-2 long pulse scenarios.

### W2.3.6 Tungsten control for low collisionality pedestal performance

As underlined by the neoclassical accumulation process, tungsten control is tightly linked to the control of the main species density and density profile. High density regimes appear to be quite favorable by leading to lowered electron temperature in the divertor, higher divertor screening efficiency, and also flat core density profile. However, high density regimes might prove to be challenging for LHCD efficiency. For several scenarios of phase-2, a low density, low collisionality regime, would be useful provided that controlled core contamination by tungsten is achieved. Such a low density H-mode scenario, with decoupled detached divertor and high performance pedestal would have two key assets. First the low core density being favorable for LHCD current drive would facilitate long pulse operation and hopefully steady state conditions. Second the high performance pedestal would lead to both an enhanced bootstrap current and an increase of the amplitude of the ELM relaxation events. This would provide additional flexibility to operate WEST with larger ELM cycling for the investigation of PFC ageing.

#### Deliverables, priority and timeline

Deliverable W2.3.1: Tungsten erosion and tungsten source pattern (phase 1)

Deliverable W2.3.2: Divertor impurity screening (phase 1)

Deliverable W2.3.3: Tungsten transport in the confined plasma (phase 1)

Deliverable W2.3.4: Tungsten transport during MHD relaxation (phase 1)

Milestone W2.3.5: Control of tungsten accumulation (phase 1 and 2; high priority)

Deliverable W2.3.6: Tungsten control for low collisionality pedestal performance (phase 2, high priority)

Developing a high density scenario without tungsten accumulation and with sufficient LHCD efficiency should be addressed during phase-1 with dedicated experimental time. A low collisionality scenario, also with controlled tungsten contamination, would ease the ageing tests of ITER PFCs during phase-2. The development of this scenario should start during phase-1 but could be completed at the beginning of phase-2.

#### W.2.4 Access to long pulse H-mode (phase-1 and phase-2)

Preliminary analysis based on existing scaling laws indicates that achieving the H-mode on WEST should not be an issue. However, since the theory of the H-mode transition is not complete, the WEST experiments will contribute to the description of the H-mode by addressing the transition physics in a high aspect ratio device. Other issues that will be addressed are the impact of magnetic field ripple, divertor geometry, and eventually the impact of a limited pumping capability. WEST will be equipped with Doppler reflectometers. This will allow one studying in details the L to H transition dynamics, in particular the radial electric field evolution and the turbulence level modification as done in DIII-D recently for example [Schmitz2012]. The dynamic of this transition will be compared to on-going non-linear turbulence modeling.

##### W2.4.1 H-mode power threshold

The uncertainty on the power required to achieve the H-mode, estimated from the present scaling laws, is quite large for ITER, although its geometry is comparable to that of most of the devices in the data base. Regarding WEST, for most of the parameters, the calculation of the threshold power appears to be an interpolation, thus reducing the error bars on the scaling laws. However, regarding several other parameters (aspect ratio, ripple, top triangularity, wall clearance) it is an extrapolation, with larger error bars. Determining the H-mode power threshold on WEST is therefore a milestone of the program. In that framework, WEST will test if the scaling laws tend to be optimistic or pessimistic with respect to the H-mode threshold. This should be an incentive to revisit the scaling laws and hopefully contribute to reducing the error bar in the projection towards ITER

##### W2.4.2 Impact of aspect ratio and magnetic ripple

The properties of the H-mode threshold on WEST can bring new evidence and help clarifying some pending issues regarding the power scaling of the H-mode threshold. The impact of magnetic field ripple as well as aspect ratio on the power threshold appears to be as an open issue. Analyzing the H-mode transition with different conditions can shed new lights on the H-mode transitions and drive a renewed theoretical effort on this issue.

**Large aspect ratio:** The aspect ratio is not used as a scaling parameter in the ITPA scaling [Martin2008]. However higher power than predicted by this scaling has been reported for spherical tokamaks [Takizuka2004] characterized by a small aspect ratio. The aspect ratio is introduced in the 2004 scaling and indicates that the threshold power decreases with increasing aspect ratio. Should this dependence be monotonic up to the WEST values of the aspect ratio would lower the H-mode threshold power.

**Ripple impact:** in WEST, at the separatrix, the ripple of the toroidal magnetic field is typically of 2%. The ripple up to 1.1% did not affect the threshold in JET [Andrew2008], but in earlier JET experiments, when switching from 32 to 16 coils, hence with a ripple factor reaching 10%, the H-mode was not obtained even with auxiliary power 6 times larger than the threshold value at low ripple [JETteam1992]. Conversely, on JT-60U, the power threshold was reduced when increasing the ripple [Tobita1995].

### W2.4.3 Impact of X-point height, main ion species and effective charge

The H-mode threshold appears to be closely linked to particle recirculation at the plasma edge. First evidence of this correlation has been the importance of machine conditioning. The density dependence of the threshold power is another indication as well as the dependence on the X-point height, the threshold power decreasing as the distance is reduced.

Radiation and consequently effective charge have also been considered as important parameters, these points being connected to the conditioning issue. Finally, the main species also seems to play a role, with a slight increase of the threshold power in helium with respect to deuterium.

The investigation of H-mode properties on WEST must therefore aim at clarifying several of these issues.

The standard operation mode in WEST is a lower single null configuration. The X-point height can be changed typically from 0 to 15 cm. The impact of the X-point height is known to reduce the H-mode threshold power [Gohil2011]. This property can also be analyzed on WEST where the large clearance with the main chamber wall can be useful to separate various parameters. The power threshold also seems to be reduced with metallic walls as observed in JET and ASDEX-Upgrade [Maggi2013, Neu2013]. Several authors have thus suggested that the effective charge could be an important parameter [Takizuka2004, Bourdelle2013]. However this reduction is also associated to a reduced improvement in confinement. Seeded light impurities, increasing radiation and the effective charge, appear to lead to an improvement of confinement. Again complex nonlinear phenomena seem at work, either changing the threshold power or changing the confinement properties.

It is to be noted however that in many cases, hidden parameters are also changed when changing species or effective charge. In WEST, the comparison between He and D operation should be more straightforward than for devices equipped with neutral beams and cryopumping. Indeed, for instance, WEST electron heating with RF should be less dependent on ion-ion slowing down properties. Similarly the WEST pumping system is less sensitive to the species than the cryopumps.

Finally, several new theoretical ideas have recently been proposed to explain the H-mode transition, for example [Fedorczak2012]. They offer a new guideline for experimental investigation.

### W2.4.4 Long pulse H mode operation

The objective is to extend the ITER reference H mode scenario on relevant plasma wall equilibrium time scale (~minutes). This requires developing an integrated scenario, addressing the issues mentioned below :

- addressing RF coupling issues in a W environment
- controlling the W sources and transport over time longer than the plasma wall equilibrium
- optimizing the compromise between W accumulation control and good energy confinement over long pulses
- controlling plasma density with a moderate pumping efficiency
- controlling the MHD activity

- demonstrating impurity seeding for power exhaust control on long pulse

In addition, the work carried out under Headline 2 will be used for supporting scenario development for Headline 1. In particular, robust H mode scenario providing high power on the divertor (in the range 10-20 MW/m<sup>2</sup>) and/or large ELMs for thermal transient testing of the ITER like W components will be required, as well as very long pulses (up to 1000 s) to optimize the cumulated particle fluence on the divertor for plasma wall interaction studies.

### **Deliverables, priority and timeline**

Deliverable W2.4.1 H-mode power threshold (high priority, phase 1)

Deliverable W2.4.2 Impact of aspect ratio and magnetic ripple (phase 1)

Deliverable W2.4.3 Impact of X-point height, main ion species and effective charge (phase 1)

Milestone W2.4.4 : long pulse H mode operation (high priority, phase 2)

The transition from L-mode to H-mode will be addressed at the beginning of phase-1 so that H-mode operation can become as early as possible the routine scenario. Step by step improvement of the H-mode performance and on the threshold power scaling will then be addressed during phase-1 and will require dedicated experimental days.

## **W.2.5 Optimizing confinement for long pulse H-mode operation (phase 1 and phase 2)**

In metallic wall machines, ASDEX-Upgrade and JET, fuelling has been shown to reduce the core tungsten contamination. However, increasing the fuelling also degrades confinement and in particular that of the pedestal [Beurskens2013]. Such a trade-off is consistent with the fact that a means to reduce the tungsten confinement is to reduce the overall confinement; this is the case of ELM and sawteeth impurity control as well as core heating to prevent impurity accumulation. It is far more challenging to reduce tungsten confinement specifically while maintaining or improving energy confinement [Putterich2012]. Two issues are at hand; regarding the tungsten source, fuelling must modify the tungsten source by increasing the particle flux to the wall and therefore reducing the electron temperature at the sheath, regarding confinement, the correlation between fuelling and confinement needs clarification. WEST, with actively cooled components and therefore true steady-state conditions for plasma wall interaction, as well as long pulse capability, longer than transient governed by density build-up, offers a unique experiment allowing one to identify the actual control parameters.

Pedestal confinement can also be investigated in terms of the pedestal width, hence the extension of the H-mode barrier, or external transport barrier, towards the core plasma, on the one hand, and into the SOL on the other hand.

Finally issues related to the energy scaling law should be addressed in WEST. The dependence on the aspect ratio is to be investigated, but also the isotope dependence as well as the degradation with  $\beta$ , the ratio of the plasma pressure and magnetic pressure.

### **W2.5.1 Particle confinement and pedestal degradation with fuelling**

Fuelling is required for two purposes, transiently to increase the density and in steady state density conditions to compensate the pumped particle outflux. There is then a conflict

between the improved confinement governed by the density dependence of the energy confinement scaling and degradation by fuelling.

Improving our understanding and the experimental investigation of the correlation between fuelling and pedestal degradation is important to address optimized confinement regimes with reduced tungsten source, reduced tungsten confinement, and good energy confinement. This physics then requires that one addresses the main species particle confinement on the same footing as heat confinement. In such a framework density is no more a control parameter, as considered in all scaling laws, but results from the balance between the particle source and transport. Alternative fuelling with pellets can offer a means to separate wall and particle recirculation control parameters, see W2.8.2.

### **W2.5.2 Pedestal height, width and location**

Pedestal width, pedestal height and consequently pedestal gradient are key parameters for plasma performance. One issue is the location of the external transport barrier. To address this point requires that one can identify clearly the separatrix, and that the latter only exhibits adiabatic displacements with respect to plasma confinement times. It is to be noted that high frequency motion of the separatrix will also be an issue for positioning the antennas and launchers.

Quite important regarding the WEST program is the extension of the region with reduced turbulent transport into the SOL. Indeed, it is often assumed that the H-mode turbulent reduction extends into the SOL, thus leading to a reduced width of the SOL heat channel. Precise investigation of this effect is required when analyzing the SOL heat channel width and the power balance.

### **W2.5.3 Obtaining low collisionality pedestal conditions**

Regarding confinement, and for the WEST PFC testing program, there is a strong interest in increasing the pedestal height in order to obtain large ELMs and to be able to cycle around the tungsten recrystallization temperature.

Large pedestal height leading to larger ELMs is shown empirically to be more easily obtained at low collisionality [Loarte2003]. There is thus a challenge in obtaining low collisionality pedestal conditions while maintaining high recycling or detached divertor conditions. A figure of merit for such operation is the ratio of the maximum density in the divertor, in practice at the target plate in the high recycling regime, and the pedestal density. Low collisionality regimes for the core plasma are also benefic regarding current drive efficiency. Such a regime is most relevant for phase-2 scenarios and is therefore a milestone of the WEST program. The pedestal width also seems to be related to the collisionality regime, as exemplified by the VH-mode.

### **W2.5.4 ELM properties and their control**

WEST large aspect ratio is likely to lead to an increase of the ballooning limit. The triangularity is known to impact the pedestal stability. In WEST the upper triangularity can be varied from 0 to 0.6 and its impact on ELMs will be studied. Also at large aspect ratio, the

fraction of trapped particles being lower, a lower bootstrap current is expected which might change the ELM nature and dynamics.

When deuterium fueling leads to a cooler pedestal, the ELMs dynamics can be slowed down as observed in JET-ILW. A hotter pedestal can probably be obtained thanks to impurity seeding as observed in Cmod, ASDEX-Upgrade and JET-ILW [Giroud2012]. The role of resistivity on the ELM time scales can then be studied and compared with JOREK simulations.

Regarding the ELMs and the connection to plasma current, one can observe during large ELMs a coupling between ELMs and loop voltage. At each ELM crash a fraction of ions carrying the bootstrap current are expelled. The feed-back system, to maintain the total current then drives a loop-voltage spike to generate plasma current. This current will develop in the coolest regions, hence in the pedestal and modify the ELM cycle. The feed-back knowledge gained on Tore Supra provides a way to feed-back control directly on the flux consumption avoiding the plasma current regeneration process in the pedestal.

Finally, WEST has significant shaping capability, in particular regarding upper triangularity and large wall clearance (with the exception of LHCD launchers and ICRH antennas). This can be used to progress on separating shaping and wall interaction effects as well as investigating the dependence of ELM properties on plasma shaping.

It should be reminded that obtaining large ELMs is required for PFC testing purposes, as described in Headline 1, and is the main priority in this area. However, ELM mitigation techniques can be investigated, such as the impact of Supersonic Molecular Beam Injection [Zou2014] or of the LH heating system. Indeed, in EAST, LH heating has been shown to mitigate ELMs while broadening the heat deposition footprint [Li 2013, Liang 2012]. NB : WEST is equipped with a pellet injection system, which has been shown to be a successful technique to mitigate ELMs [Lang NF2010]. However, the present system is not well suited for ELM pacing purposes in terms of frequency and pellet size, as it is primarily targeted at steady state plasma fuelling.

Finally, ELM free H mode regimes could be investigated, such as the I mode on C-Mod [Whyte NF2010] or the QH mode on DIII-D [Burrell PPCF2002], EAST [Hu PRL2015].

### **W2.5.5 ELM resilient matching and improved arc detection**

In case of large ELM operation, ELM resilient matching as well as improved arc detection to separate arcing and ELMs will have to be operational for the ICRH system. Similar actions, for instance regarding feed-back controlled local gas injection might also be required both for the ICRH and the LHCD system to ensure consistency between efficient and reliable heating systems and plasma density as required by the program.

### **W2.5.6 Confinement dependence on the aspect ratio and edge safety factor**

In the energy confinement time scaling law the unfavorable dependence on the aspect ratio can be compensated by the dependence on the safety factor provided large aspect ratios allow one achieving operation at lower safety factor. These opposite effects would then lead to a dependence on the ratio of the poloidal and toroidal magnetic fields. Investigating this issue would provide a way to untangle the confinement dependences on safety factor, aspect ratio and plasma current. It is often argued that the usually accepted performance

optimum at a safety factor close to three is governed by increased disruption probability as the edge safety factor approaches two. However, for the Tore Supra ergodic divertor experiments the disruptive limit was observed to be for edge safety factors smaller than two. It is to be noted that regarding many important facets of Headline-2, the plasma current is a major player: as with respect to particle confinement; operation to achieve high densities, also regarding the density limit, since it appears in the Greenwald density, and finally regarding the SOL width scaling depending on the plasma current. There is therefore an incentive to explore higher plasma current regimes, hence reducing the edge safety factor below three.

### W2.5.7 Optimizing intrinsic rotation

WEST is particularly well suited for intrinsic rotation studies and rotation predictions for ITER, with RF heating only and no external momentum source. Intrinsic rotation is thought to result from the competition between turbulent transport processes, MHD effects, fast particle effects and non-axisymmetric field effects as the ripple-induced toroidal friction. Also, scrape-off layer flows are expected to influence the core rotation through plasma boundary conditions. All those contributing effects will be assessed in WEST L-mode and H-mode Ohmic / RF heated plasmas, with accurate rotation, radial electric field, and edge flow profiles provided by X-ray imaging crystal spectroscopy, Doppler reflectometry and probe measurements. Moreover, fast sweep reflectometers will allow for turbulence measurements. Finally, an extensive set of modelling codes will be used for data interpretation and comparison with theoretical predictions, including neoclassical theory predictions [Garbet10]: thermal and fast particle ripple-induced torques will be inferred from SPOT, EVE and LUKE codes, while turbulent momentum flux will be provided by gyrokinetic code simulations such as QuaLiKiz [Cottier2013] or GYSELA.

### Deliverables, priority and timeline

Deliverable W2.5.1: Particle confinement and pedestal degradation with fuelling (phase 1)

Deliverable W2.5.2: Pedestal height, width and location (phase 1)

Deliverable W2.5.3: Obtaining low collisionality pedestal conditions (high priority, phase 1 and 2)

Deliverable W2.5.4: ELM properties and their control (phase 1 and 2)

Deliverable W2.5.5: ELM resilient matching and improved arc detection (phase 1)

Deliverable W2.5.6: Confinement dependence on the aspect ratio and edge safety factor (phase 1 and 2)

Deliverable W2.5.7: Optimizing intrinsic rotation (phase 1 and 2)

Most of the experimental issues quoted above will be addressed in the course of H-mode operation and optimization. The main experiments will thus be achieved during Phase-1. The problem of generating a low collisionality pedestal is part of the scenario development for phase-2 and should be addressed in both phases.

Although ELM observations will be part of all H-mode experiments, dedicated experiments will be a high priority to optimize the ELM size and develop the Wall Monitoring System capable of

determining the ELM deposition pattern. It will be developed during phase-1 and phase-2 to be fully operational during phase-2.

The part of the program depending on the low safety factor operation experiments could be postponed to phase-2.

Plasma rotation is an important player to investigate confinement impurity transport as well as MHD behavior. Dedicated experiments might be needed to identify the mechanisms generating the rotation profile and their interplay, during phase-1 in particular, and optimize the intrinsic rotation profile, possibly extending in phase-2.

## **W.2.6 Towards disruption-free campaigns (phase 1 and phase 2)**

### **W2.6.1 Disruption and VDE characterization**

The study of the current quench dynamics including runaway electrons and of the resulting halo current magnitude and asymmetries is of prime interest for reactor-regime tokamaks in general and for ITER in particular. Incorporation of a set of eddy current and halo current measurements combined with strain gauges in the divertor supporting structures will allow for the extension of the ITER disruption database.

### **W2.6.2 Disruption and runaway electrons mitigation**

Transition from carbon to metal environment has shown significant differences on the disruption behavior: longer current quenches, low radiation during the current quench due to the absence of carbon, less frequent runaway electrons. These features are foreseen to have consequences on the mitigation strategy for ITER. WEST will contribute to investigating the impact of a metallic environment on the disruption process. WEST has reduced risks of severe disruption damages compared with JET thus providing easier conditions for disruption and runaway studies. Burst-disc cartridges concept for ultra-fast injections (FIRE device) may also be further tested in metallic environment. Comparisons of unmitigated and mitigated disruption behavior with simulations could be performed using the 3D MHD code JOREK supplemented by a gas jet-plasma interaction modelling. Runaway electrons generation during disruptions and their dynamics could be assessed coupling the LUKE code to the transport code CRONOS.

### **W2.6.3 Disruption-free long pulse campaigns**

Disruption-free campaigns can only be achieved with a threefold action. First the long pulse scenarios must be safe with respect to operational limits of both plasma conditions and system reliability. Second disruption avoidance strategies must be put in place in particular appropriate ageing signs, such as arcing, UFOs, hot spots on components must be carefully monitored and limit must assigned to prevent the risk of driving a disruption with a component failure. This also requires strict component conditioning by plasma operation prior to the repetitive pulse campaign. Finally the disruption mitigation technique must reach sufficient maturity to be used routinely and to ensure that the heat loads or prompt energy



deposition during mitigated disruption are smaller than experienced during standard operation.

### **Deliverables, priority and timeline**

Deliverable W2.6.1: Disruption and VDE characterization (phase 1)

Deliverable W2.6.2: Disruption and runaway electrons mitigation (phase 1)

Deliverable W2.6.3: Disruption-free long pulse campaigns (phase 2)

## **W.2.7 Current profile control and MHD stability (mostly phase 2)**

As discussed in the program, repetitive pulse campaign dedicated to gradual ageing tests of PFCs require that one avoids operation near operational limits usually characterized by MHD activity. However, there is more to current profile control than disruption issues.

### **W2.7.1 Assisted plasma breakdown and current ramp-up**

Plasma breakdown and plasma current ramp-up use most of the magnetic flux. Assisting these two steps with ECRH or LHCD can provide substantial magnetic flux saving that can be used to extend the current plateau at small loop voltage. Furthermore, this know-how will be useful in for the JT60-SA program and DEMO scenarios where the available magnetic flux will be limited.

This program is relevant for phase-2 by extending the induction phase of long pulse operation. Experimental days will be required before achieving a standard procedure.

### **W2.7.2 Stability of low safety factor operation**

As stated in W2.5.4 there is a possibility of extending large aspect ratio discharges towards lower safety factor. Developing such a scenario and analyzing its density limit, or sawtooth activity, means running close to operational boundaries with higher risk of reaching an MHD limit.

Exploring the MHD stability diagram is a phase-1 program which will be refined during phase 2.

### **W2.7.3 Fast ions and electrons interplay with MHD**

WEST being heated by LH and ICRH, both fast ion and electron populations are present in the plasma. This can lead to specific instabilities for both MHD and turbulence. On the MHD side, electron fishbones could lead to a redistribution of fast electrons (and a modification of the current profile), which is possibly involved in the Oscillating Regimes. Alfvénic instabilities due to fast ions are also possible, as reported on Tore Supra [Udintsev2008]. The impact of these fast ion driven instabilities could be investigated with the XTOR-K code. On the turbulence side, Geodesic Acoustic Modes can be destabilized by fast ions [Zarzoso2013], and this could be investigated with the GYSELA code. Furthermore, the specific fast particle wall deposition pattern associated to this activity must be identified and analyzed.

Fast particle interplay with MHD can be observed during experiments of other parts of the program, mostly during phase-1. A specific program can then be built on these observations.

#### **W2.7.4 Operational space without double tearing mode**

Off axis LHCD will lead to reversed safety factor profiles and hence will be vulnerable to tearing modes. Advanced MHD models have proved to be necessary for interpreting the stability limits and nonlinear saturation of these modes in Tore Supra: both diamagnetic rotations and neoclassical forces play an important role. MHD modeling of core tearing modes with XTOR-2F will be compared to experimental results. Such a detailed study is essential for low loop voltage operation needed for the large integrated particle flux experiments during phase-2.

Lower hybrid operation will provide a first picture of the operational space free of double tearing modes. The development of long pulse scenarios in phase 2 should complete this effort without requiring specific experimental days.

#### **W2.7.5 Statistics for Neoclassical Tearing Modes in long pulse operation**

Neoclassical Tearing Modes are generated when a combination of conditions are met including excitation by sawteeth. Their occurrence then appears to follow some statistical rule for given operation conditions. As a consequence, short pulses can appear to be free of Neoclassical Tearing Modes. One is then led to use a data base of shots that always exhibit small differences, and are also quite consuming in terms of run days due to the time delay between successive shots. Long pulse operation then provides conditions to investigate these statistics in a couple of pulses.

This topic requires specific experiments once detection of Neoclassical Tearing Modes in other shots allows one to determine experimental conditions to generate them. Given the long pulse requirement this is a phase-2 experiment.

#### **Deliverables, priority and timeline**

Deliverable W2.7.1: Assisted plasma breakdown and current ramp-up (phase 2)

Deliverable W2.7.2: Stability of low safety factor operation (phase 1 and phase 2)

Deliverable W2.7.3: Fast ions and electrons interplay with MHD (phase 1)

Deliverable W2.7.4: Operational space without double tearing mode (phase 2)

Deliverable W2.7.5: Statistics for Neoclassical Tearing Modes in long pulse operation (high priority, phase 2)

### **W.2.8 Advanced tokamak scenarios (phase 2 mostly)**

#### **W2.8.1 Fully non inductive H-mode discharges**

The physics of non-inductive discharges is substantially different from that of inductively driven plasmas, which are strongly constrained by resistive effects. In fact, the evolution of the main plasma quantities is governed by different types of non-linearity affecting, e.g., the absorption and current drive efficiency of the waves that sustain the non-inductive current, the fast electrons that carry such a current, the bootstrap mechanism, transport coefficients depending on the current density profile, MHD instabilities etc. This is of course of the utmost relevance for the second phase of the ITER program and for DEMO. These peculiar physics aspects have been investigated during many years of Tore Supra operation. In the WEST configuration, issues related to the divertor, H-mode physics, pedestal etc. will make this type of R&D even more relevant to ITER and DEMO. Long pulse H-mode discharges

will be in any case the workhorse of the WEST program, for divertor component testing; however, operation at feedback controlled loop voltage,  $V_{loop} = 0$ , is not necessarily required or suitable for that part of the program. Conversely, it can be the objective of specific experiments with the aim to prove compatibility of H-mode and zero loop voltage. This issue is therefore a Milestone of the WEST program. Tore Supra experiments in this field [Giruzzi2009] have shown that substantial additional difficulties are encountered when moving from very low to exactly zero loop voltage, in particular owing to the peculiar shape of the  $q$  profile and the associated MHD phenomena.

These experiments will require a careful choice of the plasma current – density operational domain in order to have a good margin for achieving a zero loop voltage with the available Lower Hybrid power. At zero loop voltage, flat-top time duration will be progressively extended from 30 s up to 1000 s. A multiple feedback strategy will be employed, with the following actuators: (1) gas puff to keep the plasma density constant, (2) Lower Hybrid power to keep the plasma current constant, and (3) transformer flux to keep the loop voltage constant and exactly equal to zero. At the same time, the power flux to the divertor, plasma contamination by Tungsten, hot spots and ripple losses should be kept under control, which will make these experiments challenging and useful for preparation of JT-60SA, ITER and DEMO scenarios.

### W2.8.2 Pellet fuelling in LH heated discharges

WEST will be equipped with the pellet injection system already used on Tore Supra, which is compatible with long pulse operation. Since high-density operation will be needed for several experimental regimes, the pellet system is expected to be routinely used. However, it is well known that the fast electrons produced by the Lower Hybrid waves used to sustain the long pulses greatly increase the pellet ablation, thus preventing deep fuelling [Pégourié2009]. For this reason, a specific scenario has been developed on Tore Supra, based on notching the Lower Hybrid power with a well-chosen time pattern and injecting the pellets during the phases in which the Lower Hybrid power is turned off and the fast electron tail has sufficiently decayed. The use of this technique in the new WEST configuration should be explored and validated for long pulses, as a pre-requisite for various high density experiments (in particular, the program at high Greenwald fraction). These experiments will provide valuable information for the use of Lower Hybrid waves in ITER steady-state scenarios, in which pellet fuelling is mandatory.

The experiments will be performed at full Lower Hybrid power, rather high density and with flat-top duration of at least 30 s. Combination with Ion Cyclotron heating at a power as high as possible should also be assessed.

Pellet experiments can be initiated during phase-1 especially to investigate alternative fueling. The main experimental activity will take place during phase-2.

### W2.8.3 High bootstrap discharges

Maximizing the bootstrap fraction is the key ingredient for steady-state operation of ITER and DEMO. In the past, Tore Supra experiments have been limited to rather low bootstrap fractions ( $< 30\%$ ). In the new WEST configuration, significantly higher values of beta poloidal will be accessible, allowing exploration of the impact of various levels of bootstrap

current in vanishing loop voltage discharges. Alignment of the various current density components and interplay with MHD activity will be decisive elements for the success of these scenarios. The potential interest of this program will depend on the attained plasma performance and remains to be carefully assessed by modelling and by the results of the first operation phase of WEST. The possible operation at reduced magnetic field ( $\leq 2$  T) is also being considered for this experiment.

The typical conditions of these experiments are: full LHCD and ICRH power, plasma current as low as possible ( $\sim 0.5$  MA), density close to the Greenwald density and flat-top duration of at least 30 s.

### W2.8.4 Internal Transport Barrier regimes

In Tore Supra, an Internal Transport Barrier (ITB) regime has been developed and systematically investigated in conditions of strong electron heating, negligible plasma rotation and dominant non-inductive current [Giruzzi2009]. These conditions are exactly those relevant for the long pulse operation of ITER and DEMO, although the actuators used will be different. In fact, the regime discovered on Tore Supra, called LHEP (Lower Hybrid Enhanced Performance) is based on the shear reversal in the plasma center produced by the LHCD, which naturally peaks off-axis. Originally developed at rather low density and power ( $n_e < 3 \cdot 10^{19} \text{ m}^{-3}$ ,  $P_{LH} \leq 3$  MW), the LHEP regime has been subsequently extended to higher densities, with the help of higher Lower Hybrid power.

The compatibility of this regime with a H-mode plasma edge, with tungsten accumulation and strong ICRH heating, as well its controllability for long pulses at vanishing loop voltage, will be one of the targets of the WEST advanced scenario program. Additional control of the Internal Transport Barrier by ECCD could also be tested. The main obstacle to steady-state and the reliability of this regime is the specific MHD activity associated with the reversed safety factor profile, i.e., double tearing modes. Combination of Internal Transport Barrier with the H-mode confinement will allow working at higher beta, therefore pressure effects will play a more substantial role in the MHD activity, with respect to the past Tore Supra regimes.

The typical conditions of these experiments are: full Lower Hybrid power, density as low as possible compatible with the divertor protection and the impurity contamination of the core, moderate ICRH power and flat-top duration between 30 and 60 s.

### W2.8.5 Long pulse hybrid scenario

The WEST configuration should make hybrid scenarios possible, which has never been the case for Tore Supra in the circular limiter configuration. Hybrid scenarios are now considered one of the leading ITER operation regimes, and are being seriously considered for DEMO. The long pulse capability of WEST will allow specific studies on the controllability of hybrid scenarios, with the aim of making this regime fully stationary and reliable. Moreover, on WEST this scenario can be explored in conditions of dominant electron heating and negligible rotation. Careful dosing of the Lower Hybrid and ICRH powers (and therefore of the inductive/non-inductive current ratio) should allow to study the impact of various current density sources on the safety factor profile and the plasma performances.

The typical conditions of these experiments are, as usual, similar to those of the H-mode, but on the lower current, higher power side: full LHCD and ICRH power, mid-range values of plasma current and density, flat-top duration of at least 30 s.

This is a phase-2 experiment. Performance evaluation compared to ITB scenario must be assessed.

### **Deliverables, priority and timeline**

[Milestone Fully non inductive H-mode discharges \(high priority, phase 2\)](#)

Deliverable W2.8.2: Pellet fuelling in LH heated discharges (phase 1 and phase 2)

Deliverable W2.8.3: High bootstrap discharges (phase 2)

Deliverable W2.8.4: Internal Transport Barrier regimes (phase 2)

Deliverable W2.8.5: Long pulse hybrid scenario (phase 2)

## **W.2.9 Controlled high density and high radiation regimes (phase 2 mostly)**

### **W2.9.1 Controlled high radiation regimes**

The fraction of power radiated in the plasma core is one of the key parameters for the design of both pulsed and steady-state DEMO concepts, at least in the hypothesis of employing the standard radiative divertor configuration, as in ITER. Typical levels of core radiation fraction expected are of the order of 75% [Zohm2013], which of course poses significant problems of power balance and control. Tungsten is a natural core radiator; however its excessive accumulation in the plasma core may lead to quick loss of performance, which would act nonlinearly for burning plasmas in which the dominant heating source is the fusion power. For these reasons, active control of highly radiative regimes is one of the most important physics and operation issues on the way to DEMO and the reactor. Owing to its long pulse capability and its large electron heating power, WEST can give a contribution in this area, exploring real-time control strategies combining central electron heating and impurity seeding. This will be also useful in preparation of the transition to tungsten divertor operation of JT-60SA.

These experiments will explore a wide range of plasma parameters, but rather at high densities, for flat-top duration of at least 30 s.

### **W2.9.2 Operation at high Greenwald fraction (>1)**

Because the fusion power has a strong favorable dependence on density peaking, most DEMO concepts employ high values of the Greenwald fraction,  $f_G \geq 1$ . Operation beyond the Greenwald limit is of course affected by a high disruptivity and the data base of discharges of this type is extremely sparse. Moreover, there is experimental evidence that even for  $f_G < 1$ , the energy confinement of H-mode plasmas tends to decrease with increasing  $f_G$  (an effect that can be partially compensated by a high triangularity). Conversely, the density peaking is known to increase with decreasing collisionality, a favorable circumstance for the high-temperature DEMO plasmas. Therefore DEMO scenarios are ideally expected to have  $f_G > 1$  globally, however a pedestal temperature below the Greenwald limit to prevent disruptions, a large peaking in the low collisionality plasma core and high shaping to recover

a good H-mode confinement. Demonstrating that  $f_G > 1$  scenarios can be sustained in stationary, long pulse discharges and exploring their controllability is therefore a valuable scientific objective that can be pursued in WEST, using its long pulse capability and high performance pellet injection system.

The typical conditions of these experiments are: full Lower Hybrid and ICRH power, plasma current as low as possible ( $\sim 0.5$  MA), density as high as possible and flat-top duration of at least 30 s.

### **Deliverables, priority and timeline**

[Milestone W2.9.1: Controlled high radiation regimes \(high priority, phase 2 mostly\)](#)

Deliverable W2.9.2: Operation at high Greenwald fraction ( $>1$ ) (phase 2 mostly)

Increased core radiation experiments with argon for instance can start during phase-1. However, the bulk of this program will be achieved during phase-2.

Increased core density experiments can start during phase-1 but will be mainly a phase-2 program.

## **W.2.10 Control of slowly evolving burning plasmas (phase 2)**

### **W2.10.1 Cyclic scenario**

A new concept of steady-state scenario for tokamak reactors based on cyclic operations has been proposed on the basis of integrated modelling simulations [Garcia2010]. This scenario alternates phases of positive and negative loop voltage with no magnetic flux consumption on average. In the case of the ITER steady-state regime, localized non-inductive current drive by Electron Cyclotron waves could be used to trigger and sustain an Internal Transport Barrier (ITB), whereas Neutral Beam Current Drive is used to periodically recharge the tokamak transformer. The fact of operating in cycles relaxes the hard constraint of simultaneous fusion performance maximization and full non-inductive operation, within the MHD stability limits. A linear MHD analysis of the instabilities that could appear in this type of scenario has shown that MHD stability would be strongly improved with respect to a steady regime with a strong ITB. Scenarios of this type have never been investigated experimentally, although transformer recharge by non-inductive current drive has been demonstrated (even on duration of the order of one minute on Tore Supra). The long pulse capability of WEST will make an experimental investigation of this concept possible, although using different actuators with respect to the simulated ITER steady-state case.

The typical conditions of these experiments are: full Lower Hybrid power, current and density as low as possible compatible with the divertor protection and the impurity contamination of the core, moderate to high ICRH power and flat-top duration between 30 and 1000 s.

### **W2.10.2 Simulation of alpha heating & Real Time control**

The non-linearity of alpha heating in burning plasmas makes the control of tokamak reactor discharges much more challenging than in present day experiments. Optimization of the discharge parameter and of its real-time control can be simulated by integrated modelling

## Chapter 3: WEST Research Plan

codes; another technique that has been used in some experiments (see, e.g., [Takenaga2008]) consists in using some of the conventional heating systems (e.g., NBI or ICRH) to simulate alpha heating, by an appropriate controller whose response to plasma parameter variations mimics the properties of self-heating by alpha particles. Non-inductive current drive could also be used simultaneously to simulate the bootstrap current.

This type of experiments could in principle be performed in WEST, taking advantage of the long pulse capability and of the LHCD and ICRH systems. The feasibility and practical implementation of these experiments should be carefully assessed by extensive integrated modelling simulations with the METIS and CRONOS codes [Artaud2010], coupled with appropriate feedback control modules.

The typical conditions of these experiments are: full Lower Hybrid and ICRH power availability, low current and flat-top duration between 30 and 1000 s.

### **Deliverables, priority and timeline**

Deliverable W2.10.1: Cyclic scenario (phase 2)

Deliverable W2.10.2: Simulation of alpha heating & Real Time control (phase 2)

These demanding programs will be addressed during phase-2.

## Tentative timeline for WEST exploitation

A tentative timeline for Headline 1 and 2 is given in Figure 16 and Figure 17 respectively, covering phase 1 and phase 2 of WEST exploitation. The headlines sub topics and the associated deliverables as listed in the previous sections are indicated and sequenced in time. Major milestones identified for WEST exploitation are shown in red.

The full color blocks indicate the timing proposed to address the associated deliverable with a high priority, while hashed areas correspond to periods during which the topic could be either prepared or further studied. Specific campaigns related to PFC testing for Headline 1 are shown in Figure 16 (such as campaign with misaligned/pre-damaged PFC, He operation, wall loading campaigns). They are also indicated as a reminder on Figure 17 for Headline 2.

Major shutdowns are indicated (such as the shutdown between phase 1 and phase 2, where the complete ITER like divertor will be assembled), but regular additional shorter shutdowns will also take place (for PFC exchange or regulatory maintenance for instance). They are not yet shown at this stage.

Note that the present timeline proposal should be seen as an initial draft, which needs to be consolidated and will be revised as the preparation of the WEST scientific exploitation will proceed.



### Chapter 3: WEST Research Plan

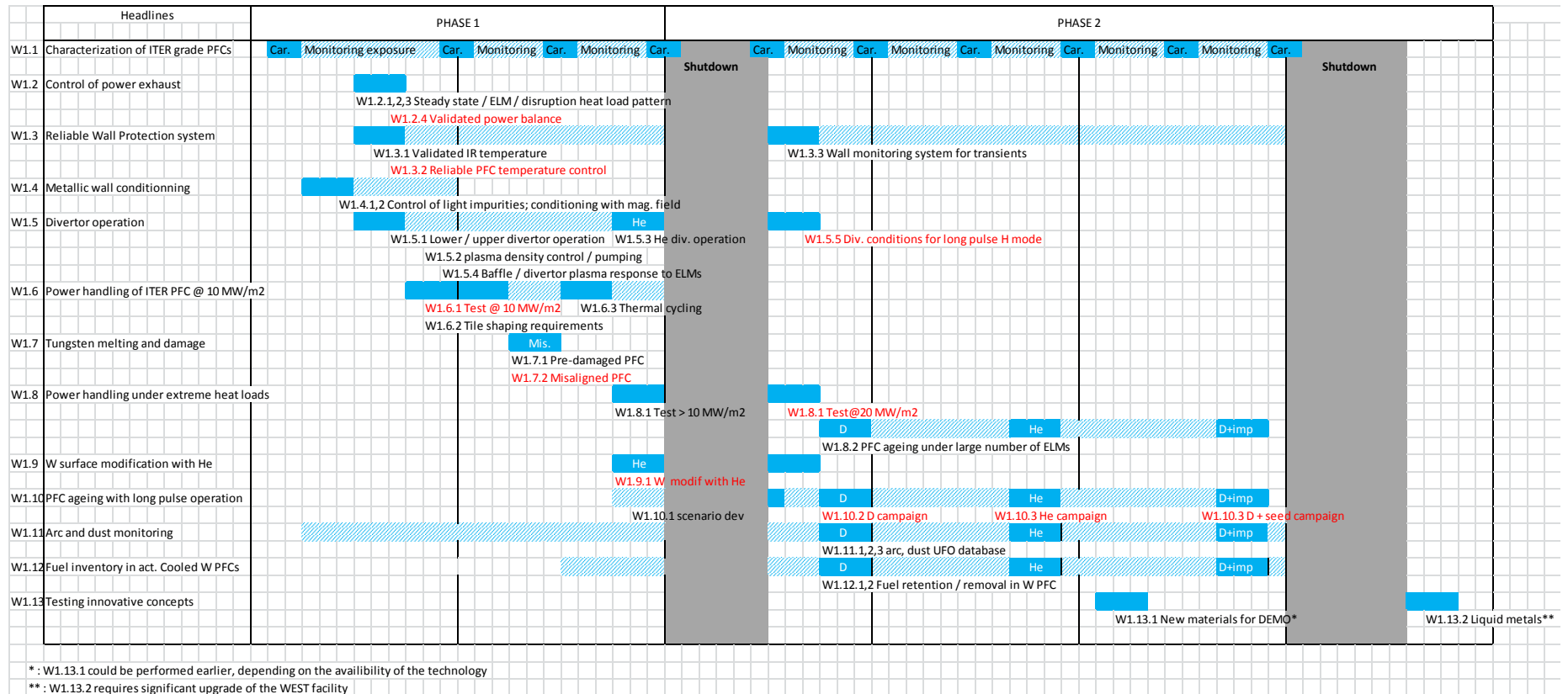


Figure 16 : tentative timeline for Headline 1. Major milestones are indicated in red. Specific campaigns related to PFC testing are also shown (campaign with misaligned/pre-damaged PFC, He operation, wall loading campaigns). Major shutdowns are indicated, but additional shorter shutdowns are to be planned.

### Chapter 3: WEST Research Plan

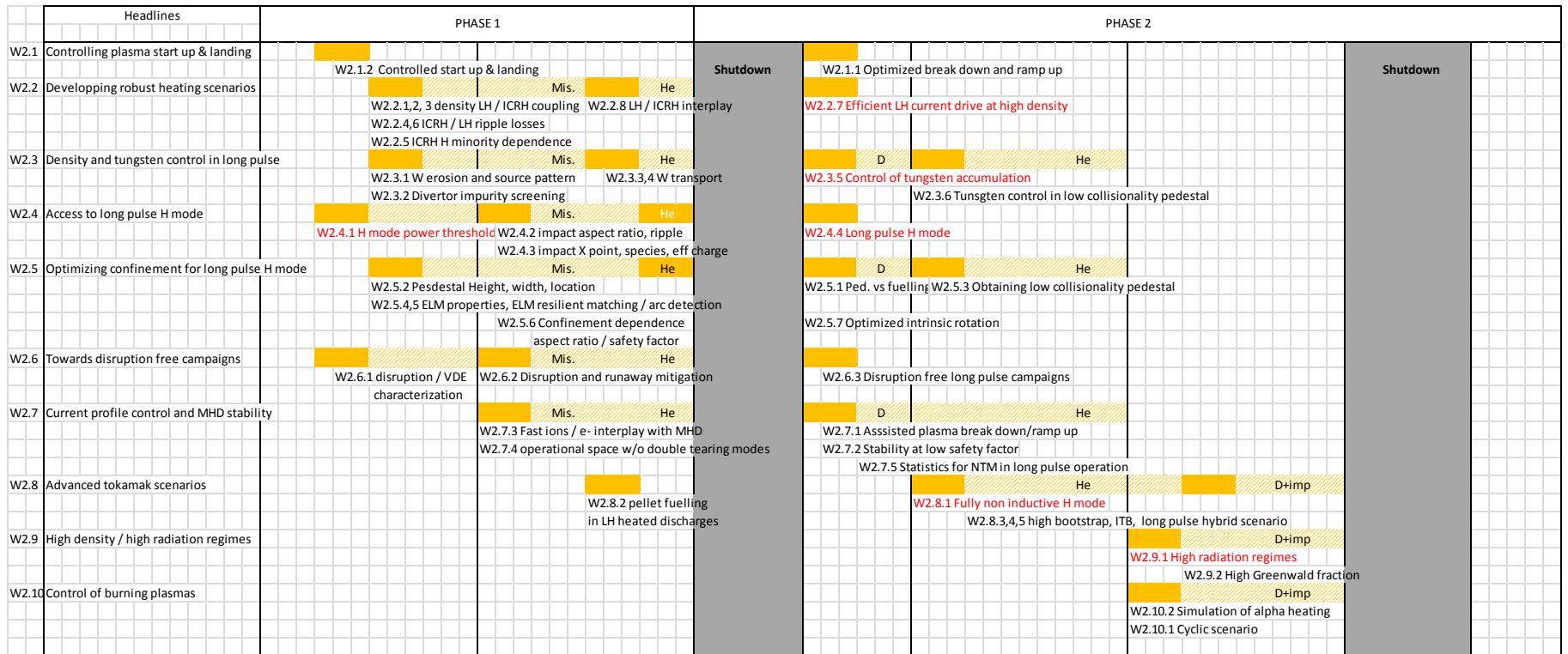


Figure 17 : tentative timeline for Headline 2. Major milestones are indicated in red. Specific campaigns related to PFC testing for Headline 1 are also shown as a reminder. Major shutdowns are indicated, but additional shorter shutdowns are to be planned.

References of Chapter 3 :

- [Andrew2008] Andrew Y et al, Plasma Phys. Control. Fusion **50** (2008) 124053
- [Artaud2010] J.-F. Artaud et al., Nucl. Fusion **50** (2010) 043001
- [Beurskens2013] Beurskens M et al, Nuclear Fusion 2013
- [Bourdelle2013] Bourdelle C et al submitted to Nuclear Fusion Letters
- [Burrell PPCF2002]
- [Bucalossi2009] J. Bucalossi et al., Fusion Sci. Techn. **56** (2009) 1366
- [Bucalossi2013] “*The WEST project: preparing power exhaust control for ITER tungsten divertor operation*”, J. Bucalossi, J.M. Travers, MH. Aumeunier et al., IAEA-TMSSO meeting, Aix en Provence, 14-17 May 2013
- [Dejarnac2007] “*Kinetic calculation of plasma deposition in castellated tile gaps*”, R. Dejarnac, J.P. Gunn, Journal of Nuclear Materials, Vol **363–365**, 15 June 2007, Pages 560-564
- [DeTemmerman2013] “*Helium effects on tungsten under fusion-relevant plasma loading conditions*”, G. De Temmerman, K. Bystrov, R. P. Doerner et al., Journal of Nuclear Materials, Vol. **438**, Supp., July 2013, Pages S78-S83
- [Dumont2013] Dumont R et al submitted to PPCF
- [Durocher2009] “*Infrared thermography inspection of the ITER vertical target qualification prototypes manufactured by European industry using SATIR*”, A. Durocher, F. Escourbiac, M. Richou, et al., Fusion Engineering Design **84** (2009) 314–318.
- [Eich2013] Th. Eich et al. Nucl. Fusion **53** (2013) 093031 (7pp)
- [Garcia2010] J. Garcia et al., Nucl. Fusion **50** (2010) 025025
- [Goldston2012] R.J. Goldston Nucl. Fusion **52** (2012) 013009
- [Giruzzi2009] G. Giruzzi et al., Fusion Sci. Techn. **56** (2009) 1381
- [Fedorczak2012] Fedorczak N et al Nucl. Fusion **52** (2012) 103013
- [Giroud2012] Giroud C et al, IAEA 2012
- [Gohil2011] Gohil P. Nucl. Fusion **51** (2011) 103020
- [Hu PRL2015]
- [JETteam1992] JET team Plasma Physics and Controlled Nuclear Fusion Research 1992 (Proc. 14th Int. Conf. Wuerzburg, 1992)
- [Kamada2013] Y. Kamada et al., Nucl. Fusion **53** (2013) 104010
- [Lang NF 2014]
- [Li 2013] A long-pulse high-confinement plasma regime in the Experimental Advanced Superconducting Tokamak, J. Li et al., Nat. physics 2013,
- [Liang 2012] Magnetic Topology Changes Induced by LHW and Its Profound Effects on ELMs in EAST, Y. Liang et al., Phys. Rev. Lett 2012
- [Maggi2013] Maggi C et al, Nuclear Fusion 2013
- [Marandet2013] Marandet Y et al Contributions to Plasma Physics (2013)
- [Meyer2013] O. Meyer, E. Belonohy, J. Bucalossi et al., “WEST Like Divertor geometry experiments in ASDEX Upgrade”, 40<sup>th</sup> European Physical Society Conference on Plasma Physics, Espoo, Finland, 2013
- [Martin2008] Y.R. Martin et al. Journal of Physics: Conference Series **123** (2008) 012033
- [Minardi1997] E.J. Minardi et al. Plasma Physics (1997), vol. **57**, part 2, pp. 449±464

- [Missirlian2011] “*The heat removal capability of actively cooled plasma-facing components for the ITER divertor*”, M. Missirlian, M. Richou, B. Riccardi, et al., Phys. Scr. T145 (2011) 014080 (7pp)
- [Missirlian2013] “*The WEST project: Current status of the ITER-like tungsten divertor*”, M. Missirlian, J. Bucalossi, Y. Corre et al., 11th International Symposium on Fusion Nuclear Technology (ISFNT), Barcelona, 2013.
- [Neu2013] Neu R et al, Journal of Nuclear Materials 2013
- [Pégourié2009] B. Pégourié et al., Fusion Sci. Techn. **56** (2009) 1318
- [Pitts2013] “*A full tungsten divertor for ITER: Physics issues and design status*”, R. Pitts, S. Carpentier, F. Escourbiac et al., Vol. **438**, Supp., July 2013, S48–S56
- [Scarabosio2013] A. Scarabosio et al. Journal of Nuclear Materials **438** (2013) S426–S430
- [Pütterich2012] Pütterich T et al IAEA 2012
- [Schmitz2012] Schmitz L et al PRL 2012
- [Takenaga2008] H. Takenaga et al., Nucl. Fusion **48** (2008) 035011
- [Takizuka2004] T. Takizuka et al., Plasma Phys. Control. Fusion **46** (2004) A227–A233
- [Travere2012] “*Imaging Challenges for the ITER Plasma Facing Components Protection*”, J.-M. Travere, M.-H. Aumeunier, M. Joanny et al., 24<sup>th</sup> IAEA Fusion Energy Conference San Diego, USA, 2012
- [Tobita1995] Tobita K et al., Nucl. Fusion, **35**, 12 (1995)
- [Udintsev2008] Udintsev V. et al, Fusion Science and Technology **53**, 88 (2008)
- [Weisen2005] Weisen et al., Nucl. Fusion **45** (2005) L1–L4 *Collisionality and shear dependences of density peaking in JET and extrapolation to ITER*
- [Zarzoso2013] Zarzoso D. et al, Phys. Rev. Lett. **110**, 125002 (2013)
- [Loewenhoff2012] : “*Combined Steady State and High Cycle Transient Heat Load Simulation with the Electron Beam Facility JUDITH 2*” (RWTH Aachen, 2012). Th Loewenhoff, PhD Thesis, <http://darwin.bth.rwth-aachen.de/opus3/volltexte/2012/4313/>
- [Maier2013] H. Maier et al., J. Nucl. Mater. **438** S921 (2013).
- [Pegourie2013] B. Pégourié et al., J. Nucl. Mater. **438** S120 (2013).
- [Rubel2011] M. Rubel et al., J. Nucl. Mater. **415** S223 (2011).
- [Ueda2013] Y. Ueda et al., J. Nucl. Mater. **442**(1-3) S267 (2013).
- [Whyte NF2010]
- [Wirtz2013] : “*Thermal shock behaviour of tungsten after high flux H-plasma loading*” M. Wirtz, J. Linke, G. Pintsuk et al., J. Nucl. Mater. **443**(1-3) S497-501 (2013)
- [Zohm2013] H. Zohm et al., Nucl. Fusion **53** (2013) 073019
- [Zou2014] X. L. Zou et al., “*Intermittent Small Scale Turbulence Driven Edge Localized Modes Mitigation and Suppression in Tokamak Plasmas*”, submitted to Phys. Rev. Lett

## Chapter 4: Conclusions and prospects

---

The WEST project will contribute to the challenge of mastering power exhaust over long pulse in preparation of ITER, and to solving the associated technological, operational and physics issues. It will benefit from the unique expertise of the French Institute of Research on Magnetic Fusion in this area, as well as from the strong international collaborative network developed with the ITER partners.

The overall objective of WEST is to prepare, but also to be prepared for ITER operation.

The project has entered a very active phase of development, with major procurement contracts being launched so that the WEST platform is operational for plasma in 2016.

The present document gives an overview of the first draft of the research plan elaborated to fulfill the mission of WEST :

- Paving the way towards the ITER actively cooled tungsten divertor procurement and operation
- Mastering integrated plasma scenario over relevant plasma wall equilibrium time scale in a metallic environment

A workshop has been organized in summer 2014 (June 30-July 2<sup>nd</sup>, Aix-en-Provence, France) to discuss the initial draft research plan with the international fusion community. Topical headlines of the research plan have been reviewed by international experts, and discussed during dedicated working sessions. This has provided the basis for the present version of document, structured around 2 headlines :

- Headline 1 : Operating and testing ITER grade Plasma Facing Components in tokamaks
- Headline 2 : Towards long pulse H mode and steady state operation

The next step will be to build a consistent experimental timeline over the exploitation phase foreseen for WEST (2016-early 2020's), taking into account the operational constraints (regulatory Tore Supra shutdowns etc). A more detailed planning will be worked out for the phase-1 of WEST exploitation. This is expected to be finalized by end 2015. The phase-1 WEST campaigns will then take place in 2016-2017. The next revision of the Research Plan is proposed at the end of phase-1.

On the physics side, a solid basis has been established to show that WEST will reach its objectives in terms of :

## Chapter 4: Conclusions and prospects

- providing ITER relevant steady state heat fluxes to assess the power handling capabilities of the ITER like divertor (Headline 1)
- reaching long pulse operation (~minutes) to demonstrate extended H mode operation over relevant plasma wall equilibrium time (Headline 2)
- cumulating high particle fluence to perform a lifetime test of the ITER like divertor and assess the evolution of its performance under combined plasma loads (Headline 1)

The WEST plasma scenarios will be further consolidated. More detailed integrated modelling of WEST plasma scenarios is planned, using the CRONOS suite to complement the preliminary METIS simulations. Efforts will also be pursued with simulations in specific areas, in particular in the field of plasma edge modelling. Issues identified through the preliminary studies performed at this stage will be further looked at (impurity seeding, LH penetration at high density, ripple losses, tungsten contamination, He scenario development, impact of internal transport barriers formation and bootstrap current for advanced scenarios). In complement to modelling activities, experimental work will continue in close connection with the AUG and JET programmes.

In summary, as shown schematically in Figure 18, WEST will contribute to progress :

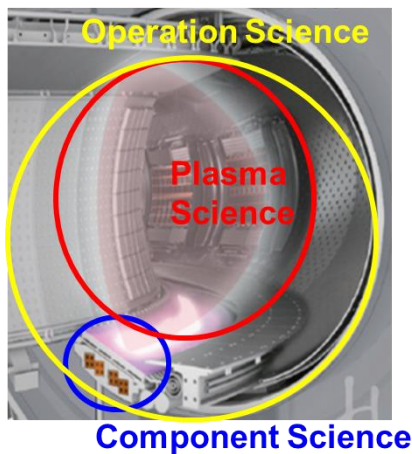


Figure 18 : schematic view of WEST contributions in terms of component science, plasma science and operation science

- The component science : optimizing the component manufacturing at industrial scale, assessing the component lifetime and material evolution in tokamak environment, identifying potential failure modes and safe operational window
- The plasma science : mastering H mode operation over relevant plasma wall equilibrium time scale, through demonstrating control of tungsten contamination, optimizing RF heating and developing integrated power exhaust schemes
- The operation science : gaining operational know how and developing specific control tools, such as the wall protection system

# Annexes of the WEST research plan

---

# Annex 1: contributions of WEST to the EU fusion roadmap for Horizon 2020

---

The WEST research plan is aligned with the orientations defined in the EU fusion roadmap, in particular in the field of power exhaust (Mission 2), which is identified amongst the highest priority topics.

WEST complements the strong effort on tungsten related issues ongoing in Europe, both in tokamaks (AUG, JET) and Plasma Wall Interaction devices (Magnum PSI, Judith, Gladis ...), by providing an integrated test environment, bringing together for the first time the high heat flux technology of the ITER divertor and tokamak operation.

The WEST platform will enter into operation in January 2016, and will be run as a user facility. It is open to EUROFUSION laboratories and to all ITER partners.

The WEST research plan addresses Mission 1 on plasma regimes of operation (investigating long pulse H mode operation and preparing advanced tokamak modes) and Mission 2 on heat exhaust systems (testing ITER tungsten Plasma Facing Components and exploring high fluence plasma wall interactions).

The high level WEST deliverables foreseen for Mission 2 include:

- Assessment of power handling capabilities of ITER high heat flux tungsten divertor components in tokamak environment
- Impact of high particle fluence plasma wall interactions on ITER tungsten PFC lifetime
- Assessment of plasma operation on damaged/melted tungsten components
- Validated scheme for actively cooled metallic PFC protection and monitoring

These deliverables require high performance diagnostics and will call for intense physics and modeling activities.

The table below summarizes the main contributions which WEST provides in the area of Mission 1 and 2 [2]. Specific assets of WEST are mentioned when applicable. In particular, the 3 following logos are used in the table:



The plasma duration foreseen for WEST is larger than several critical physics time constants (such as the plasma wall thermal equilibrium time or the resistive time). The long pulse capability of WEST also allows cumulating high plasma fluence or large number of transients.



WEST operates ITER relevant actively cooled W components, based on the ITER technology, with the same geometry (castellated structure, tile shaping etc) and temperature cycle as foreseen for ITER (stable during the shot and rapidly decreasing at the end of the shot).



## Annex 1: contributions of WEST to the EU fusion roadmap for Horizon 2020





WEST allows addressing non inductive operation at vanishing loop voltage.





The contributions described in the table below are proposed to be executed in the framework of the Work Package WP-MST1, in close connection with the Work Package WP-PFC. The corresponding support will be proposed in the framework of WP-MST2. The part of the programme dedicated to preparing advanced tokamak modes will be performed in support to the Work Package WP-SA. Finally, links with the Work Packages WP-DTT1 and 2 could be explored on a longer time scale, as WEST will be operated for ITER in the same spirit a Divertor Test Tokamak could be operated for DEMO.

[1]: “Strategic orientation of the Fusion Programme- Report of a group of experts assisting the European Commission to elaborate a roadmap for the fusion programme in Horizon 2020 – the Framework Programme for Research and Innovation” CCE-FU 53/3c, C. Cesarsky, Ph. Garderet, J. Sanchez, M. Q. Tran, C. Varandas, B. Vierkorn-Rudolph, S. Paidassi





[2]: WORK PLAN FOR THE IMPLEMENTATION OF THE FUSION ROADMAP IN 2014-2018, October 2013

Table 6 :WEST contributions to Mission 1 and 2 of the EU fusion roadmap for Horizon 2020

Mission	Headline	Sub headline	WEST contributions	WEST assets
Mission 1	Headline 1.1: Increase the margin to achieve high fusion gain on ITER	<i>Operation with metallic Plasma Facing Components</i>	WEST complements the H mode database of metallic machines, with specific features which allows challenging the models and scaling laws (large aspect ratio, dominant electron heating).	
		<i>Improved H-mode ("hybrid" regime).</i>	WEST is able to explore how hybrid regimes extrapolate towards long pulse operation.	
		<i>High radiation</i>	WEST allows exploring how highly radiating regimes extrapolate towards long pulse operation.	
		<i>Optimization of ICRH coupling</i>	WEST is equipped with dedicated local gas puffing to optimize the coupling of its RF systems.	
	Headline1.2 : Operation with reduced or suppressed ELMs		Not Applicable. In the present version, WEST is neither equipped with RMPs, nor with adequate pellet injection for ELM pacing.	
	Headline 1.3: Avoidance and mitigation of disruptions and runaway electrons	<i>Massive gas injection to mitigate heat / electromagnetic loads</i>	WEST is equipped with MGI and will contribute to the demonstration of a reliable disruption mitigation control scheme in a metallic environment	
		<i>Beams of high-energy electrons</i>	The WEST research plan includes the study of runaway beams formation and control, together with modeling activities.	
	Headline 1.4: Integration of MHD control into plasma scenarios		WEST allows addressing specific MHD issues in fully non inductive long pulse H mode discharges.	
	Headline 1.5: Control of core contamination and dilution from W Plasma Facing Components		WEST allows addressing the issue of controlling the W core concentration over long pulses, to gain confidence for both ITER and JT60 SA. The research plan also addresses the issue of ICRH impact on W contamination, including modeling of the RF sheath.	
	Headline 1.6: Determine optimum particle throughput for reactor		The WEST particle exhaust system provides a pumping efficiency in the same range as foreseen for ITER. The impact of low pumping capability on plasma operation and fuel retention will be	

	scenarios		explored.	
	Headline 1.7: Optimise fast ion confinement and current drive		WEST allows studying fast particle losses and associated MHD for fast ions generated by the ICRH system.	
	Headline 1.8: Develop integrated scenarios with controllers		WEST is equipped with an extensive real time control system, applicable to the control of long pulse non inductive operation. Specific care will be taken to prototype a reliable Wall Monitoring System, based on a multi diagnostic approach (see also Mission 2).	 
	Headline 1.9: Qualification of Advanced Tokamak regimes of operation		WEST allows developing advanced tokamak regimes of operation in support to JT60SA and ITER (internal transport barriers in steady state, hybrid regimes, operation above the Greenwald density ...). WEST also addresses fully non inductive operation.	
<b>Mission 2</b>	Headline 2.1: Detachment control for the ITER and DEMO baseline strategy		<p>WEST provides data for plasma detachment and impurity seeding for a compact divertor geometry, complementing other closed divertor studies<sup>15</sup>. In addition, it extends the demonstration of detachment control over long pulse operation.</p> <p>WEST is also equipped with different fuelling systems (gas, supersonic injection, pellets) allowing the investigation of confinement at detachment for different fuelling methods.</p> <p>The influence of detailed PFC shaping on power handling (steady state and transients) will also be investigated.</p> <p>The compatibility between impurity seeding and control of W core contamination will be explored.</p>	
	Headline 2.2: Prepare efficient PFC operation for ITER and DEMO	<i>effect of accidental melting on the plasma and on the performance of the component</i>	Experiments on damaged/melted W components and assessment of subsequent plasma operation are planned with relevant ITER like actively cooled W components.	

<sup>15</sup> \*Although WEST has a moderate Psep/R, it is optimized to produce high heat flux on the divertor target (in the range 10-20 MW/m<sup>2</sup> as foreseen for ITER), making impurity seeding and plasma detachment studies relevant.

	<i>Quantification of residual fuel retention / qualification of fuel removal techniques/ dust production</i>	WEST provides data for fuel retention / removal and conditioning studies, as well as dust production, in a relevant actively cooled W environment under high fluence plasma conditions.	 
	<i>Optimize the material choice specifically in the main chamber</i>	Main chamber data are available (wide angle IR data, extensive set of Langmuir probes, calorimetry etc).	
		<p>In addition, WEST provides the following :</p> <ul style="list-style-type: none"> <li>• Assessment of power handling capabilities of ITER high heat flux tungsten divertor components in tokamak environment under combined loads (steady state + transient + high fluence plasma)</li> <li>• Impact of high particle fluence plasma wall interactions on ITER tungsten PFC lifetime (including the impact of He operation and impurity seeding)</li> <li>• Validated scheme for actively cooled metallic PFC protection and monitoring</li> </ul>	 
	Headline 2.3: Optimise predictive models for ITER and DEMO divertor/SOL	A strong plasma edge modeling effort is ongoing in IRFM, extending plasma fluid codes up to the walls with realistic PFC geometry as well as developing first principles approach for plasma edge turbulence. WEST is a good test bed for benchmarking these codes (simple compact divertor geometry with good access for diagnostics).	
	Headline 2.4: Investigate alternative power exhaust solutions for DEMO	On a much longer time scale, test procedures for innovative divertor concepts could be developed, in collaboration with other laboratories involved (ENEA, FZJ, IPP, KIT, DIFFER, CIEMAT, IPP.CR, CCFE, CRPP ...) and in connection with the relevant work packages.	

## Annex 2: WEST partnerships

---

The WEST project and its research plan are widely open to the international fusion community.

At present, a number of key agreements have been signed, mostly dealing with the procurement of the WEST platform, and a large number of contacts have been established at various levels.

The table below shows partnerships as of December 2013.

<b>ITER Parties or countries</b>	<b>Institutions</b>	<b>Dates of signature</b>
Europe	<i>Fusion for Energy (F4E)</i>	04/10/2013
Poland	<i>Institute of Plasma Physics and Laser Microfusion (IPPLM)</i>	17/07/2013
China	<i>China National Nuclear Corporation (CNNC/SWIP)</i>	03/07/2013
China	<i>Chinese Academy of Sciences (CAS/ASIPP)</i>	03/07/2013
India	<i>Institute for Plasma Research (IPR)</i>	10/07/2013
Japan	<i>Japan Atomic Energy Agency (JAEA)</i>	29/10/2013
USA	<i>Department Of Energy (DOE)</i>	05/09/2013
Korea	<i>National Fusion Research Institute (NFRI) and Ulsan National Institute of Science and Technology (UNIST)</i>	03/12/2013

**Table 7 : signed partnership agreements with WEST (as of December 2014)**

Further contacts with other potentially interested laboratories or institutions in and outside Europe are planned.

Within Europe, preliminary discussions are ongoing with Germany, Belgium, Netherlands, Italy, Sweden, Czech Republic, Romania, Slovenia, as well as with Switzerland. Informal collaboration has already started in several areas.

In addition, WEST is part of the EUROfusion facilities, following the decision of the EUROfusion General Assembly (23-24 September 2014), based on recommendations made by an international panel in charge of evaluating WEST as a EUROfusion facility.

Outside Europe, preliminary discussions are ongoing with USA fusion laboratories and Russia.

# Annex 3: The WEST magnetic configurations

WEST will allow flexible magnetic configurations to be performed, from lower/upper single null to double null. The magnetic system of Tore Supra is unchanged (superconducting toroidal field coils, conventional copper poloidal field coils). Divertor coils (water cooled copper coils) and stabilizing plates have been added to obtain the divertor configuration of WEST.

## Standard Far/Close X-point configurations

Two standard configurations will be used to test the ITER tungsten divertor, both of them being lower single-null : the far (from the divertor target) X-point and the close X-point configurations. Figure 19 shows a flux map for the two configurations as calculated by the free-boundary equilibrium code CEDRES++ [Hertout2011] and Table 8 presents their main geometric parameters. Figure 21 also shows the position of the inner wall on the high field side, and typical position of the heating systems on the low field side, as well as the upper and lower stabilizing plates and the pumping baffle.

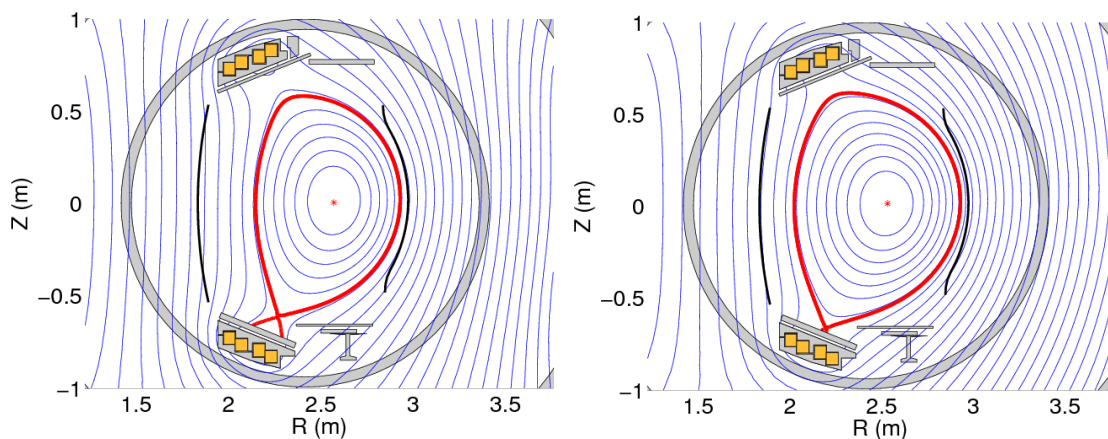


Figure 19 : Poloidal flux maps of the far X-point (left) and close X-point (right) reference configurations calculated by CEDRES++

In order to limit the vertical instability growth rate, two dedicated passive components made of copper will be used: a plate below the baffle and a beam next to the upper divertor coils casing. The feedback control of the vertical position will be done by the divertor coils.

Both configurations can be obtained for a range of  $I_p$  by scaling the PF coils currents with  $I_p$ . The maximum possible  $I_p$  for a given configuration is set by the maximum possible current in the divertor coils, which cannot exceed 20 kA due to the power supplies. In addition, it may also be limited by the Joule heating of the coils, resulting in the curves shown in Figure 20. MHD stability considerations further limit the maximum  $I_p$  achievable to 1 MA.

### Annex 3: The WEST magnetic configurations

The last columns of Table 8 give  $I_p^{\max}$  and  $q_{95}$  for steady-state operation and for 20 s operation. It can be noticed that  $I_p=1$  MA corresponds to  $q_{95}=2.4$  for the Close X-point configuration, which is about the lowest possible  $q_{95}$  in terms of MHD stability.

	$a$ (m)	$R/a$	$\kappa$	$d_x$ (cm)	$\delta$	$I_p^{\max}$ (MA) / $q_{95}$ steady-state	$I_p^{\max}$ (MA) / $q_{95}$ 20 s
Far X-pt	0.39	6.5	1.54	10	0.51	0.47 / 4.1	0.6 / 3.2
Close X-pt	0.45	5.6	1.47	3	0.48	0.78 / 3.1	1 / 2.4

Table 8 : Parameters of the reference configurations (note: the standard  $B_t^{vac}$  (T) at  $R=2.37\text{m}$  is used)

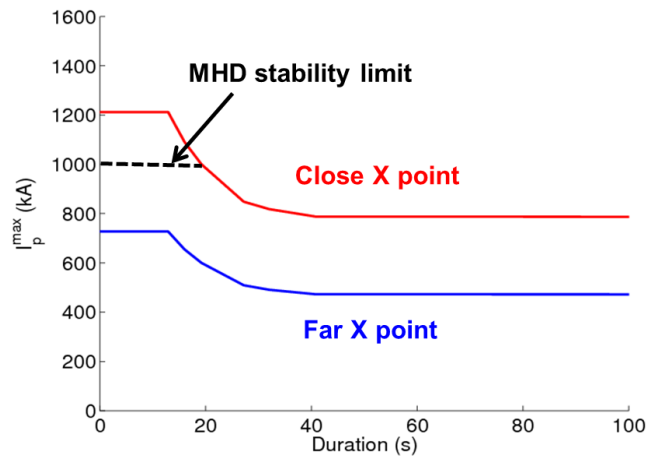


Figure 20 : Maximum possible  $I_p$  versus plasma duration for the two reference configurations, resulting from the divertor coils heating and power supplies constraints. For the close X point configuration, the maximum plasma current is further limiter to 1 MA for stability reasons ( $q_{95} = 2.4$  @ 1 MA)

### Domain of possible shapes and configurations

The PF coils system of WEST is up-down symmetric. Upper single-null or double-null configurations may thus be produced, as illustrated in Figure 21.

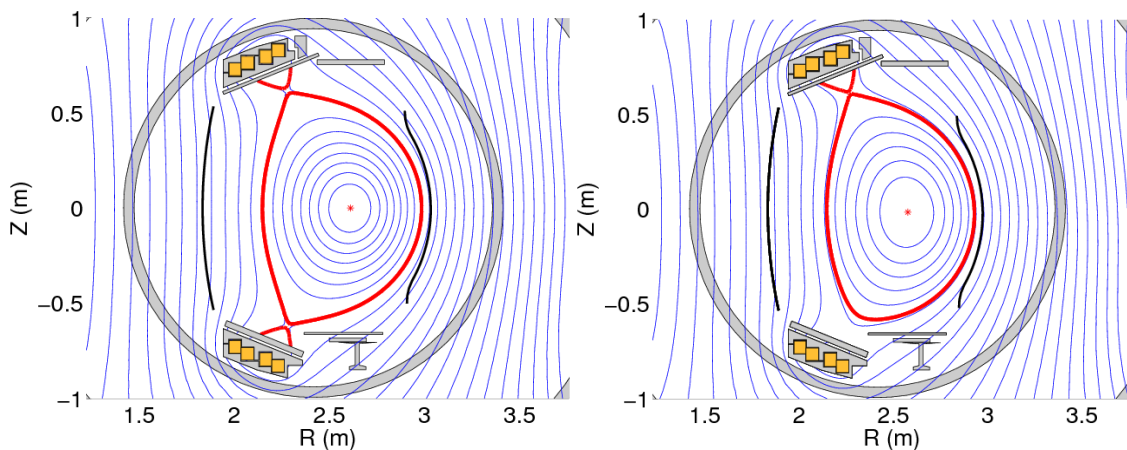


Figure 21 : Examples of double-null (left) and upper single-null (right) configurations

The 9 ex-vessel PF coils allow for a rather wide domain of possible plasma shapes. The elongation may be varied typically between 1.3 and 1.75, as illustrated in Figure 22. An ITER-like shape (scaled down by a factor  $\sim 6$ ) is also possible.

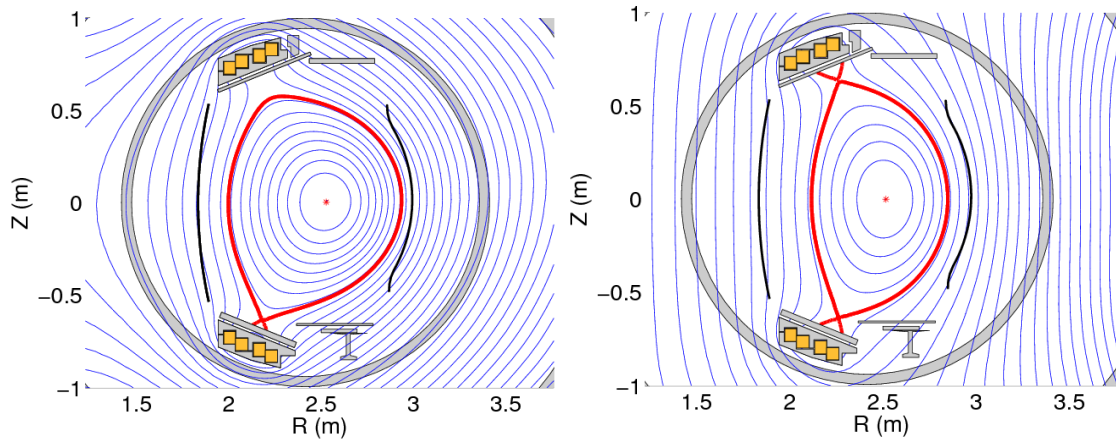


Figure 22 : Examples of configurations with  $\kappa=1.29$  (left) and  $\kappa=1.74$  (right)

**References:**

[Hertout2011] : P. Hertout et al., Fusion Eng. Des. 86 (2011) 1045



# Annex 4: The plasma facing components of WEST

WEST will provide a fully metallic actively cooled environment. The main plasma facing components include, as illustrated in Figure 23 :

- The lower divertor target, where the ITER divertor technology will be tested
- The upper divertor target, allowing upper single null operation
- The baffle, channeling neutrals towards the pumping systems in the lower vertical ports
- A set of inner bumpers and a movable outer limiter, protecting the vessel
- The ripple/VDE protections, located on upper vertical port
- The antennas protections

The lower divertor is based on the ITER technology (tungsten monoblocks), while the remaining plasma facing components will use tungsten coatings, with the exception of the heating systems antennas protections, which will use boron coatings to avoid excessive tungsten plasma contamination. The remaining vessel will be protected by water cooled stainless steel panels, not detailed in this section.

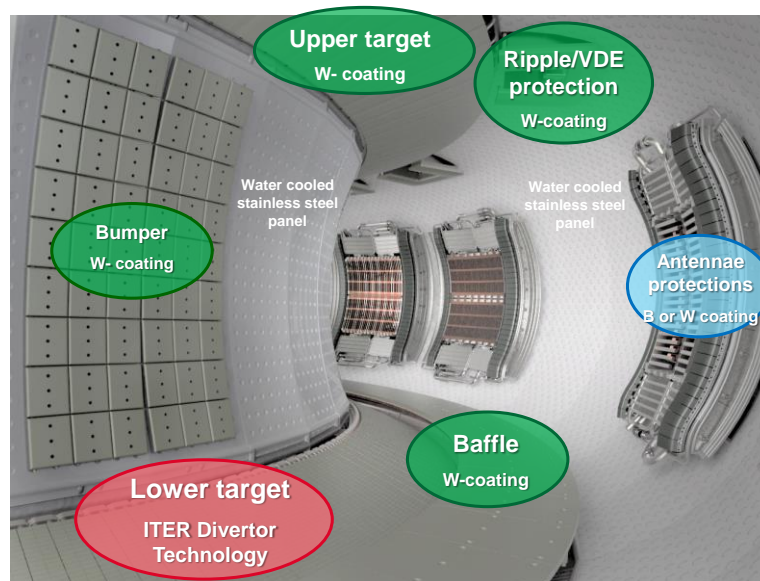
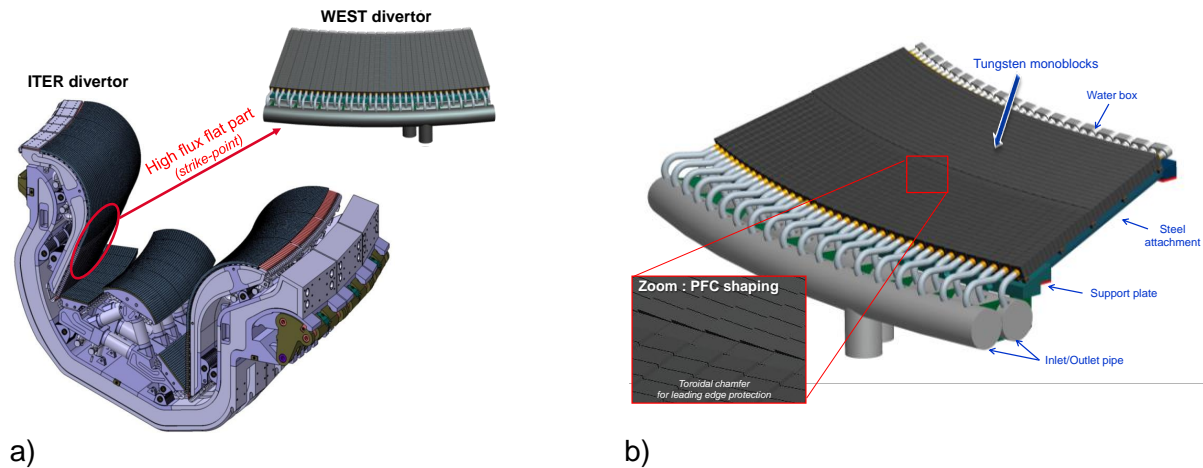


Figure 23 : overview of the WEST plasma facing components

## I. Testing ITER technology: the lower divertor

The lower divertor of WEST will reproduce the high heat flux flat part of the ITER divertor target, as is schematically shown in Figure 24. It corresponds to a scale 1 reproduction of the strike point area (the curved part of the ITER divertor target is not reproduced, but the heat loads in this area during normal operation are significantly lower).

## Annex 4: The plasma facing components of WEST



a) **Figure 24 : a) view of a WEST divertor sector, showing the similarity with the high heat flux flat part of the ITER divertor.**  
b) **detail of a WEST divertor sector, showing the cooling system, the supporting structure as well as a zoom on the monoblock shaping**

It will be a high heat flux component, fulfilling the ITER heat loads requirements [Pitts2013b] :

- 10 MW/m<sup>2</sup>, 5000 cycles
- 20 MW/m<sup>2</sup>, 300 cycles

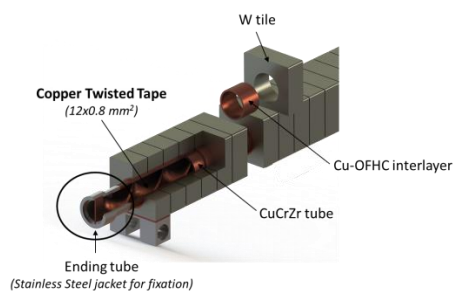
Based on the monoblock concept, the WEST divertor plasma-facing unit (PFU) will use the same monoblock geometry, materials and bonding technology that is foreseen for ITER (35 monoblocks per PFU). The cooling channel is also similar (twisted tape, Figure 25 a). The thermal hydraulic conditions will match ITER specifications (70°C,  $v = 10$  m/s). Gaps between components follow the ITER requirements (0.5 mm between PFUs of a given sector; 0.5-1 mm between PFUs from adjacent sectors for gaps in the poloidal direction; 0.5 mm between monoblocks in a given PFU for gaps in the toroidal direction). Monoblock shaping is proposed to shadow leading edges as is foreseen for ITER : a toroidal chamfer is presently planned (height 0.5 mm, see Figure 25 b). This would however induce significant tile shadowing, and discussion is still ongoing on the final shaping choice (see annex 8 for more details on the impact of tile shaping on the peak heat flux). Refined shaping could also be tested in WEST when the detailed ITER design is finalized. The comparison between the WEST and the ITER divertor is summarized in Table 9.

The large number of components foreseen for WEST (> 15 000 monoblocks, roughly 15% of the ITER vertical targets in terms of number of monoblocks) will allow for significant statistics to test the industrial scale manufacturing process as well as to optimize the qualification and control procedures. The WEST divertor procurement will follow the industrial policy developed by the Domestic Agencies in charge of providing the ITER divertor targets (F4E and JADA), involving the same manufacturers and acceptance criteria.

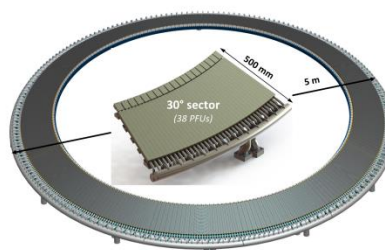
## Annex 4: The plasma facing components of WEST

	<b>WEST vs ITER</b>
<b>Plasma Facing Unit</b>	<b>Identical to high heat flux flat part</b>
<b>Assembling technology</b>	<b>Identical</b>
<b>Monoblock geometry and shape</b>	<b>Identical</b>
<b>Thermal hydraulic conditions</b>	<b>Identical</b>
<b>Area / nb of monoblocks</b>	<b>~14 % ITER</b>
<b>Length of PFU</b>	<b>Scale 1/3</b>
<b>Number of PFU</b>	<b>~ 1/4 ITER</b>

Table 9 : overview comparing WEST and ITER divertor plasma facing units (PFUs)



a)



b)

Figure 25 : a) zoom on the WEST PFU, showing the twisted tape in the cooling channel b) global view of the WEST lower divertor, composed of 12 modular sectors of 30° toroidally each [Missirlian2013b]

The WEST lower divertor consists of 12 independent toroidal sectors of 30°, each composed of 38 PFUs (see Figure 25 b). This modular design will allow for testing variants (e.g. detailed design shaping, tungsten grades...) or running dedicated experiments (e.g. deliberately damaged or misaligned components ...), as well as for post mortem analysis of the components or for refurbishment if needed. These sectors can be dismantled in a relatively short time : typically 1 month shutdown from plasma to plasma for the replacement of one sector by a new one, 2 months if the sector needs to be refurbished before going back inside the machine (leak testing is needed in the second case).

For the phase 1 of WEST operation (2016-2017), 1 to 4 ITER like divertor sectors will be available, while the complete assembly of the 12 divertor sectors is planned for phase 2 (from 2018). During phase 1, the remaining divertor sectors will be inertial tungsten coated components (called start up divertor sectors), allowing high power operation but limiting the discharge duration. They are described in the next section.

More technical details on the WEST ITER like divertor can be found in [Missirlian2013 a et b] [Missirlian2011].

## II. The coated plasma facing components

Plasma facing components other than the lower divertor targets will use coatings over various substrates, depending on the requirements. Coatings are applied to existing components (inner bumpers, outer limiters, antenna protections) or to new components when required (upper divertor, start up divertor, baffle, ripple/VDE protections). The selected technology builds on previous experience (such as W and boron coatings used in AUG and

JET [Neu2009], [Hermann2009] [Maier2006]). Specific attention is given so that carbon based substrates are fully covered (no apparent leading edges, intermediate layers between the substrate and the coating) to avoid carbon contamination in the plasma during operation. The coating thickness chosen (typically a few tens of microns) is a trade off between the coating lifetime and performance under high heat flux testing.

### **1. Start up divertor : W coatings on graphite**

The start up divertor sectors will complement the actively cooled ITER like divertor sectors during the phase 1 of operation of WEST. They are the only non actively cooled components of the WEST configuration, which will be temporarily installed during phase 1 as start up components while waiting for the complete ITER like divertor assembly. They are designed to sustain the full power available but over limited duration, as they are inertially cooled. They are made of a tungsten coating (~15  $\mu\text{m}$ ) on a graphite substrate. The exact performance of the coatings is being investigated. They should allow relevant high heat flux testing of the neighboring ITER like sectors during phase 1 (over duration of the order of the tungsten monoblock thermal equilibrium ~5 s), although operation above 10  $\text{MW}/\text{m}^2$  should be carefully assessed [Neu2009].

### **2. Upper divertor, baffle, ripple/VDE protections : W coatings on copper**

The upper divertor is designed to allow upper single null H mode operation (up to 7 MW of conducted power in steady state), while the baffle allows to run limited plasma (up to 3 MW of conducted power in steady state) and handles fast particle losses (fast electrons generated by LH, as well as ion ripple losses from ICRH). The upper ripple/VDE protections are designed to cope with a hot VDE (up to 1 MJ) and to handle fast particle losses (electron ripple losses as well as fast electrons from LH). These components are foreseen to handle heat fluxes in an intermediate range (1-5  $\text{MW}/\text{m}^2$ ). They are based on a copper heat sink with a W coatings (~30  $\mu\text{m}$ ).

It should be noted that lower and upper divertor elements are designed to be compatible, so that they can be swapped, providing flexibility for the experimental program.

### **3. Inner bumpers, outer limiter : W coatings on CFC**

The inner bumpers and the outer limiter are designed to sustain plasma start up and ramp down (or dedicated experiments) up to 3s. Both are existing actively cooled components with CFC tiles, which will be covered with W coatings (~15  $\mu\text{m}$ ). The inner bumpers are composed of 6 sets toroidally distributed, while the outer limiter is a single component, which can be moved radially and is usually retracted after the beginning of the shot.

### **4. Antenna protections : tungsten or boron coatings on CFC**

The LH and ICRH antennas are equipped with antenna protections, handling both the conducted power from the plasma and the fast particle loads generated by the RF systems. These are also existing actively cooled components with CFC tiles. The choice is still open for the antennas protections coatings, which could be W or boron coating on CFC in order to avoid excessive W production.

**References:**

- [Herrmann2009] A Herrmann, H Greuner, J C Fuchs et al., Experiences with tungsten coatings in high heat flux tests and under plasma load in ASDEX Upgrade, Phys. Scr. **T138** (2009) 014059 (4pp)
- [Maier2006] H. Maier et al., Final EFDA Report on Test Results of Tungsten Coatings on CFC for the JET ITER-like Wall Project, August 11, 2006
- [Missirlian2013a] M. Missirlian et al, Fusion Engineering and Design, Volume 88, Issues 9–10, October 2013, Pages 1793-1797
- [Missirlian2013b] M. Missirlian et al., ISFNT 2013 Barcelona, to be published in Fusion Eng Des.
- [Missirlian2011] M. Missirlian et al. Phys. Scr. T145 (2011) 014080
- [Neu2009] R Neu, H Maier, E Gauthier et al., Investigation of tungsten coatings on graphite and CFC, Phys. Scr. T128 (2007) 150–156 doi:10.1088/0031-8949/2007/T128/029 Phys. Scr. **T138** (2009) 014059 (4pp)
- [Pitts2013b] R. Pitts, ITER full W divertor Final Design Review, june 2013

# Annex 5: The heating systems of WEST

The additional heating and current drive in WEST will be provided by radiofrequency (RF) waves. Three RF systems are available [Magne2013]: Ion Cyclotron Resonance Heating (ICRH), Lower Hybrid Current Drive (LHCD) and Electron Cyclotron Resonance Heating (ECRH). A schematic layout of the RF antennas in the WEST configuration is shown in Figure 26. The three systems are detailed further in the following sections.

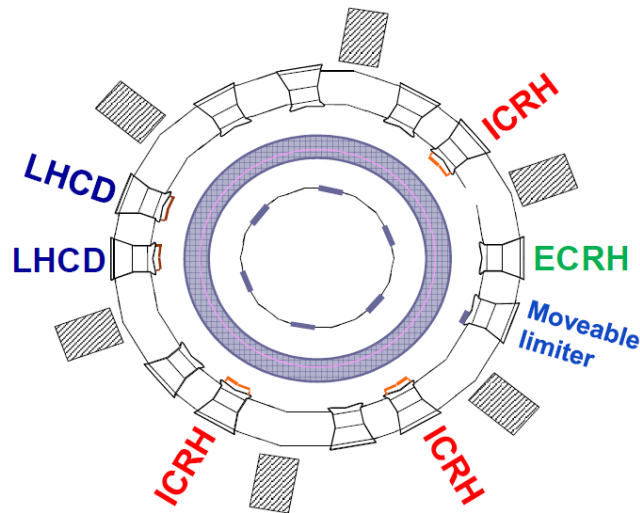


Figure 26 : Schematic layout of the RF antennas in WEST.

## I. Ion Cyclotron Resonance Heating (ICRH)

ICRH offers a large variety of applications, due to different possibilities of heating and current drive schemes, combined with active control of ion species concentrations, launched wave spectrum and resonance location. Most of these topics have been explored in Tore Supra [Colas2009], e.g. various heating scenarios, stabilization of MHD modes by localized fast ion population, and influence on the plasma rotation. For WEST, the ICRH system will be the main heating system, expected to deliver 9 MW for 30s, 6 MW for 60 s and 3 MW for up to 1000 s.

The ICRH generator plant is composed of three modules (one per antenna) of two generators each (one per radiating strap). The six ICRH generator lines are identical, each featuring a synthesizer, a modulator, a solid-state wideband amplifier, and a three-stage THALES ELECTRON DEVICES tetrode amplifier. The pulse duration is limited to 30 s at full power (i.e. 2 MW per generator; 4 MW per antenna). At 500 kW per generator (1 MW per antenna), the generator can operate up to 1000 s. The ICRH generator can operate in frequency range 40-78 MHz. For WEST, the operation class of the generator is changed from AB to B, in order to allow more power from the generator at a given VSWR-value.

A set of three ELM-resilient ICRH antennas has now been designed for WEST [Helou2014] [Vulliez2014], in order to cope with the coupling to H-mode plasmas. The nominal operating frequencies are  $53 \pm 2$  MHz and  $56 \pm 2$  MHz, in order to allow some flexibility in the localization

of the H-minority resonance layer. The chosen design for the WEST ICRH antennas is based on the concept using “internal matching capacitors” (Figure 27), already tested in Tore Supra [Vulliez2007] and in JET [Durodié2009]. This design has demonstrated load resilience during fast edge density variations and features a short resonant circuit that allows to save space and to facilitate the antenna cooling. The main drawback of this design is the use of matching capacitors under vacuum (four capacitors for each antenna), but actions are taken with the manufacturer in order to improve the reliability and maintainability of the capacitors.

Optimization of the original antenna prototype design from 2007 has been finalized [Helou2014]. All design modifications have been made in compatibility with the cooling requirements of the antenna to allow operation at 1 MW per antenna during 1000 s [Vulliez2014]. Keeping the VSWR below 2, each antenna should be able to deliver 1 MW in steady-state scenarios and more than 2 MW for 60 seconds, in ELMY plasmas. The ICRH antennas will be manufactured in collaboration with ASIPP, China.

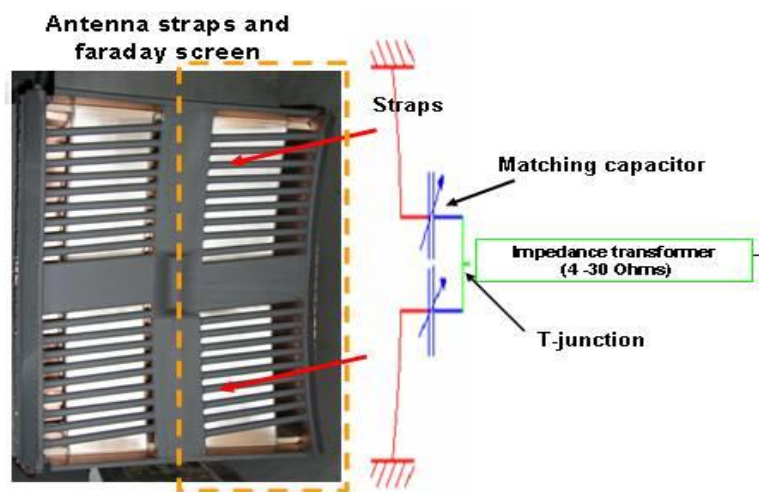


Figure 27: Electrical scheme of the Tore Supra ICRH antenna prototype, tested in 2007.

## II. Lower Hybrid Current Drive (LHCD)

The LHCD system is an indispensable tool for achieving the goals of WEST in terms of long pulse operation, in particular the high fluence scenarios (up to 1000 s long pulses). The LHCD system has recently undergone a complete upgrade, and once the final commissioning of the LHCD plant has been completed in WEST, the LHCD system will have a capability of 6-7 MW coupled to the plasma for up to 1000 s.

The generator of the LHCD system consists of 16 klystrons and their auxiliaries operating at a frequency of 3.7 GHz. The new klystrons, installed in the generator between 2009 and 2012, have a specification of 700 kW on matched load and ~ 600 kW on VSWR = 1.4 [Delpech2011] (Figure 28). The generator is divided in two parts, the first part already being commissioned on matched load and on plasma operation in 2010-2011. The second part has so far only been commissioned on test load. Once the final commissioning on plasma has been carried out for the second half of the generator plant, the maximum LHCD power available at the generator will be 9 MW CW (and 6-7 MW expected power to the plasma).

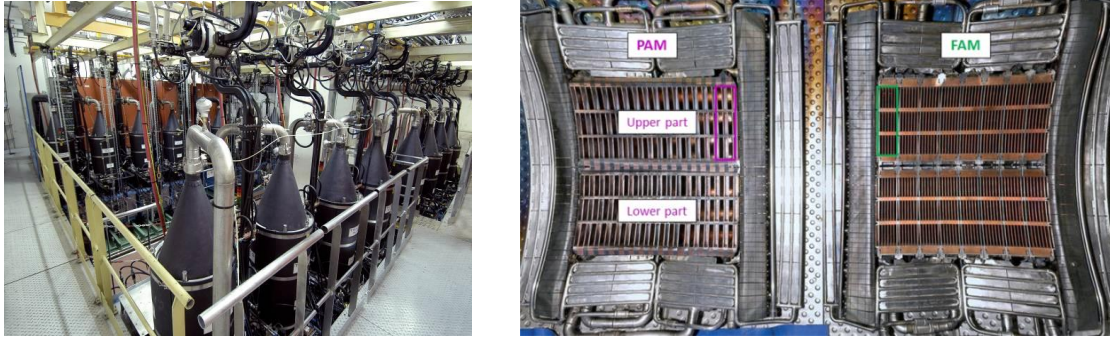


Figure 28: Photos of the LHCD system: generator plant with 16 new klystrons (left) and the two LHCD launchers (right).

For coupling the LHCD power to the plasma, two actively cooled launchers are available (Figure 28). The oldest is called Fully-Active-Multijunction (FAM) launcher, installed in 1999 and designed to operate at  $25 \text{ MW/m}^2$  (equivalent to 4 MW) for 1000 s [Bibet2000]. The second LHCD launcher is the Passive-Active-Multijunction (PAM) launcher, an ITER-relevant design that was installed in 2009 [Guilhem2011]. The target value for the power density on the PAM is also  $25 \text{ MW/m}^2$ , taking into account the active surface of the launcher, which translates into 2.7 MW. Promising results on L-mode plasmas on Tore Supra have shown that higher power density could probably be achieved [Ekedahl2010]. This will be assessed in WEST with the new high power klystrons.

Due to the smaller minor radius and plasma volume in WEST compared to Tore Supra, the LHCD launcher and ICRH antennas must be moved inwards in the vessel by  $\sim 90 \text{ mm}$ . The operating range for the LHCD and ICRH antennas are shown in Figure 29 in terms of radial position. Since the magnetic field ripple is smaller at this inward position, the toroidal shape of the launchers will no longer match the local field lines. Such a toroidal mismatch has shown to have a strong effect on the coupling properties and especially the FAM launcher exhibits a strong increase in reflected power in these conditions. The toroidal profile of the FAM launcher mouth has therefore been reshaped in order to match the toroidal profile of the WEST plasmas at the new nominal LHCD launcher position [Delpech2014].

Another method for improving the coupling of the LHCD launchers, as well as the ICRH antennas, is the use of local gas injection. Each antenna and launcher (3 ICRH + 2 LHCD) has a local gas injection valve in its vicinity, located  $\sim 20 \text{ cm}$  radially behind the protection limiters and distributed over the poloidal height of the antenna.



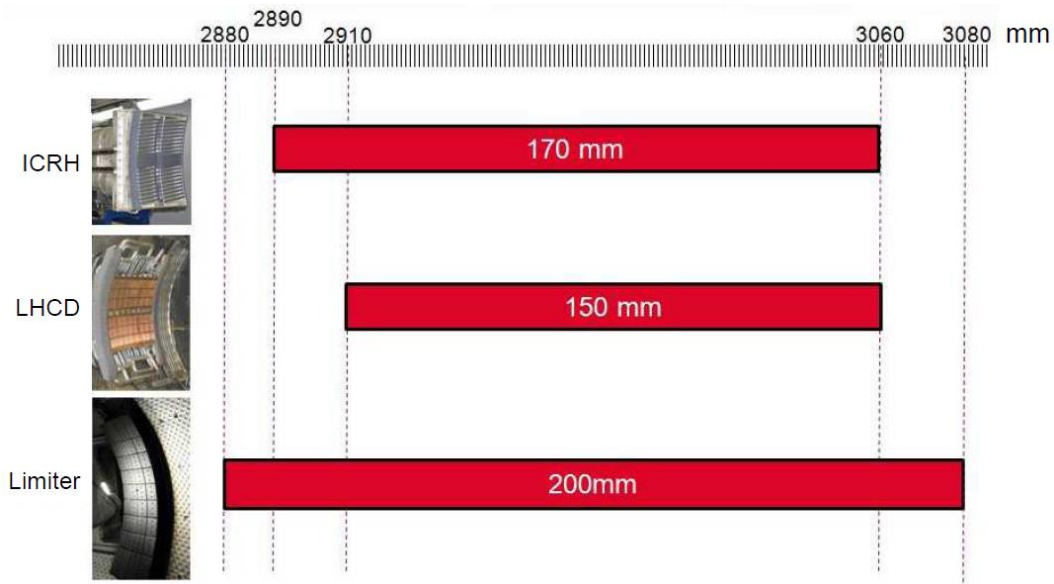


Figure 29: Operating range for the radial positions of the ICRH and LHCD antennas in WEST. The outboard limiter is also shown for comparison.

### III. Electron Cyclotron Resonance Heating (ECRH)

The present ECRH system in Tore Supra consists of two gyrotrons (500 kW x 5 s) operating at a frequency of 118 GHz [Darbos2009]. (The full design of the ECRH system can allow six gyrotrons with a frequency of 118 GHz, each connected to one waveguide transmission line.) The transmission lines power one antenna, situated in a main horizontal port, that inject two (six) beams that can be oriented to allow extensive control of the toroidal and poloidal injection angles. The Gaussian beams emitted by the waveguides are focused by spherical mirrors before being directed into the plasma by mobile mirrors. Each mobile mirror is used to direct two Gaussian beams originating from the same row of corrugated waveguides.

In spite of the relatively low power (700 kW injected power with two gyrotrons), the localized absorption property of the electron cyclotron waves has been used on Tore Supra in a wide variety of experiments, in particular in combination with LHCD or ICRH, such as synergy with LHCD [Giruzzi2004]. During ICRH, it has been shown that relatively modest ECCD power, with the power deposition adjusted by feedback control on the injection angle, can reliably reduce the sawtooth period in the presence of fast ions [Lennholm2009]. In addition, ECRH-assisted start-up has been successfully demonstrated in Tore Supra, and plasma initiation has been obtained down to 0.15 V/m at 7 mPa [Bucalossi2008]. ECRH-assisted start-up was used systematically during plasma restart after two machine shutdowns, lasting several months and causing strong impact on the machine conditioning.

The real-time control system for the ECRH antenna steering has now been upgraded [Bouquey2014], in order to increase the accuracy of the control of the wave injection angles, as well as the speed and the reliability. A more precise and resistant mechanical system with cables and pulleys has been implemented, with the requested specification of  $< 0.25^\circ$  of precision for mirror positioning (i.e.  $0.5^\circ$  for beam positioning) and with a speed of angular displacement of the mirrors of  $3^\circ/s$  on the full angular range ( $\pm 15^\circ$ ).

**References:**

- [Magne2013] R Magne et al., Proc. Topical Conf. on RF Power in Plasmas, Sorrento (2013)
- [Colas2009] L Colas et al., Fusion Sci. Tech. **56** (2009) 1173
- [Helou2014] W Helou et al., Proc. SOFT (2014), to appear in Fusion Eng. Design
- [Vulliez2014] K Vulliez et al., Proc. SOFT 2014, to appear in Fusion Eng. Design
- [Vulliez2008] K Vulliez et al., Nucl. Fusion **48** (2008) 065007
- [Durodié2009] F Durodié et al., Fusion Eng. Design **84** (2009) 279
- [Delpech2011] L Delpech et al., AIP Conf. Proc. **1406** (2011) p. 145
- [Bibet2000] Ph Bibet et al., Fusion Eng. Design **49-50** (2000) 751
- [Guilhem2011] D Guilhem et al., Fusion Eng. Design **86** (2011) 279
- [Ekedahl2010] A Ekedahl et al., Nucl. Fusion **50** (2010) 112002
- [Delpech2014] L Delpech et al., Proc. SOFT (2014), to appear in Fusion Eng. Design
- [Darbos2009] C Darbos et al., Fusion Sci. Tech. **56** (2009) 1205
- [Giruzzi2004] G Giruzzi et al., Phys. Rev. Lett. **93** (2004) 255002
- [Lennholm2009] M Lennholm et al., Phys. Rev. Lett. **102** (2009) 115004
- [Bucalossi2008] J Bucalossi et al., Nucl. Fusion **48** (2008) 054005
- [Bouquey2014] F Bouquey et al., Proc. SOFT (2014), to appear in Fusion Eng. Design

# Annex 6: The fuelling/pumping systems

---

WEST is equipped with a versatile fuelling system (gas injection, supersonic molecular beam injection, pellet injection), able to provide steady state particle injection. The pumping system is unchanged compared to the previous CIEL configuration (turbo molecular pumping) but could be upgraded if deemed necessary from the first phase of WEST operation.

## I. Fuelling

Three fuelling systems are available. By order of complexity and efficiency  $\varepsilon_\phi$  (defined as the ratio of the number of particles reaching the confined plasma to the number of particles injected), they are the conventional gas puffing (GP,  $\varepsilon_\phi < 10\%$ ), supersonic molecular beam injection (SMBI,  $\varepsilon_\phi$  of a few 10%), and pellet injection (PI,  $\varepsilon_\phi > 50\%$ ).

In addition, WEST is equipped with a massive gas injection system (MGI) to mitigate the impact of disruptions and runaways.

### 1. Gas puffing

Gas injection lines are distributed toroidally and poloidally around the vacuum chamber, see Figure 30.

Twelve are located in the upper and lower divertors : 3 toroidal  $\times$  2 radial positions (in the inner and outer legs<sup>16</sup>) to allow flexible divertor injection.

Six are located in the midplane. The first one is located in the Outboard Movable Limiter to allow for midplane injection, while the other 5 are located in the vicinity of the heating antennas to allow for coupling optimization (3 ICRH antennas, 2 LH launchers).

Finally, 1 is located at the top of the chamber, on the Low Field Side.

They are connected to 11 calibrated reservoirs of capacity  $260 \text{ Pa}\cdot\text{m}^3$  each, equipped with absolute temperature and both absolute and differential pressure measurements. The gas throughput for each reservoir is regulated by a piezoelectric valve coupled to a flow-meter of response time 2 ms and injection capability  $4 \text{ Pa}\cdot\text{m}^3\cdot\text{s}^{-1}$ . Injected gases include  $\text{D}_2$ ,  $\text{H}_2$ , He and extrinsic impurities ( $\text{N}_2$ , Ne, Ar...).

If needed, the size of the calibrated reservoirs could be increased for larger fuelling capability. An integrated injection system through a gas matrix is also being studied.

### 2. Supersonic Molecular beam injection (SMBI)

SMBI consists in injecting a massive amount of particles during a short time interval, in order to increase the neutral penetration due to the strong edge cooling [Bucalossi2002], [Patent INPI]. Practically, one uses a high-intensity collimated jet, which is obtained by allowing the gas to expand through a Laval nozzle. At the plasma boundary, the resulting Mach number is between 2 and 3 due to gas expansion. The SMBI system consists in three injectors located close to the midplane, two on the High Field Side and one on the Low Field Side to allow for comparison of fuelling efficiencies. They can inject  $10^{20}$  molecules of  $\text{D}_2$  within 1 ms at a

---

<sup>16</sup> In both cases, the gas will be injected through the plasma facing units of the WEST divertor, resulting in a mixed fuelling between the private flux region and the inner/outer divertor respectively.

repetition rate up to 10 Hz (i.e.  $20 \text{ Pa}\cdot\text{m}^3\cdot\text{s}^{-1}$  per injector), with feedback capability on the plasma central density.

### 3. Pellet injection (PI)

The PI system, developed by PELIN Laboratory (Russia), is able to produce  $\text{H}_2$  or  $\text{D}_2$  ice continuously for 1000 s or more [Vinyar2000]. In the standard configuration, the pellet length and diameter are 2 mm (i.e.  $0.7 \text{ Pa}\cdot\text{m}^3$  per pellet), but the length can be increased up to 3 mm ( $1.1 \text{ Pa}\cdot\text{m}^3$  per pellet). He at 1 to 4 bar is used for an injection at less than 200 m/s, compatible with a safe propagation of the pellet along the curved guide tubes, or  $\text{H}_2$  up to 100 bar for a higher pellet speed ( $\sim 800 \text{ m/s}$ ) in the case of direct injection. The injection frequency can vary from the single-shot mode to more than 10 Hz, with a global reliability of  $\sim 99\%$  at 10 Hz [Géraud2003]. Four injection points are poloidally distributed around the vacuum chamber: from the LFS (free flight), vertically from the top, and obliquely or horizontally from the HFS, see Figure 30. This allows for an extensive comparison of pellet fuelling physics (impact of drifts on fuelling efficiencies etc). Present fuelling capacity is between  $7$  and  $11 \text{ Pa}\cdot\text{m}^3\cdot\text{s}^{-1}$ .

It should be noted that the present PI system is well adapted for steady state fuelling, but not for ELM pacing.

If needed, the pellet size could be increased by 30 % (diameter up to 2.3 mm) and/or of the injection frequency up to 15 Hz (ultimately 30 Hz), yielding to a fuelling capacity in the range  $14\text{-}21 \text{ Pa}\cdot\text{m}^3\cdot\text{s}^{-1}$  (ultimately  $40 \text{ Pa}\cdot\text{m}^3\cdot\text{s}^{-1}$ ).

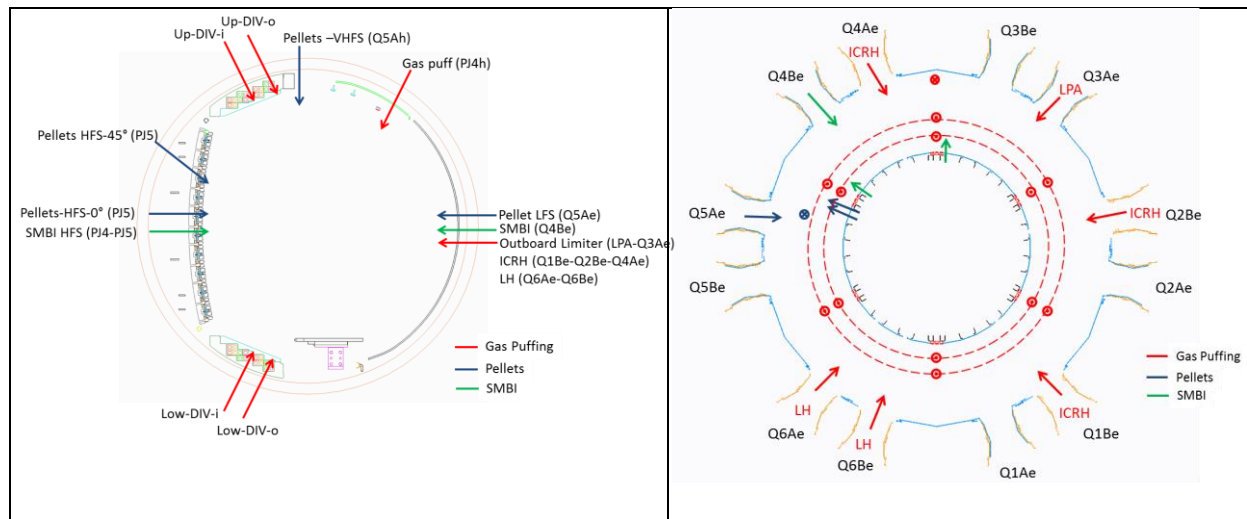


Figure 30 : overview of the fuelling systems for WEST (gas puff, supersonic molecular beam injection, pellets) with a poloidal cut (left) and a top view (right)

### 4. Massive gas injection

For disruption mitigation and runaway electrons mitigation, two gas injectors are available.

The first one is a standard Massive Gas Injector (MGI) based on a ferromagnetic valve driven by an electro-magnet [Martin IAEA2004]. It is able to inject up to  $2 \cdot 10^{23}$  atoms of noble gas (He, Ne, Ar, and mixtures). The MGI volume can be adjusted between 1.0 and 1.6 liter at filling pressure in the 0.1-10 atm range. The injector is closed by a leak-free valve connected to a Laval nozzle. It is located 1.6 m away from the plasma edge. No guiding tube is installed, thus the gas jet is in free expansion in vacuum. The opening time of the valve is less than 1 ms, and the opening duration is around 40 ms. The large valve aperture ( $4 \text{ cm}^2$ ) enables a gas flow rate reaching  $10^{25}$  atom/s.

The second injector is based on the bursting disk cartridge injector concept (BDCI), being investigated for ITER. A bundle of cartridges ( $15 \text{ cm}^3$  each) are filled at high pressure (100-150 atm). Each cartridge is sealed by a rupture disk. The rupture of the disk by electric arc occurs in less than 0.4 ms. An outflow rate as large as  $4.2 \cdot 10^{25}$  atoms/s is thus achieved at the nozzle exit. Cartridges are located 20 cm away from the plasma edge. The design of the injector maximizes the impulse pressure of the gas jet at plasma edge.

## II. Pumping

During discharges, active pumping is provided by 10 turbo-molecular pumps located at the bottom of pumping ducts under the baffle. In the present configuration, the effective pumping speed in the vacuum chamber is estimated to be  $\sim 13 \text{ m}^3 \cdot \text{s}^{-1}$  (see Figure 31) as long as the neutral pressure in the divertor remains smaller than  $\sim 0.6 \text{ Pa}$  (corresponding to the optimum regime for the turbo molecular pumps). Preliminary simulations with the SOLEDGE-2D-Eirene code package [Bufferand2013] indicate that the pressure in the WEST divertor should be in the range 0.2-0.5 Pa for the range of density considered. This leads to a gas throughput between  $2.5$  and  $8 \text{ Pa} \cdot \text{m}^3 \cdot \text{s}^{-1}$ .

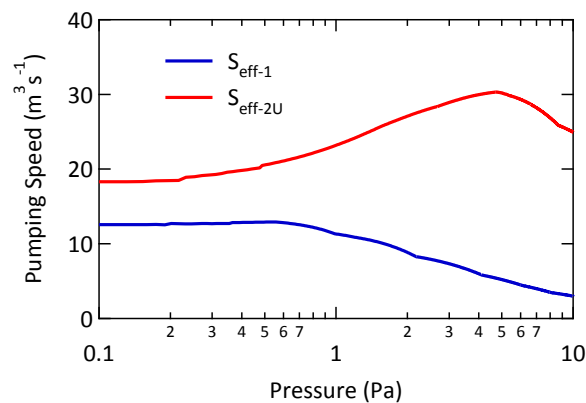


Figure 31 : Effective pumping speed in the vacuum chamber as a function of the divertor neutral pressure in the present ( $S_{\text{eff-1}}$ ) and upgrade ( $S_{\text{eff-2u}}$ ) configurations.

If the performance of the present pumping system does not fulfill the particle exhaust needs (high gas fuelling might be required to optimize coupling for the RF heating systems for instance), two possible improvements are envisaged, which could be implemented for phase 2 of WEST operation. The first option is to double the set of turbo-molecular pumps and to complement it by one Roots by pair of pumps, yielding an effective pumping speed of about  $20 \text{ m}^3 \cdot \text{s}^{-1}$  over the entire range of pressure (i.e. a gas throughput from  $\sim 4$  to  $12 \text{ Pa} \cdot \text{m}^3 \cdot \text{s}^{-1}$ , see Figure 31). The second option is to install a cryopump under the baffle, in the divertor

chamber, which could lead to a pumping capacity of up to  $\sim 100 \text{ m}^3 \cdot \text{s}^{-1}$  in deuterium (gas throughput from  $\sim 20$  to  $50 \text{ Pa} \cdot \text{m}^3 \cdot \text{s}^{-1}$ ). A feasibility study has been performed, and space reservation is made under the baffle. However, the frequency of cryopump regeneration during long pulse operation should be further assessed.

It should be noted that the rather low pumping efficiency of the present WEST system (in terms of fraction of the recycling flux) is similar to the one expected for ITER (around  $\sim 1 \%$ ).

In addition, each of the two LH-launchers is equipped with a  $2 \text{ m}^3 \cdot \text{s}^{-1}$  turbo-molecular pump and, in between discharges, the vacuum chamber is continuously pumped by a set of four  $2 \text{ m}^3 \cdot \text{s}^{-1}$  turbo-molecular pumps, installed in two pumping ports.

## References

- [Bufferand2013] : H. Bufferand et al., *J. Nucl. Mat.* 438, S445 (2013)
- [Bucalossi2002] : J. Bucalossi et al., *Proc. 29th EPS Conf. Controlled and Fusion Plasma Physics*, Montreux, Switzerland, ECA, **26B**, O-2.07 (2002).
- [Patent INPI] Patent INPI (FR) 03 00910.
- [Vinyar2000] I. Vinyar and A. Lukin, *Tech. Phys.*, **45**, 106 (2000).
- [Géraud2003] A. Géraud et al., *Fusion Eng. Des.*, **69**, 5 (2003).

# Annex 7: overview of WEST diagnostics

---

This annex gives an overview of the diagnostic set foreseen for WEST. They are grouped by research topic:

- Plasma control and operation
- Core plasma profiles
- PFC monitoring
- Plasma Wall Interaction
- Radiation and impurities
- Heating scenario
- Turbulence and MHD

We first give an overview of each topic in section I, then review the individual diagnostics in more details in section II. The whole set of WEST diagnostics can be seen in Table 10.

## I. Overview of the diagnostic set for WEST

**Plasma control and machine operation:** the real time control system of Tore Supra has been thoroughly updated. The WEST pulse schedule architecture has been developed to address advanced tokamak control needs. It features a time segmented approach to define the plasma discharge, as well as a real time event detection to deal with unexpected phenomena which may occur during the discharge. The latter will allow optimizing the experimental time, as the system can react by adjusting the plasma scenario or by changing to a backup segment, instead of aborting the discharge. The system will provide the usual control capabilities (plasma position and shape, plasma current, density, radiated fraction ...) as well as advanced control schemes (loop voltage, plasma current profile ...). A wall monitoring system (WMS), using a multi diagnostics approach (infrared, spectroscopy etc), is planned for ensuring real time PFC protection, addressing the challenge of surface temperature measurement in a metallic environment.

New magnetic sensors have been added to allow accurate reconstruction of the divertor configuration. A large number of visible cameras are also available (see Figure 32).

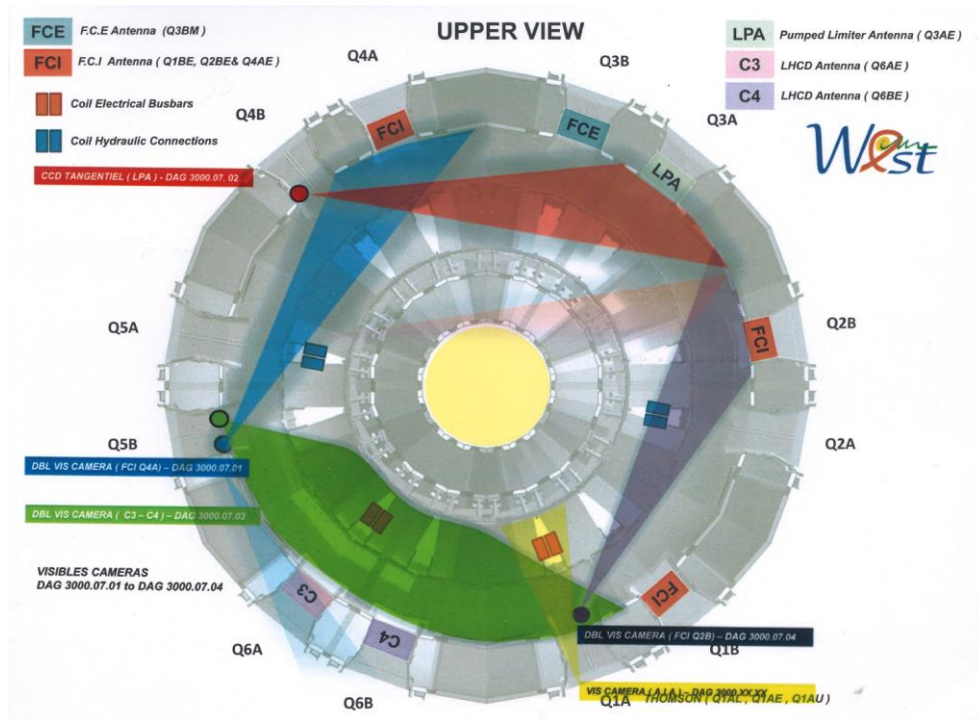


Figure 32: Location of the visible CCD cameras dedicated to tokamak operation.

**Heating system operation:** The ICRH and LHCD systems are essential tools to achieve the WEST objectives of long duration, high power density discharges. They are equipped with diagnostics providing information both for safe operation and for scenario optimisation. For safety, all lateral protections of the ICRH antennae and LH launchers, where fast particles can lead to localized high heat fluxes, are observed by infrared thermography (IR) with fiber bundles embedded in the HFS wall. For wave coupling study (specifically for RF sheath effects) and scenario optimisation purposes, the IR information will be coupled to that provided by reflectometers measuring the electron density over 10 to 20 cm in front of the LHCD launcher and ICRH antennae. A hard X ray system (horizontal camera) is also available to assess the LH power deposition profile.

**Heat and particle fluxes, SOL physics:** Measuring surface temperature and corresponding heat fluxes is at the core of the WEST programme for testing the ITER like divertor tungsten components. Every other upper port is equipped with an IR endoscope (6 in total), allowing a full coverage of the lower ITER like divertor (Figure 33). The measurements are connected to the Wall Monitoring System for real time PFC protection. An extensive set of thermocouples embedded in various PFCs allows measuring their bulk temperature (100-1300°C) and thus calibrating the IR measurements independently of the W PFC emissivity evolution. A sophisticated calorimetry system yields a detailed power and energy balance reconstruction on PFCs. More than sixty flush mounted Langmuir probes complement the IR measurements on the upper and lower divertors, the inboard limiter and the baffle (Figure 33). Two reciprocating probes in an upper port are equipped with exchangeable probe heads for measurements of e.g. electron density, electron and ion temperature, Mach number etc,



allowing for detailed SOL physics studies in complement with other diagnostics (edge reflectometer, He jet beam ...).

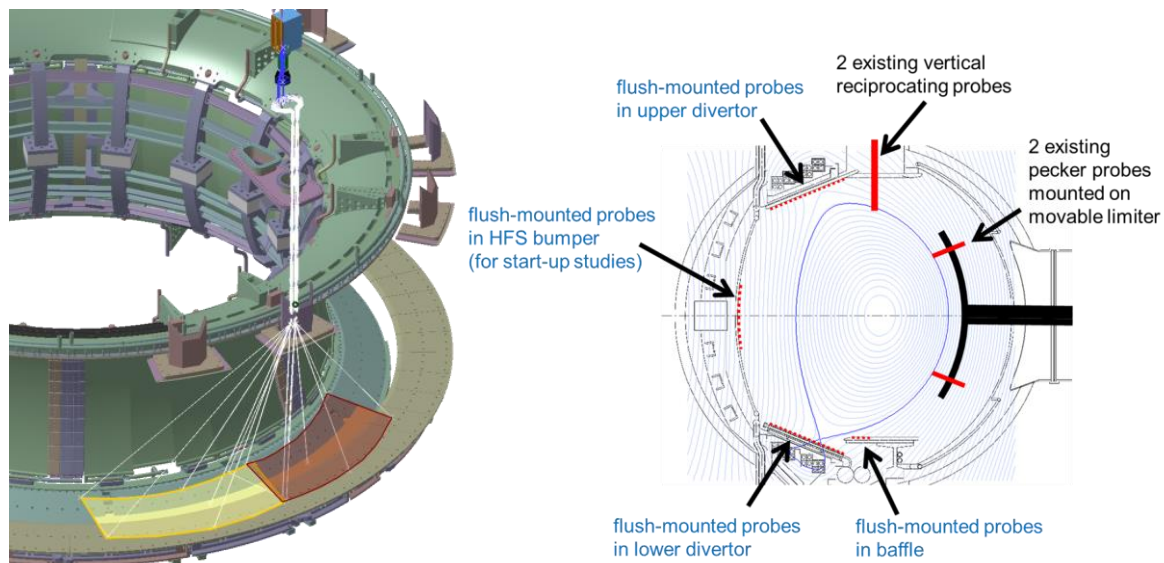


Figure 33 : : field of view of an IR endoscope (left) and Langmuir probe set-up (right)

**PFCs under high fluence exposure:** A variety of diagnostics allows characterizing the components under high fluence plasma exposure. In order to assess global material migration and PFC lifetime, erosion/deposition measurements are planned between campaigns by confocal microscopy complementing spectroscopy measurements during plasma operation. Post mortem analysis of selected PFCs is planned, while visual inspection of the PFC can be performed during the campaigns using the Tore Supra Articulated Inspection Arm (AIA).

For fuel retention studies, pressure gauges and mass spectrometers are available for residual gas analysis (including the isotope ratio of the exhaust by an optical Penning gauge) to assess particle balance. The local fuel inventory and isotope ratio can be measured by a laser based LIBS/LIDS system, which can also provide the composition of the analyzed material and the deposited layer thickness. The reciprocating probes also allow exposing well characterized samples to controlled plasma fluences, before post mortem analysis. A dust particle collector can also be mounted on the reciprocating probes for analysis e.g. by TEM or IBA. A dust particle injector for dust particle transport and dust-plasma interaction studies is also being investigated.

**Impurity sources, radiation, and transport:** The control of W contamination will be an issue for the WEST programme as a whole. Tungsten and other impurity sources, as well as recycling fluxes, are monitored by an extensive visible spectroscopy system (200 lines of sight), covering most PFCs in the vessel (lower and upper divertors, HFS limiters, antenna and launcher protection limiters). In addition to the standard time resolution, a high speed mode is also possible for ELM studies. Two VUV spectrometers are also available. The first

system has a high spectral resolution and a mobile line of sight, allowing for scans of the lower divertor region. The second system is particularly suited for impurity transport studies in conjunction with the laser blow-off system.

WEST will be equipped with three bolometric cameras in a horizontal port and one or two cameras located in an upper vertical port. The system will allow estimate of the total radiated power, but will be marginal for detailed tomographic reconstruction. A possible upgrade for a better spatial resolution would involve using in situ detectors, such as actively cooled micro-bolometers. This could be developed at a later stage through collaboration.

The soft X-ray diagnostic is going through major refurbishment based on the GEM (Gas Electron Multiplier) detector technique. An array of GEM is planned in an upper vertical port, giving a full coverage of the plasma. In addition, a second GEM based camera is planned in a horizontal port, allowing for tomographic reconstruction. Slow (ms) and fast ( $\mu$ s) acquisition modes are foreseen.

**Core and pedestal profiles** (Figure 34): The electron density profile is measured by a 10-chord interferometry diagnostic and two X-mode reflectometers which give access to the entire LFS profile and part of the HFS profile. These diagnostics allow an accurate determination of the density profile in the confined plasma with a time resolution allowing density fluctuation measurements over the entire profile. The 32-point ECE radiometer provides the  $T_e$  measurements over the same radial range with 5% accuracy and a millisecond time resolution. A new 2D X-ray crystal spectrometer is planned to provide  $T_i$ ,  $T_e$ ,  $V_\phi$  and  $V_\theta$  measurements. In a first stage, the system will be limited to central measurements (5 points around the magnetic axis). It will be further improved at a later stage, with additional measurement points including the pedestal (15 measurements in total). The  $q$  profile is deduced from the interferopolarimetry diagnostic.

The pedestal is not as well diagnosed as the core plasma. The existing Thomson scattering diagnostic is modified to focus on the electron and temperature profiles in the pedestal region, with about 10 points over a radial range of about 10 cm and a spatial resolution around 6 mm. The edge reflectometer will also provide part of the necessary density measurements. The outer views of the imaging 2D X-ray spectrometer will provide few  $T_i$  measurement points. This is clearly an area open for collaboration (e.g. for electron density measurements in the HFS pedestal with a reflectometer, or  $T_i$  measurements in the whole pedestal).

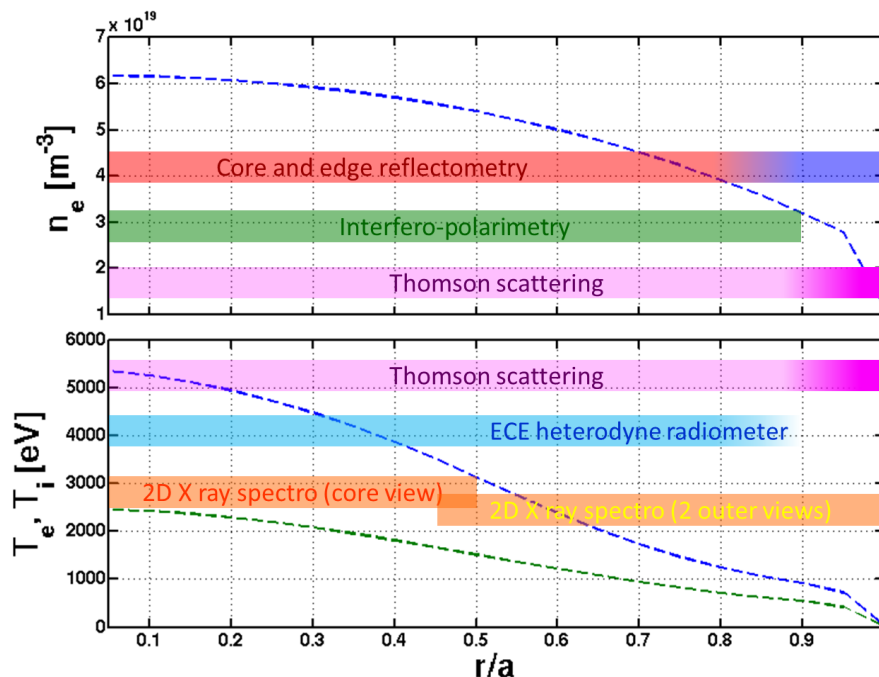


Figure 34 : Typical electron density (top) and temperature (bottom) profiles with radial intervals measured by the various profile diagnostics. The Thomson scattering diagnostic will have 6 measurement points in the pedestal region (around  $r/a$  ) 0.9-1).The overlap region between core and edge reflectometers and the outermost radius measured by ECE depend on the plasma conditions. The outer views of the 2D X ray spectrometer will not be available at the beginning of operation.

**Turbulence and MHD:** With the WEST project comes a unique set of diagnostics dedicated to fluctuation measurements. With their microsecond time resolution capability, the two reflectometers presented in the paragraph above provide fluctuation profiles over the entire LFS half of the plasma and part of the HFS half. An Upper Hybrid Resonance Scattering (UHRS) reflectometer is proposed for small scale density fluctuation measurements. The Doppler reflectometer already present on Tore Supra provides frequency spectra with a radial and wavenumber scan capability. The vertical Doppler reflectometer must go through major modifications due to the reduced space in the vertical ports and may be unavailable at the beginning of operation. A fast camera tangential view will allow observation of disruptions, gas or pellet injections and edge plasma turbulence. An ECE imaging diagnostic will record  $52 \times 18 \text{ cm}^2$  images of the electron temperature at 250 kHz for ELM dynamics and core MHD studies.

Table 10 gives an overview of the diagnostics set foreseen for WEST. The first column corresponds to diagnostics available from day 1. The second column lists the diagnostics available at a later stage (in general for phase 2 of WEST operation).

For the diagnostics foreseen at a later stage, the status is mentioned. “Approved” diagnostics correspond to diagnostics which are approved by the programme and for which integration is ongoing. “Proposed” diagnostics correspond to diagnostics for which integration is difficult, and/or for which the interest for the programme is still being discussed. Finally, diagnostics “under discussion” are in a very early stage, and are not integrated yet.

## Annex 7: overview of WEST diagnostics

Physical quantity or process	Diagnostics	
	Available from day 1	Available in a later phase
$I_p, V_{loop}, W_{dia}, Q_{95}...$	• Magnetics	
Vessel, pumping duct total and partial pressures	• pressure gauges, barometry, mass spectrometry, optical Penning gauges, etc.	
$n_e$ core profile	• 10-chord interferopolarimetry • core X-mode reflectometer	• Thomson scattering diagnostic (focus on the pedestal), approved
$T_e$ core profile	• 32-point ECE radiometer	• Thomson scattering diagnostic (focus on the pedestal), approved
$T_i, V_{tor}, V_{pol}$ core profiles	• 2D X-ray crystal spectrometer ( $-0.5 \leq \rho \leq 0.5$ )	• 2D X-ray crystal spectrometer ( $\rho \geq 0.5$ ), approved
q core profile	• 10-chord interferopolarimetry	• Reflectometer cluster (proposed)
$n_e$ pedestal profile	• edge X-mode reflectometer	• Thomson scattering diagnostic (focus on the pedestal), approved • He jet beam (approved) • HFS reflectometer (proposed)
$n_e$ HFS pedestal profile		
$T_e$ pedestal profile		• Thomson scattering diagnostic (focus on the pedestal), approved • He jet beam (approved)
$T_i, V_{tor}, V_{pol}$ pedestal profile		• 2D X-ray crystal spectrometer ( $\rho \geq 0.5$ : 1 or 2 points), approved
SOL profiles ( $n_e, T_e, T_i, Mach...$ )	• Fixed and reciprocating probes • Edge reflectometer	• He jet beam (approved)
$T_{surf}$ on PFCs	• IR thermography	
$T_{bulk}$ on PFCs	• Thermocouples	
$T_{cool}$ cooling circuit (detailed power balance)	• Calorimetry	
Net erosion/deposition on PFCs	• Confocal microscopy	
PFCs monitoring	• Visual inspection by the Articulated Inspection Arm or alternative system (depending on AIA availability)	• Visual inspection by the Articulated Inspection Arm (approved)
Fuel content and surface composition		• LIBS/LIDS (proposed)
Dust formation		• Dust particle collector on recip. probe (approved)
Dust transport		• Dust particle injector on recip.probe (proposed)
Emission of low ionisation stages of impurities	• Visible (and VUV) spectroscopy	
Emission of higher ionisation stages of impurities	• VUV spectroscopy • GEM-based soft X-ray (vertical) camera	• GEM-based soft X-ray (horizontal) camera (approved)
Radiated power	• Horizontal bolometry	• Micro-bolometer arrays for tomography (proposed)
Effective charge	• Bremsstrahlung	
Isotopic ratio	• $D\alpha$ - $H\alpha$ spectroscopy • Optical Penning gauge	• Neutral particle analyser (under discussion) • ion-ion frequency reflectometer (proposed)
$T_{surf}$ on antenna and LH grill limiters	• IR thermography	
$n_e$ in vicinity of antennae and LH grills	• Probes and reflectometers for LH coupler and ICRH antennae	
LH deposition profile	• Hard X ray	
Fast electron losses	• Cherenkov detector on recip. probe	
$n_e$ core fluctuations	• Core X-mode reflectometers	
$n_e$ edge fluctuations	• Edge X-mode reflectometer, recip. probe	
$T_e$ core fluctuations		• ECE imaging diagnostic (approved)
$T_e$ edge fluctuations	• Recip. probe	
turbulence k spectrum	• Doppler reflectometer	• Vertical Doppler reflectometer (proposed)
Small scale $n_e$ fluctuations		• Upper Hybrid Resonance Scattering (UHRS) reflectometer (approved)
Other edge fluctuations	• Fast camera (tangential view)	

Table 10 : overview of WEST diagnostics

## II. Detailed description of WEST diagnostics

The following section gives a detailed description of WEST diagnostics, sorted in the following categories:

- 1) Plasma operation and control
- 2) Core plasma and pedestal profiles
- 3) Plasma Facing Components
- 4) Plasma Wall Interactions
- 5) Radiation and impurities
- 6) Coupling of heating systems
- 7) Turbulence and MHD

### 1. Plasma operation and control

■ **Magnetic measurements:** The diagnostic will measure plasma current, plasma position and shape, current centroid vertical speed, loop voltage, low and high frequency (up to 300 kHz) MHD mode activity, eddy and halo currents. The whole diagnostic set, except high frequency (HF) sensors, is essential from the start of WEST operation, including for the first WEST X-point plasma.

The WEST magnetic diagnostics are based on conventional inductive sensors, pick-up coils and flux loops, with analog integrators [Spuig 2003]. It will also feature innovative current measurement techniques based on fiber optic current sensors to measure the current in the passive structures located in the vacuum vessel [Moreau2011]. The optimization of the number and position of sensors has been carried out in collaboration with Nice University. The diagnostic consists of a set of about 460 sensors of 9 types located around the machine with 120° symmetry (cf. Figure 35). The sampling frequency of magnetics (except MHD) will be 500 Hz. The expected relative accuracy on the X point position is about 2 mm. The absolute accuracy on the separatrix position is about 10 mm.

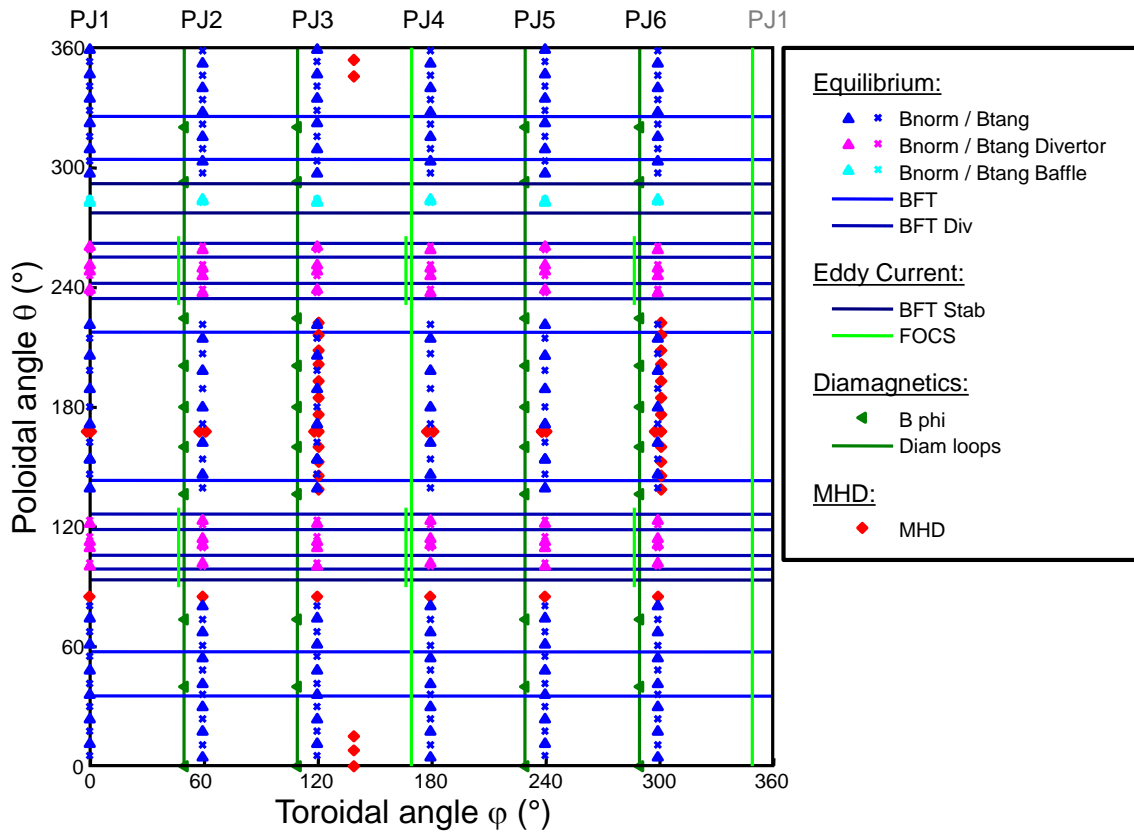


Figure 35 : Overview of magnetic sensors position

■ **Plasma Control System (PCS):** it is a key element to run any plasma discharge in a tokamak as it has to collect information from diagnostics and to orchestrate the actuators to reach the required plasma performance while ensuring the machine protection. To be able to address these advanced functionalities, the WEST PCS architecture is built around a single supervision unit which collects information from the tokamak subsystems (Figure 36).

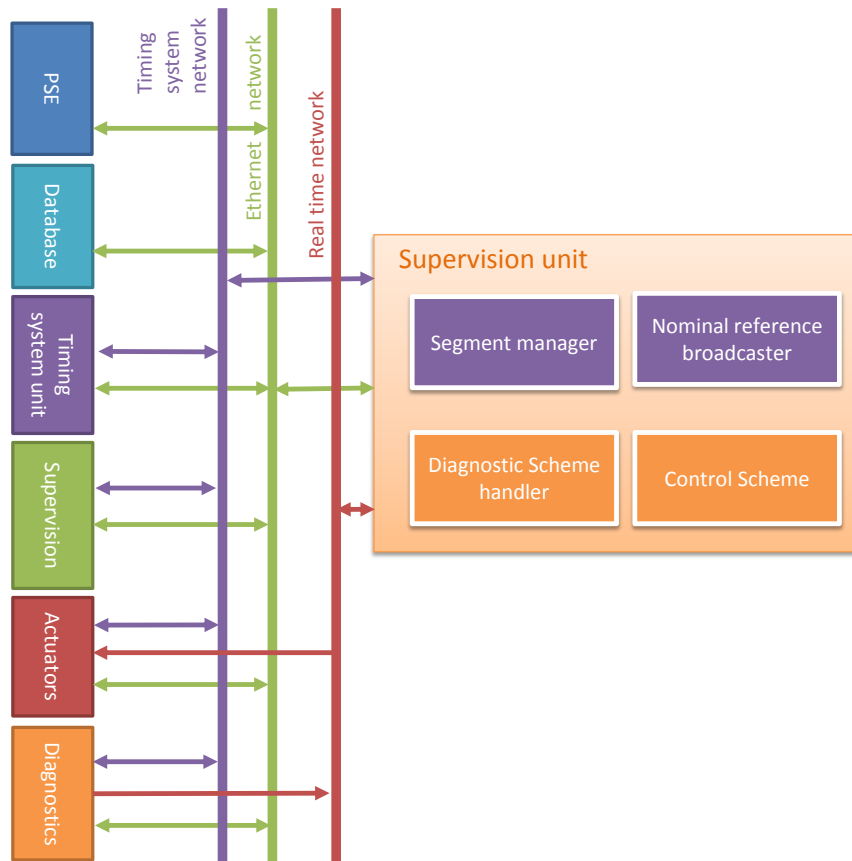


Figure 36 : Architecture of WEST Plasma Control System around a supervision unit.

This unit consists of several modules among which:

- The diagnostic scheme module's role is to check the consistency of plasma quantities provided by the diagnostics, calculate high level physics parameters, define the plasma state and identify the occurrence of an event.
- The plasma control scheme module's role is to control the plasma parameters and to optimize the use of the actuators to stay within the plasma scenario references envelope defined by the session leader.

Most of these modules may be prepared using Matlab Simulink and integrated automatically in the PCS. Existing C/C++ codes can also be integrated.

The WEST pulse schedule architecture has been developed to address modern tokamak control needs. It features especially a time segments approach to define a plasma discharge and real time event handling capabilities to deal with unexpected events which may occur during the discharge either by slightly adjusting the plasma scenario or by changing to a backup segment instead of aborting the discharge. The goal of this approach is to use as much as possible the allocated experimental time. For that purpose a segment manager module acts at the top of the PCS hierarchy. Its role is the full plasma discharge orchestration. For example, it decides (according to a preset set of rules) to move to an alternative plasma scenario when the reference scenario is no longer feasible. From the previous considerations and depending on the significance of the event, the PCS chooses between 4 levels of mitigation: 1) recovering the reference plasma quantities; 2) continuing the main

plasma scenario as long as the plasma parameters remain within preset reference envelopes; 3) changing to an alternative plasma scenario; 4) triggering a plasma shutdown.

To set all the parameters of a plasma discharge, a new pulse schedule editor will be developed.

As a starting point the control schemes available on WEST will be almost similar to those of Tore Supra with the additional controls of X-point, vertical instability and H/L mode transition. The main control and machine protection controllers are summarized in Table 11:

**Table 11: Summary of main controllers and real time protection systems (orange background) for WEST.**

Controlled Parameter	Associated measurement	Actuator
Plasma position and shape	Magnetic sensors	PF/Divertor coil power supplies
Plasma current (or edge safety factor)	Magnetic sensors	CS coil power supply
Central solenoid transformer magnetic flux (and plasma loop voltage)	Magnetic sensors	CS coil power supply and/or LHCD injected power
Line-integrated electron density (or Greenwald fraction)	Infrared interferometer	Gas piezo valves, supersonic beam molecular injector, pellets
Fraction of radiated power	Bolometers	Gas injection systems (impurities)
PFC overheating (wall protection system)	Infrared thermography or metallic impurity content (VUV spectrometer) or calorimetry	Heating system injected power
Density/radiative limit (risk of disruption)	Bolometers	Gas injection systems (deuterium / impurities)
Excessive MHD (risk of disruption)	Mix magnetic sensors and bolometers	Trigger plasma soft stop

## 2. Core plasma and pedestal profiles

■ **Interfero-polarimetry:** Tore Supra is equipped with a two wavelength far infrared interfero-polarimeter [Gil2009]. The basic set-up comprises five lines of sight in the plasma core. The beams come through a horizontal port and are reflected by HFS wall corner-cube mirrors. This set-up meets the WEST requirements in terms of real time gas injection feedback for plasma density control. Moreover, the system could provide a real-time indicator for the L-H transition using for example, the ratio of core / mid-radius line integrated densities. Three more lines of sight ( $r/a < 0.5$ )<sup>[1]</sup> are planned to enhance the spatial resolution of the diagnostic in the gradient region. Finally, two additional lines are envisaged through a vertical port : one, interferometry only, to diagnose the X point and the other to complete the spatial resolution by a measurement at  $r/a=0.9$ . The lines of sight are shown on Figure 37.

<sup>[1]</sup> One additional line of sight viewing across the X point is also proposed.



Using as inputs the line integrated densities and Faraday angles calculated by a digital electronics, real time and post processing codes calculate consistently the magnetic equilibrium and the electron and current density profiles. The default data acquisition is continuous at the millisecond rate. A 1 MHz data acquisition can be set on request for studying fast density transient events and modes triggered by e.g. pellet injections, ELM disruptions or MHD.

file : WEST-Xpt-close-776kA version number 18

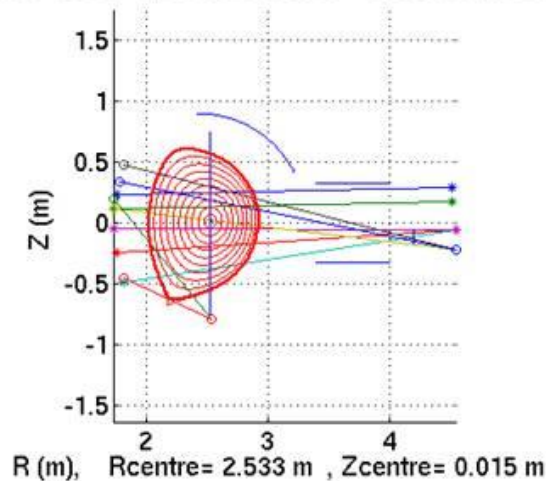


Figure 37 : Interfero-polarimetry chords in a poloidal cross section

■ **Heterodyne ECE radiometer:** the Tore Supra radiometer which has been operated and constantly updated for several years [Ségui2005] will be present on WEST. It measures the whole LFS radial  $T_e$  profile and part of the HFS profile from a midplane port. Thanks to a good gyrotron frequency rejection, it provides data in all scenarios, even when some ECRH power is injected into the plasma. It has 32 channels equipped with a low divergence beam optics of  $1.4^\circ$  giving a radial resolution of 2.5 cm. Thanks to its absolute calibration, the radiometer absolute accuracy is  $\pm 7\%$  and the relative interchannel error is  $\pm 3\%$ . Two acquisition systems can be used simultaneously: i) a standard acquisition mode allows the 32 channels to measure at 1 ms time sampling for the whole plasma duration (useful for temperature profile measurements), ii) a fast acquisition mode allows the 32 channels to measure at  $1\mu\text{s}$  time sampling for a time window either preset or triggered by a given plasma event (useful for MHD). In addition, 4 channels were equipped for correlation studies.

■ **Thomson scattering:** Using the current optical components, the Thomson scattering diagnostic is upgraded with a whole set of new lasers, replacement of the bundle of fibers with monofibers, optimisation of the polychromators and implementation of a fast acquisition system. This allow to comply with the high spatial resolution requirements for the electron temperature and plasma density measurements in the pedestal region. In order to achieve the required resolution 15 measurement points will be available in the pedestal region while a few points are kept in the plasma core region (Figure 38). The expected characteristics for the high resolution measurements are the following:

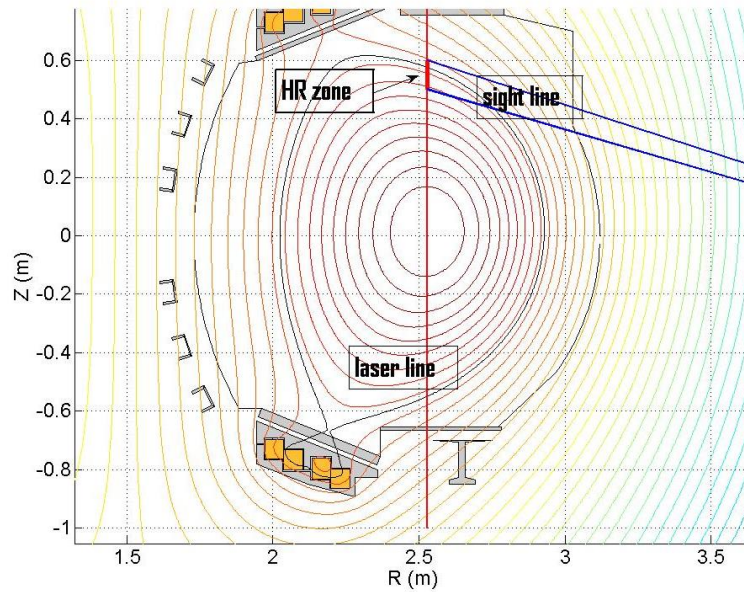


Figure 38 : Thomson scattering diagnostic laser beam (in red) and measured region (in blue).

- Spatial resolution ~ 6 mm,
- Repetition rate of the measurement > 10Hz,
- Accessible  $T_e$  range between 0.1keV and 1keV,
- Minimum density  $1.5 \cdot 10^{19} \text{ m}^{-3}$ .

■ **2D X ray crystal spectrometer:** An X-ray imaging crystal spectroscopy system will provide routinely ion temperature and toroidal velocity profiles mainly, but also electron temperature, impurity density, and poloidal velocity profiles during the whole plasma discharge duration, with a spatial resolution better than 1cm and time sampling as fast as 10ms (depending on the observed impurity). The instrument relies on the Johann type spectrometer principle, providing a direct view from the dispersion element to the plasma (there are no secondary elements in order to optimize the sensitivity and the flexibility of the device), and using Bragg reflection on the full surface of a spherically bent crystal. The latter allows for both spatial and spectral resolution, as shown on Figure 39. High count rate 2D pixilated silicon detectors with high count-rate ( $> 10^7/\text{s}/\text{mm}^2$ ) will be implemented, allowing for the full X-ray intensity available from the plasma to be processed.

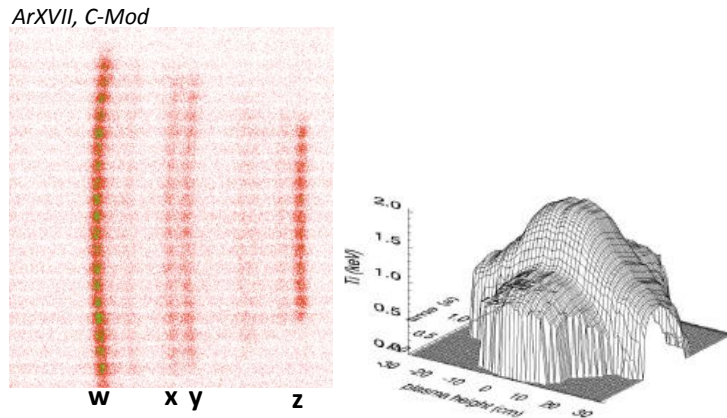


Figure 39 : Ar He-like X-ray image and time evolution of typical inferred Ti profiles

As illustrated in Figure 40, the wide probed plasma region (full plasma diameter) is obtained with a combination of three viewing lines (hence three spectrometers). The central viewing line allows for a plasma coverage  $r/a = [-0.5 \ 0.5]$ , the top viewing line for  $r/a = [0.45 \ 1]$  and the bottom viewing line for  $r/a = [-0.45 \ -1]$  (with some spatial cross-coverage between, which can be quite useful for data consistency). Each viewing line will have a  $\sim 57^\circ$  angle with respect to the magnetic axis in the horizontal plane, allowing for accurate rotation measurements. The central viewing line will be installed for WEST phase 1, collaborations being foreseen for the others.

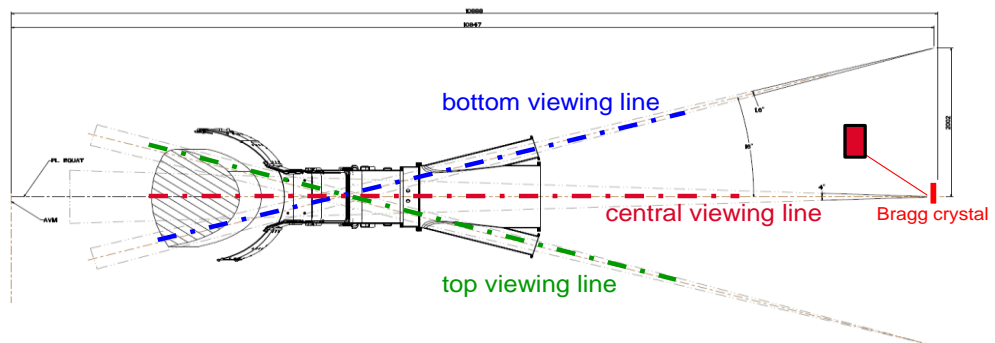


Figure 40 : (Top) Side view of the spectrometer viewing access in WEST (lower single-null initial test configuration; note that plasmas would likely be narrower).

The layout is optimized for Argon He-like, Argon H-like (injected impurity,  $n_{Ar}/n_e \sim 10^{-4} - 10^{-5}$ ) and Iron He-like measurements (intrinsic impurity), but other elements could be considered.

■ **He jet emission spectroscopy**: three supersonic helium jets ( $v_{He} \ 1.8 \text{ km/s}$ ) will be available. One will be installed horizontally in a midplane port, the second one vertically in the baffle and the third one will be in the protection limiter of an ICRH antenna. The collection optics will be telescopes (e.g. fr the midplane jet) or in situ

optics already used in the past (baffle jet). The  $n_e$  and  $T_e$  ranges will be  $10^{18}$  -  $4 \times 10^{19}$   $m^{-3}$  and 20 - 350 eV respectively. This diagnostic will thus be adapted to measurements in the pedestal. The spatial resolution and sampling are expected to be around 5 mm (depending on the location of the jet). The ultimate time resolution is defined by the type of detectors, which will probably be photomultiplier tubes, but in practice it will be determined by the signal-to-noise ratio.

### 3. Plasma facing components

■ **Calorimetry:** The calorimetric diagnostic [Chantant2005] is implemented in the cooling water system. It is composed of temperature sensors (inlet and outlet), and flowmeters (differential pressure, vortex or ultra-sonic types). Temperature sensors consist of four wires Pt100 resistors (high sensitivity  $\pm 2 \cdot 10^{-2}$  K) directly immersed into the coolant. The acquisition is working 24h/7days with variable sampling rate (4Hz during plasma operation and 1Hz between pulses). The basic data processing allows measuring the thermal exhaust power from the components using the formulae  $P_{exhaust} = \dot{m}(t) \times \rho \times Cp \times (T_{out}(t) - T_{in}(t - \tau))$ , where  $\tau$  is the time needed for the fluid to go through the cooling system of the PFC. The integral of the exhausted power recorded during the pulse provides the cumulated thermal energy exhausted from the PFCs. The sum of power/energy exhausted by each PFC enables to derive the global power/energy balance. In the Tore Supra configuration the deviation between calorimetric and input power/energy was less than 10%.

In WEST 71 PFCs will benefit of the calorimetric instrumentation, about 140 flowmeters and 140 temperature sensors are presently planned :

- Upper divertor (x12, each sector is individually monitored)
- Upper damp plate (x18)
- LHCD antenna (x2, each antenna is individually monitored)
- ICRH antenna (x3, each antenna is individually monitored)
- HFS inner vessel protections + bumper (x6)
- LFS vessel protections (x6)
- Lower divertor (x12)
- Baffle (x12)
- Single PFU for physics application (xTBD)

Advanced and off-line data processing based on inverse techniques (using the experimental transfer function of the PFC and regularisation techniques) enables to extract the time evolution of the power deposited on each PFC:

$$P_{PFC}(t) = M^{-1} \times P_{exhausted}(t),$$

where M is the regularized transfer function of the PFC.

■ **Infra-Red thermography:** The IR thermography system [Guilhem2005, Salasca2009] will be a key diagnostic for WEST, both for machine protection and

programmatic needs. The baseline IR monitoring configuration includes 6 mid-wavelength IR (MWIR, 3-5  $\mu\text{m}$ ) standard endoscopic views for lower divertor monitoring, 6 optic fiber bundles for antenna and outboard limiter views, 1 wide angle tangential view. In addition, 1 fast IR and 1 bi-colour camera will be available for divertor or wide angle tangential views according to the programmatic needs. The main characteristics and performances of the IR thermography systems are summarized in the following table:

System name	sensor / filter	T° range	Spatial resolution / Field of View (FoV)	Frequency /integration time
Standard Div monitoring	CEDIP InSb [3-5 $\mu\text{m}$ ] 256x320 pixels 30 $\mu\text{m}$ pitch Filter: 4.5 $\mu\text{m}$	35°-1800° Black Body 140°-4000°C with $\epsilon=0.2$	r=7-9mm FoV=2x30°	50Hz, automatic $\tau=11, 65, 340\mu\text{s}$
HR Div monitoring	CEDIP InSb [3-5 $\mu\text{m}$ ] 256x320 pixels 30 $\mu\text{m}$ pitch Filter: 4.5 $\mu\text{m}$	35°-1800° Black Body 140°-4000°C with $\epsilon=0.2$	r=4-5mm Fov=20°	50Hz, automatic $\tau=11, 65, 340\mu\text{s}$
Antenna views (bundle)	InGaAs [1-2 $\mu\text{m}$ ] 320x26 logarithmic	300°-2000°C Black-body	r=13mm FoV=62°	Log.
Wide angle tangential view	CEDIP 320x256 pixels of 30 $\mu\text{m}$	35°-1800° Black Body 140°-4000°C with $\epsilon=0.2$	r=20mm Fov=60°	50Hz, automatic $\tau=11, 65, 340\mu\text{s}$
Fast IR camera	IRCAM InSb [1-5 $\mu\text{m}$ ] 512x640 pixels de 15 $\mu\text{m}$		r=10 mm for the WA view r=4mm for the DIV view	640x512 @333Hz to 640x6 @5kHz
Bi-spectral SOFRADIR-IRFM	HgCdTe 3-5mm x2 640x512			

Table 12 : overview of the IR system foreseen for WEST

A basic treatment of the thermographic measurement enables to derive the surface temperature ( $T^{\text{surf}}$  [°C]) of the PFC (based on calibration routine and surface emissivity table). Advanced data processing based on thermal modeling of the PFC (2D or 3D modeling could be required in function of the material thermal properties) enables to derive the heat flux received by the PFC ( $Q$  [MW.m<sup>-2</sup>]). Transient application (ELM, VDE, disruption...) can be performed with fast IR camera (up to 5kHz).

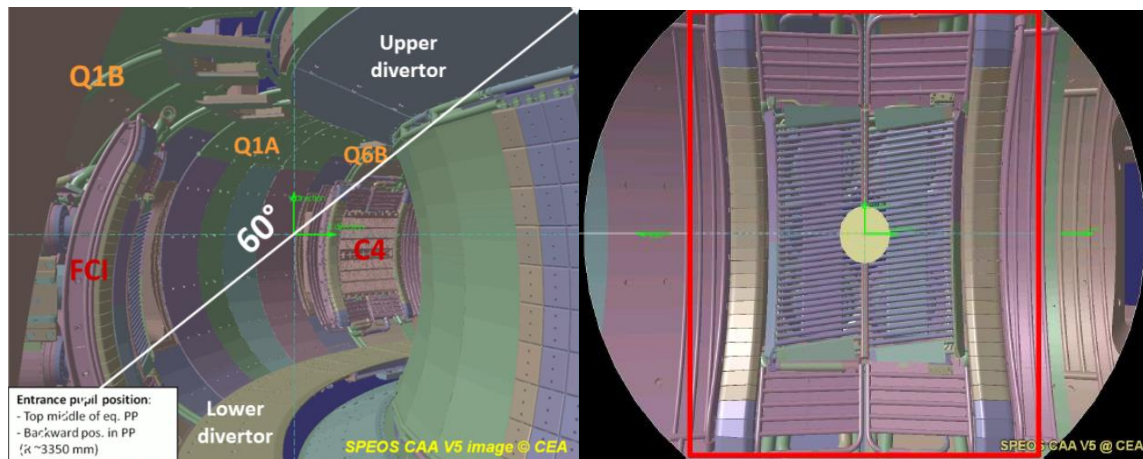


Figure 41 : (left) Field of view of the wide angle tangential viewing system, (right) Field of view of the fiber bundle system

■ **Thermocouples:** Thermocouples are used to determine the bulk temperature ( $T^{\text{bulk}}$ ) of the PFCs (see e.g. [Gaspar2013]). They can be intrusive (embedded) or non intrusive (spot welding). Type N thermocouples enable temperature measurements in the range of 100°C-1300°C. When steady state is reached for both the plasma and the component, the bulk temperature can be correlated to the surface temperature of and the heat flux onto the component (via thermal modelling). The thermocouple data can then be compared with IR data measurements. During transients, off-line inverse techniques (similarly to calorimetric measurements) are necessary to retrieve the surface temperature ( $T^{\text{surf}}$ ) and peak heat flux ( $Q^{\text{peak}}$ ). For non-actively cooled PFC tiles, it is possible to derive the cumulated tile energy from the bulk tile temperature rise for the whole pulse (the cooling curve is back extrapolated to the end of the heating pulse). This is valuable if the tile has been homogeneously heated and cools down by conduction/radiation only.

■ **Langmuir probes:** The global Langmuir probe set is essential for edge plasma characterization (temperature, density, particle and heat flux) and advanced understanding of SOL transport (SOL flows ...). It is an essential tool to characterize divertor regimes, investigate power and particle balance, interpret plasma spectroscopy as well as for RF antenna coupling physics, plasma transport studies. It will be used to constrain the edge plasma modelling, which requires both high quality upstream and divertor target plasma profiles. The Langmuir probe set is composed of:

- 64 flush mounted probes in the Upper and Lower divertor. Probes are positioned in order to measure as closely as possible the maximum heat / particle flux as expected from the toroidal distribution pattern. Basic setting enables to derive  $T_e$  [eV],  $n_e$  [ $\text{m}^{-3}$ ] near the target. Using the microsecond time resolution foreseen should allow discriminating ELMs and inter ELMs plasma parameters, which are also of high interest for the program.
- 2 ITER-like probes in the proximity of the divertor PFU
- 2 Upper reciprocating probes: 2 existing upper reciprocating probes allows to characterize the plasma in the SOL (radial profiles). Magnetic connection with one of

the RF antenna is possible to investigated RF specific heat load. Using the 2 upper reciprocating probes allows for instance simultaneous  $T_i$  measurement with the tunnel probe and  $n_e/T_e$  flows with the Mach probe.

- 2 outboard reciprocating probes (pecker types): 2 probes are located in outboard limiters with 10 cm radial excursion. This will allow the characterization of SOL transport and investigation of far SOL parameters.
- 10 Flush mounted probes in the inboard limiter
- Flush mounted probes in the pumping baffle (number to be defined)

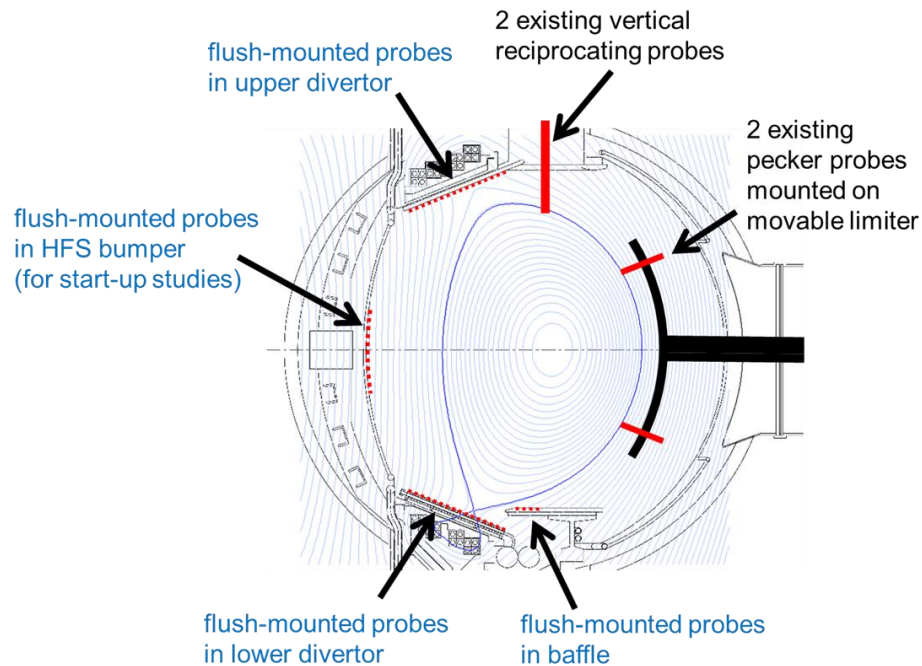


Figure 42 : schematic view of the Langmuir probes set up for WEST

■ **AIA inspection robot:** Between WEST plasma sessions, in-vessel inspection will be required for high flux components checking and wall investigation. To minimise the impact on the machine duty cycle, these operations must be performed under high vacuum and temperature conditions to keep the vessel conditioning. To that purpose, a remote-handling system called the Articulated Inspection Arm (AIA robot, Figure 43) was developed and tested by CEA to perform mini-invasive tasks into a tokamak.

The arm is a 7.3 meter long multi-link cantilever beam made of 5 titanium modules able to be deployed through a noteworthy small port of 250 mm diameter. With the deployment shuttle and the embedded vision camera, both developed concurrently, the AIA device offer up to 11 degrees of freedom and allow close inspection of all the WEST Plasma Facing Components (few centimeters from robot head to wall).

In September 2008, the operation was demonstrated into the Tore Supra vacuum vessel at 120°C and in a  $10^{-5}$  Pa vacuum without any effect on the

conditioning. Following this success, CEA has started a robot upgrade and a tokamak integration completion activity to provide a routine inspection device for WEST operations. A collision avoidance software will be implemented. The target accuracy for in-vessel robot displacement is about 5 cm and the camera snapped pictures will have a submillimetric resolution without external light source needed.

In parallel of the inspection device integration, several applications are considered to convert the AIA robot in a multi-purpose carrier able to assist the WEST operation. Developments are already started for in-vessel water leak localization and infrared diagnostic in situ calibration.

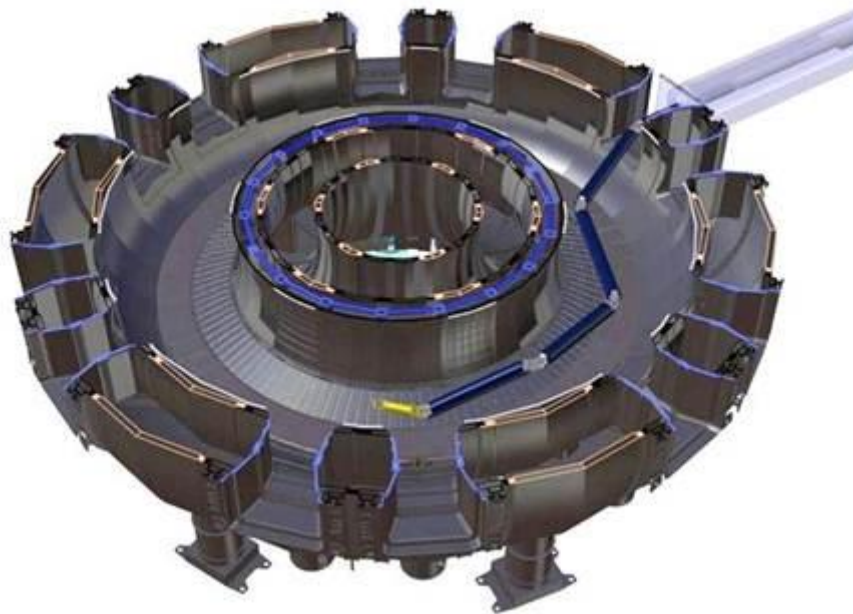


Figure 43 : AIA robot deployment in WEST

#### 4. Plasma wall interaction

■ **Barometry, mass spectrometry and Penning gauges:** Measurements for particle balance studies will be performed in WEST by a set of pressure gauges and mass spectrometers. In the WEST project, it is anticipated that fuel trapping in the metallic wall will be lower than in the carbon one. In order to get a sufficient accuracy of the particle balance measurements, it is proposed to accumulate the exhaust in a dedicated volume and to analyze the stored gas by mass spectrometry (see Fig. XX). In parallel to this measurement, an optical Penning gauge [Klepper1997] will be used for isotope ratio  $n_H/(n_H+n_D)$  assessment.



## Barométrie WEST

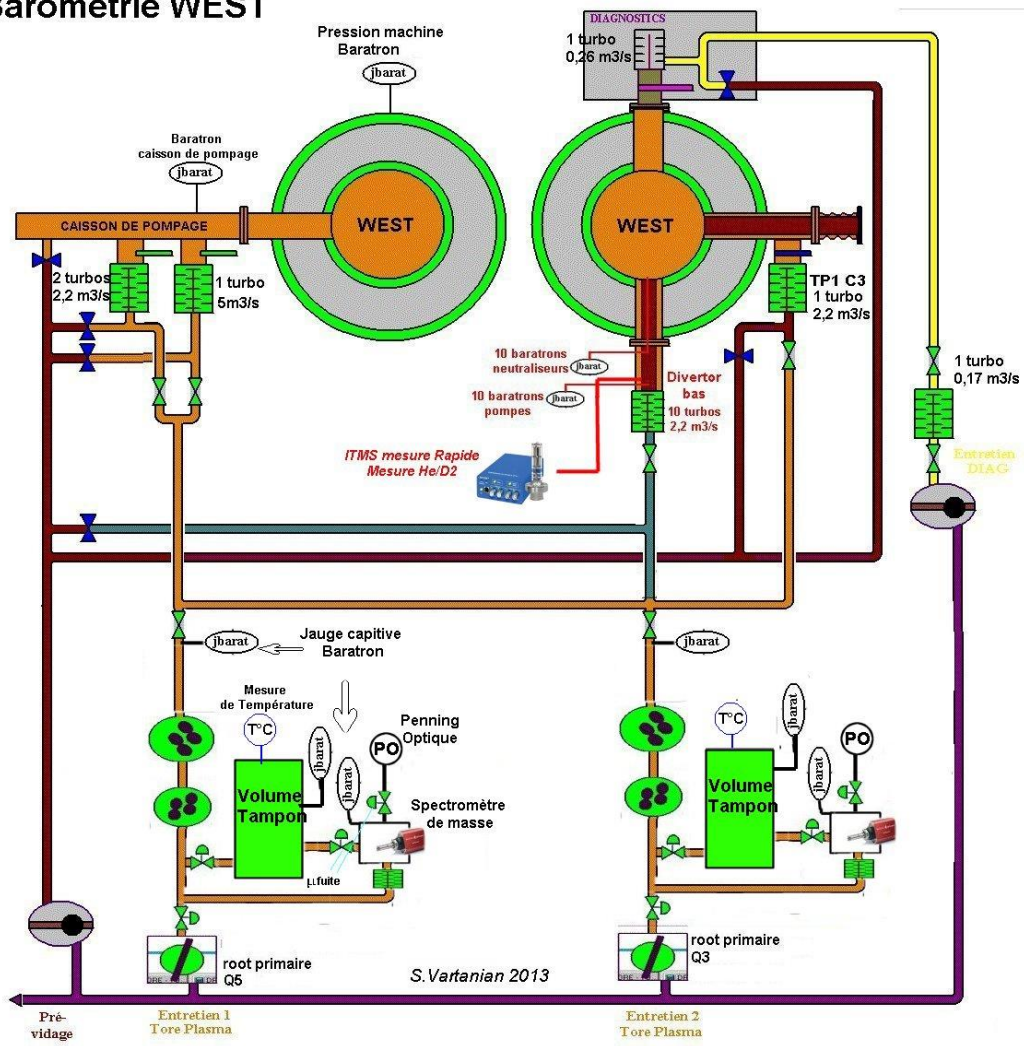


Figure 44 : Outline of the barometry set-up in WEST

These accurate measurements are complemented by baratron gauges located under the divertor which can assess the total particle outflux from the machine. The gas composition will be measured by a sensitive Ion Trap Mass Spectrometry (ITMS) device able to separate deuterium and helium.

■ **Dust injection and collection:** During tokamak operation, dust is usually produced by several processes such as material sputtering and accretion, deposited layer delamination by fast thermal heating etc. When entering the plasma, the dust particles are rapidly negatively charged and travel along the field lines in the plasma edge. In WEST, it is proposed to collect these particles in an aerogel. The aerogel will be placed in two reservoirs mounted on a dedicated head of one of the reciprocating probes. After several insertions of the aerogel in the WEST SOL, the collected sample will be extracted and analyzed by SEM (Scanning Electron Microscopy) and TEM (Transmission Electron Microscopy). The composition of the particles will be determined by IBA (Ion Beam Analysis). In Figure 45 a drawing of the dedicated tool is proposed.

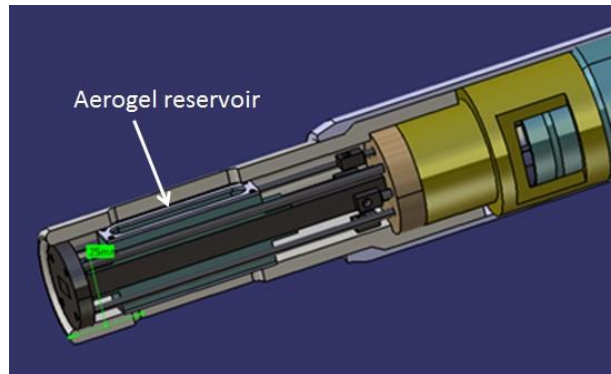


Figure 45 : Picture of the dust collector as installed on a reciprocating probe of Tore Supra.

An upgrade of this tool (see Figure 46) could also be used to insert particles of known size. A reservoir containing the particles is placed at the end of the previous tool. The deceleration of the reciprocating probe is thus used to shake the reservoir and inject the particles in the plasma.

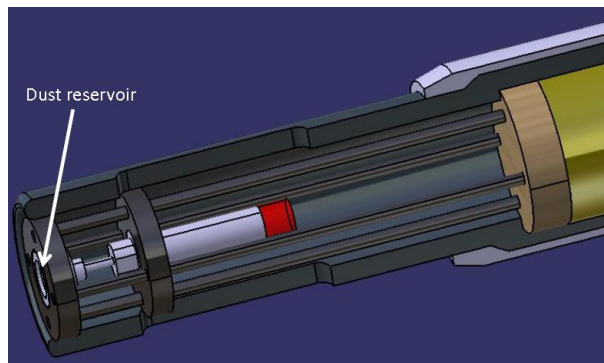


Figure 46 : Picture of the dust injector as it will be installed on the reciprocating probe of Tore Supra

The upper bound of the injected particle (mainly tungsten dust) size range is defined by a grid closing the particle reservoir (from 2.5 $\mu\text{m}$  to 250 $\mu\text{m}$ ). Each shock corresponds to a known number of injected dust particles ( $\sim 1000$ ). When entering the plasma, the particles are heated and detected by a fast CCD camera. This injection tool will be used as a SOL transport diagnostic but also as a test of plasma resilience to a calibrated influx of particles.

■ **LIBS and LIDS:** LIBS (Laser Induced Breakdown Spectroscopy) is a technique [Semerok2013] which allows to measure locally the deuterium/tritium inventory in plasma facing components. It could also be used to assess the purity of the materials facing the plasma or to evaluate the thickness of a deposited layer. The LIBS technique is based on the spectroscopic analysis of the plasma created when a powerful laser is focussed on materials of interest. It is proposed to install this LIBS diagnostic in the WEST tokamak.

A pulsed picosecond laser will be focussed on the divertor target or on the baffle of the machine between tokamak plasma discharges. The light emitted by the created plasma will be analyzed and the composition of the material retrieved. The laser beam will enter the WEST vessel through a top port as proposed in the following picture. The laser beam direction will be mobile so that the surface analyzed can be

as large as square meters (see Figure 47). Light emitted by the LIBS plasma will be collected in the same port and analyzed.

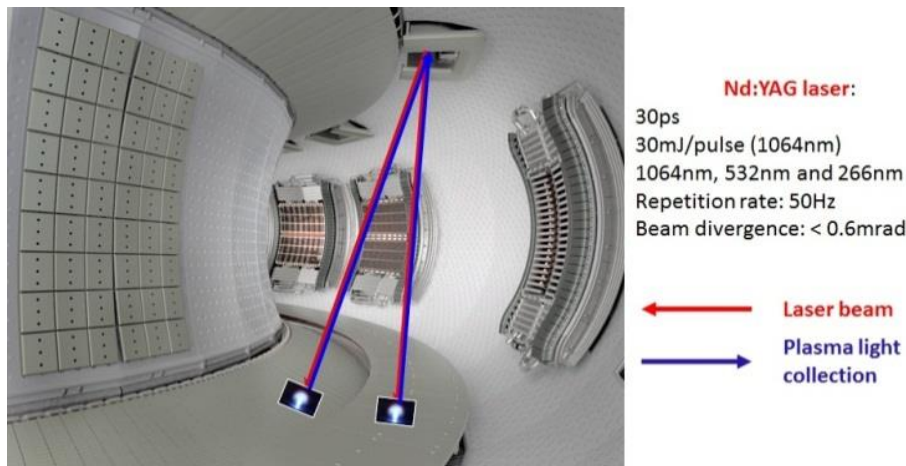


Figure 47 : Schematic view of the LIBS experiment in the WEST tokamak.

With a reduced fluence, the laser pulse heats up the materials and the trapped fuel is thermo-desorbed. The fuel escaping from the wall is then ionized by the tokamak plasma. The  $H\alpha$  and  $D\alpha$  spectral line evolution with the laser pulses is used to characterize the wall inventory. This technique called Laser Induced Desorption Spectroscopy will be implemented in WEST.

■ **Sampling on W material on the reciprocating probe:** The implantation of deuterium in different W based materials will be studied in the WEST tokamak. The samples, mainly W alloys presently considered for use in the DEMO reactor, will be placed on the reciprocating probe and plunged into the SOL. The position of the samples in the SOL will be defined in order to maintain the material at a temperature below 350°C. Some plasma immersion will be necessary to get the needed ion fluence.

Prior to implantation, the samples will be carefully characterized. Special attention will be devoted to internal defects evaluation.

After implantation, the samples will be retrieved and studied by various techniques (IBA and Thermo-Desorption Studies – TDS).

■ **Confocal microscopy:** In order to measure erosion from and redeposition onto the WEST divertor target, a diagnostic based on confocal microscopy [Gauthier2013] will be used. The principle of the chromatic confocal microscope is based on a white light source passing through a chromatic lens and focussed, depending on the wavelength, at different positions on the optical axis. Backscattered light is deflected through a pinhole toward the detector. Only the light coming from the focus point is passing through the pinhole. The light collected by the instrument presents a maximum at the wavelength corresponding to the focal distance between the lens and the surface. Therefore, at each point of the surface, the axial coordinate (z) can be determined from the maximum intensity on the instrument. By changing the focal length of the chromatic lens, the range of measurement can be varied in the range of 100  $\mu\text{m}$ –10 mm with an axial resolution from 10 nm to 0.3  $\mu\text{m}$ . The lateral

resolution is limited by the size of the spot which varies from 3 to 20  $\mu\text{m}$ . Scanning the surface, by moving either the object or the optical head, in two directions with step motors allows the acquisition of a cloud of points and produces 3D measurements of the object. An opto-mechanical bench was designed for measuring *in situ* the TPL erosion/deposition in Tore Supra after the DITS campaign (see Figure 48). A structure was assembled in the tokamak chamber and connected to the vacuum vessel. The displacements (toroidal, radial, X & Y) were remotely controlled by step motors. The same principle will be used in the WEST device.

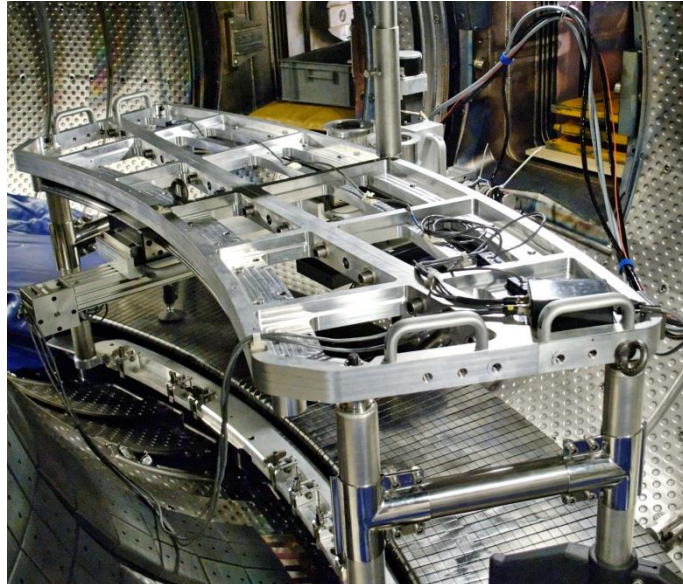


Figure 48 : In Situ confocal microscopy for erosion/deposition limiter assessment (DITS campaign)

One of the issues when using confocal microscopy for erosion/deposition studies is the need of an absolute reference surface to improve the accuracy of the measurement and reduce the errors. It will be obtained by marking the side of some of the virgin elements of the divertor target by Focussed Ion Beam (FIB). Each mark will be engraved prior to operation at different distances from the surface ensuring accurate confocal microscopy measurements.

## 5. Radiation and impurities

■ **Vacuum ultra-Violet (VUV) spectroscopy:** Two VUV, grazing incidence spectrometers are available on Tore Supra: SIR [Schwob1987] and SURVIE. SIR is equipped with two interchangeable gratings (600 g/mm, 15-340  $\text{\AA}$  and 300 g/mm, 30-700  $\text{\AA}$ ) and two remotely controlled detectors allowing to measure two spectral intervals of a few tens of angströms at the same time with a 0.2  $\text{\AA}$  spectral resolution. The SIR mobile line of sight allows to scan the lower half of the confined plasma and the lower divertor region in about 1 s (Figure 49). SURVIE is a simpler version of SIR with only one grating (600 g/mm) and one detector. It is designed for intrinsic impurity monitoring and its data acquisition is included in the plasma feedback control loop. Both systems can perform real time measurements with a sampling period as low as 10 ms.

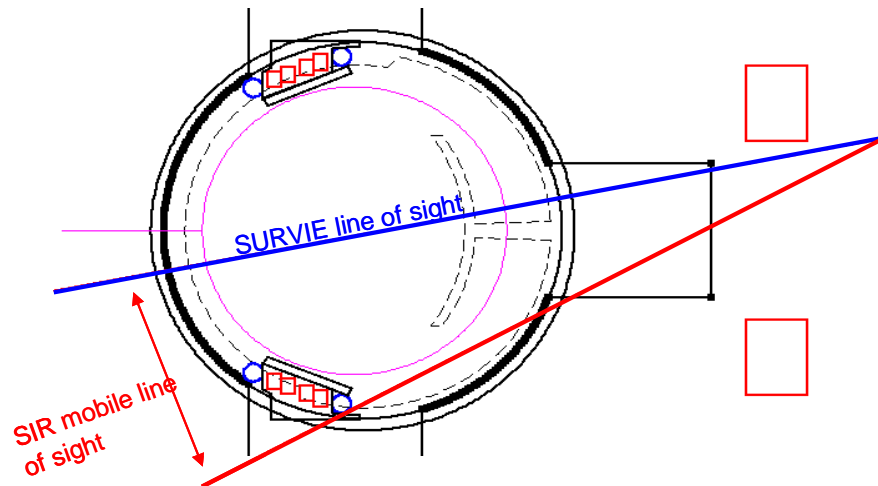


Figure 49 : SIR and SURVIE geometry for VUV spectroscopy

Development of spectral analysis and processing tools will be necessary to commission a W real time and an on-line monitoring.

■ **Visible spectroscopy:** A total of 200 lines of sight detailed in Table 13 is required to cover all the relevant components, with the aim of providing impurity (in particular W) sources and recycling fluxes. A dispatching system will be developed to easily connect the optical fibers to the spectrometers.

Table 13 : Specifications of lines of sight for visible spectroscopy

Objects : Main specifications :	Antenna protections	Inner limiters	Upper divertor	Lower divertor	Baffle
<b>Dimension</b>	94 x 504 mm	2 x 510 mm	600 mm	450 mm	200 mm
<b>Object field</b>	29°	2 x 19°	16°	29°	29°
$\phi_{spot}$ <b>(spatial resolution)</b>	90 mm	45 mm	10 mm	10 mm	10 mm
<b>D (sampling period)</b>	90 mm	60 à 70 mm	20 mm	10 mm (150→250mm / 280→380mm) 20 mm (elsewhere)	20 mm
<b><math>g_y</math> système</b>	0,004	≈ 0,01	0,04	0,04	0,04
<b><math>N_{views/object}</math></b>	2 x 5	2 x 8	3 * 10	3 x 11	10

\* 5 antennas are expected on WEST with 2 antenna protections each

Concerning optical aspects, a large aperture *in situ* optical system (F number ~ 3) will be developed for each set of ~ 10 optical fibers. The optical system and

optical fibers are designed to operate at the inner wall temperature range (80 °C to 110 °C) and to stand conditioning temperatures up to 200°C. Each system will be positioned in order to see its target under normal incidence to optimize the spatial resolution (2 to 9 cm depending on the object) and to avoid specular reflections.

The light collected by the optics and transported out of the torus hall by the optical fibers is analysed by four spectrometers. One is optimised and exclusively dedicated to the W I 4009 Å line detection. It can accommodate 27 input fibers. Two other spectrometers, accepting 28 fibers each, are of a more general use. The fourth spectrometer, with a lesser f number (about f/10 instead of f/3-4.6 for the first three), is well suited for high resolution applications (such as the H $\alpha$ /D $\alpha$  intensity ratio for plasma edge isotopic ratio estimate). To complete the set of spectrometers, a number of detection channels (4-8) made of an interference filter + a photomultiplier tube will be available.

Regarding the sampling period on the spectrometers, two acquisition modes can be selected: a “standard mode” with a 5 ms sampling period and a “high speed mode” with 0.2 ms sampling period (e.g. for ELM studies). In the case of the latter one, it may be necessary to sum adjacent lines of sight in order to reduce the camera readout time or/and increase the signal-to-noise ratio.

■ **Bolometry:** WEST will be equipped with three bolometric cameras (one camera = 8 lines of sight) in a horizontal port and one or two cameras located in a vertical port. The two wide angle (covering a 18.5° angle, brown lines on Fig. XX) horizontal cameras will provide a full scan of the vertical direction allowing to determine the total radiated power (the accuracy of the estimate depending on the degree of asymmetry of the radiation in the plasma; typically the accuracy should be between 10 and 20%). The third horizontal camera will be a narrow angle one (covering a field of 9.3°, in green on Figure 50) and set to observe the divertor region. The narrow angle vertical cameras (blue and red on Figure 50) will give information about the radiation on the low field side of the plasma including a small part of the outer divertor. The spatial resolution of the horizontal lines of sight observing the divertor will be around 9 cm at the divertor. The diagnostic can be operated typically with a sampling rate of 10 ms but a rate of 1 ms can be considered.

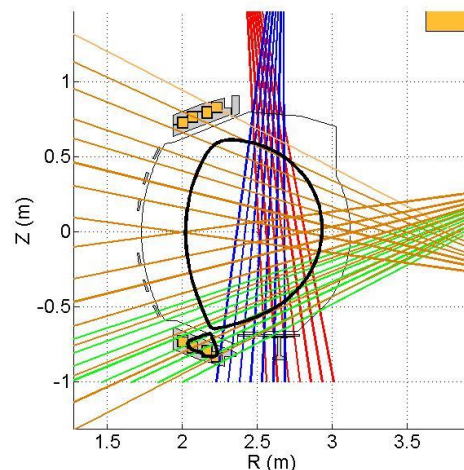


Figure 50 : Bolometric lines of sight in a poloidal cross section of WEST

■ **Soft X-ray detection:** In WEST, the number of vertical lines of sight from an upper port is restricted by the presence of the upper divertor. The proposed alternative is to install a diagnostic based on GEM (Gas Electron Multiplier) detectors [Mazon2013] working in photon counting mode. Such a detector has already been operated on Tore Supra (matrix detector) since 2011. The WEST version is made of an array of 128 detectors located inside the vertical port so as to have a full view of the plasma. The detector array is inserted into a sleeve so as to be kept under atmospheric pressure. A second GEM-based camera is proposed for the horizontal port. Tomographic reconstruction of the SXR distribution is thus available on WEST (See Figure 51). Spatial resolution will be improved with respect to the previous SXR diagnostic (3 cm in the poloidal plane with a beam width of 12 cm in the toroidal direction). Slow (1ms) and fast ( $\mu$ s) acquisition modes are foreseen. The matrix detector will be available on request for toroidal imaging of the plasma.

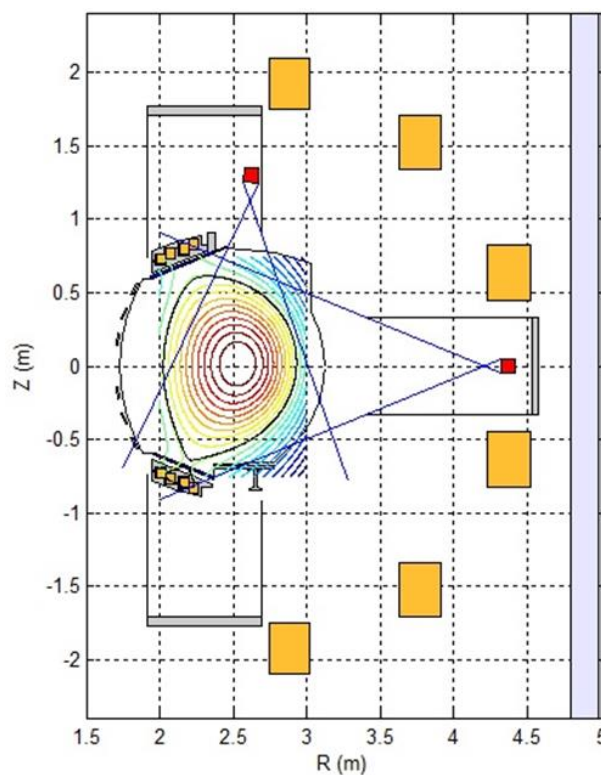


Figure 51 : Layout of the GEM detector diagnostic for SXR detection (red squares are SXR active surfaces)

■ **Bremsstrahlung measurements for effective charge assessment:** The bremsstrahlung will be measured from two different toroidal positions. One line of sight will be in the tangential direction at the mid-plane and will provide an estimate of  $Z_{eff}$  strongly weighted by the plasma centre. In another toroidal port, at least six lines of sight arranged obliquely in a poloidal plane will allow to give estimates of line integrated  $Z_{eff}$  for different radii. The photons collected by the appropriate optics are carried by optical fibers to photomultipliers equipped with interference-filters (central wavelength 523.8nm, bandwidth 1nm). The diagnostic will be sampled with a 4 to 8 ms time resolution.

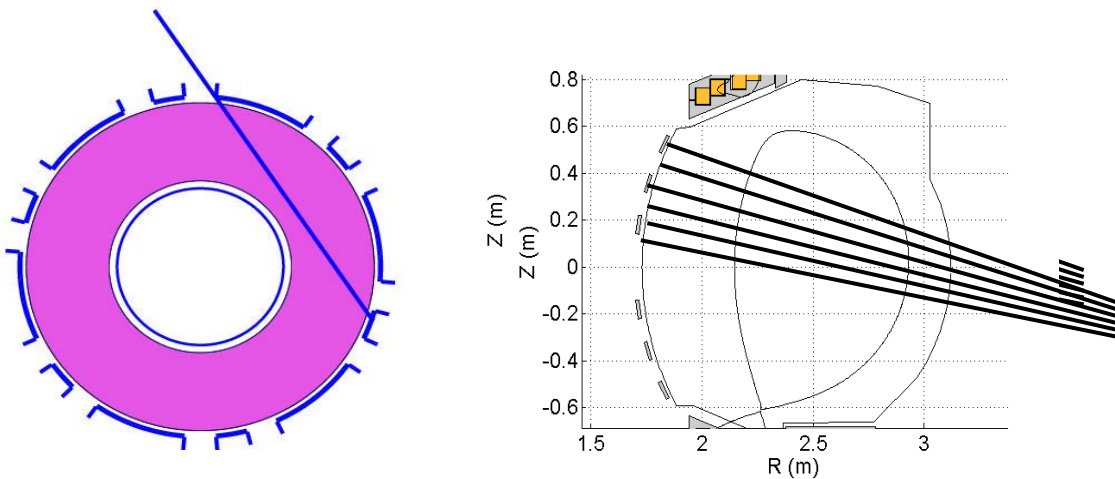


Figure 52 : line of sight for the Bremsstrahlung system

## 6. Coupling of Heating systems

■ **Fixed probes on LHCD launchers:** Tore Supra is equipped with two Lower hybrid Current Drive (LHCD) launchers, operating at  $f = 3.7$  GHz. The electron density in front of the launchers is a critical parameter for the coupling of the LH wave, since the slow wave has a cut-off at  $1.7 \times 10^{17} \text{ m}^{-3}$ . To measure the electron density near the launchers, four fixed Langmuir probes are installed in the corners on each of the two launchers (Figure 53). A swept voltage (from -100V to +20V with 16 points in 2 ms) is applied to the probes in order to yield the electron density and electron temperature locally near the launcher mouths. For WEST, the voltage sweep will be increased to 64 points during 2 ms.

In addition to eight Langmuir probes, six additional probes are available for measuring the density fluctuations in the scrape-off layer at the launcher mouths (Figure 53). A fast diagnostic allowing several triggers during the pulse to measure the ion saturation current with an acquisition frequency of 1 MHz during a time interval of 16 ms for each trigger. Four channels have been available for this diagnostic (called DFLUC). In the last experimental campaign on Tore Supra, a new diagnostic (called DCEDRE) with an acquisition frequency of 200 MHz was tested on two channels [Goniche2013]. An upgrade of the two diagnostics (DFLUC and DCEDRE) is proposed for WEST, to allow increasing the number of measurement channels of the very fast diagnostic (200 MHz) and to optimize the frequency range for these measurements, but this is outside the WEST baseline.



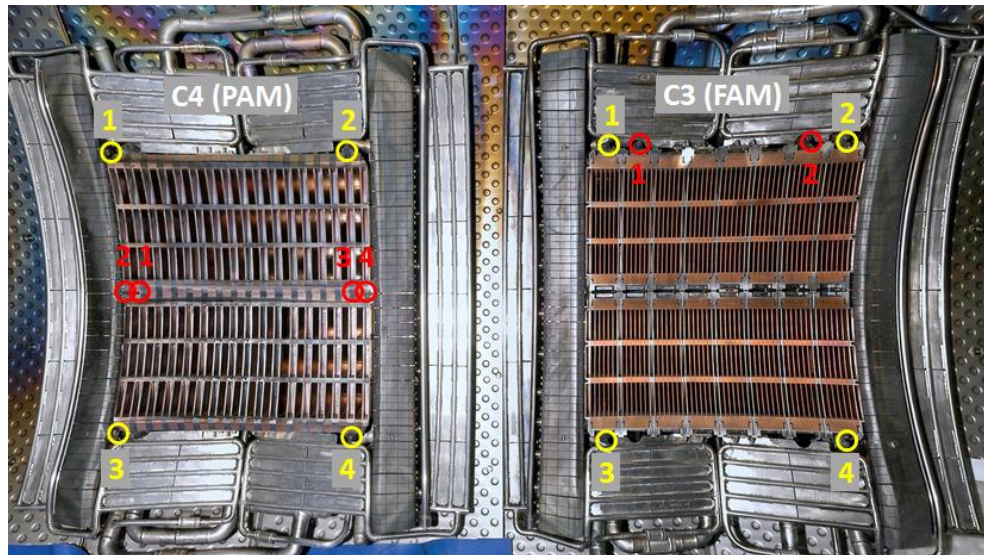


Figure 53 : Photographs of the two LHCD launchers inside the Tore Supra vessel. Each launcher has four Langmuir probes located one in each corner of the launchers (yellow circles). Four probes for fluctuation measurements are located at the mid-plane on the C4-PAM launcher and two on the upper part on the C3-FAM launcher (red circles).

■ **Reflectometers in RF heating antennas:** One of the LHCD launchers (C3-FAM, on the right in Fig. 1), is equipped with a X-mode reflectometer in E-Band (60-90 GHz), imbedded at the centre of the launcher mouth [Bottereau2011]. A modification to cover the band 75-110 GHz is planned. It is a fast frequency sweep heterodyne reflectometer based on our mature technology tested on Tore Supra and JET. The previous version of the system allowed measurements in 20  $\mu$ s, but acquisition upgrade in 2012 should allow a rate of a few microseconds. It was specifically adapted to the particular location inside an LHCD launcher. The key of our technology is the Single Side Band Mixer which allows a heterodyne detection without phase lock loop. The beat frequencies are up to 50 MHz, and a VME controlled data acquisition system sampling at 100MHz can provide up to 10000 profiles per shot, triggered on an external signal if needed. The routine scan time is 20  $\mu$ s for a profile with a dead time within 2 profiles of 5  $\mu$ s.

For WEST, it is proposed to install reflectometers in the new Ion Cyclotron Resonance Heating (ICRH) antennas, currently being designed to fulfill the requirements on ELM-resilience. Previous density distributions observed on Tore Supra [Colas2007] motivate the choice to have at least three poloidal measurement points (at the bottom, the middle and the top of the antenna. Due to mechanical constraints and cooling of the ICRH antenna, it is likely that the mid-plane reflectometer must be placed on the side of the lateral protection, either in the private region between the lateral protection and the antenna, or outside the lateral protection in the free SOL. In order to reduce the cost for this reflectometer system, the data acquisition could be shared with the LHCD reflectometer.

■ **Dynamic Stark spectroscopic measurement (DIAS):** This diagnostic has proven to be able to measure the RF electric field in the vicinity of a LHCD launcher in

Tore Supra, using the dynamic Stark effect [Klepper2013]. The spectroscopic sightline is provided by an endoscope located in a mid-plane port at the outer wall, recessed in its access port to protect from direct exposure to radiated heat during long pulse operation. The diagnostic sightline views the lateral protection and part of the grill of one of the LHCD launchers. It measures the deuterium Balmer-series spectral line profiles (which are influenced by the dynamic Stark effect). The spectra are then fitted to a time-dependent Stark effect spectral model. The results are combined with local plasma characterization and neutral transport modeling to localize the emission region. Information has been obtained about both the magnitude and the direction of the local RF electric fields and validated by comparison to LHCD antenna code. For WEST, it is proposed to increase the flexibility of the sightline to be able to view the lateral protection on either side of the LHCD launcher (by an intervention in the torus hall over night or over the weekend). The aim is to measure the RF electric field in both the co-current and counter-current directions and to compare this to the LHCD antenna modelling of the spectrum directivity of the launched wave.

■ **Hard X-Ray (HXR) cameras:** A dedicated tomographic system was installed on Tore Supra to measure the thermal bremsstrahlung emission of the fast electrons, accelerated by the electric field of the Lower Hybrid (LH) wave, in the HXR range of energy [Peysson1999]. It is made of 59 lines of sight, arranged into two cameras placed in a poloidal plasma cross section, each having a mean radial resolution  $\Delta r = 4\text{--}5$  cm. The time resolution  $\Delta t$  is usually at 8 ms, but can be as low as 2 ms. The horizontal camera consists of 38 detectors, while the vertical camera has 21 detectors (Figure 54). Photon energies  $h\nu$  between 20 and 200 keV are discriminated by an eight-channel spectrometer of width  $\Delta h\nu = 20$  keV for each chord, which allows investigating the electron dynamics from the Maxwellian bulk to the non-thermal tail at all plasma radii. Measurements are carried out at room temperature by CdTe semiconductors, and the detection efficiency of the diagnostic has its maximum at photon energy of 100 keV, where Landau resonance is expected to be dominant while the effects of the ohmic electric field contribution are almost negligible. The use of two distinct cameras enhances the spatial redundancy of the HXR measurements by covering the plasma poloidal cross-section with lines-of-sight of various inclinations, which is favorable for a well conditioning of the Abel inversion matrix. However, for WEST it is possible to keep only the horizontal HXR camera due to constraints on the available diagnostics space, but this has been considered adequate for obtaining sufficient information on the power deposition of the LH wave in the WEST plasma.

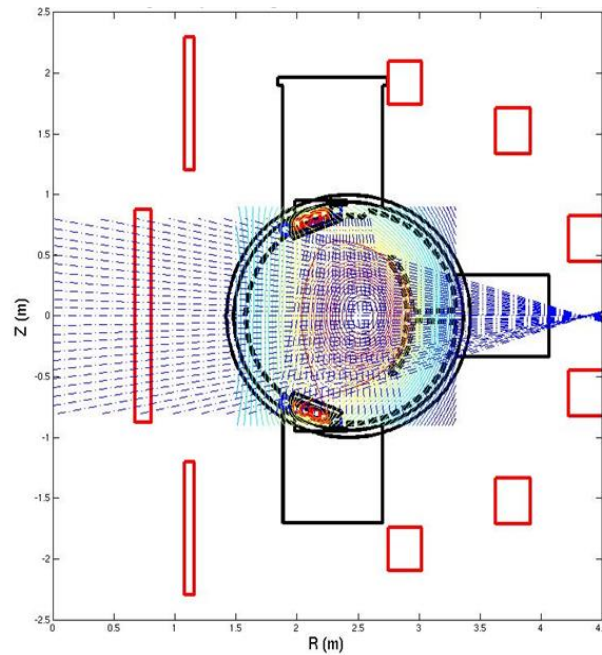


Figure 54 : Schematic view of the horizontal (38 detectors) and the vertical (21 detectors) HXR cameras in Tore Supra. Only the horizontal camera will be used in WEST

■ **Fast electron ripple loss measurements:** A new diagnostic system (DENEPR), based on Cherenkov radiation, was tested in Tore Supra in 2010 [Jakubowski2010]. The aim of this diagnostic is to measure the energy distribution of the fast electrons lost from the plasma due to the effect of the magnetic ripple. The Cherenkov radiation, which can be induced by fast electrons in appropriate solid radiators offers almost instantaneous (with a rise time of the order of  $10^{-9}$  s) information about the appearance of fast electrons. It should be also noted that under appropriate conditions the Cherenkov signals are considerably higher than those originating from X-Ray bremsstrahlung. In Tore Supra, the Cherenkov measuring head was fixed at the top of the internal movable shaft of the DENEPR probe (Figure 55), which could be shifted from the intermediate rest-position (at  $z=991$  mm above the plasma equatorial plane) to the deepest measurement point (at  $z=795$  mm, i.e. 76 mm from LCFS) in about 100 ms, and be withdrawn in about 200 ms.

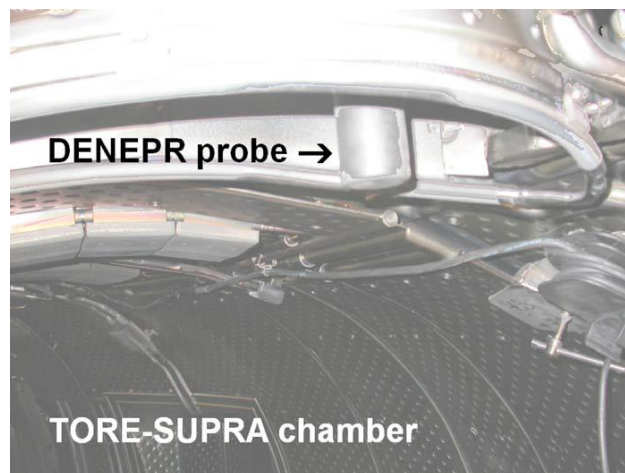


Figure 55 : Positioning of the DENEPR probe inside a vertical diagnostic port of the Tore Supra chamber

## 7. Turbulence and MHD

■ **Reflectometry:** Tore Supra is equipped with several reflectometers for measuring the density profile and characterizing density fluctuations:

- an edge reflectometer: a dual channel (50-110 GHz) swept reflectometer.
- a core reflectometer: dual channel D-band reflectometer for profile, fluctuation and correlation measurements.
- a profile reflectometer inside the FAM Lower Hybrid antenna.
- a dual channel Doppler reflectometer.
- a vertical Doppler reflectometer.

New reflectometers to be installed behind the inner wall are also considered.

Reflectometry access depends on density and magnetic value. In O-mode, the frequency band determines the density measurement range. The localisation is thus given by the density profile. In X mode, accessibility depends on the magnetic field and density. Figure 56 shows the variation of the accessibility with the magnetic field for a given density profile, and the cutoff-frequency for 2 WEST scenarios in H mode: a high density and low density case. At nominal magnetic field in-H mode, the edge reflectometer is restricted to SOL and pedestal coverage. With a peaked density profile, access to the high field side is limited. For flat density profile, the core reflectometer can probe up to the top of the pedestal on the HFS.

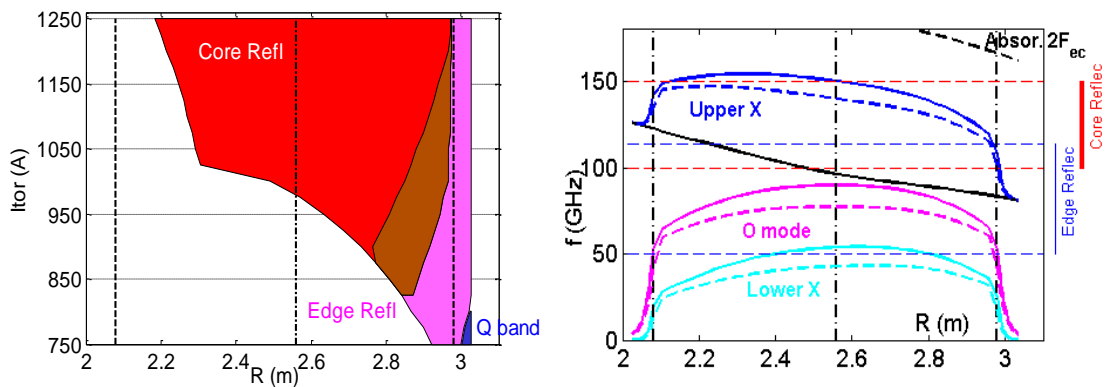


Figure 56 : left: accessibility of the X mode reflectometers for a WEST profile with  $n_e(\rho=0)=7.5 \cdot 10^{19} \text{ m}^{-3}$ ,  $n_e^{\text{ped}} = 4.5 \cdot 10^{19} \text{ m}^{-3}$ ,  $n_e^{\text{sep}} = 2 \cdot 10^{19} \text{ m}^{-3}$ . The brown zone shows the overlap between the core (red zone) and edge (pink zone) reflectometer accessibility. Right: cutoff layer profiles at nominal B ( $I_{\text{tor}}=1250$  i.e.  $B=3.6\text{T}$ ) for 2 scenarios: the high power, high density, high current, high confinement  $H=1.2$  ( $n_e(\rho=0)=10.5 \cdot 10^{19} \text{ m}^{-3}$ ,  $n_e^{\text{ped}} = 5.2 \cdot 10^{19} \text{ m}^{-3}$ ,  $n_e^{\text{sep}} = 3.5 \cdot 10^{19} \text{ m}^{-3}$ ) and the moderate power, high current, low density, low confinement  $H=0.7$  ( $n_e(\rho=0)=7.6 \cdot 10^{19} \text{ m}^{-3}$ ,  $n_e^{\text{ped}} = 4.3 \cdot 10^{19} \text{ m}^{-3}$ ,  $n_e^{\text{sep}} = 2 \cdot 10^{19} \text{ m}^{-3}$ ).

- **Edge reflectometer** [Clairet2010]: it will be re-installed without major modification since it is already well adapted to the program needs. The two channels cover the band 50-78 (V-band) and 74-110 GHz (W-band) in X-mode. They are swept simultaneously in 2 $\mu$ s. At nominal field ( $B=3.6$  T), the W-band probes the edge from the far SOL to densities up to approximately  $4 \cdot 10^{19} \text{ m}^{-3}$ . At lower field operation, the

reflectometer probes deeper inside the plasma and the V-band becomes necessary. The time resolution is flexible: the whole plasma discharge can be covered with typical time resolution of a few milliseconds. Fast acquisition can also be performed at a time resolution of 3  $\mu\text{s}$  during a maximum duration time of few tens of milliseconds limited by the memory size of the acquisition system. The fast acquisition is also used to measure the profile of density fluctuations and the radial wavenumber spectrum.

- **Core reflectometer** [Sabot2009]: The diagnostic will move to port Q5B but the implantation design has not yet started. A new access with a cluster of 5 antennas/waveguides is considered to allow poloidal correlation and pitch angle measurements. This cluster would also facilitate the installation of reflectometers from WEST partners as they could share the waveguides using optical boxes as on JET. The diagnostic was upgraded in 2012 (ultra-fast sweep, new data acquisition at 5 Ms/s for fluctuation measurements). It operates in X mode over the band 100-155 GHz probing further inside the edge reflectometer to the core and high field side at high magnetic field & moderate density. It is made of 2 independent hopping reflectometers for fluctuations / radial correlation measurements. Up to 3 seconds (distributed as desired) can be recorded per shot. Between fluctuation measurement periods, one channel measures also the density profile in few  $\mu\text{s}$ . As for the edge reflectometer, full discharge covering or high time resolution (few  $\mu\text{s}$ ) during short duration (few tens of  $\mu\text{s}$ ) can be chosen. As the first cut-off is always inside the plasma, an edge profile (either from edge reflectometer or interferometry) profile is needed to initialize the profile reconstruction.

- **Doppler reflectometer** [Sabot2009]: it will be re-installed without major modification. It offers two hopping channels: 50-75 GHz in O-mode and 75-110 GHz in X-mode. The O-mode covers the pedestal and gradient region, depending on the density profile. The X-mode channel is dedicated to edge measurements. An electric shaft modifies the tilt angle of the reflectometer during the shot. Combined with frequency flexibility, this allows radial and wavenumber scans.

- **Vertical Doppler reflectometer**: a vertical Doppler channel was mounted for the 2011 campaign. However, the top divertor structure will drastically reduce the accessibility and the number of top diagnostics. The fate of this diagnostic is still under discussion: dismantling, fixed angle Doppler in D-band to limit the beam divergence, waveguide & antenna under vacuum to get closer to the plasma ... An operation in the first days of the campaign is thus improbable.

- **High field side reflectometer project**: Installation behind the inner wall of 2 pairs of waveguides is considered for reflectometry measurements on the high field side: an O-mode profile reflectometer to compare the HFS pedestal with LFS one, an upper hybrid resonance scattering (UHRS) reflectometer to probe small scales (tens electron Larmor radius) density fluctuations. UHRS was proposed and tested by E. Gusakov et al on the FT-2 tokamak [Gurchenko2010]. It would be complementary to correlation and Doppler reflectometers that probe density fluctuation at ion Larmor radius scale.

- **Fast Camera**: Tore Supra is equipped with a fast camera system [Géraud2009] in the visible range to study fast phenomena like plasma start up,

disruptions, gas or pellets injections, plasma turbulence in the visible range. The camera is able to record movies at a speed up to 4 800 frames per second at full resolution (800 x 600), or much faster for a limited number of pixels. For instance with a 128 x 64 resolution we can record up to 100 000 frames per second. The camera is coupled with an endoscope which goal is to support an optical system compatible with a tangential view of the plasma. It is also a vacuum interface between the vessel and the camera. An optical fiber bundle is used to transport images from the front optical component to the camera. In the West configuration the diagnostic would move from the Q4Am port to the Q5bm one and the field of view would be roughly as displayed on Figure 57.

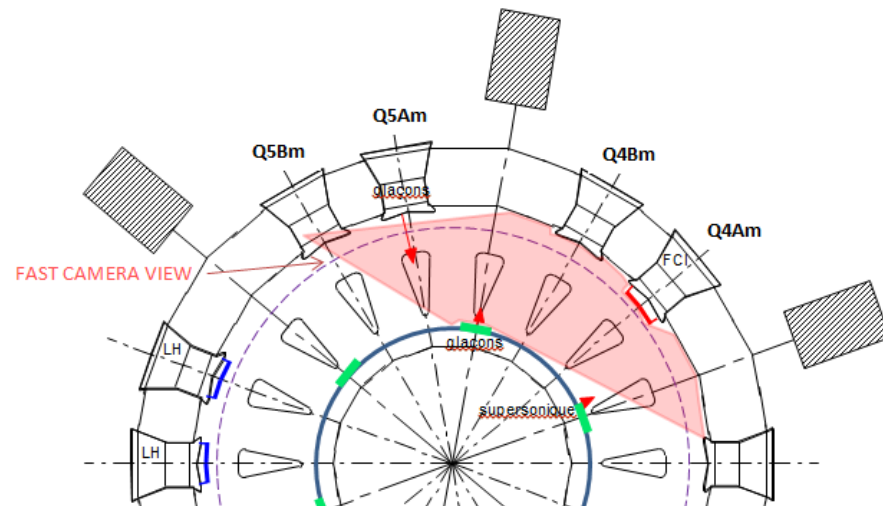


Figure 57 : position and field of view of the fast camera in WEST

■ **ECE imaging:** For WEST Phase 2, an ECE imaging diagnostic will be settled on Tore Supra to study ELM dynamics and core MHD instabilities. One (or two?) array(s) with 24x8 detectors will produce 2-D images of the electronic temperature fluctuations (<1% and <250 kHz). The observation area will be about 52x18 cm ( $\pm 0.5 \times 0.3$  r/a) and can be set from the plasma core to its outer edge (see Figure 58). The resolution will be 2  $\mu$ s and  $\sim 4$  cm<sup>2</sup>.

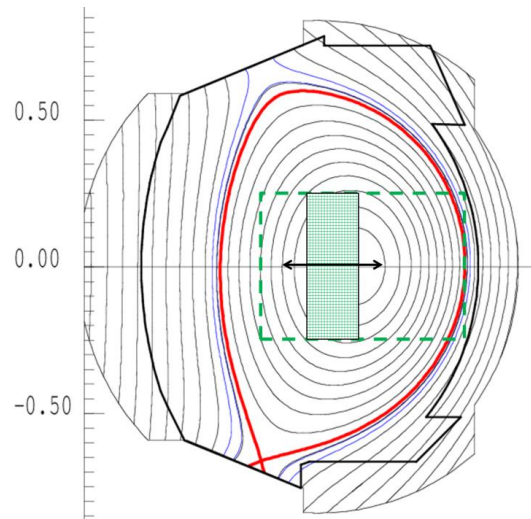


Figure 58: Dimension of the ECEI measured plasma area and coverage in a poloidal cross section.

## References

- [Bottereau2011] C Bottereau et al., Proceedings 10<sup>th</sup> International Reflectometry Workshop (2011).
- [Chantant2005] M. Chantant et al., Fusion Eng. Design **74** (2005) 897.
- [Clairet2010] F. Clairet et al., Rev. Sci. Instr. **81** (2010) 10D903.
- [Colas2007] L Colas et al., Plasma. Phys. Control. Fusion **49** (2007) B35 .
- [Gaspar2013] J. Gaspar et al., Int. J. Thermal. Sci. **72** (2013) 82.
- [Gauthier2013] E. Gauthier et al., J. Nucl. Mater. **438** (2013) S1216.
- [Géraud2009] A. Géraud et al., Rev. Sci. Instr. **80** (2009) 033504.
- [Gil2009] C. Gil et al., Fusion Sc. Technol. **56** (2009) 1219.
- [Goniche2013] M Goniche et al., Nucl. Fusion **53** (2013) 033010.
- [Guilhem2005] D. Guilhem et al., Fusion Eng. Design **74** (2005) 879.
- [Gurchenko2010] A.D. Gurchenko et al., Plasma Phys. Control. Fusion **52** (2010) 035010.
- [Jakubowski2010] L Jakubowski et al., Rev. Sci. Instr. **81** (2010) 013504.
- [Klepper1997] C.C. Klepper et al., Rev. Sci. Instrum. **68** (1997) 400.
- [Klepper2013] C.C. Klepper et al., Phys. Rev. Lett. **110** (2013) 215005.
- [Mazon2013] D. Mazon et al., Nucl. Instr. Methods **720** (2013) 78.
- [Moreau09] Ph. Moreau et al., Fusion Sci. Technol. **56** (2009) 1284
- [Moreau2011] Ph. Moreau et al., Fusion Eng. Design **86** (2011) 1222.
- [Nouailletas13] R. Nouailletas et al., Fusion Sci. Technol. **64** (2013) 13
- [Peysson1999] Y Peysson and F Imbeaux, Rev. Sci. Instr. **70** (1999) 3987.
- [Ravenel13] N. Ravenel et al., IAEA Technical Meeting, Hefei,
- [Sabot2009] R. Sabot et al., Fusion Sci. Technol. **56** (2009) 1253
- [Salasca2009] S. Salasca et al., Fusion Eng. Design **84** (2009) 1689.
- [Schwob1987] J.L. Schwob et al., Rev. Sci. Instr. **58** (1987) 1601.
- [Ségui2005] J.L. Ségui et al., Rev. Sci. Instr. **76** (2005) 123501.
- [Semerok2013] A. Semerok and C. Grisolia, Nucl. Instr. Methods **720** (2013) 31.
- [Spuig2003] P. Spuig et al., Fusion Eng. Design **66-68** (2003) 953

# Annex 8: WEST scenario modelling

---

This annex corresponds to the preprint version of the paper “WEST physic basis”, C. Bourdelle et al., submitted for publication to Nuclear Fusion. This paper describes the physics basis of WEST: the estimated heat flux on the divertor target, the planned heating schemes, the expected behaviour of the L-H threshold and of the pedestal and the potential W sources. A series of operating scenarios has been modelled, showing that ITER relevant heat fluxes on the divertor can be achieved in WEST long pulse H mode plasmas.

## 1. Introduction

Power exhaust is one of the main challenges for next step fusion devices. In ITER and DEMO, the plasma facing components (PFCs) will experience extreme heat and particle loads as well as unprecedented levels of cumulated particle fluence and gigajoules of energy to be extracted in a single discharge. WEST provides an integrated platform for testing the ITER divertor components under combined heat and particle loads in a tokamak environment [Buc14]. It will allow assessing the power handling capabilities and the lifetime of ITER high heat flux tungsten divertor technology under ITER relevant power loads (10 to 20 MW/m<sup>2</sup>), particle fluence (~10<sup>27</sup> D/m<sup>2</sup>) and time scales (above 100s). Operation in WEST will also allow validating a scheme for the protection of actively cooled metallic PFCs. The WEST research plan has been structured around two main topical headlines: “ITER grade PFC tests” and “towards long pulse H mode and steady-state operation”. The research plan is evolving with the project and revised with the WEST partners on a yearly basis. Such interactions with the fusion community have started during the 1st WEST International Workshop that took place in Aix-en-Provence in 2014 [25].

In order to fulfil its scientific objectives, WEST is equipped with upper and lower divertor coils, W coated upper divertor, baffle, inner bumper and with a flexible lower divertor made of twelve 30° sectors where the ITER like W monoblocks will be installed [Mis14]. The additional heating and current drive power is provided by high frequency heating systems, namely Ion Cyclotron Resonance Heating (ICRH) and Lower Hybrid Current Drive (LHCD), delivering up to 9 MW of ICRH power and 7 MW of LHCD power. See Fig.59 for CAD views of WEST and for a table summarizing the main plasma and heating system parameters (maximum values).

To address the programme headlines, three groups of standard scenarios have been targeted. Scenarios at medium power (12 MW) are needed for testing the ITER grade PFC and demonstrating integrated H mode long pulse operation (~60 s) while ensuring relevant heat fluxes on the divertor (in the range 10-20 MW/m<sup>2</sup>). To study plasma wall interactions at high particle fluence, scenarios up to 1000 s at 10 MW are foreseen. Finally, high power scenarios at 15 MW are developed for 30 s high performance discharges. In the WEST actively cooled environment, there is no hard technological limit on the pulse duration, 1000s is an indicative time scale.



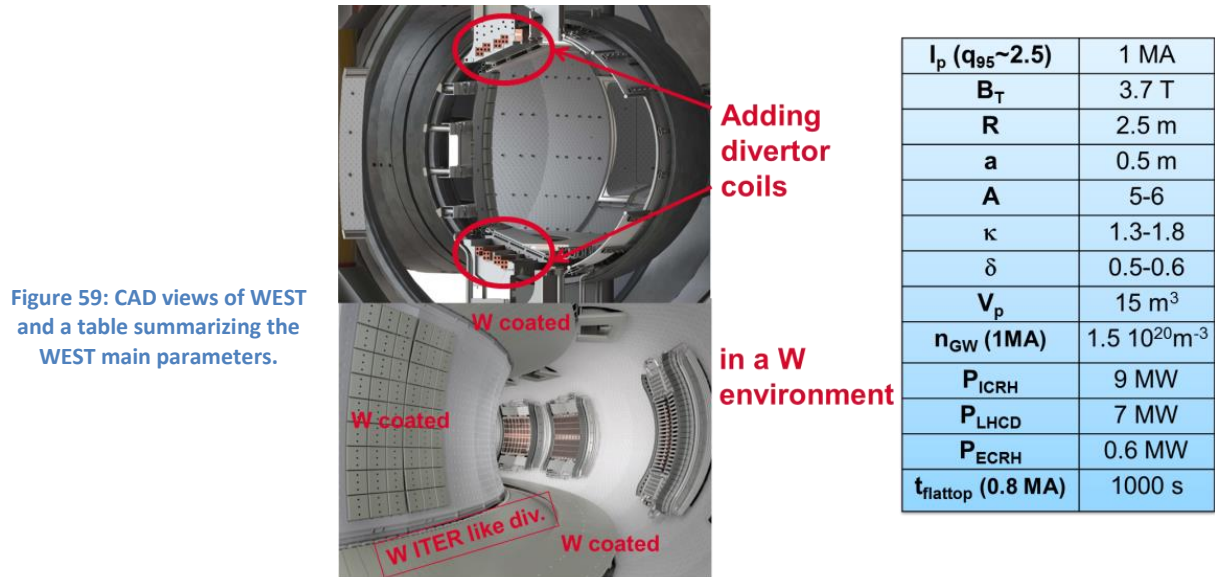


Figure 59: CAD views of WEST and a table summarizing the WEST main parameters.

To prepare these scenarios, the amount of additional power required to achieve 10 to 20 MW/m<sup>2</sup> is discussed in section 2; ICRH and LHCD modelling is presented in section 3; the fuelling and pumping capacities are detailed in section 4; the estimated L-H power threshold, pedestal and ELMs are studied in section 5; the expected density profile is reviewed in section 6; in section 7, W sources are discussed and finally in section 8 integrated modelling of four WEST scenarios are presented before concluding in section 9.

## 2. Expected heat flux on the divertor target

The peak heat flux is constrained by geometrical factors, magnetic equilibrium (flux expansion) and by the SOL physics.

The WEST magnetic configurations allow for elongated plasmas in Lower or Upper Single Null, or Double Null configurations. For a standard elongated Lower Single Null case, the X point height range, at for example 0.7 MA, is up to 10 cm, see Fig.60. The equilibria of Fig.60 are used as references equilibria in the rest of the scenario study presented here. They are constrained by a fixed toroidal magnetic field  $B_T=3.7$  T at 2.5 m and by an external radius of 2.93m which is compatible with ICRH and LHCD launchers positions. It is to note that ICRH and LHCD launchers can be moved radially between or during shots, for ICRH between 2.89 and 3.06 cm and for LHCD from 2.91 and up to 3.06 cm. All equilibria are computed with the free boundary equilibrium code CEDRES++ [cedres].

The pulse duration is constrained by the maximum current flowing in the actively cooled copper divertor coils. Steady state is reached with a total current in the divertor coils of 200 kA.turn. For shorter pulses of 15s, up to 320 kA.turn can be reached, limited by the coils power supplies capabilities (20kA). The link between the X point height and the plasma current,  $I_p$ , is illustrated in Fig.61, for the two divertor currents 200 kA.turn and 320 kA.turn. In steady-state, up to  $I_p=0.8$  MA can be reached and X point height of 12 cm corresponds to  $I_p=400$  kA while  $I_p=1$  MA is achievable with a  $q_{95}$  of 2.5, for an X point height of 1 cm for this kind of equilibria.

Figure 60: CEDRES++ free boundary set of equilibria for  $B_T = 3.7$  T (at 2.5 m); with a fixed external radius of 2.93 m and with the steady state divertor coil current of 200 kA.turn.

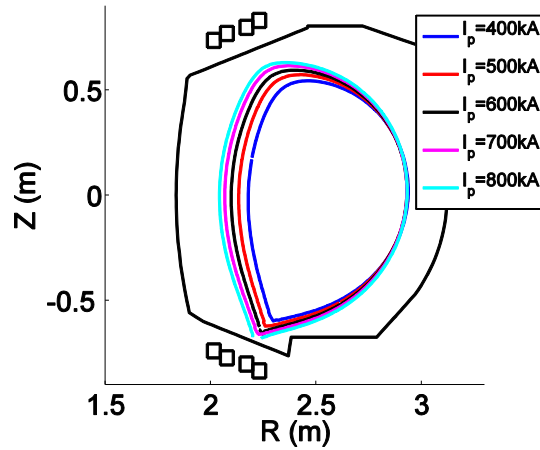
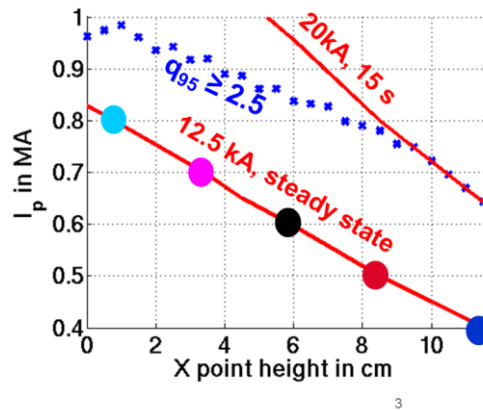


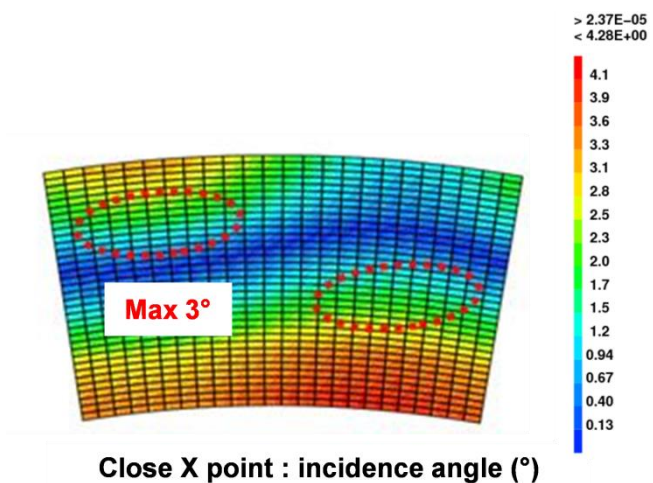
Figure 61: At fixed  $B_T=3.7$ T, range of accessible  $I_p$  and X point heights corresponding to the references equilibria illustrated by FIG.60. The limits due to the divertor coils are in red, one for the steady state and one corresponding to the maximal divertor coils current. In blue is the limit corresponding to  $q_{95}=2.5$ .



In WEST the angle of incidence of the magnetic field lines on the lower divertor is toroidally modulated by magnetic field ripple due to 18 superconducting toroidal field coils. The magnetic ripple reaches 2% at the LCFS in WEST. The angle and its modulation are illustrated for an X point height of 3 cm by a top view of 20° of the lower divertor in Fig.62. The grazing angle of incidence close to the strike points for this configuration is between 2 and 3°, i.e. in the ITER range.

Figure 62: Top view of a 30° divertor sector. The low field side is at the top of the figure and the high field side at the bottom.

Angle of incidence of the field lines in ° for the low X point configuration. The high heat flux area is circled in red.



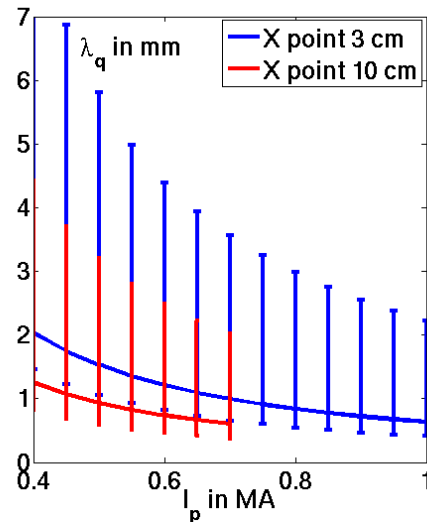
The WEST heat flux fall-off length  $\lambda_q$  in H mode is extrapolated from the scaling law published in [Eic11]:

$$\lambda_q = (0.73 \pm 0.38) \times B_T^{-0.78 \pm 0.25} q_{cyl}^{1.2 \pm 0.27} P_{SOL}^{0.10 \pm 0.11} \quad (1)$$

With  $B_T$  the toroidal magnetic field,  $P_{SOL}$ , the power flowing through the Last Closed Flux Surface in the SOL and  $q_{cyl}$  the cylindrical safety factor.

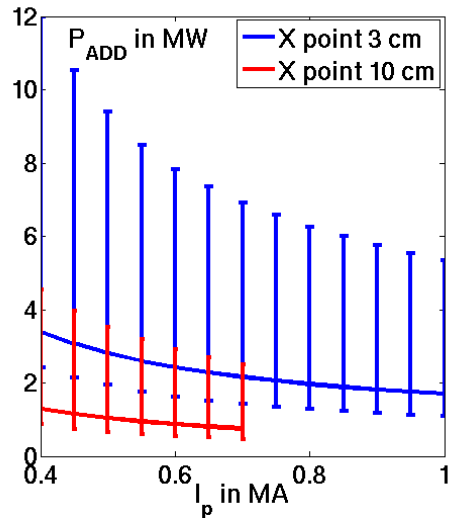
For WEST,  $B_T = 3.7$  T and  $P_{SOL}$  is iterated to match a peak heat flux on the divertor of  $10 \text{ MW/m}^2$ . One then finds  $\lambda_q$  as a function of  $I_p$  as illustrated by Fig. 63. The error bars correspond to the extremes of equation (1) taken as follows: extreme of the prefactor and the extreme of one of the two exponents on  $B_T$  or  $q_{cyl}$ . Since the constraint on  $P_{SOL}$  is a peak heat flux of  $10 \text{ MW/m}^2$ , the range of expected values for  $\lambda_q$  varies with the X point heights. Two heights, 3 and 10 cm, are illustrated in Fig.63. The range of expected  $\lambda_q$  based on the scaling law proposed in [Eic11] is rather large and varies from 0.5 to 7 mm.

Figure 63: Heat flux fall-off length  $\lambda_q$  in H mode based on the scaling law from [Eic11], for an X point height of 3 cm in red and an X point height of 10 cm in blue. The error bars represent the uncertainties on the exponents of equation (1).



The amount of additional power to reach a peak heat flux of  $10 \text{ MW/m}^2$  is estimated with the following assumptions: 40% of the additional power is supposed to be radiated before reaching the divertor; an asymmetry Low Field Side versus High Field Side with  $2/3$  of the power on the LFS is supposed; a spreading factor,  $S$ , is taken such that:  $S = 0.4 \times \lambda_q$  and the uncertainties on  $\lambda_q$  illustrated in Fig.63 are accounted for. The additional power required to reach  $10 \text{ MW/m}^2$  is plotted versus  $I_p$  in Fig. 64 for two X point heights (3 and 10 cm). For 3 cm, the flux expansion factor is 9, whereas at a higher X point it is down to 3, leading to higher peak heat fluxes for an identical amount of power reaching the divertor region.

Figure 64: Additional power required to reach  $10\text{MW/m}^2$  on WEST divertor. Using the scaling law of [Eic11], accounting for the magnetic ripple and for an X point height of 3 cm in red and an X point height of 10 cm in blue.



$10\text{MW/m}^2$  can be achieved onto the divertor with an additional power varying greatly from less than 2 MW to up to more than 10 MW [Fir14]. Given the large uncertainties, the flexibility provided in WEST through a large range of X point heights is a key feature. The large error bars are essentially due to the uncertainties on the expected  $\lambda_q$ . This points towards the importance of the heat flux fall-off length studies in progress on various machines. Such studies will be carried out, thanks to a unique IR coverage of the divertor region [Cou13], adding information on the large aspect ratio impact on SOL transport. Overall, in WEST, the level of additional power is sufficient to achieve  $10\text{MW/m}^2$ , and up to  $20\text{MW/m}^2$  for slow transients.

### 3. High frequency plasma heating

As presented in the introduction, WEST plasmas will be heated by a combination of Lower Hybrid Current Drive (LHCD) power, up to 7 MW, and Ion Cyclotron Resonance Heating (ICRH) power, up to 9 MW. It is essential to adapt the heating systems to the WEST configuration, and also to verify the adequacy of these heating schemes with H-mode operation in terms of power coupling, fast particle confinement and ELM resilience in a metallic environment. It will complement active efforts carried out in metallic environments on JET-ILW [May14], ASDEX Upgrade [Bob13, Neu11], Alcator C mod [Wuk09] and FTU [Tuc09].

#### a. Lower Hybrid Current Drive

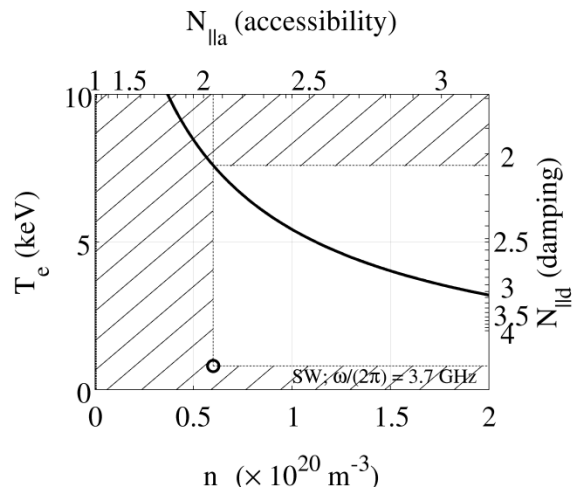
The Lower Hybrid Current Drive (LHCD) system for WEST consists of two fully actively cooled multijunction launchers, the so-called Passive Active Multijunction (PAM) [Gui11] and the Fully Active multijunction (FAM) [Bib00], where the latter has been modified to match the toroidal curvature of the WEST plasmas. These are fed by 16 klystrons, each capable of providing 600 kW / CW on matched load, leading to a total generator power of 10 MW / CW. Eight of the klystrons, feeding the FAM launcher, have been tested on high power operation in Tore Supra [Del14]. Injection of LH power in the 5.0–6.0MW range has been achieved in Tore Supra plasmas [Dum14, Gon14].

One of the crucial points for RF operation in WEST, as in any tokamak, is the coupling of the RF waves to H-mode plasmas. To ease the LH wave coupling, local gas injection valves are installed at outer mid-plane locations, magnetically connected to the launchers [Eke09]. This

method may be particularly important for the FAM launcher, which needs a density at the launcher mouth of typically  $\sim 3\text{-}5 \times 10^{17} \text{ m}^{-3}$  for optimum coupling. The ITER-relevant PAM launcher, on the other hand, has its optimum operating range close to the cut-off density ( $1.7 \times 10^{17} \text{ m}^{-3}$  at  $f = 3.7 \text{ GHz}$ ) and is therefore more suitable for operating in conditions with large plasma-launcher distance or with steep edge density gradients [Eke10].

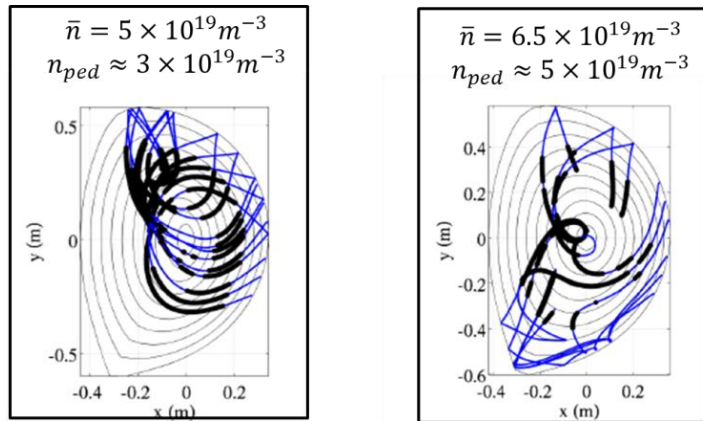
For the LH waves, the accessibility criterion implies that only waves with a launched parallel refractive index ( $N_{\parallel}$ ) larger than a critical value can penetrate beyond a certain density. The choice of the launched parallel refractive index  $N_{\parallel}$  is a trade-off between the Stix-Golant accessibility condition and the current drive efficiency. The largest  $N_{\parallel}$  that allows the LH wave to penetrate in the core of the plasma and which can be excited by the PAM or the FAM launcher is 2.0. For  $N_{\parallel}=2.0$ , the pedestal density is limited to  $6.5 \times 10^{19} \text{ m}^{-3}$  for the LH waves to propagate in the core of the plasma without prior multiple reflections between the caustic and the cut-off at the plasma edge, as shown in Fig. 65. The accessibility domain in Fig. 65 illustrates that the limit in temperature (around 8 keV) is well above the expected pedestal temperature, whereas a density limit of  $6.5 \times 10^{19} \text{ m}^{-3}$  is in the expected range for the pedestal density as discussed later.

Figure 65: LHCD accessibility diagram at 3.7 GHz



Additional sources of  $N_{\parallel}$  shifts are known to take place as the wave propagates in the plasma, as a consequence of toroidal refraction and other effects [Pey08, Dec11]. Among the latter, the interplay of the wave in the SOL can also introduce a significant  $N_{\parallel}$  spectrum broadening at the separatrix [Ces10, Gon13]. Modelling of injected  $N_{\parallel 0}=2.0$  cases has been carried out with the C3PO/LUKE codes [Pey08, Dec11] for different pedestal densities,  $n_{\text{ped}}$ , as illustrated in Fig.66 for  $n_{\text{ped}}=3 \times 10^{19} \text{ m}^{-3}$  and  $5 \times 10^{19} \text{ m}^{-3}$ . The peak of the LH absorption occurs around mid-radius for both cases. In the low density range, the wave penetrates inside the plasma core, while, at high densities, it undergoes several reflections prior to its absorption. After multiple cut-off reflections, a strong  $N_{\parallel 0}$  upshift takes place when the wave propagates in the vicinity of the X-point, which leads to a well off-axis LH wave deposition.

Figure 66: C3PO-LUKE LH modelling for two WEST scenarios.



Thanks to fast electron bremsstrahlung tomography and extensive comparisons with existing ray-tracing and Fokker-Planck codes, WEST will bring new insights in LHCD physics at high pedestal density, together with Alcator C-Mod [Wal10], EAST [Liu12] and FTU [Tuc09]. On the technological side, high power operation of the PAM launcher during ELMs will allow demonstrating that the PAM is a viable solution for LHCD in ITER [Hoa09].

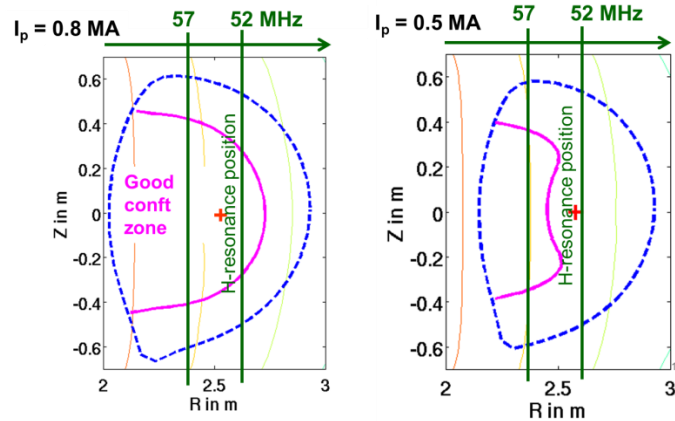
### b. Ion Cyclotron Resonance Heating

WEST will be equipped with three new ICRH antennas, designed to provide resilience to ELMs as well as capacity for steady-state operation. Their design is an upgrade of the ITER-like ICRH prototype, tested in Tore Supra in 2007 [Vul08, Arg09]. Their ELM resilience relies on vacuum conjugate T-junction. Due to the generator specifications, the maximum power available depends on the pulse duration: 3 MW/antenna during 30 s, 2 MW/antenna during 60 s and 1 MW/antenna in steady state.

The coupling of ICRH in H-mode plasmas is crucial and has longed been studied on Tore Supra plasmas [Col06]. Several gas injection points near the antennas are prepared, as well as reflectometry density measurement in front of the antennas in order to study the local SOL profiles. Comparing the observations with SOL 2D codes such as Soledge2D-EIRENE [Buf13] will allow for detailed ICRH coupling studies.

It is planned to use ICRH mostly in the H minority scheme, i.e. damping by minority hydrogen ions in deuterium or helium at the fundamental cyclotron resonance. The nominal operating frequency is adjusted in order for the wave energy to be deposited in the central region to prevent W accumulation [Dux03, Ler14]. However, due to the finite magnetic ripple level expected in WEST, the fast ions produced by ICRH can be deconfined [Bas04]. As an illustration, Fig. 67 shows the good confinement region size which is affected by the value of the plasma current. In order to reduce the resulting fast ion losses, it is therefore desirable to retain the capability to locate the fundamental absorption layer in the good confinement region, by shifting it towards the high field side. To cover both the magnetic axis and access the good confinement zone even at low  $I_p$ , two frequency bands at the generator have been selected, as shown on Fig.67, namely:  $53 \pm 2$  and  $56 \pm 2$  MHz.

Figure 67: Poloidal views of WEST equilibria at 0.8 and 0.5 MA in steady state computed by CEDRES++ see Fig.60. The unshifted H resonance positions are indicated in green for two ICRH frequencies: 52 and 57 MHz. In magenta are shown the limits of the good confinement region.



The full wave solver EVE with the Fokker–Planck module AQL are used to model the ICRH deposition profiles [Dum13]. Fig. 68 illustrates an EVE/AQL simulation for 6 MW of ICRH at 55.5 MHz and  $n_H/n_e=6\%$ . The power is deposited within  $\rho=0.4$ , essentially on minority hydrogen ions ( $\sim 5\text{MW}$ ). It is then redistributed through collisional relaxation of these fast ions between electrons ( $\sim 2.5\text{MW}$ ) and bulk ions ( $\sim 1.2\text{MW}$ ). As is often the case in the hydrogen minority scheme, the majority of the coupled power eventually heats electrons [Eri01]. Some flexibility in terms of electron/ion heating can be obtained by varying the amount of ICRH power. When the coupled power is increased from 3 to 9 MW at  $n_H/n_e=6\%$ , the fraction coupled to the electrons increases continuously from 45% to 70%, as illustrated by Fig.69. Another possibility is to vary the minority hydrogen concentration, as shown in Fig. 70. When  $n_H/n_e$  is varied between 3% and 18% for 6MW of coupled power, it is possible to transit from dominant electron heating to dominant ion heating. It should be noted, however, that operating at large minority concentrations can be difficult as the per-pass damping rate decreases as  $n_H/n_e$  increases.

Figure 68: EVE/AQL modelling of a WEST scenario for 6 MW of ICRH at 55.5 MHz and  $n_H/n_e=6\%$ . Power density absorbed by species (left y-axis, solid lines), total power (right y-axis, dashed lines).

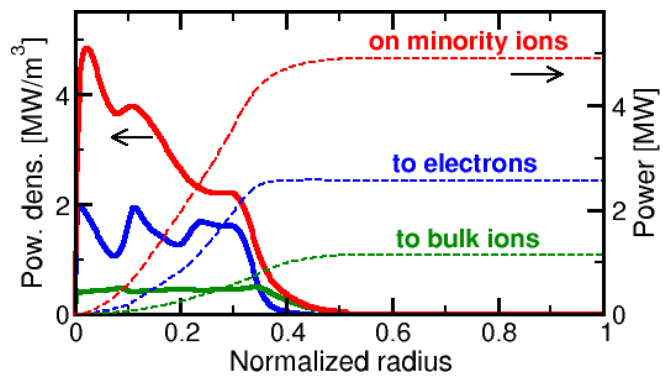


Figure 69: Power split between electrons and bulk ions (solid lines) when the coupled RF power is varied between 3MW and 9MW, at 6% H minority concentration. Also shown is the fast ion content (dashed line).

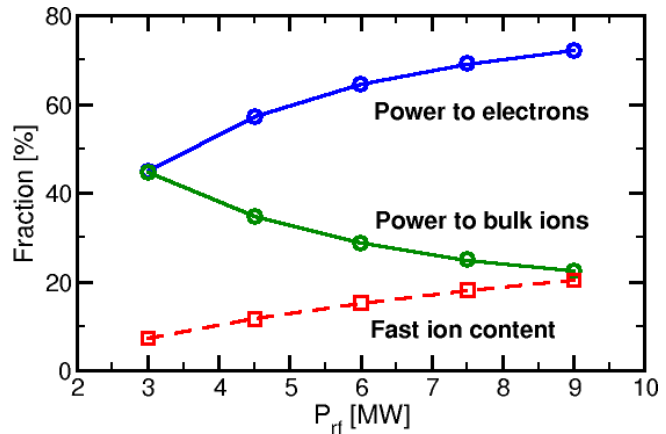
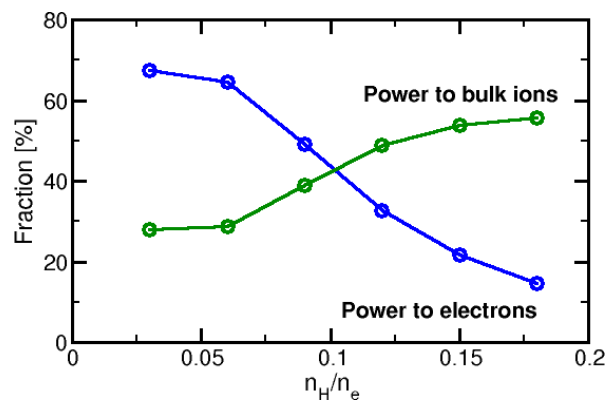


Figure 70: Influence of the hydrogen minority concentration on the power split between electrons and bulk ions.



The optimization of ICRF scenarios constitutes an important research axis of WEST. Since the three new ELM resilient ICRH antennas can be operated in steady-state conditions, critical ITER topics such as continuous wave antenna operations, fast ion losses, central heating, the ratio of power to ions and electrons and impurity production from RF sheaths will be studied. The experimental results will be compared to ICRH codes such as SSWICH [Col12], EVE coupled with fast ion modules such as AQL [Dum13] and SPOT [Sch05].

#### 4. Fuelling and pumping capabilities

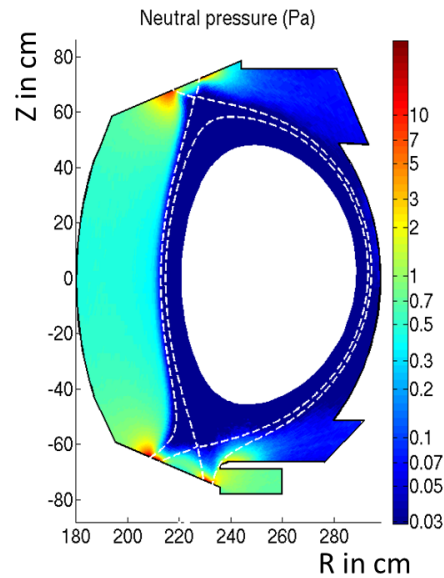
Three fuelling systems are available in WEST: 19 gas puff injection lines connected to 11 calibrated reservoirs; three Supersonic Molecular Beam Injectors and four pellet injection points. Their capacities are of  $11 \times 4 \text{ Pa} \cdot \text{m}^3 \cdot \text{s}^{-1}$  for gas puff; of  $3 \times 20 \text{ Pa} \cdot \text{m}^3 \cdot \text{s}^{-1}$  for SMBI and of  $7\text{-}11 \text{ Pa} \cdot \text{m}^3 \cdot \text{s}^{-1}$  for the pellets. In addition, a massive gas injection system (MGI) is available to mitigate the impact of disruptions and runaways.

During the discharges, active pumping is provided by 10 turbo-molecular pumps located at the bottom of pumping ducts under the baffle. The pumping baffle has been optimized to channel the neutrals towards the pumping systems, using the Soledge2D-EIRENE code package [Buf13]. Soledge2D is a 2D transport code solving fluid equations for the plasma density, parallel momentum and temperatures for the main ions in a realistic geometry [Buf13]. Sources related to neutral particles are calculated by the EIRENE kinetic transport code [Rei05]. The Soledge2D-EIRENE code package is run by puffing in D2 molecules and imposing a given energy flux on the core-edge interface. Simulations results indicate that the



pressure under the baffle, with  $n_{\text{sep}}$  between 2 and  $4 \times 10^{19} \text{m}^{-3}$ , is expected to be in the range of 0.5 to 1 Pa, as illustrated in Fig. 71. This leads to a pumping rate of the order of  $5 \times 10^{21} \text{D/s}$  or around  $10 \text{Pa} \cdot \text{m}^3 \cdot \text{s}^{-1}$  which is consistent with the installed fuelling capabilities.

Figure 71: Neutral pressure in a poloidal cross section of WEST modeled by SolEdge2D-EIRENE [Buf13]



The WEST particle exhaust system provides a moderate pumping efficiency, as will be the case for ITER. The impact of low pumping capability on plasma operation (H mode access, confinement quality, W sources) and fuel retention will be explored. The system could be upgraded to cryopumps depending on the results of the first phase of WEST operation.

### 5. L-H power threshold, pedestal and ELMs

The L-H power threshold has been estimated using different scaling laws. The ITPA 2008 scaling has been computed [Mar08] as well as the ITPA 2004 one [Tak04] where the impact of the effective charge  $Z_{\text{eff}}$  is included. The later has been recently shown to reduce the spread of JET-ILW and JET-C data points compared to the ITPA 2008 scaling law without  $Z_{\text{eff}}$  [Mag14]. Moreover, since WEST has an aspect ratio,  $A$ , between 5 and 6, larger than most tokamaks, an additional aspect ratio dependence is discussed. The aspect ratio impact was reported by comparing spherical tokamaks with standard  $A \sim 3$  tokamaks [Tak04]. A higher  $P_{\text{th}}$  at lower  $A$  in [Tak04] was found to be in qualitative agreements a scaling law based on ideas from [Min97].

Therefore, for WEST, the predictions from three scaling laws are illustrated in Fig. 72: ITPA 2008 [Mar08], ITPA2004 [Tak04] assuming  $Z_{\text{eff}}=1.2$  and ITPA 2004 with  $Z_{\text{eff}}=1.2$  and an

additional aspect ratio impact such that  $P_{\text{th}} \propto \frac{1}{\sqrt{A}}$  from [Min97]. Fig. 72 shows the available additional power in WEST is larger than the most pessimistic of these scaling laws.

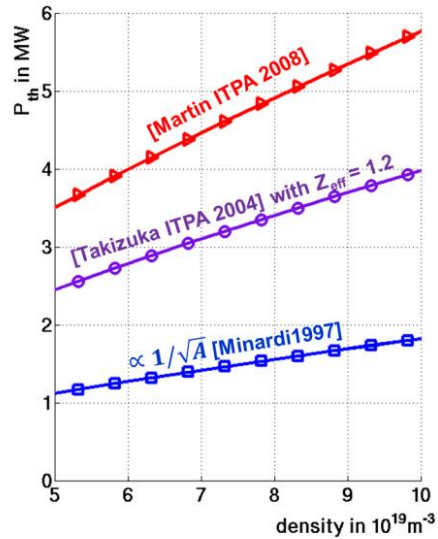
On the experimental side, the WEST compact divertor geometry has been tested in the W environment of ASDEX Upgrade and a power threshold of 2 MW was reported [Mey13].

Nonetheless, uncertainties remain, in particular in WEST the magnetic field ripple reaches 2.3 % at  $R = 2.93 \text{ m}$  (outboard midplane boundary) and it could affect the L-H power

threshold through the modified ambipolar radial electric field. Note however that in JET a ripple up to 1.1% did not affect the threshold [And08] and in JT-60U, before the installation of ferromagnetic inserts, the power threshold was even reduced with larger magnetic ripple [Tob95]. In DIII-D, local magnetic ripple of 3% from test blanket module mock-up coils did not change  $P_{th}$  [Goh11].

Figure 72: L-H power threshold expectation for WEST with respect to the core line average density. In red, triangles: ITPA 2008 [Mar08]; in purple circles: ITPA2004 [Tak04] assuming  $Z_{eff}=1.2$ ; in blue squares: ITPA 2004 with  $Z_{eff}=1.2$  and an additional aspect ratio impact such that

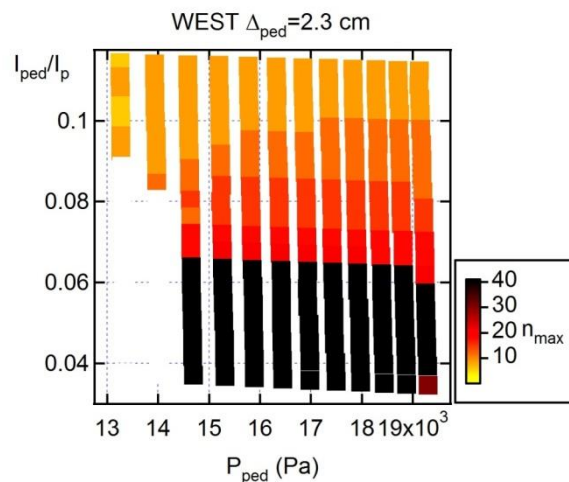
$$P_{th} \propto \frac{1}{\sqrt{A}} \text{ from [Min97].}$$



The ideal MHD stability limit in the WEST scenarios studied has been calculated using the linear MHD code MISHKA [13]. The pedestal width is assumed to be around 5% of the minor radius such that  $\Delta_{ped}=2.3$  cm. A pedestal pressure limited by the ballooning limit of 14.5 kPa was found for  $I_p=0.8$  MA, see Fig. 73. This limit scales with  $I_p^2$ , hence, at 0.5 MA, 6kPa are expected.

The impact of WEST large aspect ratio, ranging from 5 to 6, on the pedestal height and width remains to be studied. For the time being, the scenarios are prepared with a pedestal energy derived from the multi-machines ITPA scaling law given in [Mcd07] and leads to consistent pedestal pressures within 65 to 90% of the ideal MHD limit with  $\Delta_{ped}= 2.3$ cm.

Figure 73: Ideal MHD limit computed by MISHKA [Huy07] for  $I_p=0.8$  MA. The low wave number modes are the peeling modes and the higher wave number modes are the ballooning modes.

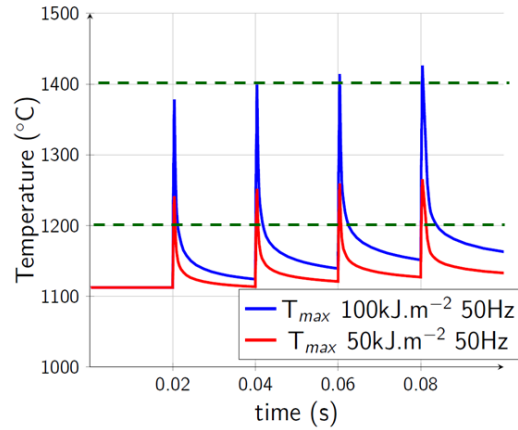


Using the ITPA 2007 pedestal energy scaling law [Mcd07], it is found that the pedestal energy,  $W_{ped}$ , is in the range of 20 to 25% of the total thermal energy,  $W_{th}$ , in WEST modelled scenarios presented in section 8. For the high power scenario illustrated by Table 1 below, a maximum  $W_{th}$  of 0.9 MJ is expected with a  $H_{98}$  factor of 1. This means that up to  $W_{ped}$  of 200kJ is anticipated. The ratio  $W_{ELM}/W_{ped}$ , where  $W_{ELM}$  is the energy expelled per ELM, varies with collisionality for baseline discharges [Loa03] but for hybrid scenarios no clear correlation can be established [Zar11].  $W_{ELM}/W_{ped}$  can be as low as a few % and as high as 20% in the case of low density type I ELMs. Therefore, ELMs of up to 40kJ are anticipated. The size of the wetted area will depend on the X point height and on the broadening of the wetted area. For a high X point height around 10 cm, without broadening, and without divertor tile shaping, a wetted area in the range of 0.3 m<sup>2</sup> is expected. Accordingly, in this case, an ELM load of more than 100 kJ/m<sup>2</sup> could be reached. Using [Her02], the associated ELM frequency,  $f_{ELM}$ , can be estimated as follows:  $f_{ELM} = 0.2 \times P_{SOL}(\text{MW}) \times 10^3 / W_{ELM}(\text{kJ})$ , leading to  $f_{ELM} = 50\text{Hz}$  for the high power scenarios and  $W_{ELM} = 40\text{kJ}$ .

On a scenario with 10 MW/m<sup>2</sup> onto the divertor, the tile surface temperature reaches 1100°C. In the case of type I ELMs with  $W_{ELM} = 40\text{kJ}$  at 50Hz, temperature excursions of 300° on the surface of the actively cooled W monoblocks are modelled by Finite Element Method thermal simulations [Cou13] as illustrated by Fig. 74. Hence, with such ELMs, cycling around the W recrystallization temperature, i.e. above 1200°C, would allow studying the actively cooled W divertor response. Experiments in WEST accumulating 100,000 transients or more would be benchmarked against laboratory experiments to assess the role of possible synergistic effects encountered in a tokamak environment. As an alternative to the utilization of large ELMs, the use of an in-situ laser tool to study the impact of combined transient / steady state heat loads is considered.

ELMs study is a strong axis of research in WEST integrating physics, operational and technological aspects. The impact of resistivity and aspect ratio on ELMs will be studied and compared to codes such as JOREK [Huy09] and MISHKA [Huy07]. The heat loads on the divertor will be monitored taking advantage of the 100% coverage of the lower divertor by Infra Red thermography and thanks to probe measurements and thermocouples, in particular the ELM wetted area and its modification with ELM size will be explored. Besides, the heat load on the main chamber will also be studied using the infrared coverage of the ICRH and LHCD antennas. Finally, the impact of more than 100,000 transients on ITER like actively cooled W divertor targets will be studied in situ using the Articulated Inspection Arm and post-mortem analysis.

Figure 74: Estimate of the temperature increase of the W monoblocks linked to ELMs, for a steady state heat load of  $10 \text{ MW/m}^2$ , and large type I ELMs of 50 and  $100 \text{ kJ/m}^2$ , red and blue curve respectively, 50 Hz frequency. The W recrystallization temperature range is bordered by green dashed lines.



## 6. Expected density profiles

The density profile prediction for WEST is based on three estimates: the density at the separatrix, the pedestal density and the core density peaking factor.

As expected from the 2 points model [Sta], the plasma temperature downstream on the divertor target is constrained by the density at the separatrix. The upper bound considered in the following is of the order of 50 eV, a temperature above which W sputtering by deuterium sharply increases [Dux09]. Figure 75 shows the target temperature from the 2 points model with hydrogen recycling included. The electron cooling of 25eV per ionization event is taken, and the 2 points model parameters are such that  $f_{mom} = 0.8$ ,  $f_{cond} = 1$  [Sta]. Different fractions of the power loss in the SOL ( $P_{loss}^{SOL}$ ) with respect to  $P_{SOL}$  are explored such that  $f_{power} = P_{loss}^{SOL}/P_{SOL}$  is varied from 0 to 50%. Here a fairly high power case is considered with  $P_{SOL} = 6 \text{ MW}$ ,  $\square_q = 5 \text{ mm}$ , i.e. a combination of parameters which should allow reaching  $10 \text{ MW/m}^2$  on the divertor plates, and relevant for H-mode operation (see sections 2 and 5). Should  $\square_q$  be lower,  $P_{SOL}$  should be lower too in order to be compatible with safe PFC operation. This simple model shows that high power operation requires separatrix densities of the order of  $3 \times 10^{19} \text{ m}^{-3}$ . These estimations for the required separatrix density are in fair agreement with Soledge2D-EIRENE modelling [Buf13] (pure deuterium cases) see open circles in Fig. 75 from [Mar14]. In Soledge2D-EIRENE a particle diffusion coefficient  $D$  has been chosen such that  $D = 0.3 \text{ m}^2 \text{ s}^{-1}$ , a convection velocity such that  $v = 0.1 \text{ m s}^{-1}$  and the assumed diffusive heat transport such that  $\chi_e = \chi_i = 1 \text{ m}^2 \text{ s}^{-1}$ . Note that these transport coefficients are compatible with an analysis of the heat deposition profiles leading to  $\lambda_q \approx 5 \text{ mm}$ .

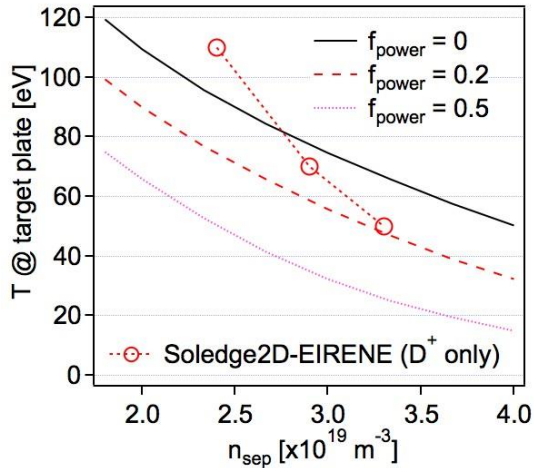


Figure 75: Plasma temperature in front of the target plates as a function of separatrix (upstream) density from a two points model, for  $P_{SOL}=6\text{MW}$  and  $\lambda_Q=5\text{mm}$  and various levels of radiated power in the SOL. Open circles are pure deuterium Soledge2D-EIRENE calculations for the same parameters.

In metallic machines, in H mode, the operation at low densities is more limited than in C wall machines. Indeed, JET-ILW [Beu14] and ASDEX Upgrade with the full W coverage [Kal11, Neu11] both operate in a  $n_{ped}/n_{gw}$  range, from 40 to 80%. In WEST, for  $I_p=0.6\text{-}0.8\text{MA}$ , the Greenwald density,  $n_{gw}$ , ranges from 10 to  $12 \times 10^{19}\text{m}^{-3}$ . Therefore  $n_{ped}$  between 4 to  $9 \times 10^{19}\text{m}^{-3}$  is expected.

On the other hand, a multi-machine database shows that  $n_{ped}/n_{sep}$  correlates with  $n_{sep}/n_{gw}$  [Kal05]. As discussed above,  $n_{sep}$  of the order of 2 to  $3 \times 10^{19}\text{m}^{-3}$  is projected, i.e.  $0.15 \leq n_{sep}/n_{gw} \leq 0.3$ . Therefore based on [Kal05],  $n_{ped}$  between 3 and  $9 \times 10^{19}\text{m}^{-3}$  are anticipated. This range is coherent with the previously expected constraint on  $n_{ped}/n_{gw}$ .

The density peaking factor has been extensively studied in H modes in JET and ASDEX Upgrade [Ang07]. Multiple regression analyses show that in the combined database collisionality is the most relevant parameter. Based on these works, a core density peaking with  $\frac{n_0}{\langle n \rangle} - 1 = 0.28 - 0.17 \ln v_{eff}$  from [Wei05] is used for WEST scenarios extrapolation,

where  $v_{eff}$  is the normalized collisionality,  $n_0$  the central electron density and  $\langle n \rangle$  the volume averaged electron density. It is to note that WEST has an aspect ratio significantly larger than JET and ASDEX Upgrade, 5 to 6 in WEST to be compared to 3 in JET and ASDEX Upgrade. A larger aspect ratio is expected to modify the core turbulent transport due to a reduced trapped particle fraction, in particular Trapped Electron Modes should be less unstable. The high aspect ratio in WEST will expand the existing databases beyond possible future DEMO values of about  $A=4$ , allowing firmer projections from the large existing  $A=3$  database. This means that ideally the core particle transport in the large aspect ratio WEST should be modelled using first principle transport codes such as TGLF [Sta07] or QuaLiKiz [Bou07] in CRONOS [Art10]. Such studies are planned. For the time being, the modelled density profile peaking is based on [Wei05].

Since WEST will operate without NBI, hence without central particle fuelling, and at low loop voltage, hence reduced neoclassical Ware pinch, core particle transport at high aspect ratio will be analysed as done in the past [Hoa03]. The density profiles will be measured precisely thanks to a full coverage by reflectometry measurements together with 10 interferometry chords. The peaking factor will be compared to first principle non-linear and quasilinear gyrokinetic codes [Bou07, Ang12].

## 7. W sources and contamination

Experience from ASDEX Upgrade and JET shows that tungsten sources as measured by spectroscopy are usually dominated by W sputtering caused by light impurities [Neu11]. This is due to (1) the fact that even in the inter-ELM regime sputtering by light impurities is usually not extinguished, and (2) the contribution of ELMs [Dux09]. In ASDEX Upgrade, the main chamber tungsten source is dominant for the core plasma W content, due to the efficient divertor retention for sputtered W. So, it should be stressed that one of the main source of uncertainties in foreseeing W sources in WEST is the fact that the concentration of light impurities (O, C, B) cannot be predicted accurately. Preliminary calculations with SOLPS4.0 and DIVIMP including C as a representative impurity have shown tolerable contamination levels, that is, comparable to those observed in ASDEX Upgrade, for conditions where peak heat fluxes are of the order of  $10 \text{ MW/m}^2$  [Buc11]. These simulations have been made assuming that the power flowing through the separatrix is such that  $P_{\text{SOL}}=4\text{-}8 \text{ MW}$ . A specific feature of a W machine compared to a low-Z machine is the existence of potentially strong core-edge coupling, due to the fact that W radiates in the core. As a result, an increase of W sources and thus contamination would reduce  $P_{\text{SOL}}$  at a given injected heating power, hence lower the temperatures in front of the target plates and in turn act as a feedback on W sources [Zag09]. Roughly speaking, the temperature in the divertor would then settle around the effective sputtering threshold value, for the mix of low Z-impurities present in the plasma. This situation pertains to low density cases, for which W screening is inefficient. At higher densities, one would expect lower W contamination, hence lower radiation losses in the core and thus reduced core-edge coupling. Addressing the full picture is very challenging, because core transport physics (accumulation, saw teeth) and pedestal physics (transport through the pedestal, ELMs flushing) have to be taken into account. However, simplified tools such as Corediv, which simulates both core and edge plasmas have proven to be valuable to analyse ASDEX Upgrade and JET discharges [Zag12]. Coupled core-edge modelling for WEST has been performed with Corediv first in pure deuterium [Iva13]. Then, to mimic a light impurity content, boron is included as a typical light impurity [Mar14]. In these simulations, a concentration of boron of 1% typically reduces the power flowing to the target plates by 50% compared to a pure deuterium case, essentially due to W radiation in the core (edge radiation by boron is then comparable to deuterium radiation) for coupled power above 8 MW and a volume averaged density of  $6 \times 10^{19} \text{ m}^{-3}$ . As an illustration, Fig. 76 shows the radiation fraction in the core and in the SOL for a heating power of 14 MW, as a function of boron concentration in %. In these simulations, the edge radiation is fairly low because boron is not an efficient radiator. Note that estimates for the peak power flux density in section 2 assumed 40% of coupled power radiated, and are thus consistent with these results. Also, reaching  $P_{\text{SOL}}=6 \text{ MW}$  as assumed e.g. for Fig. 75 would then require about 12 MW of auxiliary power.

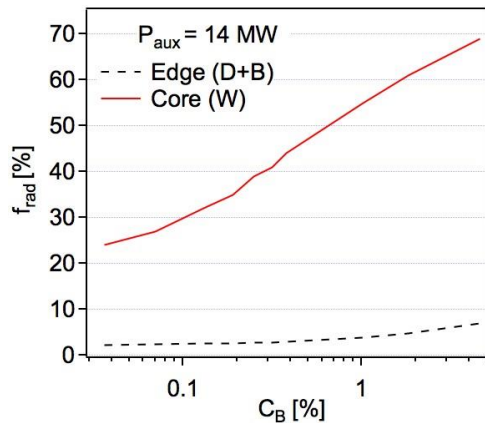


Figure 76: Fraction of the heating power radiated in the core (solid red) and in the edge (dashed black), as a function of boron concentration in % obtained by Corediv for  $P_{aux}=14$  MW. Core radiation is almost exclusively from W while edge radiation is essentially from D and B.

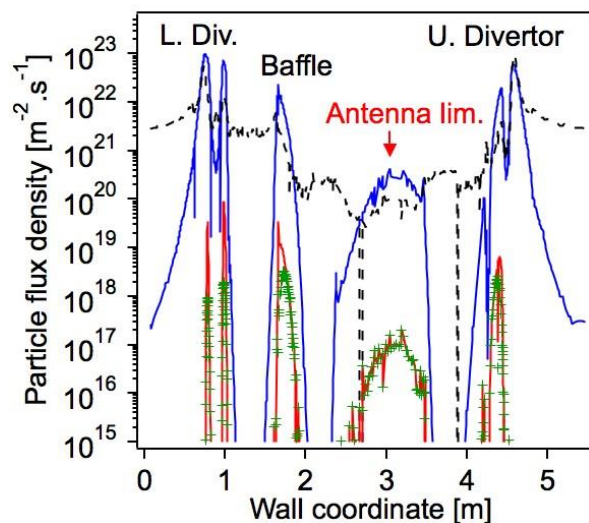
However, even if W divertor sources are dominant in terms of gross sputtered fluxes, the contamination of the main plasma seems to be often controlled by main chamber sources [Dux09, Lip01], which were not included in either the SOLPS/DIVIMP or Corediv simulations mentioned earlier. It should be emphasized that in WEST most of the first wall elements are farther from the plasma than in ASDEX Upgrade, with the exception of a few objects such as the pumping baffle and the antenna guard limiters. Also, unlike most other machines, all the antennas on WEST are moveable radially in the chamber [Col06]. While a low radial gap between the radiating straps and a characteristic density layer is beneficial for the ICRH power coupling, a minimal antenna-separatrix clearance was found necessary on Tore Supra to maintain safe steady-state surface temperatures on the antenna structures [Col06]. Similar operational trade-off will probably have to be found in WEST to limit the impurity accumulation in the main plasma over long pulses. In this empirical optimization, localized gas injection in the main chamber, initially designed as a tool to ease ICRH wave coupling, might also influence the impurity production near the antennas, as suggested experimentally on ASDEX-Upgrade [Bob13] and JET [Ler14].

Calculating main chamber sources is a challenge for modelling since most of the current versions of transport codes cannot simulate the plasma up to the first wall. This issue is currently being addressed with the Soledge2D-EIRENE code [Buf14], and first calculations of W sources have been presented in [Mar15]. But these simulations will have to be complemented by additional modelling to address a possible influence of turbulent fluctuations in the far SOL (filaments) [Mar11], penetration of neutrals [Mek12] and transport of impurities in such fluctuating plasmas [Guz15]. Last but not least, prompt redeposition has to be taken into account [Chan14]. The latter is shown to play an important role in the balance between divertor and main chamber sources, as illustrated on Fig. 77. In the simulations presented in [Mar15], the pumping baffle is found to be a substantial source of W (between 15 to 40% of the total net W influx, that is with prompt redeposition taken into account, in the absence of ICRH). DIVIMP modelling has been initiated to provide an estimate for the W contamination resulting from these sources.

Finally, it must be emphasized that calculations presented on Fig. 77 do not take the effect of ICRH operation into account (hence the very low sources on the antenna limiter) [Bob13, Wuk09]. It should also be mentioned that these 2D simulations do not take the limited toroidal extent of the antenna limiters into account, so that the sources reported on Fig. 77 (with ICRH switched off) are actually overestimated. In addition, the antennas are movable, so that their position in the simulations is only representative of a typical situation. One

expects enhanced potentials in region magnetically connected with the antennas [Och14] and a maximum of the potential is observed in region connected with the antenna side limiters [Col14, Wuk13, Kub13, Czi12]. Nonetheless, it is still difficult to extrapolate because enhanced potentials are also observed in unconnected regions on Alcator C-mod [Och14], in some cases similar enhanced potentials are measured with an unexpected smaller impurity production [Wuk13]. ICRH-induced convective cells are also supposed to enhance the perpendicular penetration of the impurities [Czi12]. Therefore, predicting the W sources during ICRH operation from first principle is not possible at this time. The sources will depend on the type of antenna, on its operation mode, as well as light impurity concentrations and conditions in front of the antenna (fluxes, ionization degree). Nevertheless, experience gained during Tore Supra operation in L-mode can be used to estimate particle fluxes and typical ion energies on the antenna protections [Rit13, Cor11]. Both probe data mapped onto the antenna protections and analysis of IR data lead to particles fluxes of up to a few  $10^{22}$   $D^+/m^2/s$ , and ions energies of the order of 200eV. Using an ASDEX Upgrade relevant effective sputtering yield of  $Y_{\text{eff}} \sim 10^{-4}$ , one typically would get gross tungsten influxes in the range  $\Gamma_W = 10^{18} - 10^{19} \text{ m}^{-2} \cdot \text{s}^{-1}$  if the WEST antennas are operated in similar conditions as on Tore Supra, i.e. with a strap potential between 10 to 30 kV. The surface area of the antenna limiter, assuming that the three ICRH antennae are operating, is of the order of  $0.1 \text{ m}^2$ . The total W influx can thus be estimated as  $10^{17} - 10^{18} \text{ s}^{-1}$ , noting that prompt redeposition is likely to be low (as observed on Fig. 77) because of the fairly low temperatures in front of the antennas. These values are comparable to those obtained in Soledge2D-EIRENE simulations for the net divertor sources (i.e. including prompt redeposition effects), while easier W penetration to the plasma core is expected from the antenna limiters than from the divertor. From this analysis, it can be concluded that W sources on antenna protections are indeed likely to play a substantial role in the W contamination, as is the case elsewhere [Wuk13]. Note that enhanced floating potentials during ICRH were measured by Langmuir probes located at the top of Tore Supra, several meters away toroidally from the powered antennas [Kub13]. Therefore ICRH operation might also increase sources elsewhere in the machine, in particular on divertor baffle and target areas magnetically connected to the antennas.

Figure 77: Particle flux densities as a function of the poloidal location, from the lower to the upper divertor via the low field side elements (baffle and antenna limiters).  $D^+$  flux (solid blue), D flux (dashed black), W gross influx from ions (solid red) and net influx from ions (green crosses), i.e. accounting for prompt redeposition, but without sheath rectification.





In order to address these issues, the  $W$  sources will be closely monitored thanks to the comprehensive visible spectroscopy diagnostic which will be available on WEST, with 200 lines of sight aiming at both divertors, baffle, antenna limiters, and inner bumpers. The compact divertor geometry allows good optical access to study the physics of, e.g. prompt  $W$  redeposition. The good diagnostic coverage of antenna protections will be an asset for HF sheaths code validation [Jac14].

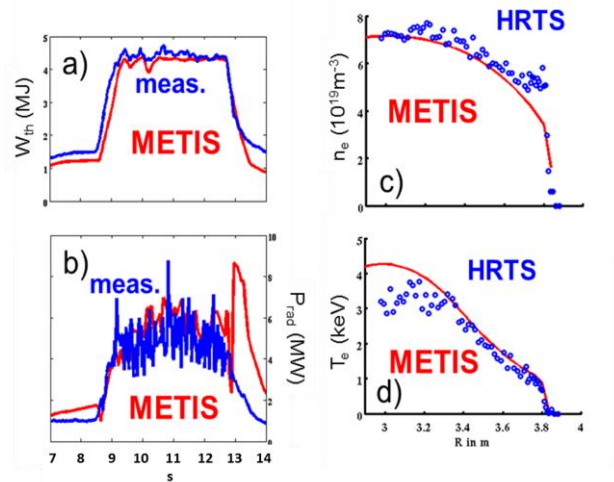
### 8. Integrated standard scenarios

The integrated modelling of WEST scenarios has been performed with the 0D version of CRONOS code called METIS [Art10]. METIS stands for **M**inute **E**MBEDDED **T**OKAMAK **I**ntegrated **S**imulator. 300 time slices are modelled within one minute. The heat transport equations are simplified by separating the time and radial dimensions, which allows a fast solution to the heat transport problem based on scaling law prescriptions. The current diffusion is carried out in 1.5D with moment equilibrium, as in traditional integrated modelling solvers. The heat and particle source profiles are deduced from simple models. The global energy content comes from 0D scaling laws. The temperature profiles are stationary 1D solution scaled to reproduce  $W_{th}$ . All non-linearities are solved (dependence of sources on profiles ...). The inputs are: the additional power,  $I_p$ , the line average density,  $Z_{eff}$ , the LCFS geometry. The outputs are all standard 1D and 0D data from a transport code. METIS is included in the CRONOS suite of codes, as a first step scenario design to prepare full integrated modelling simulations.

Before using METIS to predict WEST scenarios, it has been used to model eleven JET-ILW and one ASDEX Upgrade pulses. With a choice of reasonable sets of input parameters, METIS outputs could simultaneously reproduce the energy content, the radiated power level as well as the density and temperature profiles, in particular the pedestal and LCFS values. One of the pulses used is shown on Fig. 78. It is a JET-ILW pulse with ICRH and NBI heating. The thermal energy content,  $W_{th}$ , is reproduced by adjusting the H factor [ITE99]. H factors ranging from 0.7 to 1 have been found, for the case of Fig.78 a,  $H=0.8$  has been required. The radiated power,  $P_{rad}$ , is reproduced using the revised  $W$  cooling rate [Put10], assuming flat  $W$  profiles and adjusting  $C_W$  at the LCFS.  $C_W$  from 1 to  $7 \times 10^{-4}$  has been found necessary to reproduce the core  $P_{rad}$  value, for the case of Fig.78 a,  $C_W = 7 \times 10^{-4}$  has been required. The separatrix density value is from the scaling proposed in [Mah03] and agrees well with the measured values, as it can be seen for the example illustrated by Fig. 78.c. The pedestal width is fixed and chosen to be 5% of the minor radius. The pedestal density is then constrained by the line average density and the density peaking chosen, here [Wei05]. In some cases, density peaking from [Wei05] leads to underestimated  $n_{ped}$  as in can be seen for the case illustrated on Fig.78.c.  $T_{ped}$  is deduced from  $W_{ped}$  based on [Mcd07] multiplied by the H factor. It is usually in good agreement with the measured values, as illustrated for one of the cases on Fig.78.d.

Figure 78: JET-ILW pulse 84746

- The thermal energy versus time. In blue the measured one and in red the simulated one with METIS.
- $P_{\text{rad}}$  versus time in s.
- The electron density profile at 11s measured by HRTS in blue and modeled by METIS in red.
- The electron temperature profile at 11s.



Based on a fair agreement obtained on these 12 cases and using the information gathered through the previous reported studies (ICRH, LHCD, pedestal density value,  $W$  content, etc), WEST pulses have been modelled. For ICRH a power absorption within  $\rho=0.4$  is modelled, based on EVE/AQL results of section 3, with a ratio of 50% of the power coupled to the bulk ions and 50% to the electrons (see Fig.68). LH waves are absorbed at mid radius (see Fig.66) with a CD efficiency from 0.07 to  $0.1 \times 10^{20} \text{ A} \cdot \text{W}^{-1} \cdot \text{m}^{-2}$  consistent with C3PO/LUKE simulations reported in section 3. The density peaking from [Wei05] is used, based on the relative success in reproducing JET profiles. A density at the separatrix from [Mah03] coherent with SOLEDGE2D-Eirene expectations presented in section 6 is assumed. A pedestal width of 5% is taken, which was found coherent with JET observations as illustrated by Fig. 78.c. A  $W$  concentration at the separatrix such that  $n_W/n_e = 5 \times 10^{-4}$  is taken, in the range used to reproduce the radiated power of the 12 studied cases. Such a  $W$  concentration is in the right order of magnitude, in case of target temperatures around 50 eV and some light impurity content [Dux09] as presented in section 7. A flat  $n_W$  profile is assumed for the moment. In the future simultaneous turbulent and neoclassical transport should be accounted for. The radiative power,  $P_{\text{rad}}$ , is determined using the revised  $W$  cooling rate from [Put10]. The H factor from [ITE99] is taken to be 1 and sensitivity tests in the range 0.7 to 1.2 have been carried out. The pedestal energy based on the ITPA scaling [Mcd07] adjusted to the H factor is used. It was shown to be below the ideal MHD limit for  $\Delta_{\text{ped}}=2.3 \text{ cm}$  in section 5 and to reproduce well 12 cases as the one illustrated on Fig. 78.d.

All scenarios are for 3.7 T at 2.5 m. Accounting for the fact that ICRH power is limited by the generator to 9 MW / 30 s, 6 MW / 60 s or 3 MW / 1000 s, three types of scenarios have been designed. The high power one with 9 MW of ICRH and 6 MW of LH lasting 30s at 0.8 MA; so called “standard” cases with 6MW of ICRH and 6 MW of LH lasting 60 s at 0.6 MA (and lasting less if operated at higher current, 25 s at 0.8 MA) and finally a high particle fluence scenario lasting 1000s with 3MW of ICRH and 7 MW of LH power. The three scenarios are summarized in Table 1.

In particular, one can note that the Greenwald fraction is between 60 to 70%, which is coherent with the fraction at which metallic wall machines such as JET-ILW [Beu13] and ASDEX Upgrade [Kal11] routinely operate. The pedestal density is at most  $5 \times 10^{19} \text{ m}^{-3}$  which should be compatible with LH wave accessibility discussed in section 3. The bootstrap fraction is around 30 to 35% and the fraction of LH driven current up to 60%. On Fig. 79, the

profiles for the 3 scenarios are illustrated. The density profiles are peaked due to the scaling used [Wei05], this should be revisited using CRONOS and realistic transport codes. The electron temperature reaches up to 6 keV in the core of the high power case. The q profiles do not go below 1 for the two scenarios at 0.6 MA. The q profile is even expected to be strongly reversed in the high fluence scenario due to the off-axis LHCD absorption. No ITB model has been included here.

Table 14: summary of some key parameters characterizing 3 scenarios for WEST suited with the code METIS.

Scenario	High power	standard	High fluence
$I_p$ (MA)	0.8	0.6	0.6
$n_e$ ( $10^{19}m^{-3}$ )	8.0	7.0	7.0
$f_{GW}$ (%)	70	70	70
$P_{heat}$ (MW)	15	12	10
LHCD (MW)	6	6	7
ICRH (MW)	9	6	3
$P_{rad}$ (MW)	5.0	3.0	3.0
$\beta_N$	2.7	2.2	1.7
$T_{ped}$ (keV)	0.7	0.4	0.4
$n_{ped}$ ( $10^{19}m^{-3}$ )	5.0	5.0	4.5
$W_{th}$ (MJ)	0.9	0.6	0.5
Bootstrap fraction (%)	30	35	35
LHCD fraction (%)	30	50	60
Pulse length (s) min(14 Wb or IC time limit)	30	60	1000
Expected heat load (MW/m <sup>2</sup> ), 2/3 vs 1/3 asym.	10 to 20 depending on X point height and $\lambda_q$		
Operation time to reach one ITER pulse fluence	~6 months	~2 months	few days

15 MW, 0.8 MA, 30 s 12 MW, 0.6 MA, 60 s 10 MW, 0.6 MA, 1000 s

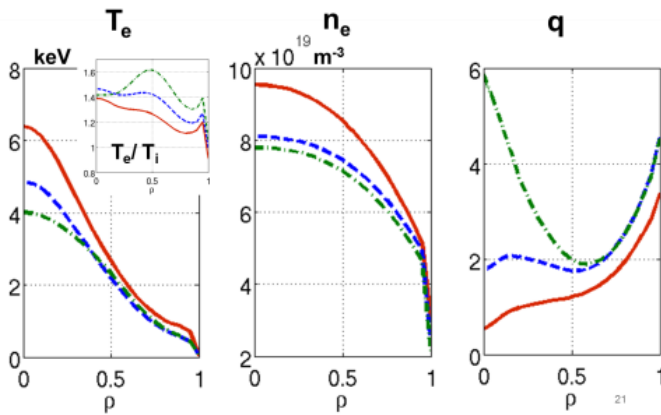


Figure 79: Temperature, density and q profiles of the 3 scenarios summarized in Table 1.

Moreover advanced tokamak modes are expected to be accessible thanks to the LHCD long-pulse capability at high power and their investigation will be an important research axis of WEST. Note that a 30 s pulse is as long as 20 resistive times. These scenarios will allow developing real-time control expertise for long pulse scenarios, exploring some advanced regimes and their control. This programme will participate to JT60-SA operation preparation.

## 9. Conclusions

Sustainment of ELMy H mode up to 1000s with 10 to 20 MW/m<sup>2</sup> onto the divertor is achievable. WEST will thus allow operating an actively cooled tokamak equipped with an ITER-like divertor and studying simultaneously the related technology, operation and physics a phase ahead of ITER. The WEST scientific program has been discussed extensively during the 1st WEST International in Aix-en-Provence, France, from June 30 to July 2, 2014 [WWS14]. It is organized around two main axes: “ITER grade PFC tests” and “towards long pulse H mode and steady-state operation”. WEST operation is to be started in 2016 [Buc14].

The research activities on WEST will address a very large variety of topics such as: steady-state and transient heat loads on an ITER-like actively cooled tungsten divertor, IR monitoring of the surface temperatures in a metallic environment, LHCD absorption at high density, ICRH coupling with ELMs, W source survey and understanding, density control over long time, large aspect ratio impact on core turbulent transport, W transport, L-H power threshold in large aspect ratio machine, advanced tokamak scenarios, etc. A helium campaign is also foreseen to address PFC and confinement ITER relevant issues.

The WEST platform and its research plan are fully open to all ITER partners. It will contribute to train professionals and newcomers on a long pulse superconducting tokamak integrating high heat flux tungsten PFCs and thus actively prepare ITER divertor operation

## Acknowledgements:

The authors wish to acknowledge the active and fruitful participation to the 1<sup>st</sup> WEST International Workshop of D. Campbell, F. Escourbiac, R. Pitts and J. Snipes from ITER Organization, P. Lorenzetto from F4E, K. Ezato from JADA, X. Litaudon from EUROfusion, D. Hillis from ORNL, C. Angioni, V. Bobkov and Th. Eich from IPP Garching, S. Brezinsek, J. Coenen, C. Linsmeier and T. Loewenhoff from FZJ, S. Kajita from Nagoya University, A. Tuccillo from ENEA and P. Chiappetta from Aix-Marseille University.

This work has been carried out within the framework of the EUROfusion Consortium and has received funding from the European Union's Horizon 2020 research and innovation programme under grant agreement number 633053. The views and opinions expressed herein do not necessarily reflect those of the European Commission. The views and opinions expressed herein do not necessarily reflect those of the European Commission.

- [And08] Andrew Y et al Plasma Phys. Control. Fusion 50 (2008) 124053
- [Ang07] C. Angioni, H. Weisen, O.J.W.F. Kardaun et al Nucl. Fusion 47 (2007) 1326–1335
- [Ang12] C. Angioni et al Nucl. Fusion 52 (2012) 114003
- [Arg09] A. Argouarch et al., FED 84 (2009) 275–278
- [Art10] J.-F. Artaud et al, Nucl. Fusion 50 043001 (2010)
- [Bas04] V. Basiuk et al 2004 Nucl. Fusion 44 181 doi:10.1088/0029-5515/44/1/020
- [Beu14] M. Beurskens et al Nucl. Fusion 54 (2014) 043001 (13pp)
- [Bib00] Ph. Bibet et al., FED 51-52 (2000) 741–746
- [Bob13] V. Bobkov, et al., Nucl. Fusion 53 (2013) 093018
- [Bou07] C. Bourdelle et al Phys. Plasmas 14, 112501 (2007)
- [Buc11] J. Bucalossi et al Fusion Engineering and Design 86 (2011) 684–688

- [Buc14] J. Bucalossi, M. Missirlian, P. Moreau et al *Fusion Engineering and Design* 89 (2014) 907–912
- [Buf13] H. Bufferand et al., *J. Nucl. Mat.* 438, S445 (2013)
- [Buf14] H. Bufferand et al., *Contrib. Plasma Phys.* 54, 378 (2014)
- [cedres] H. Heumann, et al, submitted to *J. Plasma Phys*
- [Ces10] Cesario R. et al, *Nature Commun.* 1 55 (2010)
- [Cha14] A. Chankin et al *Plasma Phys. Control. Fusion* **56** (2014) 025003 (11pp) doi:10.1088/0741-3335/56/2/025003
- [Cir13] G. Ciruolo et al., *Contributions to Plasma Physics* (2013)
- [Coe14] J.W. Coenen et al., *J. Nucl. Mater.* (2014), <http://dx.doi.org/10.1016/j.jnu>
- [Col06] L. Colas et al 2006 *Nucl. Fusion* 46 S500
- [Col07] L. Colas et al. *Journal of Nuclear Materials* 363–365 (2007) 555–559
- [Col12] L. Colas *Phys. Plasmas* 19, 092505 (2012); <http://dx.doi.org/10.1063/1.4750046>
- [Col13] L. Colas et al., *J. Nucl. Mater.* (2014), <http://dx.doi.org/10.1016/j.jnucmat.2014.10.011>
- [Cou13] X. Courtois, M. Firdaouss, P. Gavila et al *Fusion Science and Technology* 64 (2013) 727-734
- [Cor11] Y. Corre, et al *Fusion Engineering and Design* 86 (2011) 429–441
- [Czi12] I Cziegler et al *Plasma Phys. Control. Fusion* 54 (2012) 105019 (9pp) doi:10.1088/0741-3335/54/10/105019
- [Dec11] Decker J. et al, *Nucl. Fusion* 51 073025 (2011)
- [Del14] L. Delpech et al *Nucl. Fusion* 54 (2014) 103004 (12pp)
- [Dum13] R.J. Dumont and D. Zarzoso, *Nucl. Fusion* 53, 013002 (2013)
- [Dum14] R.J. Dumont et al., *Plasma Phys. Control. Fusion* 56 (2014) 075020
- [Dux03] R. Dux et al *Plasma Phys. Control. Fusion* 45 (2003) 1815–1825
- [Dux09] R. Dux et al *Journal of Nuclear Materials* 390–391 (2009) 858–863
- [Eic11] T. Eich et al, *PRL* 107, 215001 (2011)
- [Eke09] A Ekedahl et al 2009 *Plasma Phys. Control. Fusion* 51 044001
- [Eke10] A. Ekedahl et al, *Nucl. Fusion* 50 (2010) 112002 (5pp)
- [Eri01] L.-G. Eriksson et al 2001 *Nucl. Fusion* 41 91 doi:10.1088/0029-5515/41/1/307
- [Fir14] M. Firdaouss, et al, to be published in the SOFT2014 proceedings
- [Goh11] P. Gohil et al *Nucl. Fusion* 51 (2011) 103020 (9pp)
- [Gon13] M. Goniche, et al., *Nucl. Fusion* 53 (2013) 033010, <http://iopscience.iop.org/0029-5515/53/3/033010>
- [Gon14] M. Goniche et al., *Phys. Plasmas* 21, 061515 (2014) <http://dx.doi.org/10.1063/1.4884357>
- [Gui11] D. Guilhem et al., *FED* 86 (2011) 279–287
- [Guz15]. F. Guzman-Fulgencio et al., *J. Nucl. Mater. cmat.2014.08.062* (2015)
- [Her02] A. Herrmann, *Plasma Phys. Control. Fusion* 44 (2002), 883-903
- [Hoa03] G.T. Hoang et al *PRL* 90 (2003)
- [Hoa09] G.T. Hoang et al 2009 *Nucl. Fusion* 49 075001
- [Huy07] Huysmans G.T.A. *Nucl. Fusion* 47 659 (2007)
- [Huy09] Huysmans G et al *Plasma Phys. Control. Fusion* 51 (2009) 124012
- [ITE99] ITER Physics *Nucl. Fusion* 39 2175 (1999)
- [Iva13] I. Ivanova-Stanik et al., IAEA technical meeting on Steady State Operation, Aix-en-Provence, 14-17 May, 2013.
- [Jac14] J Jacquot, et al *Phys. Plasmas* **21**, 061509 (2014)
- [Kal05] A. Kallenbach et al *Journal of Nuclear Materials* 337–339 (2005) 381–385
- [Kal11] A. Kallenbach et al *Nucl. Fusion* **51** (2011) 094012 (11pp) doi:10.1088/0029-5515/51/9/094012
- [Kub13] M. Kubic et al *Journal of Nuclear Materials* 438 (2013) S509–S512
- [Ler14] E. Lerche et al, Proc. 25th IAEA Fusion Energy Conf., St Petersburg (2014), Paper EX/P5-22
- [Liu12] Z X Liu et al 2012 *Plasma Phys. Control. Fusion* 54 085005 doi:10.1088/0741-3335/54/8/085005
- [Loa03] Loarte A et al, PPCF 2003

- [Mag14] C.F. Maggi et al EPS, Berlin, 2014
- [Mah03] Mahdavi et al. Phys. Plasmas, Vol. 10, No. 10, (2003)
- [Mar08] Y.R. Martin et al. Journal of Physics: Conference Series 123 (2008) 012033
- [Mar11] Y. Marandet et al., Nucl. Fusion 51 083035 (2011).
- [Mar14] Y. Marandet et al., Contrib. Plasma Phys. 54, No. 4-6, 353 – 357 (2014).
- [Mar15] Y. Marandet et al., J. Nucl. Mater. <http://dx.doi.org/10.1016/j.jnucmat.2014.11.030>
- [May14] M-L Mayoral et al Nucl. Fusion 54 (2014) 033002
- [Mcd07] D C McDonald et al, Nucl. Fusion 47 (2007) 147–174
- [Mek12] A. Mekkaoui et al., Phys. Plasma 19 122310 (2012).
- [Mey13] O. Meyer, et al, 40th EPS Conference on Plasma Physics, Espoo, Finland, (2013)
- [Min97] E.J. Minardi et al. Plasma Physics (1997), vol. 57, part 2, p. 449
- [Mis14] M. Missirlian, J. Bucalossi, Y. Corre et al Fusion Engineering and Design 89 (2014) 1048–1053
- [Neu11] R. Neu et al 2011 Plasma Phys. Control. Fusion **53** 124040 [doi:10.1088/0741-3335/53/12/124040](https://doi.org/10.1088/0741-3335/53/12/124040)
- [Par11] A. Paredes et al., J. Nucl. Mater. 415, S579 (2011)
- [Pey08] Peysson, Y. and Decker, J., Phys. Plasmas, 15, 092509 (2008)
- [Put10] Pütterich T et al Nucl. Fusion 50 (2010) 025012
- [Rei05] D. Reiter, M. Baelmans and P. Boerner, Fusion Science and Technology 47,172 (2005)
- [Rit13] G. Ritz et al, Fusion Engineering and Design. 88 (2013) 899-902
- [Sch05] M. Schneider et al, Plasma Phys. Control. Fusion 47 (2005) 2087–2106
- [Sta07] G. Staebler et al Phys. Plasmas 14, 055909 (2007)
- [Stan] [Stangeby, Peter](#) The Plasma Boundary of Magnetic Fusion Devices. Series: Series in Plasma Physics, ISBN: 978-0-7503-0559-4. Taylor & Francis, Edited by Peter Stangeby, vol. 7
- [Tak04] T. Takizuka et al. Plasma Phys. Control. Fusion 46 (2004) A227–A233
- [Tob95] Tobita K et al Nucl. Fusion, Vo1.35. No.12 (1995)
- [Tuc09] A.A. Tuccillo et al 2009 Nucl. Fusion 49 104013
- [Vul08] K. Vulliez et al., NF 48 (2008) 065007
- [Wal10] G. M. Wallace et al Phys. Plasmas 17, 082508 (2010); <http://dx.doi.org/10.1063/1.3465662>
- [Wei05] Weisen et al. Nucl. Fusion 45 (2005) L1
- [Wuk09] Wukitch S.J. et al 2009 J. Nucl. Mater. 390–391 951
- [Wuk13] S Wukitch et al. Phys. Plasmas 20, 056117 (2013)
- [WWS14] <http://west.cea.fr/Workshop2014/>
- [Zag09] R. Zagórski et al., J. Nucl. Mater. 390, 404 (2009).
- [Zag12] R. Zagórski et al., Contrib. Plasma Phys. 52, 379 (2012).
- [Zar11] Zarzozo D et al, Nuclear Fusion 2011

# Annex 9 : theory and modelling

---

Theory and modeling activities need to cover the broad range of expertise that is required for an efficient use of the WEST results. This will be achieved thanks to the strong collaborative network that is in place around the IRFM, both in France through the French Fédération Fusion par Confinement Magnétique - ITER (FR-FCM, <http://www.fr-fcm.fr/>), as well as at the European and International levels. We describe here the tools that we intend to use at this preliminary stage. A broader range is expected to be available as international collaborations will grow up.

The relevant activities, although connected at several levels, can be grouped into the following issues

- the Tungsten cycle, from its erosion at the PFCs to the core contamination and exhaust;
- the transport and L-H transition issue;
- the scenario development, with the issues of Heating and Current Drive (including the induced fast particle losses), and the fuelling;
- the MHD related issues, that covers the stability of the pedestal, its relaxation into Edge Localized Modes (ELMs), and the core stability;
- the disruptions and the runaway electron issue.

## I. The Tungsten cycle

The modeling of the Tungsten issue is extremely complex because of the number of factors that enters into its erosion, transport and exhaust, all being nonlinearly coupled with the actual Tungsten distribution. This complexity can be somewhat reduced at the price of using adjustable heuristic models, or by isolating specific problems. In the first case, a global self-consistent description of the Tungsten cycle can be made with 1D models, and arbitrary coefficients adjusted by simple rules or fits with experimental measurements. In the second case, more “first-principle” results obtained from partial problems can be used in a non-consistent manner as inputs for other issues. Both approaches are needed, the simplified one for understanding the main trends and design plasma scenarios, while the more elaborated one will provide a deep understanding of the most important issue and participate in the scientific outcome of the experimental exploitation.

### 1. Global simplified approaches

The fusion community in Europe uses the COREDIV code [Zagorski2008] that solves the 1D transport problem of impurity transport in the plasma core, and relies on a 2D module for the edge part. COREDIV yields : radiative losses, erosion and screening. This code, after adjusting free parameters, proved to give sound results on metallic devices such as AUG [Zagorski2012] and JET [Zagorski2009]. Simulations for WEST scenarios have already been performed (see annex 8) [Marandet2013]. Another simpler code, METIS [Artaud2010], was

developed at IRFM for scenario modeling, and it includes several extensions that make it able to simulate diverted plasmas with tungsten impurities. This code is being tested on JET discharges for validation.

## 2. SOL / Edge physics at prescribed transport coefficients

The level above the global simplified approach covers codes that provide edge profiles consistent with the neutral and impurity fluxes that they generate. In contrast, these codes require both a long and deep expertise for being used properly, as well as long computation time for providing the expected results. A package of codes, named SOLPS, has been used for this purpose in order to provide inputs for ITER [Kukushkin2009]. This package contains a fluid code (B2 or B2.5) with prescribed diffusion coefficients that solves the dynamics of density, parallel momentum and temperature, while the kinetic Monte Carlo code EIRENE [Reiter2005] calculates the sources related to neutral species. Several versions exist, the one being maintained in the FR-FCM is SOLPS5.X. The SOLEDGE-2D code [Bufferand2013] solves a similar problem as B2, but it benefits from a more recent numerical implementation. Its main originality in terms of physics is that it solves the equations for the plasma up to the first wall, using the so-called penalization technique [Isoardi2010]. It has been successfully coupled to EIRENE in 2012/2013. Moreover SOLEDGE2D can also solve transport equations for the entire core region with the perspective of integrating further nonlinear interactions (for example with the coupling to externally computed heat sources). An example is shown in Figure 80 for the neutral pressure in WEST.

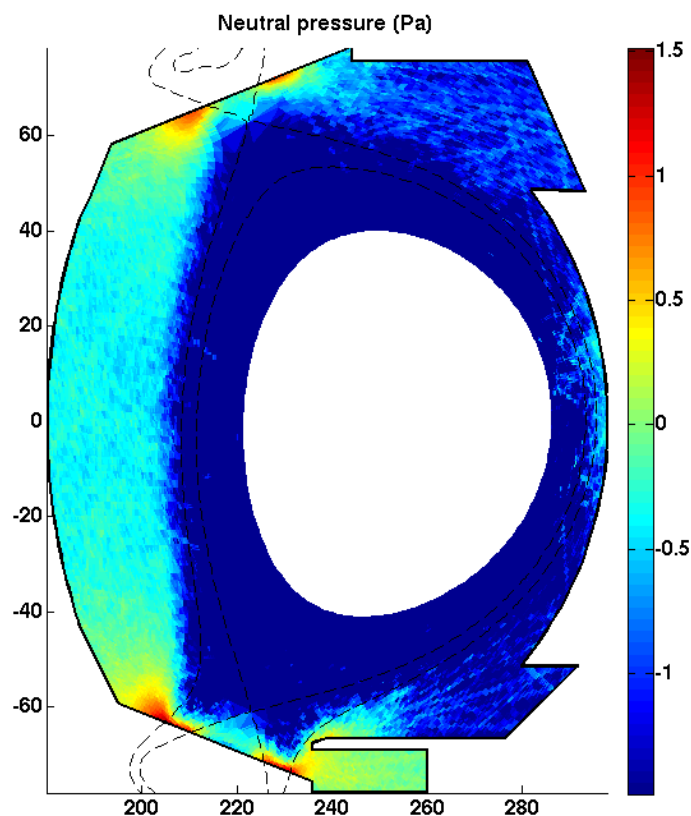


Figure 80: Neutral pressure in WEST for a discharge heated by 8 MW and a gas puff of  $8 \times 10^{20}$  particles/s in the private region (SOLEDGE-2D simulation, log scale).



As far as the wall response is concerned, we have at our disposal several numerical tools. First, the exact 3D distribution of the heat flux on the wall components is not computed in SOLEDGE or TOKAM [Tamain2013] codes, which assume a 2D axisymmetric wall. This 3D distribution can however be computed by using the output of these codes in the PFCFLUX tool [Firdaouss2013]. This code, based on an engineering approach with a realistic 3D geometry for the plasma facing components but a simplified plasma model, has been widely used in Tore Supra and JET. Then, local tungsten erosion and re-deposition can be computed with the ERO code [Kirschner2000]. A fit of ERO result is used in METIS as redeposition model for tungsten. Although a version of ERO has been recently adapted and successfully used in the Tore Supra configuration, the expertise for this code will need to be developed through collaboration with the Juelich laboratory, where it is maintained and developed. Finally, to address the global tungsten transport, it is planned to use the DIVIMP code [Stangeby1995], where tungsten is followed as a trace impurity in a plasma background defined by the output from the plasma edge code packages (such as SOLPS. The coupling of DIVIMP to a SOLEDGE2D background, in order to have a plasma defined up to the walls, is also planned).

The particle implantation and release from the tungsten wall is being addressed through collaboration between several laboratories in the FR-FCM (WHISKI project).

### **3. Synthetic diagnostics for interpreting W related data**

The survey of tungsten and plasma edge characterization will be achieved with dedicated diagnostics (spectroscopy, Langmuir probes ...). The interpretation of these measurements is often not directly connected with the information given by numerical tools. Therefore, an effort is being made in developing synthetic diagnostics. This is the objective of the ANR project (granted by the French Agence Nationale de la Recherche) SEDIBA as far as the SOL measurements are concerned. Synthetic diagnostics are also developed for Langmuir probes [Colin 2014]. A photonic code, SPEOS (developed by the OPTIS company), has proved useful also for reconstructing the origin of the light captured by a given optical component, and provide the correct interpretation of a signal that, especially in a metallic environment, can contain a large part of reflected light [Aumenier2012]. The diagnostic coverage of the discharge can also be synthesized using the PINup environment [Martin2012], where the diverse information can be mapped onto its respective plasma facing components. This tool has been used on Tore Supra, JET and is being installed on EAST in China.

### **4. Nonlinear edge transport models**

At this level, one would like to determine the self-consistent particle and energy transport going to the plasma facing component by computing the turbulent transport dynamics. This level of sophistication is required because not only the losses going into the SOL and later on the walls are to a large extent unknown, but also their poloidal distribution and their radial profile, which will impact the spatial distribution of heat and particle fluxes onto the wall. Having in mind that these will determine the level of Tungsten erosion, it appears that a detailed understanding of the tungsten cycle requires this level of description.

To this end, we dispose of the turbulent electrostatic code TOKAM-3X [Tamain2013], developed by IRFM with the FR-FCM community. This is a fluid code adapted to an X-point configuration that has the potential to be coupled to EIRENE in the same way as SOLEDGE-2D. This code provides the relevant self-consistent density and temperature profiles in the SOL, with the 2D equilibrium flows, as well as heat and particle transport up to the plasma facing materials.

#### Core W transport modelling

More inside the plasma, kinetic effects become important players in the regulation of heat and particle transport, and other codes provide a more advanced computation of heat, particle and impurity transport. First, the Qualikiz code [Bourdelle2007] provides a Quasi-linear estimate of transport coefficients for several plasma species. Being quasi-linear and therefore relatively fast in terms of computer time, it allows a coupling with global scenario simulations, as done in CRONOS. This code has been benchmarked with nonlinear codes and has proved to give sound results. The extension of Qualikiz to multiple ion species and charge states is planned in 2014. Moreover, CRONOS-ITM is being coupled to an impurity transport solver (in fact, this is the core solver of the COREDIV package) and a first verification of the coupling was done in 2013. The 2D neoclassical transport code, essential for poloidal asymmetries modeling is planned to be coupled to CRONOS. These developments, when completed, will provide a full package for integrated transport modeling of tungsten in the plasma core.

Then an intermediate complexity is reached by using local gyrokinetic codes such as GWK [Peeters2009], together with 2D neoclassical transport with NEO [Belli2008]. Such analyses are carried out on JET and AUG. We have the local expertise to do similar work on WEST plasmas using either GWK or GENE [Jenko2000].

Finally, the self-consistent interplay between turbulent and neoclassical transport in a flux driven system will be studied thanks to a 5D gyro kinetic approach allows going further by computing the nonlinear heat fluxes for arbitrary sources. The GYSELA code [Grandgirard2006], developed at IRFM, covers the transport of two ion species, and is expected to describe as well electron transport in the coming years. It is able to compute the turbulent and neoclassic heat and particle flux in presence of an impurity ion, and the self-consistent back reaction of this impurity on the transport of the main species. The implementation of synthetic diagnostics allows validating the results of these simulations. In particular, the density fluctuations can be used to compute the signal seen by reflectometry diagnostics.

The codes that have been described here will provide information about the steady state transport of both the main species and tungsten in the WEST plasma. This will allow an understanding of impurity accumulation in the plasma core, which is a crucial issue in metallic wall devices, and provide inputs for modeling the wall response. The control of tungsten erosion and accumulation can also be modeled. Indeed, the injection of specific impurities that radiates in the SOL can decrease the heat flux impacting the tungsten components and reduce their erosion. Soledge2D-EIRENE will be used to model this control tool, when turned into a multifluid solver. Tungsten itself does not alter SOL conditions very much [Marandet2013], and will be handled by the impurity transport code DIVIMP [Stangeby1995] on SolEdge2D-EIRENE backgrounds.

Also, impurity accumulation is known to be sensitive to the ratio of electron to ion heating: the nature of micro turbulence changes from Ion Temperature Gradient (ITG) to Trapped

Electron Mode (TEM) as electron temperature rises and the impurity flux is then directed outward. This effect can be modeled by Qualikiz. The GYSELA code can address impurity neoclassical and turbulent transport for ITG turbulence, i.e. the competition between neoclassical accumulation and turbulent diffusion (Figure 81).

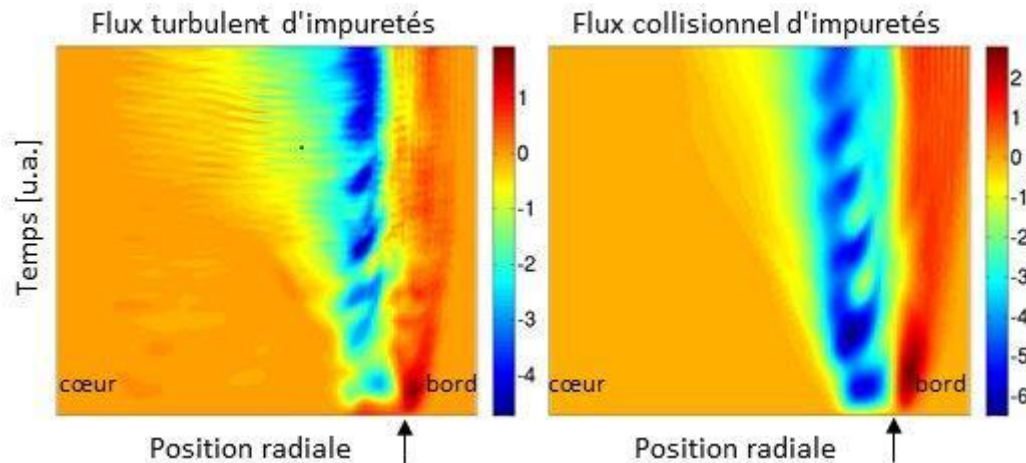


Figure 81: Turbulent (left) and collisional (right) impurity fluxes, showing a predominant inward (blue) contaminating trend (GYSELA simulation).

Apart from the steady state turbulent transport, several other sources should be considered as impacting the wall: transient MHD events, RF sheaths, and fast particle losses from the plasma core.

- The description of transient MHD related events is also an important issue. At the plasma edge, Edge Localized Modes (ELMs) are expected to impose severe constraint on transient power fluxes hitting the wall. This will be discussed in the section relative to MHD issues. In the core plasma, magnetic reconnection is well known for mitigating impurity accumulation, but as well for sometimes accelerating the tungsten transport towards the core, as observed (but not explained so far) in JET. This aspect will be studied with the XTOR code [Lütjens2010], which has already shown a good agreement with experimental observations for the internal kink mode activity when the current profile is monotonic (typically when LHCD is off) in Tore Supra [Nicolas2012]. The sensitivity to magnetic islands may also be an issue in the WEST experiments, and the control of these instabilities with a localized source (ECCD) will be modelled.
- RF sheaths potentials are generated by the RF electric field parallel to the static magnetic field generated in the vicinity of ICRH antennas. It is known that the reduction of such sheath is essential to reduce the W production. Similar phenomenology can also appear away from wave launchers due to unabsorbed RF power. Enhanced sheaths can accelerate ions along magnetic field lines that will hit the wall and produce localized heating. This phenomenon can be mitigated by acting on the phasing of the radiating elements (strap) for improving the single pass absorption, or by an increase of the plasma density. This will be modeled with the SSWICH code [Jacquot2013]. In its present simple version, SSWICH was compared

with Tore Supra measurements and could reproduce qualitatively some experimental observations: the relative behavior of two types of antennas, the poloidal distribution of plasma potential enhancement and the related convective cells in the SOL. Quantitative results were shown sensitive to loosely constrained simulation parameters. Developments are foreseen to improve the physics model.

- Fast particles originate from the coupling of RF waves to the plasma and when impacting the wall can increase the W sputtering. Lower Hybrid waves accelerate electrons for driving parallel plasma current, while ICRH accelerate minority ions. The fast electron losses will be computed using the LUKE code, and the fast ion losses will be computed using the coupling of the EVE code [Dumont2009] with the Monte Carlo SPOT code [Schneider2005].

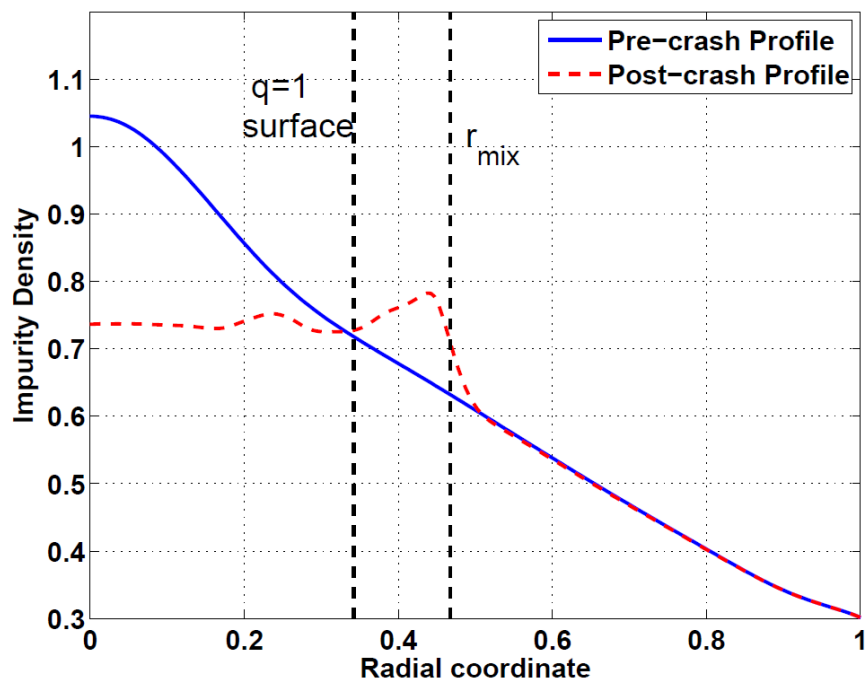


Figure 82 : Impurity redistribution by a sawtooth crash as modeled with XTOR.

## II. Transport and L-H transition

In addition to the specific issue of tungsten contamination, transport physics is investigated for the understanding of the confinement scaling and anomalous transport mechanisms. Related to this issue, the transition from a low to a high confinement regime at the plasma edge, known as the L-H transition, is particularly important and still not fully understood. This transition allows an increase of the energy confinement time of about a factor 2. At present, several reduced models have been derived that recover characteristic features of this transition, and could give some clues about the triggering mechanism and its relation with the size of the improved confinement region. A simplified turbulent fluid code, EMEDGE-3D [Beyer2005], developed at the PIIM laboratory (Aix-Marseille University AMU, partner of the

FR-FCM) recovers a confinement reduction triggered above a threshold in the input heat flux, as observed experimentally.

We are therefore at a stage where ab-initio models could be tested for a comprehensive description of the L-H transition. The main tools that we are using for investigating this issue are the fluid TOKAM-3X code [Tamain2013], which covers both the confined region and the SOL, including the X-point, and the gyro-kinetic code GYSELA [Strugarek2013] which only covers the confined plasma. Depending on the role of the SOL in the L-H transition triggering, one of the two codes may give a better agreement with experimental findings. On this issue as well, the comparison of code results with experimental measurements will guide the progress of our understanding: equilibrium flows and fluctuations are two examples of the possible characterizations of the plasma in this transition regime.

Electrons are currently being implemented in the GYSELA code in order to address particle and impurity transport situations where Ion Temperature Gradient (ITG) and Trapped Electron Modes (TEM) are involved.

### III. Scenario development

The WEST scenario preparation is being performed with the 0D METIS code, and more detailed simulations use the 1D CRONOS suite [Artaud2010]. While the 0D code uses simple laws for the power and current drive sources, the 1D CRONOS suite is coupled to specific codes for LH, ICRH and ECRH sources. The ITM integrated modeling tool, ETS (European Transport Solver), which is equivalent to CRONOS but is developed in a European framework, has not reached at the moment the same level of integration, in particular for heat and current drive sources. Nonetheless it starts to implement new functionalities with respect to the original Matlab version, such as an impurity transport solver.

A particular attention is being paid to the coupling of RF sources to the plasma. For LH, we use the linear coupling code ALOHA code [Hillairet2010], while non-linear effects on the LH wave coupling (ponderomotive force) has been investigated in the PICCOLO-2D code which incorporates non-linear couplings [Preynas2013]. The generation of fast electrons in the SOL, which has been evidenced by probe measurements [Gunn2009] and infrared measurements [Goniche1998, Ritz2013] on Tore Supra, will be further investigated by modeling using the tools developed in [Fuchs2003]. The LH Current Drive and heat deposition is computed using the C3PO/LUKE codes [Peysson2012] which has been improved to take into account regimes at high plasma densities. This module also computed the electron ripple losses [Ju2002]. The comparison with experimental measurements is possible thanks to the Hard X-ray tomography, and a synthetic diagnostic (R5X2 [Peysson2008]) is integrated to the code for providing this information. A particular attention must be put on the LH absorption modeling in the WEST magnetic configuration, since the increase of the aspect ratio will lead to a larger spectral gap [Nilsson2013]. For the ICRH source, the coupling to the plasma is computed with the TOPICA code [Milanesio2010], provided by the Politecnico di Torino. The amplitude of the RF driven sheath can be computed with the SSWICH code. The heat and current drive source is computed either with PION [Eriksson1993], which is coupled to the CRONOS suite, or EVE [Dumont2009], which

is run independently. Fast ion losses are not yet modeled properly, and to this purpose, a coupling between EVE and SPOT [Schneider2005] is in progress.

The ECRH source can be computed with either the REMA code [Krivenski1985] or the C3PO/LUKE code [Peysson2012].

Finally, particle sources can be computed for gas puff by the SOLEDGE-EIRENE coupling, and by HPI2 for pellet injection [Pégourié2005, Pégourié2007]. HPI2 is coupled to CRONOS.

#### **IV. Magneto-Hydro-Dynamics issues**

The Magneto-Hydro-Dynamic (MHD) stability of tokamak plasmas sets not only the performance limitations but it can also degrade the energy confinement and trigger a disruption. Performance limitations are understood here as the boundary of the operational domain, described by the ideal MHD model, where the growth rate of instabilities is too fast to allow any control. The energy confinement degradation by MHD modes is in contrast produced by resistive instabilities, with a relatively slow growth rate that allows a control on their dynamics.

Ideal MHD instabilities are limiting the height of the H-mode pedestal, and their non-linear development results in Edge Localized Modes (ELMs). The characterization of the pedestal stability is computed using the linear code MISHKA [Mikhailovskii1997], and this procedure allows deriving the maximum pedestal temperature for a given density [Maget2013]. The MHD limit is here a useful input for setting the boundary condition for the integrated modeling of the core plasma. In this respect, the quality of the confinement (measured by the H factor [ITER1999]), is strongly dependent on the pedestal stability, as well as the RF coupling, pellet fuelling and the SOL properties. The non-linear evolution of the mode is addressed with the JOREK code [Huysmans2007], which has been regularly used for comparison with experimental findings. The code describes both the confined plasma and the open field lines up to the plasma facing components. This provides information about the heat and particle fluxes to the plasma facing components, which is required for evaluating the material erosion. The triggering of ELMs by pellets can also be addressed with the JOREK code.

In the plasma core, the expected MHD limits are mainly of resistive nature. Global ideal MHD modes are not expected to be a problem in WEST, since the plasma performance in terms of normalized beta remains moderate. The hollow current profile achieved with LHCD represents however an unfavorable configuration for MHD modes, as experienced with Tore Supra when developing the non-inductive scenarios [Zabiégo1999]. Also, the sawtooth instability will play an essential role in the flushing of core impurities. The modeling of these instabilities will be addressed with the XTOR-2F code [Lütjens2010], which covers essential ingredients like diamagnetic rotations [Halpern2011, Meshcheriakov2012] or neoclassical physics [Mellet2013]. The fast particle transport by MHD modes will also be important to study, because of ICRH heating that produces a significant population of energetic particles. This will be studied with the coupling of XTOR with a kinetic module (Particle In Cell), achieved during the ANR ANIKA (ANR-09-BLAN-0044-01). The on-going implementation of a localized current source term in the code will allow modeling the effect of ECCD that could be used for the control of both the sawtooth period and magnetic islands.

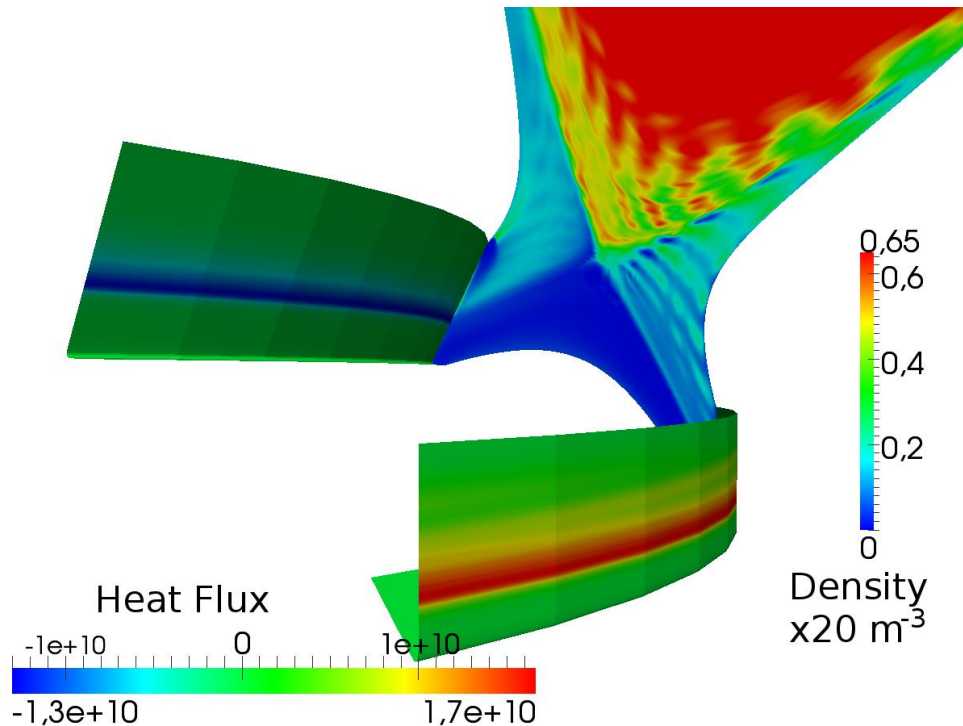


Figure 83 : Density contours and heat flux on divertor plates modelled with JOEAK (ITER case shown here) .

Instabilities driven by energetic electrons (like the ones produced by LH) can be studied with the MIKE code [Merle2012] in their linear regime. If these instabilities were to have a deleterious impact on the operation of WEST, the non-linear MHD code XHMGC developed by our colleagues from ENEA [Vlad2013] would help in interpreting experimental observations and propose solutions for improving the scenario design.

## V. Disruptions and Runaway electrons

Heat loads and mechanical forces induced by disruptions are high enough to require mitigation techniques. The main instrument that produces an efficient reduction of the peak heat flux is Massive Gas Injection (MGI), a method that triggers as well large MHD modes during the thermal quench. The modeling of the thermal quench requires the coupling of an MHD code with atomic data. This implementation is being done in the JOEAK code [Huysmans2007] extended with atomic physics [Reux2011], and the validation is performed on JET experiments.

During the disruption, the large electric field sometimes accelerates electrons at velocities where they are no longer experiencing significant collisions: these are the runaway electrons that circulate at velocities approaching that of light, and can damage the plasma wall when hitting it. By coupling the CRONOS/METIS codes with LUKE which can describe time evolution of the primary and secondary (avalanches) runaway electron generation, it is possible to model this issue, in collaboration with Chalmers University in Sweden who developed several years ago the Monte-Carlo code ARENA for this purpose [Eriksson2003]. The aim is to better understand the generation of runaways, and to make comparison with

experiments. This code could be later coupled to JOEKE for studying the interplay between MHD and the distribution of runaway electrons.

**References of annex 9 :**

- [Artaud2010] J.-F. Artaud et al, Nucl. Fusion 50 043001 (2010)
- [Aumeunier2012] M.-H. Aumeunier , et al., Rev. Sci. Instruments 83, 10D522 (2012)
- [Belli2008] E. A. Belli and J. Candy, Plasma Phys. Controlled Fusion 50, 095010 (2008)
- [Beyer2005] P. Beyer et al, Phys. Rev. Letters 94, 105001 (2005)
- [Bourdelle2007] C. Bourdelle, et al Physics Plasmas 14 :112501 (2007).
- [Bufferand2013] H. Bufferand et al., J. Nucl. Mat. 438, S445 (2013)
- [Colas2012] Colas L., Jacquot J. et al., Physics of Plasma 19 (9): 092505 (2012)
- [Colin2014] C Colin et al, Contrib. Plasma Phys., to appear
- [Dumont2009] R. J. Dumont, Nucl. Fusion 49, 075033 (2009).
- [Eriksson1993] L.-G. Eriksson et al, Nucl Fusion 33 1037 (1993)
- [Eriksson2003] L. -G. Eriksson and P. Helander, Comp. Phys. Comm. 154: 175 (2003)
- [Firdaouss2013] M. Firdaouss et al, Journal of Nuclear Materials, 438, S536 (2013)
- [Fuchs2003] V Fuchs et al., Nucl. Fusion 43:341 (2003)
- [Goniche1998] M Goniche et al., Nucl. Fusion 38: 919 (1998)
- [Grandgirard2006] V. Grandgirard, et al Journal of Computational Physics 217: 395 (2006)
- [Gunn2009] J Gunn et al., J. Nuc. Mat. 390-391 904 (2009)
- [Halpern2011] F. Halpern et al, Plasma Physics and Controlled Fusion 53, 015011 (2011)
- [Hillairet2010] J Hillairet et al., Nucl. Fusion 50 125010 (2010)
- [Huysmans2007] Huysmans G.T.A. Nucl. Fusion 47 659 (2007)
- [Isoardi2010] L Isoardi, J Comp Phys., **229**, 2220–2235 (2010).
- [ITER1999] ITER Physics Expert Group on Confinement, Transport, ITER Physics Expert Group on Confinement Modelling, Database, and ITER Physics Basis Editors Chapter 2: Plasma confinement and transport Nucl. Fusion 39 2175 (1999)
- [Jacquot2013] J Jacquot et al Plasma Phys. Control. Fusion 55 115004 (2013)
- [Jenko2000] F. Jenko et al Phys. Plasmas 7 1904 (2000)



- [Ju2002] M. Ju et al., Phys. Plasmas 9 (11) :4615 (2002)
- [Kirschner2000] Kirschner A. et al., Nucl. Fus., 40 989 (2000)
- [Krivenski1985] Krivenski V. et al Nuclear Fusion, 25(2): 127 (1985)
- [Kukushkin2009] A. Kukushkin et al., Nucl. Fusion 49, 075008 (2009)
- [Lütjens2010] Lütjens H. et al, Journal of Computational Physics, 229(21) :8130 (2010).
- [Maget2013] Maget P. et al, Nuclear Fusion 53 093011 (2013)
- [Marandet2013] Marandet Y. et al, submitted to Contributions to Plasma Physics (2013)
- [Martin2012] Martin V. et al, IEEE Transactions on Plasma Science, 40(3), 646 2012
- [Mellet2013] Mellet N. et al, Nuclear Fusion, 53(4) :043022, (2013)
- [Meshcheriakov2012] Meshcheriakov D. et al, Physics of Plasmas, 19(9) :092509, (2012)
- [Merle2012] Merle A. et al, Phys. Plasmas 19, 072504 (2012)
- [Mikhailovskii1997] Mikhailovskii A.B. et al., Plasma Phys. Rep. 23 844–57 (1997)
- [Milanesio2010] D. Milanesio and R. Maggiora Nucl. Fusion 50 025007 (2010)
- [Nicolas2012] Nicolas T. et al, Phys. Plasmas 19, 112305 (2012)
- [Nilsson2013] E. Nilsson, et al. Nucl. Fusion 53 :083018 (2013)
- [Pégourié2005] B. Pégourié et al, Plasma Phys. and Contr. Fus. 47 17 (2005)
- [Pégourié2007] B. Pégourié et al Nucl. Fusion 47 44 (2007)
- [Peeters2009] Peeters A. et al, Computer Physics Communications 180, 2650 (2009)
- [Peysson2008] Peysson, Y. and Decker, J., Phys. Plasmas, 15(9) :092509 (2008)
- [Peysson2012] Y. Peysson et al., Plasma Phys. Control. Fusion 54 045003 (2012)
- [Preynas2013] M Preynas et al., Nucl. Fusion 53 013012 (2013)
- [Reiter2005] D. Reiter et al. , Fusion Sci. Technol. 47, 172 (2005)
- [Reux2011] C. Reux et al., 38th EPS Conference on Plasma Physics, page O3.117 (2011)
- [Ritz2013] G Ritz et al., Fusion Eng. Des. (2013), article in press
- [Schneider2005] M. Schneider et al, Plasma Phys. Control. Fusion 47 2087 (2005)
- [Stangeby1995] Stangeby P C and Elder J D Nucl. Fusion 35 1391(1995)
- [Strugarek2013] A. Strugarek, et al Phys. Rev. Lett. 111, 145001 (2013)
- [Tamain2013] P. Tamain et al., submitted to Contrib Plasma Phys (2013)
- [Vlad2013] Vlad et al, Nucl. Fusion 53 083008 (2013)

[Zabiégo1999] Zabiégo M. et al, Plasma Phys. Control. Fusion 41 B129 (1999)

[Zagòrski2008] Zagòrski R. et al, Contrib. Plasma Phys. 48, 179 (2008).

[Zagòrski2009] Zagòrski R. et al, J. Nucl. Mater. 241-243, 914 (2009).

[Zagorski2010] R. Zagorski et al. C. Plasma Phys. 50, 306 (2010)

# Annex 10 : risk assessment for the WEST programme

---

## W3. I - Methodology

The same criteria used for the risk quantification of the WEST project were applied, with minor adaptation. They are summarized in the tables below. In particular, the definition of occurrence is the same (Table 15) while for the severity, the impact on the programme objectives and the operation schedule have been considered (Table 17). The resulting criticality (Table 17) is identical.

Level	Definition	Scaling
1	Negligible	< 5 %
2	Very unlikely	5 - 10 %
3	Unlikely	10 - 30%
4	Likely	30 - 70 %
5	Very likely	> 70 %

Table 15 : definition of occurrence

Level	Definition	Impact operation schedule	Impact on programme objectives
1	Negligible	< 2 days	< 5%
2	Marginal	Between 2 days -1 week	Between 5 & 10%
3	Significant	Between 1-2 weeks	Between 10 & 20%
4	Major	Between 2-4 weeks	Between 30 & 20%
5	Critical	> 1 month	> 30%

Table 16: definition of severity impact

Severity	5					
	4					
	3					
	2					
	1					
		1	2	3	4	5
<b>OCCURRENCE</b>						

Table 17 : definition of criticality

The main assumptions are summarized below :

- All the components of the WEST baseline are delivered on time, and are working according to specifications.

#### W4. II - Main risks identified for the WEST programme

The main top 15 risks identified for the WEST programme are shortly described below. The impact on the programme and/or the operation schedule is discussed. When applicable, the impact on separate headlines of the programme is mentioned (see list below). Finally, possible mitigation measures are proposed. It should be noted that although further simulations are given here as mitigation measures, it should rather be considered as a way to refine the risk quantification. Results are summarized in Table 18.

It should be noted that there is some overlap between the programme and the project risk analysis, in particular in areas dealing with operation (for instance WP on integrated commissioning, Plasma Control System, Wall Monitoring System, diagnostics etc).

List of programme headlines :

- H1 :testing ITER PFCs
- H2 : towards long pulse H mode operation
- H3 : exploring plasma wall interactions at high fluence
- H4 : preparing advanced tokamak modes

##### 1) Difficult plasma breakdown

- Description : the constraints for plasma breakdown will be higher in the WEST configuration than it was in the CIEL configuration. Present estimates ok, but less margin than for CIEL.
- Impact : whole programme
- Mitigation : 1) refined simulations of plasma breakdown 2) maintain valve 3) use ECRH assisted breakdown. The latter has a strong impact on request on ECRH availability.

##### 2) H mode power threshold on the high side

- Description : the power needed to access H mode has been estimated for WEST conditions according to empirical scalings [note C. Bourdelle]. Present estimates ok compared to installed power, but large uncertainties on power threshold from scalings (role of metallic walls, large aspect ratio, ripple, pumping/recycling, high density ...).

- Impact : whole programme
- Mitigation : 1) pursue AUG experiments in WEST configuration 2) operation at lower Bt (but gain marginal) 3) implementation of ferritic inserts if the main cause is ripple

### 3) Difficult coupling of power at multi MW level

- Description : combined ICRH-LH coupling in H mode conditions is a challenge (metallic walls, ELMs resilience, operational conditions for combined LH-ICRH ...) and will require fine tuning to reach high power operation.
- Impact : whole programme if prevents access to H mode (see point 2), mainly high power scenario for H1 and H4 otherwise.
- Mitigation : 1) pursue AUG experiments in WEST configuration for ICRH 2) refined simulations of RF heating in WEST scenarios (such as high density accessibility for LH) 3) operational tools for coupling optimization (such as local gas injection with commensurate pumping) 4) establish what performance can be reached with one heating system only (in particular with 7 MW of LH alone, should the availability of ICRH be delayed).

### 4) Excessive Tungsten contamination

- Description : WEST will operate with in a full W environment (except the ICRH protection with boron coatings). Control of W contamination has been demonstrated in AUG and JET (through central heating and minimum fuelling/ELM frequency), but the operational window will have to be worked out for WEST conditions (with ICRH as main central heating tool, compact divertor etc).
- Impact : low density scenarios foreseen for H3 (long pulse) and H4 might be difficult to achieve.
- Mitigation : 1) pursue AUG experiments in WEST configuration and check W contamination control with ICRH only 2) additional central heating through ECRH (but available for 0.5 MW/0.5 s only at the moment) 3) boronisation

### 5) Excessive Carbon and/or Boron levels

- Description : WEST will use W coated PFC with a carbon substrate and boron coated guard limiters for heating systems. C and B are therefore expected to be present in the plasma, and could cause tungsten erosion (see risk 4) and play a role in PWI (fuel retention etc).
- Impact : excessive W erosion (see risk 4) and impact on fuel retention studies (H3).
- Mitigation : 1) thorough in vessel cleaning to remove remaining carbon from the CIEL phase 2) careful coverage of the C substrate with the coatings, use of interlayers to avoid C diffusion in the coatings 3) further assessment of B erosion and migration (experiments in AUG, simulations)

### 6) Lack of density control

- Description : lack of density control can limit pulse duration (cf pre-CIEL operation of Tore Supra). WEST will operate with a rather moderate pumping [ref note B. Pégourié] (but will retain the actively cooled vessel coverage to mitigate uncontrolled particle source).
- Impact : low density scenarios foreseen for H3 (long pulse) and H4 might be difficult to achieve. Transition from L to H mode might be difficult to control in terms of target density.

- Mitigation : 1) pursue AUG experiments in WEST configuration with poor pumping 2) install additional pumping (cryopump) if needed.

#### **7) Lack of impurity control**

- Description : lack of intrinsic impurity control other than W handled in point 4 and C/B handled in point 5 (such as oxygen etc) could be detrimental to overall plasma performance as well as cause an increased erosion of W. In addition, control of extrinsic impurities injected for high radiated fraction experiments is also needed.
- Impact : could delay operation if extended conditioning needed and/or impact programme if no other solution than boronisation is found. Highly radiating scenarios of H4 could also be impacted in case of problem with extrinsic impurities control.
- Mitigation : 1) extend conditioning of vacuum chamber 2) boronisation 3) install additional pumping (cryopump) if needed

#### **8) Inaccurate control of the magnetic configuration**

- Description : the magnetic configuration will be strongly modified with WEST. New features, such as control of the vertical instability, control of the X point/strike point position or control during ELMs perturbations, will be needed.
- Impact : whole programme if vertical instability not adequately controlled, mainly H2 and H3 if strike point position not controlled.
- Mitigation : 1) refined simulations of magnetic equilibria and control 2) margin on power supplies

#### **9) Insufficient disruption/runaways control and mitigation**

- Description : although the overall disruptions forces are similar for the CIEL and WEST configurations, the radiated fraction during disruptions with metallic walls is lower than with carbon walls, so that PFC heat loads are higher. In addition, the new WEST configuration can experience Vertical Displacement Events (VDE) with strong associated heat loads. Control and mitigation of disruptions/runaways should therefore be carefully assessed.
- Impact : significant delay in operation if PFC damage.
- Mitigation : 1) refined simulations of disruptions/runaways in WEST conditions and impact on PFCs 2) routine use of massive gas injection

#### **10) Excessive MHD**

- Description : the WEST configuration will exhibit new features in terms of MHD compared to CIEL (NTM ?). Excessive MHD could impact plasma performance and/or pulse duration, in particular for long pulse H mode operation at  $V_{loop} \sim 0$ .
- Impact : mainly H4 for scenario at  $V_{loop} \sim 0$  or high beta/high bootstrap.
- Mitigation : 1) refined simulations of MHD stability in WEST conditions 2) ECRH as control tool (would imply ECRH upgrade) ?

#### **11) ELMs too weak for PFC testing**

- Description : ELMs expected in WEST are benign compared to ITER, but should allow to test PFC power handling under a large number of sub threshold events. In particular, operation above the recrystallization temperature of W due to transients should be

explored. This is only possible if ELMs allow for a sufficient temperature excursion of the W PFC.

- Impact : mainly H2 and H3.
- Mitigation : 1) refined predictions of ELMs characteristics in WEST 2) development of large ELMs scenarios if needed

### **12) Excessive ripple losses**

- Description : the ripple in WEST will be significant. This implies ripple losses from RF heating, impacting PFC and restraining the operational domain.
- Impact : might limit ICRH power, for high power scenario (H4 mainly)
- Mitigation : 1) refined simulations of ripple losses under WEST conditions to assess operational domain 2) implementation of ferritic inserts if needed (see also point 2)

### **13) Available power not sufficient**

- Description : even if all available power is adequately coupled to the plasma (see point 3), it could not be sufficient to fulfill some of the objectives of the programme (for instance the extreme heat loads in H1, the current drive needed for long pulse operation in H3 or high beta/bootstrap in H4). This is unlikely from present estimates, but should be further investigated.
- Impact : H1 for the 20 MW/m<sup>2</sup> objective, H3 for the 1000 s objective, H4 for the high beta/bootstrap
- Mitigation : 1) refined simulations 2) upgrade of power if needed

### **14) Insufficient / non consistent diagnostic data**

- Description : WEST will be equipped with set of new diagnostics, as well as with previous CIEL updated diagnostics. The output of the scientific programme is closely related to the quality of the diagnostics data of the new system (see examples below). In particular, consistency of the available measurements should be checked in the new WEST configuration. In addition, it should be noted that the new wall protection system could limit performance or on the contrary fail to prevent PFC damage, if not properly calibrated.
- Impact : H1 if power balance/surface temperature not consistent, H2 if profiles measurements/turbulence measurements not consistent, H3 if particle loads not consistent, H4 if current profile not consistent etc ...
- Mitigation : 1) thorough calibration and validation, to be included in the integrated commissioning and operation schedule 2) diagnostics upgrades if needed

### **15) New Plasma Control System difficult to operate**

- Description : WEST includes the procurement of a new Plasma Control System (PCS), which will require fine tuning before being fully operational.
- Impact : delay in operation
- Mitigation : 1) refined simulations 2) keep previous control system operational as fall back solution

Finally, an additional risk could be insufficient expertise in key physics areas.

## Annex 10 : risk assessment for the WEST programme

- Description : WEST will open new physics area compared with CIEL (H mode physics, axisymmetric divertor physics, operation with metallic walls, tungsten melting experiments ...). This requires new competences from IRFM staff, currently being worked out.
- Impact : delay in operation, output from experiments not optimized
- Mitigation : 1) training of IRFM staff in relevant programmes (AUG, JET, EAST ...) and development of adequate analysis/modeling tools 2) strengthening of collaboration in key areas, in particular in EU



Annex 10 : risk assessment for the WEST programme

Table 18 : overview of the top 15 risks identified for the WEST programme

	Risk	Impact	Occ	Sev	Mitigation
1	Difficult plasma breakdown	WEST program	2	5	Refined simulations, valve, ECRH assisted breakdown
2	H mode power threshold on the high side	WEST prog. H1, H2, H4 mainly	2	5	AUG experiments, lower Bt, ferritic inserts if due to ripple
3	Difficult coupling of power at multi MW level	H1, H4 mainly	3	4	AUG experiments, refined simulations, tools for coupling optimization
4	Excessive W contamination (in particular with ICRH)	WEST program (H3, H4 at low density)	3	4	AUG experiments, ECRH for additional central heating, boronisation
5	Excessive Carbon / Boron level	WEST prog, H3	2	3	Vessel cleaning, careful C substrate coverage, AUG experiments + refined simulations of B impact
6	Lack of density control	WEST prog, H3, H4	2	3	AUG experiments, additional pumping (cryopump) if needed
7	Lack of impurity control	WEST prog	2	2	Extended conditioning, boronisation, additional pumping (cryopump) if needed
8	Inaccurate control of magnetic configuration	WEST program if vertical instability, H1 if strike points	2	3	Refined simulations, margin on power supplies
9	Unsuccessful disruption/runaway mitigation	Delay in operation for PFC damage	2	4	Refined simulations, routine use of massive gas injection
10	Excessive MHD	H4 mainly (Vloop = 0)	2	3	Refined simulations, ECRH

Annex 10 : risk assessment for the WEST programme

11	ELMs too weak	H1	3	1	Refined simulations
12	Excessive ripple losses	H1, H4 mainly	2	2	Refined simulations, ferritic insert
13	Not enough power	H1, H4 mainly	1	4	Refined simulations, power upgrade
14	Unsufficient / Non consistent diag data	Delay on WEST program	2	2	Calibration and validation, diag upgrade
15	Use of new PCS longer than planned	Delay in operation	2	2	Refined simulations, previous control system operational as fall back solution

# Annex 11 : Commissioning and power ramp up

---

The WEST platform is expected to be operational for plasma in 2016. Before the physics programme as defined in the headlines of the research plan can be started, an intermediate period will be dedicated to high level commissioning and ramping up the additional power available from the heating systems. The objective of this initial research phase will be to achieve robust H mode operation for duration > 5s.

This period is divided in 3 steps <sup>17</sup>:

- Commissioning : this first step goes from first plasma up to plasmas in divertor configuration with a moderate amount of RF heating (few hundreds of kW), to demonstrate the heating systems are running properly. Once this milestone is achieved, the WEST platform is considered as fully operational.
- Power increase in L mode : this step goes from the previous milestone up to L mode plasmas with a few MW of heating power, over several seconds of plasma operation. Combined LH and ICRH operation will be demonstrated.
- Achievement of H mode : this final step goes from L mode heated plasmas up to stable H mode operation over several seconds. The expected L-H threshold is in the range  $P_{sep} \sim 4-6$  MW (see **Table 5** in Chapter 2 and annex 8 for more details on the L-H threshold).

Although this commissioning phase is described separately here, it is expected to be interleaved with dedicated physics experiments (for instance SOL physics under Headline 1 in preparation for testing the ITER like tungsten divertor, or RF physics under Headline 2 in preparation of optimized coupling). It should be considered as the initial research phase for WEST. In particular, it will bring the first results on H mode operation in WEST, as well as on divertor characterization, levels of W plasma contamination or optimizing the RF power coupling.

## I. Step 1 : Commissioning the WEST platform

The aim of the commissioning phase is to produce reference plasmas in divertor configuration with a moderate amount of RF heating, which will allow for the subsequent exploitation of the WEST platform. The commissioning plan is presented below in chronological order.

---

<sup>17</sup> Durations have been assigned to the different steps in this chapter, but are highly tentative at this stage.

The commissioning will begin with individual tests of the subsystems, which will be especially important for new subsystems such as the divertor coils, the IR imaging system or the ICRH antennas. We will then proceed with a sequence of “integrated objectives” testing several systems together.

The first 3 weeks will be without plasma, with 2 main objectives:

- Machine conditioning, including vessel baking at 200°C and glow discharges
- Production of a new premagnetisation map, which will have been prepared in advance based on modeling with the CEDRES code

The next 8 weeks will be dedicated to Ohmic plasmas, with the following objectives and underlying validations:

- First sustained breakdown and first limiter configuration (~circular) plasmas at low  $I_p$ 
  - o Validation of the new Plasma Control System (PCS) and its basic functions (control of  $I_p$ , plasma position and shape,  $\langle n_e \rangle$ )
- First elongated plasmas in limiter configuration at low  $I_p$ 
  - o Validation of the vertical control system
- First X-point plasmas at low  $I_p$ 
  - o Validation of the capability of the PCS to produce an X-point configuration
  - o Verification of disruption loads before going to higher  $I_p$  and stored energy
- Longer duration (~10 s) X-point plasmas with high  $I_p$  (~800 kA) and  $\langle n_e \rangle$  suitable for RF heating
  - o Validation of basic operation and machine protection diagnostics: magnetics, interferometry, Wall Monitoring System (IR imaging, thermocouples, etc.), spectrometers, bolometry, etc.
  - o Validation of backup strategies to handle exceptions or events (full consumption of the available flux, overheating of PFCs, default of the poloidal field system, etc.)
  - o General validation of diagnostics
  - o Validation of real-time and off-line data processing
- Investigation of the operational domain

The scenarios used in the above phase will have been prepared in advance via modeling with the CEDRES, CRONOS and METIS codes. The control systems (especially for position and shape control) will also have been tested in simulation.

The last 3 weeks of commissioning will focus on L-mode plasmas with a small amount of RF heating (the LH couplers and ICRH antennas will have been conditioned in vacuum in parallel to the above program):

- Coupling of a few hundreds kW of LH power
  - o Validation of machine protection systems and strategies related to LH power: hot spots monitoring (IR/visible imaging), arc detection (IR/visible imaging and Cu monitoring using spectroscopy)
- Coupling of a few hundreds kW of ICRH power (including with ELM-like perturbations mimicked by Supersonic Molecular Beam Injection)

- Validation of machine protection and mitigation strategies related to ICRH power: hot spots monitoring (IR/visible imaging), ion ripple losses monitoring

## II. Step 2 : Power ramp up in L mode

The power increase phase will start with operating the LHCD and ICRH systems separately and increasing the power on the antennas (2 LHCD and 3 ICRH) individually, before combining the 2 LHCD launchers and the 3 ICRH antennas, respectively. A typical procedure for the power increase is given below. When applicable, the associated modelling is cited. This phase is expected to last 3 weeks, and will be performed in close connection with the WEST partners involved in the exploitation of the heating systems.

In addition to the focus on power ramp up as described below, first studies on divertor characterization (heat load patterns, density regimes etc) will be carried out. Tungsten accumulation is not expected to be an issue in L mode, but the first survey on tungsten sources will be performed.

NB : . It should be noted that the LH and ICRH systems of WEST can be moved radially, which will be used for coupling optimization.

LHCD only:

- Assess LH coupling on the two different LHCD launchers for different plasma launcher gap, radial gap between the Fully-Active-Multijunction (FAM) launcher and the Passive-Active-Multijunction (PAM) launcher (see annex 5 for details on the LH launchers), triangularity, density, local gas puff rate, etc.
  - Using IR monitoring, assess hot spots on the LHCD side limiters and on magnetically connected components, in the different conditions above. Define best scenario for increasing the power.
  - First, increase the LHCD power separately on the two launchers, up to 2MW / 5s, per launcher.
  - In optimum coupling conditions, as found above, validate the eight new high power klystrons connected to the PAM launcher during plasma operation. The klystrons have been tested on matched load, but not yet on plasma. The goal is to reach ~ 600 kW / klystron for ~ 5s. (Four klystrons will be operated simultaneously, leading to up to ~2.4MW generated power.)
  - Assess the power density limit on the PAM. The nominal power density of 25MW/m<sup>2</sup> was achieved in 2010, without signs of reaching a limit in power handling. The new high power klystrons will allow testing the PAM at higher power density, i.e. up to 4MW coupled power and 37MW/m<sup>2</sup>.
  - Increase the power on the FAM launcher alone to ~ 4MW / 5s.
- Modelling: ALOHA, COMSOL, fast electron power flow modeling.*

ICRH only:

- Apply the power on the ICRH antennas separately in short pulses, ~ 2s / antenna.
- Assess the coupling on the different ICRH antennas for different plasma antenna gap, triangularity, density, local gas puff rate, etc.
- Assess effect of H-minority concentration on metallic impurity emission. A diagnostic for measuring the isotopic ratio is mandatory.
- Assess the effect of ICRH resonance location (by small variation in  $B_T$  or ICRH frequency) on the W emission.
- Using IR monitoring, identify the main contributions to the front face heat loads (ELMs excluded) in different regions of interest and the relevant actuators to act on them via real-time control. Ideally, this identification should be made far from the operational limits of the antennas. Define best scenario for increasing the power.
- Mapping with reciprocating probes to measure the potential in front of the ICRH antenna in different plasma conditions (varying gas puff, triangularity, etc). Assess sheath radial extension → can they reach field lines connected to the W-divertor?
- Identify/quantify the sources of RF-induced impurity production and their geometry on the antenna front face and on the magnetically connected chamber elements (LH launchers, upper divertor, baffle).
- Impact of new ICRH electric schemes on the heat loads and impurity production (for example left/right asymmetry in antenna heat flux in the presence of unbalanced strap feeding).
- In optimum coupling conditions, increase the ICRH power on each antenna separately to 2MW / 5s per antenna.

*Modelling: COMSOL, TOPICA, SSWICH.*

First combined heating scenario with LH and ICRH will be tried in L mode (typically < 4 MW of total power to stay below the L-H threshold).

The ECRH system will also be commissioned during this phase (up to 0.5 MW/ 5 s).

The following fuelling aspects need to be studied:

- Study the simultaneous impact of fuelling on various aspects: the power coupling, the divertor regime and so the heat load, the tungsten migration from the wall to across the pedestal.
- Assessment of local gas puffing for LHCD and ICRH.
  - Several aspects, such as wave coupling, heat load, sputtering, arcing, pedestal, need to be studied simultaneously, leading to an operational domaine/compromise.
  - Ideally the outcome of the study should be the design of a local gas injector for ITER → best radial/poloidal/toroidal position of the gas valve with respect to the antenna, gas flow rate, parametric scaling ?

*Modeling SOLEDGE-Eirene*

Finally, the risk of disruptions must be correctly treated during the power increase phase:

- Consequences of disruptions to be evaluated both in terms of PFC damage and operation (how easy to start next discharge) to assess need for disruption mitigation system (when, operating instructions)

### III. Step 3 : Achievement of H mode operation

The objective of this phase will be the achievement of robust H mode over several seconds. This requires that the power crossing the separatrix is larger than the L-H threshold, which is foreseen in the range 4-6 MW for WEST, depending on the plasma scenario (see **Table 5** in Chapter 2). The typical target for the heating systems is therefore above 5 MW to reach H mode operation. The main challenges foreseen are to optimize the coupling of ICRH and LHCD systems in H-mode plasmas in presence of ELMs, and to avoid the risk of W production during ICRH (cf JET, AUG). This phase is expected to last 4 weeks.

This phase will yield the first results on the levels of tungsten contamination in H mode and will be studied under Headline H2 (towards long pulse H mode operation). The divertor heat load pattern in H mode will also be looked at, in preparation for the Headline W1 (testing ITER tungsten plasma facing components).

In terms of the heating systems, the following procedure is planned :

LHCD only:

- Use both LHCD launchers together to increase power > 5MW. Can H-mode be produced by LHCD alone? Or is additional ICRH power required?
- If H-mode can be achieved with LHCD alone, assess LH coupling on PAM and FAM for different plasma launcher gap, radial gap between FAM and PAM, triangularity, density, local gas puff rate.
- Using IR monitoring, assess heat loads on the LH grills and side limiters during H-mode. Assess hot spots on magnetically connected components, in the different conditions above. Compare hot spots intensity in L-mode versus H-mode, at same LHCD power.

ICRH only:

- Combine the three ICRH antennas to reach > 5MW to attain H-mode.
- Assess the ICRH inter-ELM coupling in H-mode for different plasma antenna gap, triangularity, density, local gas puff rate, etc.
- Assess/optimize ELM-resilience of the ICRH system. In particular, dedicated sessions will be necessary to adapt the length of the RF transmission lines and ensure the best ELM-resilience of the generators.
- Using IR monitoring, assess hot spots on the ICRH screens and side limiters, in the different conditions above. Assess impact of ELMs on the Faraday screens, and the behavior of the heat load real-time control in the presence of ELMs.
- Assess effect of ICRH H-minority concentration on W impurity concentration.
- Assess the effect of the ICRH resonance location (high field side, centre, low field side) as a means for controlling the W impurity accumulation, by varying the toroidal magnetic field of the ICRH source frequency.

LHCD + ICRH:

- If H-mode power threshold is above the power that can be attained by ICRH or LHCD alone, the two systems will be combined.

- A pre-requisite is that the radial positions of the launchers and antennas are accurately measured. This has previously been verified by using IR cameras and checking the hot spots from the electron beam from the LHCD launchers that impinge on side limiters on the magnetically connected antennas.
- Combine LHCD and ICRH and increase the power gradually, starting from 1MW per antenna and launcher. Then follow the procedures described above in the sections for LHCD alone and ICRH alone.
- Using LHCD + ICRH will require a trade-off between various aspects, such as hot spots on LHCD launchers due to fast ion ripple losses, LHCD and ICRH coupling, LH current drive efficiency.

Once the LHCD and ICRH systems have been commissioned and brought to high enough power to reach the H-mode power threshold, the following aspects will be addressed under Headline 2 (see chapter 4) :

- ICRH absorption and ripple losses : the ripple at the LCFS is ~ 2% for WEST. Significant ICRH ripple losses (~20-25%) are expected, especially at low plasma current. The impact on PFC will be assessed, and a trade-off between ripple losses and central ICRH absorption needed for W accumulation control will be investigated.
- Hydrogen minority concentration : the hydrogen minority heating scheme will be the main ICRH heating scheme used in WEST. Ideal H/D ratio will be investigated for an optimized coupling and electron to ion heating ratio.
- LHCD efficiency at high density: The H-mode high density edge can hinder the LH wave propagation beyond the pedestal region and affect the current drive efficiency of the LH waves. Experiments will be carried out to find the optimum  $n_{//}$  spectra and plasma density for efficient current drive.



# Annex 12 : Summary of the 1<sup>st</sup> WEST international workshop

---

This annex corresponds to the summary of the 1st International WEST workshop, organized in Aix-en-Provence, France, June 30th – July 2th 2014 (see, <http://west.cea.fr/Workshop2014/> for more details). The present summary has been written by the 5 international experts in charge of reviewing the various research areas as organized in the version 0 of the WEST Research Plan. Their output has been used as guidelines to revise the WEST Research Plan and produce the present updated version 1.

## Summary 1st International WEST workshop

June 30th – July 2th 2014, Aix-en-Provence

<http://west.cea.fr/Workshop2014/>

R Doerner<sup>1</sup>, A Kallenbach<sup>2</sup>, J Linke<sup>3</sup>, ML Mayoral<sup>4,5</sup>, M Yoshida<sup>6</sup>

<sup>1</sup> Univ Calif San Diego, Energy Res Ctr, La Jolla, CA 92093 USA.

<sup>2</sup> Max Planck Inst Plasma Phys, EURATOM Assoc, Boltzmannstr 2, D-85748 Garching, Germany.

<sup>3</sup> Forschungszentrum Julich, D-52425 Julich, Germany.

<sup>4</sup> CCFE, Culham Science Centre, Abingdon, Oxon, OX14 3DB, UK

<sup>5</sup> EUROfusion Programme Management Unit, D-85748 Garching, Germany

<sup>6</sup> Japan Atom Energy Agency, Tokai, Ibaraki, Japan.

The Institute of Research on Magnetic Fusion (IRFM) of CEA and the Aix Marseille University have organized the 1st WEST international workshop, held in Aix en Provence, France, from June 30 to July 2, 2014.

The WEST project (W-tungsten Environment in Steady-state Tokamak) has been launched by CEA in March 2013. WEST is targeted at minimizing risks for the ITER tungsten divertor procurement and operation, as well as mastering integrated plasma scenarios over long pulses in a metallic environment. It consists of implementing a divertor configuration and installing an ITER like actively cooled tungsten divertor in the Tore Supra tokamak, taking full benefit of its long pulse capability. The WEST platform will be run as a user facility, open to the ITER partners. First plasma is expected in 2016.

The objective of the workshop was for the participants to contribute to building the WEST scientific program. As international fusion experts we have chaired discussion sessions along topical headlines. The outputs of these sessions are summarized below. The summary is followed by some recommendations to be used as a basis to produce an updated version of the WEST research plan by end 2014.

Outline:

1. Summary of the session “Restart, heating and operational aspects” chaired by ML Mayoral.
  2. Summary of the session “Headline 1: Testing ITER Tungsten PFCs” chaired by J Linke.
  3. Summary of the session “Headline 2: Towards long pulse H mode operation” chaired by A Kallenbach
  4. Summary of the session “Headline 3: Exploring high fluence PWI” chaired by R Doerner
  5. Summary of the session “Headline 4: Preparing advanced tokamak modes” chaired by M Yoshida
  6. Recommendations towards the version 1 of WEST Reasearch Plan.
- .....

### 1. Summary of the session “Restart, heating and operational aspects” chaired by ML Mayoral.

The topics addressed in this session were related to the WEST work plan “Commissioning and power ramp-up ...up to H-mode” aiming at achieving LHCD ~ 5-6 MW, 10-30s and ICRF ~ 5-6 MW, 10-30s. There are several physics issues that need to be investigated during the restart phase of the additional heating systems, even before entering the phase of H-mode plasmas. Once H-mode plasmas have been reached, optimisation of the ICRF and LHCD systems for coupling during ELMs need to be carried out.

The optimisation of ICRF/LH Heating and current drive in a W-wall machine includes the following:

- LHCD efficiency and LH wave penetration at high pedestal density
- H minority concentration optimisation for heating efficiency, ICRF absorption & ripple losses
- Control of the W production and transport: W transport with dominant electron heating, W source in the presence of RF, H-mode and actively cooled PFC

These issues are addressed in two topics

#### a. Tokamak operation:

- The content of low Z impurity content will have a strong impact on the subsequent WEST operation due to enhanced W sputtering. Therefore the light impurity content will be carefully monitored and will bring an insight on a full W machine conditioning.
- The Plasma Wall Monitoring System is a very important element for the safety of the PFCs and will be a very interesting contribution for ITER. The issue of IR temperature measurements in a metallic environment is crucial. The control of the surface temperatures in long pulses need to be addressed and WEST will bring a significant input.

#### b. Increasing HF power (ICRF and LH up to 2x6 MW, 10-30s):

- WEST has a unique LHCD capability, in particular an ITER-like LHCD launcher (the passive-active-multijunction, PAM). This launcher has been validated on L-mode plasmas at its nominal, ITER-relevant, power density ( $25\text{MW}/\text{m}^2$ , i.e. 2.7MW). WEST will now allow assessing the real power capability of the PAM (probably higher than 3MW) by using the new high power CW-klystrons. In addition, high power operation of the PAM during ELMs will allow demonstrating that the PAM is a viable solution for LHCD in ITER.
- Studying the LH wave propagation and absorption in high density pulses will be an important activity in the power increase phase. Measurement of the hard X-ray emission from the 2D hard X-ray diagnostic, combined with ray-tracing + Fokker-Planck modelling, will allow comparing the measured hard X-ray emission with that predicted by modelling. Note that LHCD at high density is an ongoing ITPA IOS task, for which WEST can contribute significantly and allow to progress in the understanding of the LHCD physics.
- Modelling of RF sheath is very complex matter and still not mastered. WEST with its good diagnostics coverage & strong modelling expertise could be an asset for RF sheaths code validation. The RF sheaths lead to enhanced heat load (due to ions accelerated in  $V_{\text{DC}}$ ) on magnetically connected surfaces. Therefore, the choice of the limiters and faraday

screen material is crucial. There are two options for the limiter material: Boron or W. If the limiters are made of low Z material (B), B sputtering due to D ions accelerated in the DC potential takes place. The consequence is an increased W sputtering by B in the divertor/baffle region. On the other hand, if the limiters are made of high Z material (W), there will be W sputtering due to (C, O) ions that are accelerated in the DC potential. In AUG, the divertor W source is 5-10 times stronger than the main chamber source. Nevertheless, the core W content is dominated by the main chamber sources due to a better penetration [Dux IAEA2012]. In AUG, W-coated and Boron-coated antenna limiters have been operated and compared [Bobkov NF2013]. The W concentration is larger when operating W-coated limiters. Moreover, the balance between central electron heating (for W control) and the W source is significantly better for antennas with B-coated limiters. The use of W-coated antenna limiters will likely limit the operational window in order to decrease W sputtering, by using methods such as: operating at high density, use ICRF scenarios that guarantee high single pass absorption (not during ramp-up), keep the antennas far away from the main plasma, apply ICRF only late in the discharge.

- The operation of 3 NEW antennas with ELM resilience relying on vacuum conjugate T-junction will be a very active field of research. The solution is mastered, BUT in order to be “ELM-resilient” it is necessary to optimise the impedance at the T-junction (by changing the capacitor value). The optimal settings depend mainly on coupling in between ELMs and hence a change in coupling during ELMs will depend on the H-mode nature (i.e. ELM amplitude). Additionally, a too low coupling between ELMs will (1) limit the power and (2) affect the conjugate-T ELM tolerance. Gas injection could be a solution for WEST (and ITER). WEST has several gas injection points and a good density measurement in front of the antennas, as well as SOL 2D codes to address this issue. An extension to SOL 3D codes would allow improving the modelling of the SOL density behaviour during local gas injection.
- Concerning the arc detection in the ICRF antennas, it becomes more difficult during ELMs since the discrimination between reflection due to an ELM and to an arc is difficult. Development in this area carried out in WEST could be useful for ITER. A stable H mode is needed to ensure such investigation; hence enough LH power needs to be available to ensure a well-established ELMy H mode.

The list of new challenges is long: new wall behaviour, new plasma shape & control, new ICRF antennas, operation on ELMs... Reaching a stable H-mode with ICRF / LH only is critical (both for the WEST programme but also for the HF community). This part of WEST scientific programme is rich in new and useful physics experiments.

## **2. Summary of the session “Headline 1: Testing ITER Tungsten PFCs” chaired by J Linke.**

WEST, by allowing for the test in a tokamak environment of ITER Tungsten PFCs, is filling a gap between the tests carried out in PWI devices and operation in ITER. Indeed test of such components in a tokamak are needed to be benchmarked against laboratory experiments and codes used for ITER such as: FEM, PIC, PFCFLUX, MEMOS... Test in WEST is also essential to qualify the manufacturing process of PFCs. Different materials have to be qualified: new tungsten grades, W-composite, W-alloyed or doped as well as tungsten coatings (incl. CVD, FGMs etc.), effect of different orientations and grain size effects and the performance of recrystallized tungsten. Different components also have to be qualified: ITER divertor target and dome, FW and divertor targets solutions for DEMO (incl. testing of He-cooled components?) as well as W-armoured divertor targets for W-7X and JT60SA (e.g. W coatings on CFC). A question on the time scale of PFU procurement was raised. How many PFUs can be supplied by 2015: a few PFUs? / One full sector? Provided by Japan and Europe.

Below are listed some recommended research axis:

- a. A full sector should be reserved for long term exposure of ITER like PFUs such that the following aspects are taken into account:
  - detailed pre-characterization
  - well-diagnosed sector
  - PFUs with different manufacturing technologies and shaping
  - post-mortem analysis after long term exposure to all WEST plasma scenarios
- b. Helium discharges should take place at the end of phase 1, with a set of extensive diagnostics.
- c. Study the impact of combined steady state and transients (ELMs) heat loads to study the screening under steady-state and pulsed transient heat loads and the effect of very high transients  $\gg 10^5$  (aim:  $\geq 10^7$ ). Indeed in PWI devices, high transients number can be tested but without a plasma pressure, in absence of magnetic field, missing H- / He-impact and with loaded spot size in mm-range. WEST with its tokamak environment tokamak allow exploring all synergistic effects to be encountered in ITER except neutrons. This aspect of the programme depends on the ELMs obtained in WEST which are expected to be at most of  $5\text{MW/m}^2\cdot\text{s}^{1/2}$  leading to a temperature rise of  $300^\circ$  allowing to cycle around the recrystallization temperature when starting from a steady state at  $10\text{MW/m}^2$ .
- d. W melting experiment: tokamak experiments can be carried out in WEST on ITER relevant geometries. The impact of melting on operation has to be studied for both local melting on the leading edge and surface melting. It requires heat loads clearly above melting threshold (thanks to prepared misalignment for example). It will be interesting to study the melt motion for repeated events (high pulse numbers) and the performance of re-solidified tungsten (under steady state and sub-threshold ELMs)
- e. Shaping and leading edges issues require tokamak experiments for the experimental verification. Indeed, experiments with shallow incidence angles are extremely difficult in beam experiments (HHF tests require parallel beams). The gap width analysis (monoblock gap (*poloidal gap*) and inter PFU-gap (*toroidal gap*)) has to include gyration of particles. The edges could be exposed to flux tubes penetrating through the monoblock gaps. An important question to be answered for ITER is which are the acceptable tolerances for misalignments: 0.3mm or larger?.
- f. Damaging mechanisms for W mono blocks require also tokamak experiments. Indeed synergistic load tests using electron- laser beams or linear plasma devices are limited to relatively small spot sizes. Moreover He- and H-effects are difficult to realize with high pulse numbers (up to now sequential loading only). Tokamak experiments such as WEST, comprising all load types are urgently needed. The studies will be on thermal shock induced damaging mechanism: roughening leading to crack development, self-castellation and ultimately molten droplet. Other damage such as macroscopic cracking of tungsten monoblock tile and thermally induced deformation of the CuCrZr-tube can also be observed. The subsequent performance of re-solidified W surfaces has to be investigated.
- g. Investigation of pre-loaded and pre-damaged components is important to optimize the rejection rate. WEST divertor is flexible and could allow for the investigation of specific PFCs such as repaired PFCs (joints or plasma facing surface), PFCs with calibrated defects at the interface, deliberately misaligned components and potentially investigate self-healing technologies. Importantly for ITER, PFCs which do not meet the acceptance criteria could also be tested to optimize the ITER criteria.
- h. Concerning the diagnostics, an IR view with a resolution down to 0.1mm is desirable. The multicolor camera technique is desirable to avoid biases due to the inevitable surface emissivity evolution. It would provide a detailed surface temperature and flux map of (at

least) a few mono blocks, an invaluable piece of information to study the physics involved in the shaping and gaps.

### 3. Summary of the session “Headline 2: Towards long pulse H mode operation” chaired by A Kallenbach

Under this headline, a list of physics topics with particular relevance for WEST have been pointed out.

- a. An operational threat to H-mode is the potential W accumulation. This point will have to be carefully addressed by the WEST programme. Indeed, central peaking of the density leads to neoclassical W inward transport, then W radiation influences central power balance, having the consequence of a reduced anomalous transport leading to a runaway accumulation. It is to note that plasmas with lower current are less prone to W accumulation (higher anomalous diffusivity). In WEST, the use of ICRH will require an optimizing of ICRF operation for central W suppression with low additional W source (may require antenna modifications). See also the summary on „restart, heating and operational aspects“.
- b. In WEST, core turbulent transport will be modified due to reduced trapped particle fraction at higher aspect ratio, in particular TEMs will be less unstable compared to tokamaks with lower aspect ratio. The dominant electron transport will also affect the core transport. It will be interesting to compare the transport, in particular the aspect ratio impact, to the current modelings. The high aspect ratio in WEST will expand the existing databases beyond possible future DEMO values of about  $A=4$ , allowing firmer projections from the large existing  $A=3$  database. Further, WEST can contribute to the physics study associated to current profile variation, , analyse the turbulent transport in presence of less trapped electrons and finally test the neoclassical effects on W profiles (high T minority ions, ICRF induced asymmetries).
- c. The physics of power loads and PWI are also key to WEST programme. The mechanism of power transmission to ITER like target, the ELM heat loads on the first wall, ELM characteristics from good IR and probe measurements in combination with JOEKE modelling, taking advantage of the open divertor geometry for good optical access to study the physics of prompt W redeposition, dust production in long H-mode discharges and last but not least the validation of edge codes against well diagnosed experiments.
- d. It will be interesting to study the ELM wetted area and its modification with ELM size as seen on AUG and DIII-D. . The broadening during ELMs is a crucial issue for ITER. The current assumption for ITER is based on the lowest  $\lambda_{q,ELM}$  values measure on JET, resulting in  $\lambda_{q,ELM}=5-6\text{mm}$ . The ELM width is also an issue for the main chamber PFCs. Thanks to its very good wall and divertor IR coverage, WEST could give a valuable input.
- e. In the WEST divertor, the prompt redeposition can be experimentally studied using spectroscopic line ratio measurements of  $W_{II} / W_{I}$ . It is expected to be above 50% [R. Dux et al. & G. v. Rooij et al. JNM 2013]. The mechanisms at play need to be compared to various models to improve our capacity to extrapolate towards ITER.
- f. The main WEST scenario development, database contributions and MHD are as follows: development of scenarios without tungsten accumulation, optimization of RF heating and current drive in a W environment, NTMs at low rotation (probing metastable conditions over long durations), ELM pacing (pellets, SMBI, kicks) with good divertor diagnostics, comparing different disruption mitigation regimes, low  $q_{95}$  operation, operation with He plasmas.

#### **4. Summary of the session “Headline 3: Exploring high fluence PWI” chaired by R Doerner**

ITER’s W divertor solution is an ambitious jump in technology readiness levels. WEST provides the intermediate technology development necessary for the actively cooled ITER W divertor (technical readiness level ~4).

Concerning WEST programme with respect to linear devices, linear devices/off-line facilities are well adapted to study changes in material properties and structures with high fluence (cracking, swelling, blisters, nano-bubbles, melt layers, fuzz...). WEST will need to focus on how those materials changes feedback and affect the confined plasma. Existing confinement devices can study many of the interactions of W with a confined plasma (W core accumulation, transport, radiation, sources...), but only in a transitory environment. WEST must focus on the way the W wall and plasma behave when they come into equilibrium.

- a. WEST (even in phase 2) is not, necessarily such a high fluence experiment. WEST in phase 2 is, however, long pulse and this could play a significant role in PMI related to diffusion aspects.
- b. Priority of retention in WEST phase 2 campaigns should be re-evaluated. Is it a high priority?
- c. WEST in phase 2, has for the first time the opportunity to investigate very large number of ELMs (~millions) and their impact of the evolution of surfaces. This requires to prioritize and define diagnostic specifications for measuring  $\Delta T$  changes during ELMs over large number of discharges. Calibration with ‘reference’ laser pulse at beginning of each day might be mandatory.
- d. During phase 2 of WEST operation, avoidance of infrequent large transient (i.e. Disruptions) should be emphasized. As one large infrequent transient could dominate surface changes from the very large number of small, frequent transients (i.e. ELMs).
- e. He campaign should be scheduled at the conclusion of WEST phase 1 operations, prior to installation of the full actively cooled divertor structure and phase 2 operation. This allows immediate access for analysis of the He-exposed sector while minimizing risk to the entire divertor structure.
- f. It is recognized that the Research Plan for headline 3 is presently less well defined due to its long time horizon, but thought should be put into DEMO-relevant research that can be conducted during long-pulse plasma operation.

#### **5. Summary of the session “Headline 4: Preparing advanced tokamak modes” chaired by M Yoshida**

WEST allows studying steady state scenarios in a W environment. Steady state means that 100% of the current is non-inductively produced. Various such scenarios have been presented. Overall, significant contributions to advanced operation are well discussed capitalizing on the WEST characteristics. The scenarios are relevant to various ITPA topics such as W divertor heat flux control and W impurity profile control, PAM on H mode, ICRF & LH coupling, current density profile control, control of fast ion transport and Alfvén eigenmodes, simultaneous heat flux, profile, stability, & transport control. WEST could be an excellent test bed for ITER advanced scenario development

More precisely:

- a. For particle control in long pulses, non-inductive H mode and long pulse hybrids are two scenarios on which WEST programme should focus to provide relevant information to ITER.
- b. To explore the controllability of high performance plasmas the priority should be given to the high bootstrap fraction scenarios, the large Greenwald fraction pulses and the large radiated fraction operation. Such scenarios are interesting to prepare JT-60SA operation and explore DEMO relevant aspects.
- c. Plasma start-up toward an advanced scenario (ex. Non-inductive plasma current start-up) could contribute to JT-60SA operation and a compact DEMO concept.
- d. Other topics to be studied are MHD stability analysis: mode evaluation, consider fast ion beta component in models, integration with scenarios, control tools (ECCD for NTM, ICH for beta of the ions).
- e. A systematic analysis of the fast ions content is required.
- f. Concerning the accessibility to steady state (in high beta scenarios) the q profile range and the necessity to avoid MHD have to be taken into account.
- g. The W accumulation and the interplay with the transport have to be predicted considering central electron heating,  $R/L_{Te}$  (TEM) and rotation effects.
- h. Particle control might be limited at low density due to the lack of a cryo-pump. The installation of such a pump might be needed for low density operation.
- i. WEST contribution to switch the divertor of JT-60SA to a W-divertor will be very important. WEST operation will also contribute to JT-60SA steady state operation.
- j. In all scenarios it will be mandatory to optimize of LHCD ( $n_{//}$ ) and ICRH (gas). There are many advantages of HFS launch for LH, it is worth examining its practical installation.

## 6. Recommendations towards the version 1 of WEST Research Plan.

The version 1 of WEST research plan should be organized in around topics targeting more precise operational issues. In each topic, the phase one of operation (one or more sector of ITER like divertor together with inertial divertor sectors) should be emphasized and well detailed. The main objectives of phase 2 (360° of ITER like divertor) should be more broadly overviewed.

The following key topics are proposed to be studied:

- Conditioning (compare technics for a low impurity content)
- HF heating (coupling with ELMs, RF sheath, absorption of LH at high density, etc)
- ITER divertor experiments (shaping/misalignment, melting and subsequent operation, He operation, test of PFUs which do not meet the acceptance criteria, test predamaged element, etc)
- Optimizing the pedestal confinement for large ELMs (towards low gas puff, towards large  $I_p$ ). Here, the avoidance of tungsten accumulation will be the most challenging task.
- Plasma Facing Components surface temperature (diagnostics validation, control, etc)
- W source studies (ELMs, sheath, divertor vs main chamber, etc)
- SOL regimes (towards detachment, code benchmark, etc)
- Core multi-channel confinement (aspect ratio impact on heat and particle, W transport, MHD impact)
- Steady-state regimes (non-inductive H mode, long pulse hybrid, controllability of high performance plasmas, associated MHD, etc)

# Annex 13 : List of figures

---

Figure 1 : comparison of the ITER and WEST divertor procurement and operation phases. The timing foreseen for the main inputs of WEST to ITER is also indicated. (NB : the dates shown here are subject to revision, see <sup>11</sup> ).....	19
Figure 2 : building the WEST network .....	20
Figure 3 : the worldwide family of superconducting long pulse tokamaks (in operation or under construction). WEST is presently the only superconducting tokamak located in Europe [courtesy Y. Kamada].....	21
Figure 4: going from the CIEL (left) to the WEST (right) configuration of Tore Supra .....	25
Figure 5: Internal view of Tore Supra in the previous CIEL configuration (left) and the foreseen WEST configuration (right) .....	26
Figure 6: Typical magnetic configurations foreseen for WEST: the far X-point (left) and close X-point (right) configurations.....	28
Figure 7: WEST plasma size compared to ITER and the other EU tokamaks.....	28
Figure 8 : overview of the WEST plasma facing components .....	29
Figure 9 : comparison of the ITER and WEST divertor. WEST reproduces at scale 1 the flat high heat flux part of the ITER divertor. ....	30
Figure 10 : field of view of an IR endoscope (left) and Langmuir probe set-up (right).....	32
Figure 11: Typical electron density (top) and temperature (bottom) profiles with radial intervals measured by the various profile diagnostics. The Thomson scattering diagnostic will have 6 measurement points in the pedestal region (around $r/a = 0.9-1$ ).The overlap region between core and edge reflectometers and the outermost radius measured by ECE depend on the plasma conditions. The outer views of the 2D X ray spectrometer will not be available at the beginning of operation.....	33
Figure 12: Temperature, density and q profiles of the 3 scenarios summarized in Table 5.....	36
Figure 13 : illustration of a WEST like close X point configuration run on the upper divertor of AUG [Meyer2013].....	36
Figure 14 : PFCFLUX calculations of the heat load pattern on the WEST divertor for PSOL = 10 MW and $\lambda_q = 5$ mm for the 2 standard magnetic configuration, the close X point (a) and the far X point (b) .....	50
Figure 15 : preliminary estimate of the temperature increase of the W monoblocks linked to ELMs, showing that the temperature excursion can allow cycling around the recrystallisation temperature $T_r$	



## Annex 13 : List of figures

(for a steady state heat load of $10 \text{ MW/m}^2$ , and ELMs of $50$ and $100 \text{ kJ/m}^2$ , red and blue curve respectively, $400 \mu\text{s}$ duration, $50 \text{ Hz}$ frequency).....	56
Figure 16 : tentative timeline for Headline 1. Major milestones are indicated in red. Specific campaigns related to PFC testing are also shown (campaign with misaligned/pre-damaged PFC, He operation, wall loading campaigns). Major shutdowns are indicated, but additional shorter shutdowns are to be planned. ....	89
Figure 17 : tentative timeline for Headline 2. Major milestones are indicated in red. Specific campaigns related to PFC testing for Headline 1 are also shown as a reminder. Major shutdowns are indicated, but additional shorter shutdowns are to be planned. ....	90
Figure 18 : schematic view of WEST contributions in terms of component science, plasma science and operation science .....	94
Figure 19 : Poloidal flux maps of the far X-point (left) and close X-point (right) reference configurations calculated by CEDRES++ .....	102
Figure 20 : Maximum possible $I_p$ versus plasma duration for the two reference configurations, resulting from the divertor coils heating and power supplies constraints. For the close X point configuration, the maximum plasma current is further limiter to $1 \text{ MA}$ for stability reasons ( $q_{95} = 2.4 @ 1 \text{ MA}$ ).....	103
Figure 21 : Examples of double-null (left) and upper single-null (right) configurations .....	103
Figure 22 : Examples of configurations with $\kappa=1.29$ (left) and $\kappa=1.74$ (right) .....	104
Figure 23 : overview of the WEST plasma facing components .....	105
Figure 24 : a) view of a WEST divertor sector, showing the similarity with the high heat flux flat part of the ITER divertor. b) detail of a WEST divertor sector, showing the cooling system, the supporting structure as well as a zoom on the monoblock shaping .....	106
Figure 25 : a) zoom on the WEST PFU, showing the twisted tape in the cooling channel b) global view of the WEST lower divertor, composed of 12 modular sectors of $30^\circ$ toroidally each [Missirlian2013b] .....	107
Figure 26 : Schematic layout of the RF antennas in WEST.....	110
Figure 27: Electrical scheme of the Tore Supra ICRH antenna prototype, tested in 2007.....	111
Figure 28: Photos of the LHCD system: generator plant with 16 new klystrons (left) and the two LHCD launchers (right). ....	112
Figure 29: Operating range for the radial positions of the ICRH and LHCD antennas in WEST. The outboard limiter is also shown for comparison. ....	113
Figure 30 : overview of the fuelling systems for WEST (gas puff, supersonic molecular beam injection, pellets) with a poloidal cut (left) and a top view (right).....	116

## Annex 13 : List of figures

Figure 31 : Effective pumping speed in the vacuum chamber as a function of the divertor neutral pressure in the present ( $S_{\text{eff-1}}$ ) and upgrade ( $S_{\text{eff-2u}}$ ) configurations. ....	117
Figure 32: Location of the visible CCD cameras dedicated to tokamak operation. ....	120
Figure 33 : : field of view of an IR endoscope (left) and Langmuir probe set-up (right).....	121
Figure 34 : Typical electron density (top) and temperature (bottom) profiles with radial intervals measured by the various profile diagnostics. The Thomson scattering diagnostic will have 6 measurement points in the pedestal region (around $r/a$ ) 0.9-1).The overlap region between core and edge reflectometers and the outermost radius measured by ECE depend on the plasma conditions. The outer views of the 2D X ray spectrometer will not be available at the beginning of operation..	123
Figure 35 : Overview of magnetic sensors position .....	126
Figure 36 : Architecture of WEST Plasma Control System around a supervision unit. ....	127
Figure 37 : Interfero-polarimetry chords in a poloidal cross section .....	129
Figure 38 : Thomson scattering diagnostic laser beam (in red) and measured region (in blue). ....	130
Figure 39 : Ar He-like X-ray image and time evolution of typical inferred Ti profiles .....	131
Figure 40 : (Top) Side view of the spectrometer viewing access in WEST (lower single-null initial test configuration; note that plasmas would likely be narrower).....	131
Figure 41 : (left) Field of view of the wide angle tangential viewing system, (right) Field of view of the fiber bundle system.....	134
Figure 42 : schematic view of the Langmuir probes set up for WEST.....	135
Figure 43 : AIA robot deployment in WEST .....	136
Figure 44 : Outline of the barometry set-up in WEST .....	137
Figure 45 : Picture of the dust collector as installed on a reciprocating probe of Tore Supra.....	138
Figure 46 : Picture of the dust injector as it will be installed on the reciprocating probe of Tore Supra .....	138
Figure 47 : Schematic view of the LIBS experiment in the WEST tokamak.....	139
Figure 48 : In Situ confocal microscopy for erosion/deposition limiter assessment (DITS campaign)	140
Figure 49 : SIR and SURVIE geometry for VUV spectroscopy.....	141
Figure 50 : Bolometric lines of sight in a poloidal cross section of WEST .....	142
Figure 51 : Layout of the GEM detector diagnostic for SXR detection (red squares are SXR active surfaces) .....	143
Figure 52 : line of sight for the Bremsstrahlung system .....	144

## Annex 13 : List of figures

Figure 53 : Photographs of the two LHCD launchers inside the Tore Supra vessel. Each launcher has four Langmuir probes located one in each corner of the launchers (yellow circles). Four probes for fluctuation measurements are located at the mid-plane on the C4-PAM launcher and two on the upper part on the C3-FAM launcher (red circles). .....	145
Figure 54 : Schematic view of the horizontal (38 detectors) and the vertical (21 detectors) HXR cameras in Tore Supra. Only the horizontal camera will be used in WEST.....	147
Figure 55 : Positioning of the DENEPR probe inside a vertical diagnostic port of the Tore Supra chamber.....	147
Figure 56 : left: accessibility of the X mode reflectometers for a WEST profile with $n_e(\rho=0)=7.5 \cdot 10^{19} \text{ m}^{-3}$ , $n_e^{\text{ped}} = 4.5 \cdot 10^{19} \text{ m}^{-3}$ , $n_e^{\text{sep}} = 2 \cdot 10^{19} \text{ m}^{-3}$ . The brown zone shows the overlap between the core (red zone) and edge (pink zone) reflectometer accessibility. Right: cutoff layer profiles at nominal B ( $I_{\text{tor}}=1250$ i.e. $B=3.6\text{T}$ ) for 2 scenarios: the high power, high density, high current, high confinement $H=1.2$ ( $n_e(\rho=0)=10.5 \cdot 10^{19} \text{ m}^{-3}$ , $n_e^{\text{ped}} = 5.2 \cdot 10^{19} \text{ m}^{-3}$ , $n_e^{\text{sep}} = 3.5 \cdot 10^{19} \text{ m}^{-3}$ ) and the moderate power, high current, low density, low confinement $H=0.7$ ( $n_e(\rho=0)=7.6 \cdot 10^{19} \text{ m}^{-3}$ , $n_e^{\text{ped}} = 4.3 \cdot 10^{19} \text{ m}^{-3}$ , $n_e^{\text{sep}} = 2 \cdot 10^{19} \text{ m}^{-3}$ ). .....	148
Figure 57 : position and field of view of the fast camera in WEST.....	150
Figure 58: Dimension of the ECEI measured plasma area and coverage in a poloidal cross section. ....	151
Figure 59: CAD views of WEST and a table summarizing the WEST main parameters. ....	153
Figure 60: CEDRES++ free boundary set of equilibria for $B_T = 3.7 \text{ T}$ ( at 2.5 m); with a fixed external radius of 2.93 m and with the steady state divertor coil current of 200 kA.turn. ....	154
Figure 61: At fixed $B_T=3.7\text{T}$ , range of accessible $I_p$ and X point heights corresponding to the references equilibria illustrated by FIG.60. The limits due to the divertor coils are in red, one for the steady state and one corresponding to the maximal divertor coils current. In blue is the limit corresponding to $q_{95}=2.5$ . .....	154
Figure 62: Top view of a 30° divertor sector. The low field side is at the top of the figure and the high field side at the bottom.....	154
Figure 63: Heat flux fall-off length $\lambda_q$ in H mode based on the scaling law from [Eic11], for an X point height of 3 cm in red and an X point height of 10 cm in blue. The error bars represent the uncertainties on the exponents of equation (1). .....	155
Figure 64: Additional power required to reach $10\text{MW}/\text{m}^2$ on WEST divertor.Using the scaling law of [Eic11], accounting for the magnetic ripple and for an X point height of 3 cm in red and an X point height of 10 cm in blue.....	156
Figure 65: LHCD accessibility diagram at 3.7 GHz .....	157
Figure 66: C3PO-LUKE LH modelling for two WEST scenarios. ....	158

Annex 13 : List of figures

Figure 67: Poloidal views of WEST equilibria at 0.8 and 0.5 MA in steady state computed by CEDRES++ see Fig.60. The unshifted H resonance positions are indicated in green for two ICRH frequencies: 52 and 57 MHz. In magenta are shown the limits of the good confinement region. .... 159

Figure 68: EVE/AQL modelling of a WEST scenario for 6 MW of ICRH at 55.5 MHz and  $n_H/n_e=6\%$ . Power density absorbed by species (left y-axis, solid lines), total power (right y-axis, dashed lines).159

Figure 69: Power split between electrons and bulk ions (solid lines) when the coupled RF power is varied between 3MW and 9MW, at 6% H minority concentration. Also shown is the fast ion content (dashed line). .... 160

Figure 70: Influence of the hydrogen minority concentration on the power split between electrons and bulk ions. .... 160

Figure 71: Neutral pressure in a poloidal cross section of WEST modeled by SolEdge2D-EIRENE [Buf13]. .... 161

Figure 72: L-H power threshold expectation for WEST with respect to the core line average density. In red, triangles: ITPA 2008 [Mar08]; in purple circles: ITPA2004 [Tak04] assuming  $Z_{eff}=1.2$ ; in blue squares: ITPA 2004 with  $Z_{eff}=1.2$  and an additional aspect ratio impact such that  $P_{th} \propto \frac{1}{\sqrt{A}}$  from [Min97]. .... 162

Figure 73: Ideal MHD limit computed by MISHKA [Huy07] for  $I_p=0.8$  MA. The low wave number modes are the peeling modes and the higher wave number modes are the ballooning modes. .... 162

Figure 74: Estimate of the temperature increase of the W monoblocks linked to ELMs, for a steady state heat load of  $10 \text{ MW/m}^2$ , and large type I ELMs of  $50$  and  $100 \text{ kJ/m}^2$ , red and blue curve respectively,  $50 \text{ Hz}$  frequency. The W recrystallization temperature range is bordered by green dashed lines. .... 164

Figure 75: Plasma temperature in front of the target plates as a function of separatrix (upstream) density from a two points model, for  $P_{SOL}=6\text{MW}$  and  $\lambda_Q=5\text{mm}$  and various levels of radiated power in the SOL. Open circles are pure deuterium Soledge2D-EIRENE calculations for the same parameters. .... 165

Figure 76: Fraction of the heating power radiated in the core (solid red) and in the edge (dashed black), as a function of boron concentration in % obtained by Corediv for  $P_{aux}=14 \text{ MW}$ . Core radiation is almost exclusively from W while edge radiation is essentially from D and B. .... 167

Figure 77: Particle flux densities as a function of the poloidal location, from the lower to the upper divertor via the low field side elements (baffle and antenna limiters).  $D^+$  flux (solid blue), D flux (dashed black), W gross influx from ions (solid red) and net influx from ions (green crosses), i.e. accounting for prompt redeposition, but without sheath rectification. .... 168

Figure 78: JET-ILW pulse 84746. .... 170

Figure 79: Temperature, density and q profiles of the 3 scenarios summarized in Table 1. .... 171

Annex 13 : List of figures

Figure 80: Neutral pressure in WEST for a discharge heated by 8 MW and a gas puff of  $8 \times 10^{20}$  particles/s in the private region (SOLEEDGE-2D simulation, log scale)..... 176

Figure 81: Turbulent (left) and collisional (right) impurity fluxes, showing a predominant inward (blue) contaminating trend (GYSELA simulation)..... 179

Figure 82 : Impurity redistribution by a sawtooth crash as modeled with XTOR. .... 180

Figure 83 : Density contours and heat flux on divertor plates modelled with JOREK (ITER case shown here) . .... 183

# Annex 14 : List of tables

---

Table 1 : overview of the high level deliverables expected from WEST .....	17
Table 2 : comparison of the main features of the 2 operation phases foreseen for WEST. ....	18
Table 3: Main parameters of WEST.....	27
Table 4 : comparison of the main characteristics of the ITER and WEST divertor .....	30
Table 5: overview of the plasma scenarios foreseen for WEST .....	35
Table 6 :WEST contributions to Mission 1 and 2 of the EU fusion roadmap for Horizon 2020 .....	98
Table 7 : signed partnership agreements with WEST (as of December 2014).....	101
Table 8 : Parameters of the reference configurations (note: the standard $B_t^{vac}$ (T) at $R=2.37m$ is used) .....	103
Table 9 : overview comparing WEST and ITER divertor plasma facing units (PFUs) .....	107
Table 10 : overview of WEST diagnostics .....	124
Table 11: Summary of main controllers and real time protection systems (orange background) for WEST.....	128
Table 12 : overview of the IR system foreseen for WEST .....	133
Table 13 : Specifications of lines of sight for visible spectroscopy.....	141
Table 14: summary of some key parameters characterizing 3 scenarios for WEST suited with the code METIS.....	171
Table 15 : definition of occurrence.....	187
Table 16: definition of severity impact.....	187
Table 17 : definition of criticality.....	188
Table 18 : overview of the top 15 risks identified for the WEST programme.....	193